



THE UNIVERSITY OF QUEENSLAND  
A U S T R A L I A

# Planar-algebraic models

Xavier Poncini  
B.Adv.Sc. (Hons. I)



0000-0001-5727-6436

*A thesis submitted for the degree of Doctor of Philosophy at  
The University of Queensland in 2023  
School of Mathematics and Physics*

# Abstract

This thesis studies algebraic aspects of two-dimensional statistical mechanical models. Centred around the transfer operator, we develop a framework to describe such models with planar algebras, generalising features of the Quantum Inverse Scattering Method. To each planar algebra, we thus assign a model on the strip and a model on the cylinder, and refer to these as planar-algebraic models.

Within this framework, we develop a set of sufficient conditions that imply a planar-algebraic model is integrable, which include generalised Yang–Baxter equations. We refer to planar-algebraic models satisfying these conditions as Yang–Baxter integrable. For each such model, we outline a general procedure to identify a countable set of Hamiltonians that each share a set of eigenvectors with the transfer operator. We consider the algebraic relations among the Hamiltonians, and for a particular class of planar algebras, identify when they are all algebraically related to a single Hamiltonian. In this case, the transfer operator is expressible as a polynomial in this same Hamiltonian, and we say that the model is polynomialisable.

These general considerations are then applied to the class of so-called singly generated planar algebras. We show that the planar-algebraic models on the strip and on the cylinder are Yang–Baxter integrable if and only if the underlying planar algebra satisfies a Yang–Baxter relation. To establish this result, we develop a new model whose algebraic structure owes to the recently introduced Liu planar algebra. Moreover, we show that each such Yang–Baxter integrable model on the strip is polynomialisable, although the polynomials are not determined explicitly. Again on the strip, we consider an eight-vertex model and a model described by the Temperley–Lieb planar algebra. In each case, we determine explicit expressions for the transfer operator as a polynomial in a Hamiltonian. Putting integrability aside, we apply the planar-algebraic framework to determine the critical behaviour of two models of non-intersecting loop segments defined on causal triangulations.

## **Declaration by author**

This thesis is composed of my original work, and contains no material previously published or written by another person except where due reference has been made in the text. I have clearly stated the contribution by others to jointly-authored works that I have included in my thesis.

I have clearly stated the contribution of others to my thesis as a whole, including statistical assistance, survey design, data analysis, significant technical procedures, professional editorial advice, financial support and any other original research work used or reported in my thesis. The content of my thesis is the result of work I have carried out since the commencement of my higher degree by research candidature and does not include a substantial part of work that has been submitted to qualify for the award of any other degree or diploma in any university or other tertiary institution. I have clearly stated which parts of my thesis, if any, have been submitted to qualify for another award.

I acknowledge that an electronic copy of my thesis must be lodged with the University Library and, subject to the policy and procedures of The University of Queensland, the thesis be made available for research and study in accordance with the Copyright Act 1968 unless a period of embargo has been approved by the Dean of the Graduate School.

I acknowledge that copyright of all material contained in my thesis resides with the copyright holder(s) of that material. Where appropriate I have obtained copyright permission from the copyright holder to reproduce material in this thesis and have sought permission from co-authors for any jointly authored works included in the thesis.

## Publications included in this thesis

Publications included in this thesis are the following:

- [1] B. Durhuus, X. Poncini, J. Rasmussen, M. Ünel, *Critical behaviour of loop models on causal triangulations*, J. Stat. Mech. (2021) 113102, arXiv:2104.14176 [hep-th].
- [2] X. Poncini, J. Rasmussen, *Integrability of planar-algebraic models*, J. Stat. Mech. (2023) 073101, arXiv:2206.14462 [math-ph].

## Submitted manuscripts included in this thesis

Submitted manuscripts included in this thesis are the following:

- [3] X. Poncini, J. Rasmussen, *A classification of integrable planar-algebraic models*, arXiv:2302.11712 [math-ph].

## Other publications during candidature

Other publications completed during the candidature are the following:

- [4] T. Jones, K. Steven, X. Poncini, M. Rose, A. Fedorov, *Approximations in transmon simulation*, Phys. Rev. Appl. **16** (2021) 054039, arXiv:2102.09721 [quant-ph].

## Contributions by others to the thesis

The works on integrability [2,3] were jointly conceptualised with Jørgen Rasmussen. Jørgen Rasmussen also contributed at all stages of the project including the design of the study, the development of the theory, performing calculations and writing the manuscripts [2,3].

The work on causal dynamical triangulations [1] was conceptualised by Bergfinnur Durhuus and Jørgen Rasmussen. Bergfinnur Durhuus, Jørgen Rasmussen and Meltem Ünel contributed at all stages of the project including the design of the study, the development of the theory, performing calculations and writing the manuscript [1].

Jørgen Rasmussen and Jon Links have provided feedback on drafts of this thesis.

## Statement of parts of the thesis submitted to qualify for the award of another degree

No works submitted towards another degree have been included in this thesis.

## **Research involving human or animal subjects**

No animal or human subjects were involved in this research.

## Acknowledgments

First, I would like to thank my adviser Jørgen Rasmussen for your patience, generosity and vision. With your guidance, this journey has been a true joy. I would also like to thank Bergfinnur Durhuus and Meltem Ünel for your invaluable contribution and for being wonderful collaborators.

I am indebted to those who took the time to answer my questions or to offer comments, Jon Links, Eric Ragoucy, Yvan Saint-Aubin, Paul Pearce, Christopher Raymond, Alexi Morin-Duchesne, Bernard Nienhuis, Deniz Stiegemann and Zhengwei Liu; thank you. I would also like to thank UQ for fostering a productive work environment and to LAPTh and QMATH at KU for their hospitality.

To my friends, thank you for lunch and for all of our games. To my family, thank you for your unwavering support and encouragement throughout my academic journey. Finally, to my partner, thank you for being there at every step.

## **Financial support**

This research was supported by an Australian Government Research Training Program Scholarship and by the Australian Research Council under the Discovery Project scheme, project number DP200102316.

## **Keywords**

planar algebras, statistical mechanics, Yang–Baxter integrability, causal dynamical triangulation, quantum field theory

## **Australian and New Zealand Standard Research Classifications (ANZSRC)**

ANZSRC code: 010501 Algebraic Structures in Mathematical Physics, 30%

ANZSRC code: 010502 Integrable Systems (Classical and Quantum), 30%

ANZSRC code: 010505 Mathematical Aspects of Quantum and Conformal Field Theory, Quantum Gravity and String Theory, 10%

ANZSRC code: 010506 Statistical Mechanics, Physical Combinatorics and Mathematical Aspects of Condensed Matter, 30%

## **Fields of Research (FoR) Classification**

FoR code: 0105 Mathematical Physics, 100%

---

# Contents

---

Abstract . . . . .	ii
<b>Contents</b>	<b>viii</b>
<b>1 Introduction</b>	<b>1</b>
1.1 Statistical and quantum mechanics . . . . .	1
1.2 A motivating example . . . . .	5
1.3 Statistical-quantum duality . . . . .	12
1.4 Outline . . . . .	13
<b>2 Planar algebras</b>	<b>17</b>
2.1 Planar algebras . . . . .	17
2.2 Shaded planar algebras . . . . .	20
2.3 Subfactor planar algebras . . . . .	24
2.4 Yang–Baxter relation planar algebras . . . . .	27
2.5 Unshaded planar algebras . . . . .	28
2.6 The affine category of a planar algebra . . . . .	29
<b>3 Integrable models</b>	<b>37</b>
3.1 Transfer operators . . . . .	37
3.2 Baxterisation and integrability . . . . .	41
3.3 Sklyanin’s formulation . . . . .	45
3.4 Hamiltonian limits . . . . .	47
3.5 Hamiltonians and integrals of motion . . . . .	49
3.6 Polynomial integrability . . . . .	50
<b>4 Algebraic integrability</b>	<b>53</b>
4.1 Block Toeplitz . . . . .	53
4.2 Semisimple algebras . . . . .	55
4.3 Spectral degeneracies . . . . .	57
4.4 Cellular algebras . . . . .	58

<b>5 Yang–Baxter relation planar algebras</b>	<b>63</b>
5.1 Temperley–Lieb planar algebra . . . . .	64
5.2 Proto-singly-generated algebra . . . . .	67
5.3 Fuss–Catalan algebra . . . . .	75
5.4 Birman–Wenzl–Murakami algebra . . . . .	79
5.5 Liu algebra . . . . .	83
5.6 Polynomial integrability . . . . .	86
<b>6 Hamiltonians and polynomial integrability</b>	<b>89</b>
6.1 Revisiting the Temperley–Lieb planar algebra . . . . .	89
6.2 Tensor planar algebra: an eight-vertex model . . . . .	102
<b>7 Loop models on causal triangulations</b>	<b>113</b>
7.1 Background . . . . .	113
7.2 Loop models . . . . .	115
7.3 Tree correspondences . . . . .	127
7.4 Tree partition function analysis . . . . .	135
7.5 Critical behaviour of loop models . . . . .	139
7.6 Outlook . . . . .	150
<b>8 Quantum field theory</b>	<b>153</b>
8.1 Conformal nets . . . . .	153
8.2 Semicontinuous models . . . . .	156
<b>9 Conclusion</b>	<b>165</b>
<b>A Appendix</b>	<b>169</b>
A.1 TL algebra Baxterisation . . . . .	169
A.2 FC algebra Baxterisation . . . . .	170
A.3 BMW algebra Baxterisation . . . . .	170
A.4 Liu algebra Baxterisation . . . . .	171
A.5 $TL_n(\delta)$ polynomials . . . . .	172
<b>Bibliography</b>	<b>177</b>



# Chapter 1

---

## Introduction

---

We begin this thesis with a brief review of statistical and quantum mechanics and highlight some analogies between the two formalisms. Turning to an example, we show that these analogies are far deeper than initially presented if the statistical mechanical system possesses the property of *integrability*. Moreover, this example will serve to introduce many objects that will reoccur throughout the thesis including, *transfer operators*, *R-operators*, *Yang–Baxter equations*, *integrals of motion* and *quantum Hamiltonians*. Distilling insights from this case, we present the *statistical-quantum duality* in general and highlight the role played by integrability. We conclude by presenting an outline of the thesis and a summary of the chapters to come.

### 1.1 Statistical and quantum mechanics

#### 1.1.1 Statistical mechanics

In the canonical formulation of *classical mechanics*, a system with  $n$  degrees of freedom consists of a  $2n$ -dimensional manifold  $M$  called the *configuration space* and a differentiable function  $L$  of  $M$ , known as the *Lagrangian* [5]. The space  $M$  is parameterised by generalised positions  $\mathbf{q} = (q_1, \dots, q_n)$  and generalised momenta  $\dot{\mathbf{q}} = (\dot{q}_1, \dots, \dot{q}_n)$  where the ‘dot’ notation indicates a time derivative. The Lagrangian is a function of  $\mathbf{q}$  and  $\dot{\mathbf{q}}$ , specifying the energy contributions to the system and is decomposed as

$$L(\mathbf{q}, \dot{\mathbf{q}}) = T(\mathbf{q}, \dot{\mathbf{q}}) - V(\mathbf{q}, \dot{\mathbf{q}}), \quad (1.1)$$

where  $T$  and  $V$  are the kinetic and potential energies respectively. A *state* of the system is a point in  $M$ , whose time evolution is governed by the *Euler-Lagrange equations*:

$$0 = \frac{\partial L}{\partial \mathbf{q}} - \frac{d}{dt} \left( \frac{\partial L}{\partial \dot{\mathbf{q}}} \right). \quad (1.2)$$

From this simple set of equations, one can derive forces, momenta, torques or any other mechanical property associated with the system.

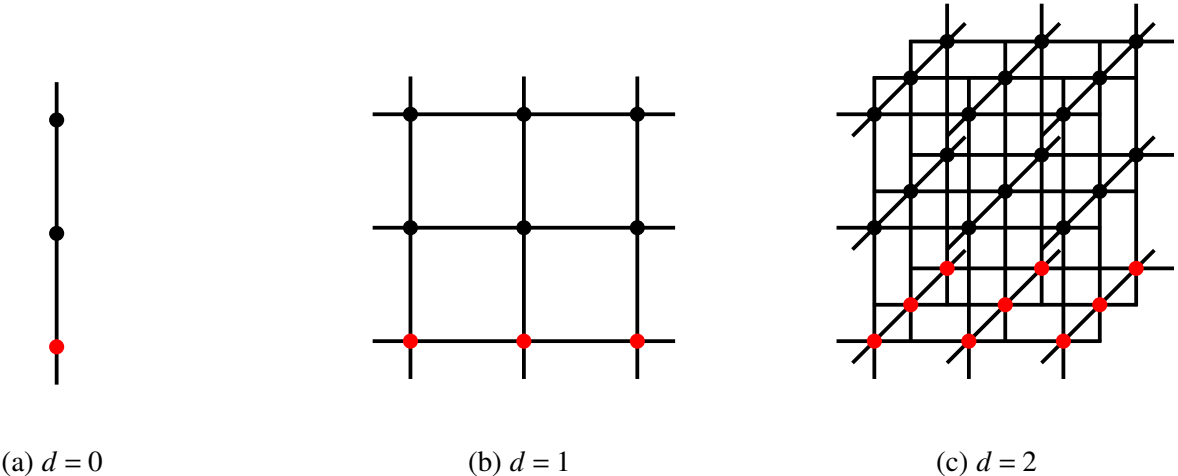


Figure 1.1: A  $\mathbb{Z}^{d+1}$  lattice can be constructed by a sequence of  $\mathbb{Z}^d$  lattices that connect to neighbouring subsystems only, here the first in the sequence is highlighted red.

While the Euler-Lagrange equations can, in principle, describe mechanical systems exactly, practical limitations arise as the number of degrees of freedom becomes large. *Statistical mechanics* provides a powerful framework for analysing systems when solving the Euler-Lagrange equations becomes intractable. Instead of evaluating the positions and momenta of every particle in a system, statistical mechanics treats each particle and their interactions probabilistically, from which one derives macroscopic properties such as energy, pressure and entropy.

All statistical mechanical systems considered here are assumed to be in thermal equilibrium with a bath at temperature  $T$ . With this in hand, the probability of a system occupying a state  $s$  is given by

$$p(s) = \frac{1}{Z} e^{-E(s)/k_B T}, \quad (1.3)$$

where  $E(s)$  is the energy associated with  $s$ ,  $k_B$  is *Boltzmann's constant*, and  $Z$  is a central object in statistical mechanics [6]. The *partition function*  $Z$  is defined such that the sum of all probabilities (1.3) is equal to one, and can therefore be expressed as

$$Z = \sum_{s \in S} e^{-E(s)/k_B T}, \quad (1.4)$$

where  $S$  denotes the set of all states of the system. For each  $s$ , the quantity  $e^{-E(s)/k_B T}$  is referred to as the *Boltzmann weight*. Intuitively, the partition function can be thought of as a measure of the energy content of state space. To illustrate the utility of the partition function, we present here some thermodynamic properties that can be determined from this quantity [6]:

$$F = -k_B T \ln Z, \quad S = \frac{\partial}{\partial T} (k_B T \ln Z), \quad C = T \frac{\partial^2}{\partial T^2} (k_B T \ln Z), \quad (1.5)$$

where  $F$ ,  $S$  and  $C$  are free energy, entropy and heat capacity respectively. To assist in the computation of the partition function, it is often convenient to introduce a *transfer matrix*.

Consider a  $d+1$ -dimensional system that can be decomposed into a sequence of  $d$ -dimensional subsystems, each of which is connected to neighbouring subsystems only, and is spaced uniformly

by a distance denoted by  $\delta\tau$ . For example, the  $\mathbb{Z}^{d+1}$  lattice can be decomposed into a sequence of  $\mathbb{Z}^d$  dimensional lattices where  $\delta\tau = 1$ , see Figure 1.1 illustrating this example for  $d = 0, 1, 2$ . For systems that can be decomposed in this way, we introduce the *transfer matrix*  $\mathcal{T}$  as the algebraic object that *generates* each configuration of a  $d$ -dimensional subsystem and assigns the appropriate Boltzmann weights. By construction, the product of  $m$  transfer matrices generates each  $d+1$ -dimensional configuration consisting of  $m$ ,  $d$ -dimensional subsystems, up to boundary conditions. Accordingly, the partition function can be written as

$$Z_m = \mathbf{v}_0 \cdot \mathcal{T}^m \cdot \mathbf{v}_{m+1}, \quad (1.6)$$

where if  $\mathcal{T}$  is a  $k \times k$  matrix, then  $\mathbf{v}_0$  and  $\mathbf{v}_{m+1}$  are  $1 \times k$  and  $k \times 1$  vectors respectively, which encode the boundary conditions of the system. As a special case of (1.6), the partition function of systems with periodic boundary conditions can typically be expressed as

$$Z_m = \text{tr}(\mathcal{T}^m) = \lambda_1^m + \dots + \lambda_k^m, \quad (1.7)$$

where  $\text{tr}$  denotes the matrix trace and  $\lambda_1, \dots, \lambda_k$  are the eigenvalues of  $\mathcal{T}$ . It is transparent in (1.7) that the eigenvalues of  $\mathcal{T}$  provide a great deal of insight into determining the partition function  $Z_m$ . Moreover, under reasonable physical circumstances, the matrix elements of the transfer operator are strictly positive. In this case, it follows from the Perron–Frobenius theorem [7], that the transfer operator has a unique largest eigenvalue which dominates the behaviour of the partition function as  $m \rightarrow \infty$ . To see this, we express (1.7) as

$$Z_m = \lambda_1^m \left[ 1 + \left( \frac{\lambda_2}{\lambda_1} \right)^m + \dots + \left( \frac{\lambda_k}{\lambda_1} \right)^m \right] \quad (1.8)$$

where  $\lambda_1 > \lambda_i$  for all  $i = 2, \dots, k$ , and observe that the terms inside the square brackets tend to one in the limit  $m \rightarrow \infty$ . We note that the eigenvalues of the transfer matrix are similarly illuminating for arbitrary boundary conditions (1.6), with details depending on the form of  $\mathbf{v}_0$  and  $\mathbf{v}_{m+1}$ .

### 1.1.2 Quantum mechanics

A *Hilbert space*  $\mathcal{H}$  is an inner product space, that is complete with respect to the metric induced by the inner product. *Dirac notation* expresses elements of  $\mathcal{H}$  by  $|\psi\rangle$  and the inner product between two elements by  $\langle\phi|\psi\rangle$ . Define the equivalence relation  $\sim$  on  $\mathcal{H}$  as

$$|\psi\rangle \sim |\phi\rangle \iff |\psi\rangle = \lambda|\phi\rangle, \quad \lambda \in \mathbb{C}^\times. \quad (1.9)$$

A *ray* in  $\mathcal{H}$  is the set of all  $|\psi\rangle \in \mathcal{H}$  related by  $\sim$ . A Hilbert space is *separable* if it admits a basis  $\{|\psi_i\rangle \mid i \in S\}$ , satisfying

$$\langle\psi_i|\psi_j\rangle = \delta_{ij}, \quad \forall i, j \in S, \quad (1.10)$$

where  $\delta_{ij}$  is the *Dirac delta function* and  $S$  is a countable set.

A *quantum mechanical system* consists of a separable Hilbert space  $\mathcal{H}$  and a self-adjoint operator  $H$  that acts on  $\mathcal{H}$ , known as the *Hamiltonian* [8]. Similar to the role of the Lagrangian in classical mechanics, the Hamiltonian defines the energy of the system and is decomposed as

$$H = T + V, \quad (1.11)$$

here  $T, V \in \text{End}(\mathcal{H})$  are the kinetic and potential energy operators respectively. A state of the system is a ray in  $\mathcal{H}$ , whose time evolution is governed by the *Schrödinger equation*

$$i\hbar \frac{d}{dt} |\psi(t)\rangle = H|\psi(t)\rangle, \quad (1.12)$$

where  $\hbar$  is Planck's constant. For a time-independent Hamiltonian, the Schrödinger equation is solved by

$$|\psi(t)\rangle = U(t)|\psi(0)\rangle, \quad U(t) = e^{-itH/\hbar}, \quad (1.13)$$

where  $U(t)$  is a unitary operator that *generates* time-evolution.

Physical quantities such as position and momentum, correspond to self-adjoint operators that act on  $\mathcal{H}$  and are known as *observables*. Measurements of these quantities correspond to *expectation values*. For an observable  $A$  and a state  $|\psi\rangle$ , the corresponding expectation value is given by

$$\langle A \rangle_\psi = \langle \psi | A | \psi \rangle. \quad (1.14)$$

At face value, the differences between classical and quantum systems are stark. Despite these initial appearances, there exist formal analogies between statistical and quantum mechanics, these are discussed in the following section.

### 1.1.3 Analogies

Let  $\mathcal{T}$  denote the transfer matrix for a statistical mechanical system in  $d+1$ -dimensions, and let  $U(t)$  denote the unitary operator generating time translations for a quantum system in  $d$ -dimensions. Similarities between these formalisms arise when considering the roles of  $\mathcal{T}$  and  $U(t)$  in their respective domains – each generates a dimension of sorts. On the quantum side  $U(t)$  generates the time dimension, while on the statistical side,  $\mathcal{T}$  generates a spacial dimension. Taking a ‘quantum’ view of the transfer operator, we can think of this object as the *Euclidean time-evolution operator*

$$\mathcal{T} \text{ “=} e^{-\delta\tau H/k_B T}, \quad (1.15)$$

where  $\delta\tau$  denotes the lattice spacing and  $H$  denotes a  $d$ -dimensional *quantum* Hamiltonian [9]. We use “=” to indicate that the equality should not be taken literally. Contrasting (1.13) and (1.15), we can read off the following analogies:

$$U(t) \leftrightarrow \mathcal{T}^m, \quad it \leftrightarrow m\delta\tau, \quad \hbar \leftrightarrow k_B T, \quad (1.16)$$

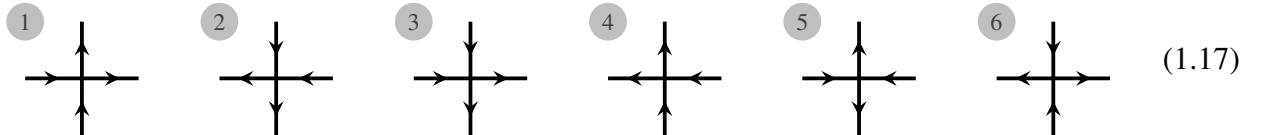
where  $U(t)$  and  $\mathcal{T}^m$  generate time-evolution and imaginary time-evolution respectively, and where  $\hbar$  and  $k_B T$  parameterise quantum and thermal fluctuations respectively [9].

The relation between  $d+1$ -dimensional statistical mechanics and  $d$ -dimensional quantum mechanics discussed here has been purely analogical. As will be demonstrated in the following section, if we endow a statistical mechanical model with *integrability*, the correspondence is far deeper than just a formal analogy. While we have stressed that (1.15) should not be taken literally, integrability implies, at least to linear order, that the equality holds up to an overall factor.

## 1.2 A motivating example

### 1.2.1 Six-vertex model

Let  $\mathcal{S}_{m,n}$  denote the set of all  $m \times n$  square lattices with periodic boundary conditions in both the horizontal and vertical direction, and where each vertex corresponds to one of the following states:

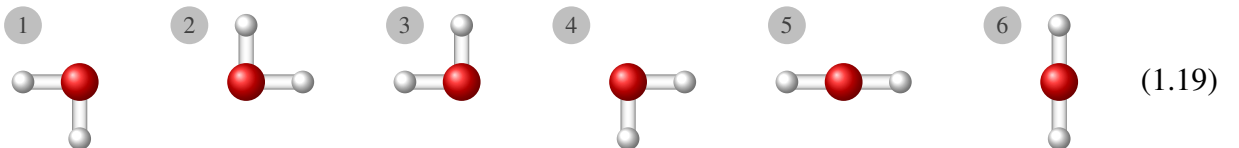


as indicated, each of the above vertices is labelled from one to six. The *six-vertex model* is defined by assigning the energy  $E_k$  to each  $k$ -labelled vertex in a given configuration. For each  $m, n \in \mathbb{N}$ , the partition function of the model is given by

$$Z_{m,n} = \sum_{C \in \mathcal{S}_{m,n}} e^{-E(C)/k_B T}, \quad E(C) = \sum_{k=1}^6 n_k(C) E_k, \quad (1.18)$$

where  $n_k(C)$  denotes the number of  $k$ -labelled vertices in the configuration  $C$ . See Figure 1.2a for an example of a six-vertex model configuration.

Physically, this model can be interpreted as an idealisation of crystalline  $\text{H}_2\text{O}$ , and is often referred to as an *ice-type model*. To see this, we identify each vertex of the lattice with an oxygen atom and each incoming arrow with a hydrogen atom – *covalently bonded* to the oxygen at that site. Reinterpreting the states in (1.17) accordingly, we have:



which are viewed as orientations of a  $\text{H}_2\text{O}$  molecule. Arranging these states on a square lattice, hydrogen-oxygen neighbours that are not bonded covalently represent *hydrogen bonds* between adjacent  $\text{H}_2\text{O}$  molecules, giving rise to the crystalline structure characteristic of ice. See Figure 1.2b for an example of a six-vertex model configuration interpreted as ice. The *ice model* is defined as the following specialisation

$$E_1 = E_2 = E_3 = E_4 = E_5 = E_6 = 0, \quad (1.20)$$

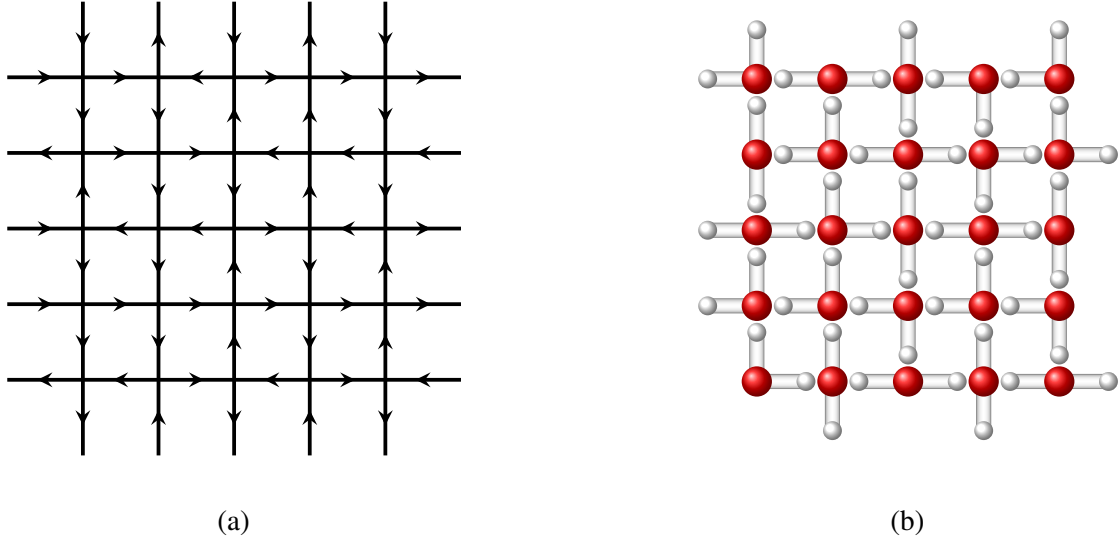


Figure 1.2: An example configuration of the six-vertex model; in (a) the configuration is expressed using the arrow notation of (1.17), while in (b) the configuration is expressed using the molecule notation of (1.19).

where the Boltzmann weight of each state in (1.19) is one, and the corresponding partition function simply counts the number of possible configurations.

Another specialisation of the six-vertex model relevant to our analysis employs the so-called *zero-field* assumption. In the absence of an external electric or magnetic field, which would serve to privilege a given direction, the energy of a configuration remains invariant under the reversal of all arrows. Accordingly, the energies of the zero-field six-vertex model are defined such that

$$E_1 = E_2, \quad E_3 = E_4, \quad E_5 = E_6. \quad (1.21)$$

We will return to this model in Section 1.2.3.

To determine the partition function of the six-vertex model, we introduce the corresponding transfer matrix. By construction, this algebraic object generates each single-row configuration of the model (with periodic boundary conditions in the horizontal direction only) and assigns the appropriate Boltzmann weights. The transfer matrix of the six-vertex model is given by

$$\mathcal{T}_n := \sum_{\substack{\alpha_1, \dots, \alpha_n = \pm \\ a_1, \dots, a_n = \pm \\ b_1, \dots, b_n = \pm}} (R_{\alpha_1 a_1}^{b_1 \alpha_2} R_{\alpha_2 a_2}^{b_2 \alpha_3} \dots R_{\alpha_{n-1} a_{n-1}}^{b_{n-1} \alpha_n} R_{\alpha_n a_n}^{b_n \alpha_1}) e_{a_1}^{b_1} \otimes e_{a_2}^{b_2} \otimes \dots \otimes e_{a_{n-1}}^{b_{n-1}} \otimes e_{a_n}^{b_n}, \quad (1.22)$$

where

$$R_{++}^{++} := e^{-E_1/k_B T}, \quad R_{+-}^{+-} := e^{-E_3/k_B T}, \quad R_{+-}^{+-} := e^{-E_5/k_B T}, \quad (1.23)$$

$$R_{--}^{--} := e^{-E_2/k_B T}, \quad R_{-+}^{+-} := e^{-E_4/k_B T}, \quad R_{-+}^{+-} := e^{-E_6/k_B T}, \quad (1.24)$$

are the Boltzmann weights associated with the model, and

$$e_+^+ := \begin{bmatrix} 1 & 0 \\ 0 & 0 \end{bmatrix}, \quad e_+^- := \begin{bmatrix} 0 & 1 \\ 0 & 0 \end{bmatrix}, \quad e_-^+ := \begin{bmatrix} 0 & 0 \\ 1 & 0 \end{bmatrix}, \quad e_-^- := \begin{bmatrix} 0 & 0 \\ 0 & 1 \end{bmatrix}. \quad (1.25)$$

The transfer matrix can be expressed diagrammatically as

$$\mathcal{T}_n = \sum_{\substack{\alpha_1, \dots, \alpha_n = \pm \\ a_1, \dots, a_n = \pm \\ b_1, \dots, b_n = \pm}} \begin{array}{c} b_1 & b_2 & \dots & b_{n-1} & b_n \\ \alpha_1 & \alpha_2 & \dots & \alpha_{n-1} & \alpha_n \\ \hline a_1 & a_2 & \dots & a_{n-1} & a_n \end{array} , \quad (R_{\alpha a}^{b \beta}) e_{\alpha}^{\beta} \otimes e_a^b = \begin{array}{c} b \\ \alpha \quad \quad \quad \beta \\ \hline a \end{array} . \quad (1.26)$$

The transfer matrix admits an equivalent, arguably neater, description in terms of *R-matrices*. For the six-vertex model, the relevant *R*-matrix is defined

$$\check{R} := R_{++}^{++} e_+^+ \otimes e_+^+ + R_{+-}^{+-} e_+^+ \otimes e_-^- + R_{+-}^{+-} e_+^- \otimes e_+^+ + R_{-+}^{-+} e_-^+ \otimes e_-^- + R_{-+}^{-+} e_-^- \otimes e_+^+ + R_{--}^{--} e_-^- \otimes e_-^-, \quad (1.27)$$

and corresponds to the matrix

$$\check{R} = \begin{bmatrix} R_{++}^{++} & 0 & 0 & 0 \\ 0 & R_{+-}^{+-} & R_{+-}^{+-} & 0 \\ 0 & R_{-+}^{-+} & R_{-+}^{-+} & 0 \\ 0 & 0 & 0 & R_{--}^{--} \end{bmatrix}. \quad (1.28)$$

By definition  $\check{R} \in \text{End}(\mathcal{V} \otimes \mathcal{V})$  where  $\mathcal{V} = \mathbb{C}^2$ . Now consider  $\mathcal{V}_0 \otimes \mathcal{V}_1 \otimes \dots \otimes \mathcal{V}_n$  where  $\mathcal{V}_k = \mathcal{V}$  for all  $k = 0, \dots, n$ , we define  $\check{R}_{ij} \in \text{End}(\mathcal{V}_0 \otimes \dots \otimes \mathcal{V}_n)$  as the operator that acts as  $\check{R}$  on  $\mathcal{V}_i \otimes \mathcal{V}_j$  and as the identity elsewhere. To avoid excess notation, we have not indicated the  $n$  dependence of the operator  $\check{R}_{ij}$ . In places where this may be confusing, we have included a remark. Expressing the transfer operator (1.22) in terms of *R*-matrices, we have

$$\mathcal{T}_n = \text{tr}_0(L_n), \quad L_n := \check{R}_{01} \check{R}_{02} \dots \check{R}_{0n}, \quad (1.29)$$

where  $\mathcal{T}_n \in \text{End}(\mathcal{V}_1 \otimes \dots \otimes \mathcal{V}_n)$  and  $L_n \in \text{End}(\mathcal{V}_0 \otimes \dots \otimes \mathcal{V}_n)$ , and  $\text{tr}_0$  denotes the matrix trace over the tensor factor  $\mathcal{V}_0$ . As in (1.26), the transfer matrix and the *R*-matrix can be expressed diagrammatically as

$$\mathcal{T}_n = \begin{array}{c} 1 & 2 & \dots & n-1 & n \\ \check{R} & \check{R} & \dots & \check{R} & \check{R} \\ \hline 0 & \quad \quad \quad \dots \quad \quad \quad 0 \end{array} , \quad \check{R}_{ij} = \begin{array}{c} i \\ \check{R} \\ \hline j \end{array} , \quad (1.30)$$

where we identify the left- and right-most horizontal edges. In (1.30), we have indicated the factors in  $\mathcal{V}_0 \otimes \dots \otimes \mathcal{V}_n$  where the operators act non-trivially, accordingly, the identification of the left- and right-most horizontal edges implement the trace over  $\mathcal{V}_0$ .

The natural algebraic structure of  $\mathcal{T}_n$  facilitates the construction of  $m$ -row configurations by taking

the product of  $m$  transfer matrices, which can be expressed diagrammatically as

$$\mathcal{T}_n^m = \sum_{\substack{a_{11}, \dots, a_{m+1n} = \pm \\ a_{11}, \dots, a_{mn} = \pm}} \begin{array}{|c|c|c|c|c|c|} \hline a_{m+11} & a_{m+12} & a_{m+13} & a_{m+1n-1} & a_{m+1n} & a_{m1} \\ \hline \alpha_{m1} & \alpha_{m2} & \alpha_{m3} & \dots & \alpha_{mn} & \alpha_{m1} \\ \hline a_{m1} & a_{m2} & a_{mn-1} & a_{mn} & a_{m-1n} & a_{m-11} \\ \hline \alpha_{m-11} & \alpha_{m-12} & \alpha_{m-13} \alpha_{m-1n-1} & \dots & \alpha_{m-1n} & \alpha_{m-11} \\ \hline a_{m-11} & a_{m-12} & a_{m-1n-1} & a_{m-1n} & \dots & a_{31} \\ \hline \vdots & \vdots & \vdots & \vdots & \vdots & \vdots \\ \hline a_{31} & a_{32} & a_{3n-1} & a_{3n} & a_{2n} & a_{21} \\ \hline \alpha_{21} & \alpha_{22} & \alpha_{23} & \dots & \alpha_{2n-1} & \alpha_{21} \\ \hline a_{21} & a_{22} & a_{2n-1} & a_{2n} & a_{1n} & a_{11} \\ \hline \alpha_{11} & \alpha_{12} & \alpha_{13} & \dots & \alpha_{1n-1} & \alpha_{11} \\ \hline a_{11} & a_{12} & a_{1n-1} & a_{1n} & & \\ \hline \end{array} = \begin{array}{ccccccc} \check{R} & & \check{R} & & \dots & \check{R} & \check{R} \\ \check{R} & & \check{R} & & \dots & \check{R} & \check{R} \\ \vdots & & \vdots & & \dots & \vdots & \vdots \\ \check{R} & & \check{R} & & \dots & \check{R} & \check{R} \\ \check{R} & & \check{R} & & \dots & \check{R} & \check{R} \\ \check{R} & & \check{R} & & \dots & \check{R} & \check{R} \end{array} . \quad (1.31)$$

By imposing periodic boundary conditions in the vertical direction, we have

$$Z_{m,n} = \text{tr}(\mathcal{T}_n^m) = \lambda_{n,1}^m + \lambda_{n,2}^m + \dots + \lambda_{n,2^n}^m, \quad (1.32)$$

where  $\text{tr}$  denotes the matrix trace and  $\lambda_{n,1}, \lambda_{n,2}, \dots, \lambda_{n,2^n}$  are the eigenvalues of the transfer matrix  $\mathcal{T}_n$ . As indicated in (1.7) and again in (1.32), the thermodynamic details of the six-vertex model are encoded in the spectrum of the transfer matrix.

## 1.2.2 XXZ model

Following Section 1.1, quantum systems are distinguished from their classical counterparts by occupying states in a Hilbert space. We consider here a two-dimensional Hilbert space  $\mathcal{H} = \mathbb{C}^2$ . The space  $\text{End}(\mathcal{H})$  is spanned by *Pauli matrices*:

$$\mathbb{1} := \begin{bmatrix} 1 & 0 \\ 0 & 1 \end{bmatrix}, \quad \sigma^x := \begin{bmatrix} 0 & 1 \\ 1 & 0 \end{bmatrix}, \quad \sigma^y := \begin{bmatrix} 0 & -i \\ i & 0 \end{bmatrix}, \quad \sigma^z := \begin{bmatrix} 1 & 0 \\ 0 & -1 \end{bmatrix}. \quad (1.33)$$

Accordingly, an arbitrary quantum state  $|\psi\rangle \in \mathcal{H}$  admits a geometric interpretation as a vector in  $\mathbb{R}^3$  with coordinates  $(\langle \sigma^x \rangle_\psi, \langle \sigma^y \rangle_\psi, \langle \sigma^z \rangle_\psi)$ . Define

$$|0\rangle := \begin{bmatrix} 1 \\ 0 \end{bmatrix}, \quad |1\rangle := \begin{bmatrix} 0 \\ 1 \end{bmatrix}, \quad (1.34)$$

which form an orthonormal basis for  $\mathcal{H}$ . An arbitrary quantum state is a ray in  $\mathcal{H}$ , and can therefore be represented by

$$|\psi\rangle = r_0|0\rangle + r_1 e^{i\varphi}|1\rangle, \quad (1.35)$$

where  $r_0, r_1, \varphi \in \mathbb{R}$  satisfy  $r_0^2 + r_1^2 = 1$ . Note that we have conveniently selected the representative to satisfy  $\langle \psi | \psi \rangle = 1$  and have no *global phase*. Parameterising trigonometrically, each quantum state in  $\mathcal{H}$  can be expressed uniquely as

$$|\psi\rangle = \cos(\frac{\theta}{2})|0\rangle + e^{i\varphi} \sin(\frac{\theta}{2})|1\rangle, \quad (1.36)$$

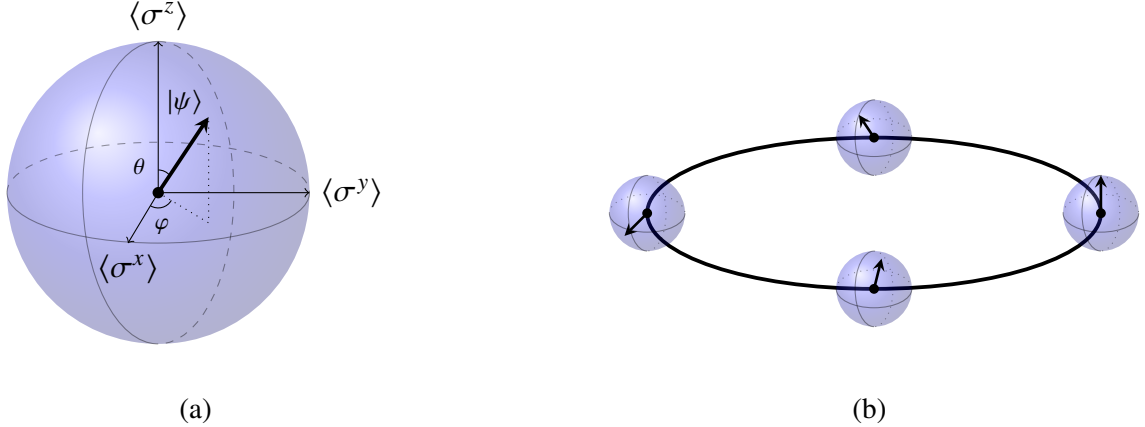


Figure 1.3: In (a) we present an example of a quantum state in  $\mathcal{H}$ . While in (b) we present an example of a quantum state in the four-site XXZ vector space  $\mathcal{H}^{\otimes 4}$ .

where  $\theta \in [0, \pi]$  and  $\varphi \in [0, 2\pi)$ . Computing the coordinates  $(\langle \sigma^x \rangle_\psi, \langle \sigma^y \rangle_\psi, \langle \sigma^z \rangle_\psi)$  of a state parameterised as (1.36), we have

$$\langle \sigma^x \rangle_\psi = \cos(\varphi) \sin(\theta), \quad \langle \sigma^y \rangle_\psi = \sin(\varphi) \sin(\theta), \quad \langle \sigma^z \rangle_\psi = \cos(\theta), \quad (1.37)$$

which corresponds to an angular parameterisation of the unit sphere. It follows that a quantum state in  $\mathcal{H}$  can be represented by a point on the unit sphere, often referred to as the *Bloch sphere* [10]. See Figure 1.3a for an example of a state expressed on the Bloch sphere.

We now consider a one-dimensional *chain* with  $n$  sites, each of which occupies a state in  $\mathcal{H}$ . The *periodic XXZ model* describes the interaction of sites within the chain when equipped with a nearest-neighbour interaction described by the Hamiltonian

$$H_{\text{XXZ}} = -\frac{1}{2} \sum_{i=1}^n (\sigma_i^x \sigma_{i+1}^x + \sigma_i^y \sigma_{i+1}^y + \Delta \sigma_i^z \sigma_{i+1}^z), \quad \sigma_i^p = \mathbb{1}^{\otimes i-1} \otimes \sigma^p \otimes \mathbb{1}^{\otimes n-i}, \quad (1.38)$$

where  $\sigma_{n+1}^p \equiv \sigma_1^p$  and  $\Delta \in \mathbb{R}$ , and we note that  $H_{\text{XXZ}} \in \text{End}(\mathcal{H}^{\otimes n})$ . See Figure 1.3b for an example of an XXZ model configuration. Physically, the XXZ model offers a quantum mechanical treatment of an idealised magnet, consisting of spin- $\frac{1}{2}$  particles dominated by a nearest-neighbour interaction induced by the spin-statistics theorem. This model has been shown to exhibit *ferromagnetism*, a feature absent in classical counterparts.

### 1.2.3 Duality

At face value, the zero-field six-vertex model and the periodic XXZ model appear mathematically and physically distinct. On the one hand, we have a two-dimensional classical statistical mechanical model and on the other, a one-dimensional quantum mechanical model. Despite this, we show that a six-vertex model with the property of *integrability*, is intimately related to the XXZ model.

A statistical mechanical model is considered *integrable* if it is described by a transfer matrix  $\mathcal{T}(u)$  satisfying

$$[\mathcal{T}(u), \mathcal{T}(v)] = 0, \quad \forall u, v \in \Omega, \quad (1.39)$$

where  $\Omega \subseteq \mathbb{C}$  is some suitable domain. Consider a transfer matrix  $\mathcal{T}_n(u)$  of the form (1.30), where the  $u$ -dependence of the  $R$ -matrix is expressed diagrammatically as

$$\mathcal{T}_n(u) = \begin{array}{c} u \\ \text{---} \\ \bullet \\ \text{---} \\ u \end{array} \quad \dots \quad \begin{array}{c} u \\ \text{---} \\ \bullet \\ \text{---} \\ u \end{array} \quad , \quad \check{R}_{ij}(u) = \begin{array}{c} u \\ \text{---} \\ \bullet \\ \text{---} \\ \text{---} \end{array} . \quad (1.40)$$

A model described by  $\mathcal{T}_n(u)$  is integrable if the  $R$ -matrix satisfies the Yang–Baxter equation (YBE) and inversion identity (Inv):

where  $w$  is a function of  $u$  and  $v$ , and  $\bar{u}$  is a function of  $u$ . To illustrate, we use the following diagrammatic manipulations

$$\begin{aligned}
 \mathcal{T}_n(u)\mathcal{T}_n(v) &= \begin{array}{c} \text{Diagram of a grid with nodes } u \text{ and } v \text{ at the top and bottom respectively.} \end{array} \\
 &\stackrel{(\text{Inv})}{=} \begin{array}{c} \text{Diagram showing a crossing between } u \text{ and } v \text{ with labels } w \text{ and } \bar{w}. \end{array} \\
 & \quad \begin{array}{c} \text{Diagram of a grid with nodes } u \text{ and } v \text{ at the top and bottom respectively.} \end{array} \quad (1.42) \\
 &\stackrel{(\text{YBE})}{=} \begin{array}{c} \text{Diagram showing a crossing between } u \text{ and } v \text{ with labels } w \text{ and } \bar{w}. \end{array} \\
 & \quad \begin{array}{c} \text{Diagram of a grid with nodes } u \text{ and } v \text{ at the top and bottom respectively.} \end{array} \\
 & \quad = \begin{array}{c} \text{Diagram showing a crossing between } v \text{ and } u \text{ with labels } \bar{w} \text{ and } w. \end{array} \\
 & \quad \stackrel{(\text{Inv})}{=} \mathcal{T}_n(v)\mathcal{T}_n(u).
 \end{aligned}$$

Let  $u, \lambda \in \mathbb{C}$  and parameterise the zero-field six-vertex model as

$$\check{R}(u) := \begin{bmatrix} a(u) & 0 & 0 & 0 \\ 0 & b(u) & c(u) & 0 \\ 0 & c(u) & b(u) & 0 \\ 0 & 0 & 0 & a(u) \end{bmatrix}, \quad \begin{aligned} a(u) &= \frac{\sinh(\lambda-u)}{\sinh(\lambda)} \\ b(u) &= \frac{\sinh(u)}{\sinh(\lambda)} \\ c(u) &= 1 \end{aligned} \quad (1.43)$$

we observe that this  $R$ -matrix satisfies (1.41), and that the model is integrable [11]. Expanding the transfer matrix in powers of  $u$ , we have

$$\mathcal{T}_n(u) = \sum_{i=0}^{\infty} u^i Q_i, \quad (1.44)$$

where  $Q_i \in \text{End}(\mathcal{V}^{\otimes n})$ . Integrability implies that

$$[\mathcal{T}_n(u), Q_j] = 0, \quad [Q_i, Q_j] = 0, \quad \forall i, j \in \mathbb{N}_0, \quad (1.45)$$

and we refer to each  $Q_i$  as an *integral of motion* of the model. It follows from (1.45) that the transfer matrix and the integrals of motion are closely related – each sharing a common set of eigenvectors.

Following [12], we will make contact with the XXZ model by determining  $Q_0$  and  $Q_1$  of the six-vertex model. To this end, it is convenient to expand the  $R$ -matrix to linear order in  $u$  as

$$\check{R}(u) = \mathcal{P} + u \check{R}^{(\delta)} + \mathcal{O}(u^2), \quad (1.46)$$

where

$$\mathcal{P} := \begin{bmatrix} 1 & 0 & 0 & 0 \\ 0 & 0 & 1 & 0 \\ 0 & 1 & 0 & 0 \\ 0 & 0 & 0 & 1 \end{bmatrix}, \quad \check{R}^{(\delta)} := \begin{bmatrix} -\frac{\cosh(\lambda)}{\sinh(\lambda)} & 0 & 0 & 0 \\ 0 & \frac{1}{\sinh(\lambda)} & 0 & 0 \\ 0 & 0 & \frac{1}{\sinh(\lambda)} & 0 \\ 0 & 0 & 0 & -\frac{\cosh(\lambda)}{\sinh(\lambda)} \end{bmatrix}. \quad (1.47)$$

Note that  $\mathcal{P}$  and  $\check{R}^{(\delta)}$  satisfy

$$\mathcal{P}^2 = \mathbb{1}^{\otimes 2}, \quad \check{R}_{0j}^{(\delta)} \mathcal{P}_{0j+1} = \mathcal{P}_{0j} \mathcal{P}_{0j+1} \mathcal{P}_{j,j+1} \check{R}_{j,j+1}^{(\delta)}, \quad [\check{R}_{j,j+1}^{(\delta)}, \mathcal{P}_{0k}] = 0, \quad \forall k < j, j+1 < k. \quad (1.48)$$

Expanding the  $L_n$  operator in (1.29) to linear order in  $u$ , we have

$$L_n = \prod_{i=1}^n (\mathcal{P}_{0i} + u \check{R}_{0i}^{(\delta)}) + \mathcal{O}(u^2) = \prod_{i=1}^n \mathcal{P}_{0i} + u \sum_{j=1}^n \left( \prod_{i=1}^{j-1} \mathcal{P}_{0i} \right) \check{R}_{0j}^{(\delta)} \left( \prod_{i=j+1}^n \mathcal{P}_{0i} \right) + \mathcal{O}(u^2). \quad (1.49)$$

**Remark.** Here and elsewhere we use left-to-right ordering of products i.e.  $\prod_{i=1}^n x_i \equiv x_1 x_2 \dots x_n$ .

Applying the relations (1.48), we have

$$\begin{aligned} L_n &= \prod_{i=1}^n \mathcal{P}_{0i} \left( \mathbb{1}^{\otimes(n+1)} + u \mathcal{P}_{0n} \check{R}_{0n}^{(\delta)} \right) + u \sum_{j=1}^{n-1} \left( \prod_{i=1}^{j+1} \mathcal{P}_{0i} \right) \mathcal{P}_{j,j+1} \check{R}_{j,j+1}^{(\delta)} \left( \prod_{i=j+2}^n \mathcal{P}_{0i} \right) + \mathcal{O}(u^2) \\ &= \left( \prod_{i=1}^n \mathcal{P}_{0i} \right) \left( \mathbb{1}^{\otimes(n+1)} + u R_{0n}^{(\delta)} + u \sum_{j=1}^{n-1} R_{j,j+1}^{(\delta)} \right) + \mathcal{O}(u^2) \end{aligned} \quad (1.50)$$

where we have introduced  $R^{(\delta)} := \mathcal{P} \check{R}^{(\delta)}$ . Tracing over the zeroth tensor factor, we have

$$\begin{aligned} \mathcal{T}_n(u) &= \text{tr}_0 \left( \left( \prod_{i=1}^n \mathcal{P}_{0i} \right) \left( \mathbb{1}^{\otimes(n+1)} + u R_{0n}^{(\delta)} + u \sum_{j=1}^{n-1} R_{j,j+1}^{(\delta)} \right) \right) + \mathcal{O}(u^2) \\ &= \text{tr}_0 \left( \left( \prod_{i=1}^n \mathcal{P}_{0i} \right) \right) \left( \mathbb{1}^{\otimes n} + u \sum_{j=1}^{n-1} R_{j,j+1}^{(\delta)} \right) + u \text{tr}_0 \left( \left( \prod_{i=1}^n \mathcal{P}_{0i} \right) R_{0n}^{(\delta)} \right) + \mathcal{O}(u^2) \end{aligned} \quad (1.51)$$

and note the relations

$$\text{tr}_0 \left( \left( \prod_{i=1}^n \mathcal{P}_{0i} \right) \right) = \tau_n, \quad \text{tr}_0 \left( \left( \prod_{i=1}^n \mathcal{P}_{0i} \right) R_{0n}^{(\delta)} \right) = \tau_n R_{n1}^{(\delta)}, \quad \tau_n := \prod_{i=1}^n \mathcal{P}_{n-i, n+1-i}. \quad (1.52)$$

**Remark.** We highlight that in equations (1.51) and (1.52), operators within the partial trace operation act on  $\mathcal{V}^{\otimes(n+1)}$ , while the operators outside the partial trace operation act on  $\mathcal{V}^{\otimes n}$ .

Applying (1.52) to the transfer matrix, we have

$$\mathcal{T}_n(u) = \tau_n \left( \mathbb{1}^{\otimes(n+1)} + u \sum_{j=1}^n R_{j,j+1}^{(\delta)} \right) + \mathcal{O}(u^2), \quad R_{nn+1} \equiv R_{n1}, \quad (1.53)$$

and read off the first two integrals of motion as

$$Q_0 = \tau_n, \quad Q_1 = \tau_n \sum_{j=1}^n R_{j,j+1}^{(\delta)}. \quad (1.54)$$

Expressing  $R_{j,j+1}^{(\delta)}$  in terms of Pauli matrices, we have

$$R_{j,j+1}^{(\delta)} = -\frac{1}{2} \cosh(\lambda) \mathbb{1}^{\otimes n} + \frac{1}{2} \left( \sigma_j^x \sigma_{j+1}^x + \sigma_j^y \sigma_{j+1}^y - \cosh(\lambda) \sigma_j^z \sigma_{j+1}^z \right) + \mathcal{O}(u^2), \quad (1.55)$$

and we recognise the appearance of the XXZ model in  $Q_1$

$$Q_1 = -\tau_n \left( \frac{n}{2} \cosh(\lambda) \mathbb{1}^{\otimes n} + H_{XXZ} \right), \quad \Delta = -\cosh(\lambda). \quad (1.56)$$

It immediately follows from (1.45) that  $[\mathcal{T}_n(u), \tau_n] = 0$  and

$$[\mathcal{T}_n(u), H_{XXZ}] = 0. \quad (1.57)$$

Consequently, the transfer matrix of a zero-field six-vertex model and the Hamiltonian of the XXZ model share a common set of eigenvectors! This is a remarkable result. From a practical perspective, a solution to one of the models can be immediately passed to the other via the ‘duality’ (1.57). In fact, this approach was the first to yield a solution to the XXZ model, where the initial breakthrough was achieved via an application of the algebraic Bethe ansatz to the six-vertex model [11].

### 1.3 Statistical-quantum duality

Taking lessons from the six-vertex and XXZ example, we proceed by stating the *statistical-quantum duality* in a general setting. Let  $\mathcal{T}$  denote the transfer matrix describing a  $d+1$ -dimensional statistical mechanical system, and let  $\mathcal{V}$  denote the vector space acted on by  $\mathcal{T}$ . Let  $\mathcal{H}$  denote the Hilbert space of a quantum system described by a Hamiltonian  $H$ . These two systems are dual if  $\mathcal{V}$  can be viewed as a Hilbert space such that  $\mathcal{V} = \mathcal{H}$ , and if the transfer operator and Hamiltonian satisfy

$$[\mathcal{T}, H] = 0. \quad (1.58)$$

As illustrated in Section 1.2, the integrability of a statistical mechanical model described by  $\mathcal{T}(u)$  naturally gives rise to a statistical-quantum duality (1.58), provided that  $\mathcal{V}$  is a Hilbert space. For an arbitrarily parameterised transfer matrix  $\mathcal{T}(u)$ , we demonstrate how to determine a countable set of dual Hamiltonians. Let  $\mathcal{B}$  denote a basis for  $\text{End}(\mathcal{V})$ , expressing the transfer matrix in terms of elements in the basis  $\mathcal{B}$ , we have

$$\mathcal{T}(u) = \sum_{a \in \mathcal{B}} t_a(u) a, \quad (1.59)$$

where  $t_a : \Omega \rightarrow \mathbb{C}$  for each  $a \in \mathcal{B}$ . Define the space of scalar functions

$$\mathcal{F} := \text{span}_{\mathbb{C}} \{ t_a : \Omega \rightarrow \mathbb{C} \mid a \in \mathcal{B} \} \quad (1.60)$$

and denote by  $\mathcal{B}_{\mathcal{T}}$  a basis for  $\mathcal{F}$ . Determining the dual Hamiltonians associated with  $\mathcal{T}(u)$ , it is convenient to express the transfer matrix in terms of elements from the basis  $\mathcal{B}_{\mathcal{T}}$

$$\mathcal{T}(u) = \sum_{f \in \mathcal{B}_{\mathcal{T}}} f(u) Q_f, \quad (1.61)$$

where  $Q_f \in \text{End}(\mathcal{V})$  for each  $f \in \mathcal{B}_{\mathcal{T}}$ . The integrability of the model implies that

$$[\mathcal{T}(u), Q_f] = 0, \quad [Q_f, Q_g] = 0, \quad \forall f, g \in \mathcal{B}_{\mathcal{T}}. \quad (1.62)$$

It follows from (1.62) that any Hamiltonian defined as a multi-variate function of elements in  $\{Q_f \mid f \in \mathcal{B}_{\mathcal{T}}\}$ , is dual to the statistical mechanical system described by  $\mathcal{T}(u)$ . We return to the analysis (1.59)–(1.62) in a general setting in Chapter 3.

## 1.4 Outline

This thesis describes two-dimensional statistical mechanical models in a *planar-algebraic* setting. We develop a framework, centred around the *transfer operator* (which takes the role of the transfer matrix) but is not necessarily a matrix, instead it is an element of a so-called *planar algebra*. Planar algebras were developed by Vaughan Jones to study inclusions of *von Neumann algebras* [13], but have found applications ranging from knot theory [14–16] to various areas of mathematical physics [17–20]. Intuitively, planar algebras describe the ‘multiplication’ of vectors in the plane and therefore are natural objects to describe two-dimensional statistical mechanical systems. While we are not the first to observe the utility of planar algebras to describe statistical mechanical systems [13, 17], nor are we the first to express the transfer operator as an element of a planar algebra [21]; the novelty in this thesis owes to the generality of the framework, which can be summarised in the following: to each planar algebra, we assign a model on the strip and a model on the cylinder. We refer to these as *planar-algebraic models*.

Within this framework, we develop sufficient conditions that imply that a planar-algebraic model is integrable, which generalises and translates the Yang–Baxter equation and inversion identities introduced in Section 1.2 to the planar-algebraic setting. We present an algebraic characterisation of integrals of motion of a planar-algebraic model and consider algebraic relations among them. For a general class of planar algebras, we identify when each integral of motion arising from the transfer operator is algebraically related to a single element of the planar algebra. In this case, we can express the transfer operator as a polynomial in a single algebraic element, suggesting that, in some instances, (1.15) may be taken literally. We also highlight that the planar-algebraic framework recovers the standard formulation of transfer operators as matrices by specialising to the tensor planar algebra.

Stepping back, we present three motivations for studying planar-algebraic models. The first and most straightforward is that planar algebras offer an inherently two-dimensional setting to describe models native to the plane. The second is that the planar-algebraic framework is more general than the standard matrix formalism. To see this, observe that planar-algebraic models can only be described in

the standard formalism via a representation, which is typically unable to capture the structure of the underlying planar algebra. On the other hand, each model in the standard formalism is expressible as a planar-algebraic model by specialising to the tensor planar algebra. Finally, planar-algebraic models offer new perspectives on statistical mechanical systems, in particular, by suggesting new integrable models and connections to other areas of mathematics.

To conclude this section, we present an overview of the upcoming chapters. Chapter 2 serves to introduce many of the planar-algebraic objects used throughout the thesis. We begin by defining *shaded* and *unshaded* planar algebras. Imposing additional structure on shaded planar algebras, we introduce *subfactor*, *singly generated* and *Yang–Baxter relation* planar algebras. Using [22], we show that shaded planar algebras consistent with our Yang–Baxter integrability framework necessarily admit an unshaded description. We conclude by presenting planar algebras in a categorical setting.

In Chapter 3, we develop the planar-algebraic framework. We begin by defining  $R$ - and  $K$ -operators from which we construct a transfer operator on the strip and a transfer operator on the cylinder. For each of these transfer operators, we develop a finite set of relations, including generalised Yang–Baxter equations, that serve as sufficient conditions for integrability. A planar-algebraic model satisfying these sufficient conditions is referred to as *Yang–Baxter integrable*. Integrals of motion of each model are determined by identifying *identity points*, about which a power series expansion of the transfer operator is performed. We refer to the linear order term in this expansion as the *principal Hamiltonian* of the model. We conclude this chapter with an algebraic characterisation of the integrals of motion and quantum Hamiltonians associated with a planar-algebraic model and introduce the notion of *polynomial integrability*.

Chapter 4 develops the groundwork to establish algebraic relations among integrals of motion arising from the transfer operator of an integrable planar-algebraic model. Specifically, we identify necessary and sufficient conditions for a parameter-dependent matrix to be expressible in terms of a polynomial in a parameter-independent matrix. This result is then extended to parameter-dependent elements of a semisimple algebra. We also review *cellular algebras* and establish results relevant to the spectral analysis of planar-algebraic models.

In Chapter 5, we apply the planar-algebraic framework to show that a singly generated planar algebra underlies a Yang–Baxter integrable model if and only if it is a Yang–Baxter relation planar algebra. According to a result by Liu, there are three singly generated Yang–Baxter relation planar algebras: the well-known Fuss–Catalan and Birman–Wenzl–Murakami planar algebras, in addition to a new planar algebra, that we refer to as the Liu planar algebra. The Fuss–Catalan and Birman–Wenzl–Murakami planar algebras have long been known to admit integrable models, which we review and place within our framework. While, to the best of our knowledge, no such model has been introduced for the Liu planar algebra. We address this absence by constructing an integrable model from the Liu planar algebra, which fits naturally within our framework. We conclude this chapter by showing that all of the singly generated Yang–Baxter relation planar algebras encoding Yang–Baxter integrable models on the strip are polynomially integrable, that is, the transfer operator is expressible in terms of a polynomial in a single Hamiltonian.

In Chapter 6, we focus on an eight-vertex model and a model with an underlying Temperley–Lieb planar-algebraic structure, both defined on the strip. In each case, we determine the principal Hamiltonians of the model and establish conditions for which the model is polynomially integrable. For the eight-vertex model, we find that it is polynomially integrable for all  $n \in \mathbb{N}$ , while for the Temperley–Lieb model, we show that it is polynomially integrable for all but finitely many  $\delta \in \mathbb{C}$  and all  $n \leq 17$ . For both models, we find that the transfer operator can be expressible as a polynomial in the corresponding principal Hamiltonian, and we determine these polynomials explicitly in each case.

Chapter 7 is distinct from the preceding chapters in two main ways: (i) we consider models defined on *causal triangulations*, and (ii) our primary interest is the critical behaviour of the model, not whether it is integrable. We introduce a dense and a dilute loop model on causal triangulations and describe each model by a transfer operator different from those introduced in Chapter 3. We show that the dense loop model can be mapped to a planar tree model, which can be solved exactly to determine the critical behaviour. The dilute loop model can similarly be mapped to a planar tree model, albeit one that cannot be solved exactly using the methods employed in the dense case. Instead, we develop transfer operator techniques to determine the critical behaviour of the dilute loop model, which we show to be distinct from the dense loop model.

In Chapter 8, we extend the scope of planar-algebraic models beyond statistical mechanics by showing how such models relate to quantum field theories (QFTs). After defining the relevant class of QFTs, we introduce Jones’ semicontinuous models as ‘almost’ examples of this class and detail some recent efforts to endow these models with the properties of actual examples. Within semicontinuous models, we outline the relevance of the planar-algebraic framework and highlight the central role played by the single-row transfer operator.

We conclude in Chapter 9, by summarising the main results and by offering some directions for future study. The Appendix consists of technical details deferred from Chapter 5 and Chapter 6.

Components of the following publications have been incorporated into Chapter 2.

- [2] X. Poncini, J. Rasmussen, *Integrability of planar-algebraic models*, J. Stat. Mech. (2023) 073101, arXiv:2206.14462 [math-ph].
- [3] X. Poncini, J. Rasmussen, *A classification of integrable planar-algebraic models*, arXiv:2302.11712 [math-ph].

# Chapter 2

---

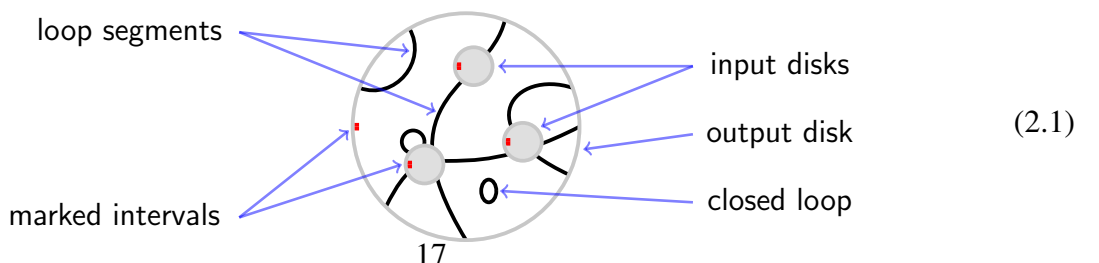
## Planar algebras

---

In this chapter, we introduce planar algebras and define much of the planar-algebraic machinery used in subsequent chapters. We begin by defining planar algebras and their shaded incarnation. We follow up by constructing planar-algebraic versions of familiar linear-algebraic operations such as multiplications, traces and inner products. By imposing additional structure on shaded planar algebras, we introduce *subfactor planar algebras* as a planar-algebraic version of a  $C^*$ -algebra, and present *singly generated* and *Yang–Baxter relation* variants of these. We show that singly generated planar algebras relevant to our integrability framework (introduced later in Chapter 3) must admit an *unshaded* description. We conclude by presenting planar algebras in a categorical setting that will be convenient for describing models on the cylinder.

### 2.1 Planar algebras

Informally, an (*unshaded*) *planar algebra* is a collection of vector spaces  $(P_n)_{n \in \mathbb{N}_0}$  whose elements can be combined in the plane such that the resulting object is identified as an element of a given  $P_k$  for the appropriate  $k \in \mathbb{N}_0$ . A basis for  $P_n$  consists of a set of disks whose boundary is decorated by  $n$  connection points or *nodes* and a marked interval, basis vectors are distinguished by some internal structure specific to the particular planar algebra. Vectors are combined in the plane by connecting each available node to a single non-intersecting loop segment defined up to ambient isotopy, that is, the loop segments can be bent or stretched without affecting the result but cannot be cut or made to intersect. *Planar tangles* are the diagrammatic objects that facilitate the combination of vectors, for example:



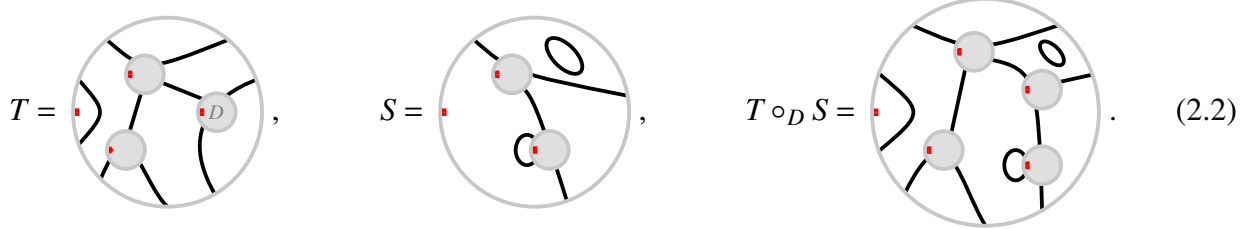
**Definition 2.1.1.** An (unshaded) planar tangle  $T$  consists of the following components in  $\mathbb{R}^2$ :

- A disk  $D_0^T$ , called the output disk.
- A finite set of non-overlapping disks  $\mathcal{D}_T$  in the interior of  $D_0^T$ , called input disk(s).
- A finite number of non-intersecting loop segments within the output disk and outside of the input disk(s), connecting pair-wise, distinct points on the boundary of the disks in  $\{D_0^T\} \cup \mathcal{D}_T$  called nodes, or closing on themselves forming loops. Denote by  $\eta(D)$  the number of nodes on the boundary of  $D \in \{D_0^T\} \cup \mathcal{D}_T$ . The boundary of each disk is thus composed of nodes and boundary intervals: the open intervals between the nodes or if there are no nodes, a whole circle.
- For each disk in  $\{D_0^T\} \cup \mathcal{D}_T$ , a choice of boundary interval, here marked graphically by a red rectangle.

Each planar tangle  $T$  is defined up to ambient isotopy of  $D_0^T \subset \mathbb{R}^2$ .

**Remark.** One can consider variants of planar algebras by equipping the planar tangles with additional structure, for example, by assigning each loop segment a label. After introducing the simplest version here, Section 2.2 is devoted to so-called *shaded planar algebras*.

There exists a natural product structure among planar tangles known as *glueing* or composition. Consider two planar tangles  $T$  and  $S$ , we say  $S$  is  *$D$ -compatible* with  $T$  if  $D \in \mathcal{D}_T$  satisfies  $\eta(D) = \eta(D_0^S)$ , in this case, it is possible to deform  $S$  so that it takes the place of  $D$  in such a way that the nodes and marking of both are aligned. The image of the product, denoted by  $T \circ_D S$ , is identified as a planar tangle by replacing  $D$  with  $S$  and by removing both the output disk and associated marking of  $S$ . If  $S$  is not  $D$ -compatible, then  $T \circ_D S = 0$ . To illustrate, the following quadratic tangle  $S$  can be glued inside the cubic tangle  $T$ :



**Definition 2.1.2.** The set of planar tangles endowed with compositions is called the *planar operad*.

Planar tangles also act naturally as multilinear maps on the vector spaces  $(P_n)_{n \in \mathbb{N}_0}$ . To each planar tangle, we associate the linear  $|\mathcal{D}_T|$ -ary operator

$$\mathsf{P}_T: \bigotimes_{D \in \mathcal{D}_T} P_{\eta(D)} \rightarrow P_{\eta(D_0^T)}, \quad (2.3)$$

where we note that for  $\mathcal{D}_T = \emptyset$  there is no domain, in which case  $\mathsf{P}_T$  is a 0-ary operator (or nullary) and we denote its image by  $\mathsf{P}_T()$ . The action of  $\mathsf{P}_T$  is similar to the composition of tangles but at the

level of vectors. Each input disk  $D$  of  $T$  is replaced with elements of the vector space  $P_{\eta(D)}$  in such a way that the nodes and the marking of both are aligned, for example:

$$T = \text{Diagram of } T \text{ with nodes labeled 1, 2, 3 and 0, and red dots at the boundary.}, \quad P_T(v_1, v_2, v_3) = \text{Diagram of } T \text{ with nodes labeled } v_1, v_2, v_3 \text{ and 0, and red dots at the boundary.} \in P_8. \quad (2.4)$$

The markings of the input disks are then removed and the resulting vector is identified in  $P_{\eta(D_0^T)}$ .

**Remark.** Unlike in the picture of  $T$  in (2.4), disks in  $\mathcal{D}_T$  are not labelled; however, to apply the ordered-list notation for the vectors in  $P_T(v_1, v_2, v_3)$ , it is convenient to label the disks accordingly. Once drawn as in the second picture in (2.4), no labelling is needed.

The identification of an appropriate output vector depends on the specific action of the planar tangles as linear maps, which is specified when defining a particular planar algebra. To illustrate, consider a planar algebra whose vector spaces  $(P_{2n})_{n \in \mathbb{N}_0}$  are spanned by planar tangles with zero input disks, and take the action of the planar tangles to be the composition of tangles. Revisiting (2.4) with a particular set of input vectors, we identify the image of  $P_T$  in  $P_8$  as

$$P_T(\text{Diagram 1}, \text{Diagram 2}, \text{Diagram 3}) = \text{Diagram of } T \text{ with nodes labeled 0 and red dots at the boundary.} = \text{Diagram of } T \text{ with nodes labeled 0 and red dots at the boundary.} = \text{Diagram of } T \text{ with nodes labeled 0 and red dots at the boundary.} \quad (2.5)$$

Having defined both the action of planar tangles on themselves and on arbitrary vector spaces, we now consider their interaction. A basic requirement is that these actions are consistent, that is, for any tangle  $S$  that is  $D$ -compatible with  $T$ , we have

$$P_{T \circ_D S} = P_T \circ_D P_S, \quad (2.6)$$

where the right-hand side is defined concretely after (2.7). The condition (2.6) is known as *naturality* and is much akin to a homomorphism property among planar tangles and their associated linear maps. To specify the action of the right-hand side, we introduce

$$g : \left( \bigtimes_{d \in \mathcal{D}_S} P_{\eta(d)} \right) \times \left( \bigtimes_{d \in \mathcal{D}_T \setminus \{D\}} P_{\eta(d)} \right) \rightarrow P_{\eta(D)} \times \left( \bigtimes_{d \in \mathcal{D}_T \setminus \{D\}} P_{\eta(d)} \right), \quad (x, y) \mapsto (P_S(x), y). \quad (2.7)$$

We can now write the right-hand side as  $P_{T \circ_D S} := P_T \circ g$ , where here  $\circ$  denotes standard function composition, and the domain of  $P_T$  is ordered such that the input  $D$  is first, followed by the inputs  $\mathcal{D}_T \setminus \{D\}$ . To illustrate, suppose that the domain of  $P_{T \circ_D S}$  is ordered such that all of the  $\mathcal{D}_S$  inputs come first and are denoted by  $v_S$ , followed by the  $\mathcal{D}_T \setminus \{D\}$  inputs denoted by  $v_{T'}$ . For  $\mathcal{D}_S, \mathcal{D}_T \setminus \{D\} \neq \emptyset$ , we can express the naturality condition as

$$P_{T \circ_D S}(v_S, v_{T'}) = P_T(P_S(v_S), v_{T'}). \quad (2.8)$$

We also list the exceptional cases

$$\mathsf{P}_{T \circ D S}(v_S) = \mathsf{P}_T(\mathsf{P}_S(v_S)), \quad \mathcal{D}_S \neq \emptyset, \quad \mathcal{D}_T \setminus \{D\} = \emptyset \quad (2.9)$$

$$\mathsf{P}_{T \circ D S}(v_{T'}) = \mathsf{P}_T(\mathsf{P}_S(), v_{T'}), \quad \mathcal{D}_S = \emptyset, \quad \mathcal{D}_T \setminus \{D\} \neq \emptyset \quad (2.10)$$

$$\mathsf{P}_{T \circ D S}() = \mathsf{P}_T(\mathsf{P}_S()), \quad \mathcal{D}_S, \quad \mathcal{D}_T \setminus \{D\} = \emptyset \quad (2.11)$$

which, together with (2.8), must hold for all  $v_S \in \bigtimes_{d \in \mathcal{D}_S} P_{\eta(d)}$  and  $v_{T'} \in \bigtimes_{d \in \mathcal{D}_{T'} \setminus \{D\}} P_{\eta(d)}$ , and all tangles  $T$  and  $S$ .

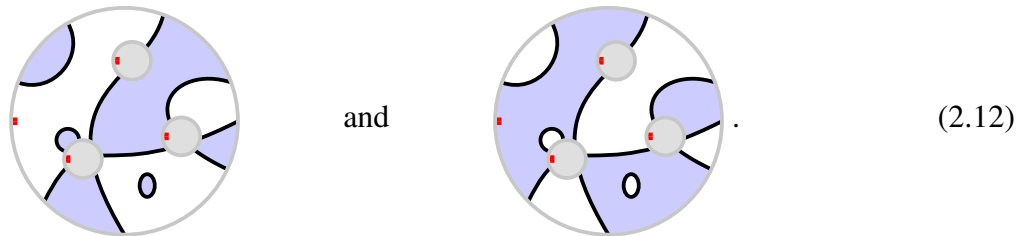
We now give a precise definition of planar algebras.

**Definition 2.1.3.** *A planar algebra is a collection of complex vector spaces  $(P_n)_{n \in \mathbb{N}_0}$ , together with the action of each element of the planar operad as a multilinear map, such that naturality is satisfied.*

In the following section, we describe a type of planar algebra whose planar tangles (and consequently vector spaces) are equipped with additional structure.

## 2.2 Shaded planar algebras

Shaded planar algebras are a simple variant of planar algebras where the planar tangles possess a ‘checker-board’ shading. A planar tangle is *shaded* if each region (excluding the interior of input disks) is one of two colours, such that two regions separated by a single loop segment do not possess the same colour. For a planar tangle to admit a shading, the output disk and each input disk must have an even number of connection points. Each planar tangle admitting a shading can be shaded in exactly two ways, for example:



Accordingly, each disk in a *shaded planar tangle* carries *both* node information *and* shading information. As for planar tangles in Definition 2.1.1, we denote the output disk of the shaded planar tangle  $T$  by  $D_0^T$  and the set of input disks by  $\mathcal{D}_T$ . The number of nodes on the (exterior) boundary of  $D \in \{D_0^T\} \cup \mathcal{D}_T$  is denoted by  $\eta(D)$  and is even, while the *shading* of  $D$  is denoted by  $\zeta(D)$  and is  $+$ , respectively  $-$ , if the (exterior) marked boundary interval corresponds to a white, respectively blue, region.

Composition among shaded planar tangles works much in the same way as for planar tangles. Let  $T$  and  $S$  be shaded planar tangles and suppose there exists  $D \in \mathcal{D}_T$  satisfying  $\eta(D) = \eta(D_0^S)$  and  $\zeta(D) = \zeta(D_0^S)$ . It is then possible to isotopically deform  $S$  such that it can take the place of  $D$ , as

illustrated by

$$T = \text{Diagram } T, \quad S = \text{Diagram } S, \quad T \circ_D S = \text{Diagram } T \circ_D S. \quad (2.13)$$

**Definition 2.2.1.** *The set of shaded planar tangles endowed with compositions is called the shaded planar operad.*

To accommodate the presence of shading, the relevant collection of vector spaces is  $(A_{n,\varepsilon})_{n \in \mathbb{N}_0}^{\varepsilon \in \{+,-\}}$  which is commonly abbreviated as  $(A_{n,\pm})_{n \in \mathbb{N}_0}$ . A basis for  $A_{n,\pm}$  consists of disks with  $2n$  nodes (connection points) on their boundary, whereby a boundary is composed of nodes and boundary intervals, and the boundary intervals are labelled alternately by + or -. Shaded planar tangles act naturally as multilinear maps on the vector spaces  $(A_{n,\pm})_{n \in \mathbb{N}_0}$ . To each shaded planar tangle  $T$ , we associate the linear  $|\mathcal{D}_T|$ -ary operator

$$P_T: \bigotimes_{D \in \mathcal{D}_T} A_{\eta(D)/2, \zeta(D)} \rightarrow A_{\eta(D_0^T)/2, \zeta(D_0^T)}, \quad (2.14)$$

where for  $\mathcal{D}_T = \emptyset$ , we denote the image by  $P_T()$ . The action of  $P_T$  is similar to the unshaded case, each input disk  $D$  of  $T$  is replaced with elements of the vector space  $A_{\eta(D)/2, \zeta(D)}$  in such a way that the nodes, the shading, and the marking of both are aligned, for example:

$$T = \text{Diagram } T, \quad P_T(v_1, v_2, v_3) = \text{Diagram } P_T(v_1, v_2, v_3) \in P_8. \quad (2.15)$$

The markings of the input disks are then removed and the resulting vector is identified in  $A_{\eta(D_0^T)/2, \zeta(D_0^T)}$ .

Naturality for shaded planar tangles can be stated as in (2.8) as

$$P_{T \circ_D S}(v_S, v_{T'}) = P_T(P_S(v_S), v_{T'}), \quad (2.16)$$

where  $v_S \in \bigotimes_{d \in \mathcal{D}_S} A_{\eta(d)/2, \zeta(d)}$  and  $v_{T'} \in \bigotimes_{d \in \mathcal{D}_{T'} \setminus \{D\}} A_{\eta(d)/2, \zeta(d)}$ . For the exceptional cases, translate (2.9)–(2.11) accordingly.

We now give a precise definition of shaded planar algebras.

**Definition 2.2.2.** *A shaded planar algebra is a collection of complex vector spaces  $(A_{n,\pm})_{n \in \mathbb{N}_0}$ , together with the action of each element of the shaded planar operad as a multilinear map, such that naturality is satisfied.*

The naturality condition is quite restrictive, it allows us, under very mild conditions, to determine the action of some of the shaded planar tangles. For each  $n \in \mathbb{N}_0$ , the *identity tangles* are defined

$$\text{id}_{n,+} := \text{Diagram of a shaded disk with 2n spokes and a central dot, shading on the left half-plane}, \quad \text{id}_{n,-} := \text{Diagram of a shaded disk with 2n spokes and a central dot, shading on the right half-plane}, \quad P_{\text{id}_{n,\pm}} : A_{n,\pm} \rightarrow A_{n,\pm}, \quad (2.17)$$

each having  $2n$  ‘spokes’. We say that a nonzero  $v \in A_{n,\pm}$  is a *null vector* if  $P_T(v) = 0$  for every shaded planar tangle  $T$  for which  $P_T$  has domain  $A_{n,\pm}$ . With that, we have the following result.

**Proposition 2.2.3.** *If  $A_{n,\pm}$  has no null vectors, then  $P_{\text{id}_{n,\pm}}$  is the identity operator.*

*Proof.* Let  $v \in A_{n,\pm}$  and  $T$  be a shaded planar tangle for which  $P_T$  has domain  $A_{n,\pm}$ . By naturality, we then have

$$P_{T \circ D \text{id}_{n,\pm}}(v) = P_T(P_{\text{id}_{n,\pm}}(v)), \quad (2.18)$$

hence

$$P_T(v - P_{\text{id}_{n,\pm}}(v)) = 0, \quad (2.19)$$

so  $v - P_{\text{id}_{n,\pm}}(v) \in \ker(P_T)$ . Since  $A_{n,\pm}$  has no null vectors, it follows that  $P_{\text{id}_{n,\pm}}(v) = v$  for all  $v \in A_{n,\pm}$ .  $\square$

**Remark.** An analogous result holds for unshaded planar algebras by considering unshaded planar tangles and elements of the graded vector space  $(P_n)_{n \in \mathbb{N}_0}$ .

In general, there are no constraints on the dimensions of the vector spaces  $A_{n,\pm}$ , but a planar algebra is called *evaluable* if  $\dim(A_{0,\pm}) = 1$  and  $\dim(A_{n,\pm}) < \infty$  for all  $n \in \mathbb{N}$ . In that case, the *evaluation map*

$$e : A_{0,\pm} \rightarrow \mathbb{C}, \quad (2.20)$$

which acts by mapping the ‘empty disk’ to the scalar 1, provides an isomorphism,  $A_{0,\pm} \cong \mathbb{C}$ , for each shading  $+/-$ .

Many familiar linear algebraic operations have counterparts in shaded planar algebras. We proceed by introducing the shaded planar tangles and corresponding linear maps that implement operations relevant in forthcoming sections.

**Remark.** Omitting the subscript indicating the shading of a given shaded tangle, we are referring to the corresponding unshaded version of the tangle. A similar convention is adopted for vector spaces.

For each  $n \in \mathbb{N}_0$ , the planar tangles

$$\text{tr}_{n,+}^{(l)} := \text{Diagram of a shaded disk with concentric circles and a central dot, shading on the left half-plane}, \quad \text{tr}_{n,-}^{(l)} := \text{Diagram of a shaded disk with concentric circles and a central dot, shading on the right half-plane}, \quad \text{tr}_{n,+}^{(r)} := \text{Diagram of a shaded disk with concentric circles and a central dot, shading on the right half-plane}, \quad \text{tr}_{n,-}^{(r)} := \text{Diagram of a shaded disk with concentric circles and a central dot, shading on the left half-plane}, \quad (2.21)$$

induce notions of *left* and *right traces* respectively

$$P_{\text{tr}_{n,\pm}^{(l)}} : A_{n,\pm} \rightarrow A_{0,\pm(-)^n}, \quad P_{\text{tr}_{n,\pm}^{(r)}} : A_{n,\pm} \rightarrow A_{0,\pm}. \quad (2.22)$$

**Remark.** If the shading of a region is unspecified, as it may depend on the parity of  $n$ , we use the banded pattern illustrated in (2.21). For simplicity, the region containing the ‘dots’ is coloured white.

A planar algebra is said to be *spherical* if

$$P_{\text{tr}_{n,\pm}^{(l)}} = P_{\text{tr}_{n,\pm}^{(r)}} \quad (2.23)$$

for all  $n \in \mathbb{N}_0$ . We note that sphericity requires  $A_{0,+} \cong A_{0,-}$ .

Similarly, the *partial trace* tangles

$$\tau_{n,+}^{(l)} := \text{Diagram } 1, \quad \tau_{n,-}^{(l)} := \text{Diagram } 2, \quad \tau_{n,+}^{(r)} := \text{Diagram } 3, \quad \tau_{n,-}^{(r)} := \text{Diagram } 4, \quad (2.24)$$

induce notions of *left-* and *right-partial traces* respectively

$$P_{\tau_{n,\pm}^{(l)}} : A_{n,\pm} \rightarrow A_{n-1,\mp}, \quad P_{\tau_{n,\pm}^{(r)}} : A_{n,\pm} \rightarrow A_{n-1,\pm}, \quad (2.25)$$

where  $\text{tr}_{n,\pm}^{(l)} = \tau_{1,\pm(-)^{n-1}}^{(l)} \circ \tau_{2,\pm(-)^{n-2}}^{(l)} \circ \dots \circ \tau_{n,\pm}^{(l)}$  and  $\text{tr}_{n,\pm}^{(r)} = \tau_{1,\pm}^{(r)} \circ \tau_{2,\pm}^{(r)} \circ \dots \circ \tau_{n,\pm}^{(r)}$ .

For each  $n \in \mathbb{N}_0$ , the planar tangles

$$M_{n,+} := \text{Diagram } 1, \quad M_{n,-} := \text{Diagram } 2, \quad P_{M_{n,\pm}} : A_{n,\pm} \times A_{n,\pm} \rightarrow A_{n,\pm}, \quad (2.26)$$

induce a *multiplication* on  $A_{n,\pm}$ , and we write  $vw = P_{M_{n,\pm}}(v, w) \in A_{n,\pm}$  for  $v, w \in A_{n,\pm}$ , where  $v$ , respectively  $w$ , is replacing the lower, respectively upper, disk in  $M_{n,\pm}$ . Naturality ensures that the resulting algebra  $A_{n,\pm}$  is associative, and under mild conditions (see Proposition 2.2.4 below), also unital, with unit

$$1_{n,\pm} := P_{\text{Id}_{n,\pm}}(), \quad \text{Id}_{n,+} := \text{Diagram } 1, \quad \text{Id}_{n,-} := \text{Diagram } 2, \quad (2.27)$$

whose dependence on  $n$  may be suppressed by writing  $1_{\pm}$  for  $1_{n,\pm}$ .

**Proposition 2.2.4.** *If  $A_{n,\pm}$  has no null vectors, the algebra induced by the multiplication tangle  $M_{n,\pm}$  is unital, with unit  $1_{n,\pm}$ .*

*Proof.* Observe that naturality implies

$$\mathsf{P}_{M_{n,\pm} \circ_2 \text{Id}_{n,\pm}}(v) = \mathsf{P}_{M_{n,\pm}}(v, \mathbb{1}_{n,\pm}), \quad \mathsf{P}_{M_{n,\pm} \circ_1 \text{Id}_{n,\pm}}(v) = \mathsf{P}_{M_{n,\pm}}(\mathbb{1}_{n,\pm}, v), \quad (2.28)$$

which can be simplified to

$$\mathsf{P}_{\text{Id}_{n,\pm}}(v) = v = v \mathbb{1}_{n,\pm}, \quad \mathsf{P}_{\text{Id}_{n,\pm}}(v) = v = \mathbb{1}_{n,\pm} v, \quad (2.29)$$

and holds for all  $v \in A_{n,\pm}$ . Note that in the first equality of both expressions, we have applied Proposition 2.2.3.  $\square$

**Remark.** A *zero planar algebra* [23], where the vector spaces  $(A_{n,\pm})_{n \in \mathbb{N}_0}$  are arbitrary and all planar tangles act as the zero map, exclusively contains null vectors. We note (i) that each vector space of a planar algebra can be extended to include arbitrarily many null vectors, and (ii) for each planar algebra with null vectors, except for a zero planar algebra, there exists a corresponding planar algebra without null vectors (obtained by omitting them).

In this section, we have considered shaded planar algebras in a general setting. In the following, we impose additional structure on the vector spaces and linear maps to define variants of shaded planar algebras. For us, this will culminate in the definition of *Yang–Baxter relation planar algebras*. But first, we meet *subfactor planar algebras*, which play a significant role in the theory of von Neumann algebras. For more on this, see [24].

## 2.3 Subfactor planar algebras

One can endow (shaded) planar algebras with a  $*$ -algebraic structure by introducing two involutions, one acting on (shaded) planar tangles and the other acting on vectors. First, let  $\cdot^\dagger$  denote the operator that acts by reflecting a planar tangle about a line perpendicular to the marked exterior boundary interval, and let  ${}^* : A_{n,\pm} \rightarrow A_{n,\pm}$ ,  $n \in \mathbb{N}_0$ , denote a conjugate linear involution. Analogous to naturality, compatibility between the two maps manifests itself in a simple relation,

$$\mathsf{P}_{T^\dagger}(v_1^*, \dots, v_{|\mathcal{D}_T|}^*) = \mathsf{P}_T(v_1, \dots, v_{|\mathcal{D}_T|})^*, \quad (2.30)$$

which must hold for all planar tangles  $T$  and all  $(v_1, \dots, v_{|\mathcal{D}_T|}) \in \bigtimes_{D \in \mathcal{D}_T} A_{\eta(D)/2, \zeta(D)}$ . A planar algebra  $(A_{n,\pm})_{n \in \mathbb{N}_0}$  endowed with the maps  $\cdot^\dagger$  and  ${}^*$  satisfying (2.30) is known as *involutive*. In that case,

$$\mathsf{P}_{\text{Id}_{n,\pm}^\dagger}() = \mathsf{P}_{\text{Id}_{n,\pm}}()^*, \quad \mathbb{1}_{n,\pm} = \mathbb{1}_{n,\pm}^*, \quad (2.31)$$

and for  $p \in A_{n,\pm}$ , we have

$$p^2 = p \quad \implies \quad (p^*)^2 = p^*, \quad (2.32)$$

with the indicated multiplication induced by  $M_{n,\pm}$ .

An involutive planar algebra  $(A_{n,\pm})_{n \in \mathbb{N}_0}$  admits the sesquilinear maps

$$\langle \cdot, \cdot \rangle_{n,\pm}^{(c)} : A_{n,\pm} \times A_{n,\pm} \rightarrow A_{0,\pm}(-)^{n\delta_{cl}}, \quad (a, b) \mapsto \mathsf{P}_{\text{tr}_{n,\pm}^{(c)}}(a^* b), \quad (2.33)$$

labelled by  $c \in \{l, r\}$  and known as the *left* and *right trace map* for  $c = l$  and  $c = r$ , respectively. Here,  $\delta_{cl} = 1$  for  $c = l$ , and  $\delta_{cl} = 0$  for  $c = r$ . Composed with the evaluation map (2.20) for  $\dim A_{0,\pm} = 1$ , we obtain the sesquilinear *trace forms*

$$e \circ \langle \cdot, \cdot \rangle_{n,\pm}^{(c)} : A_{n,\pm} \times A_{n,\pm} \rightarrow \mathbb{C}. \quad (2.34)$$

An involutive planar algebra inherits the qualifier *positive (semi-)definite* if both trace forms enjoy it for all  $n \in \mathbb{N}_0$ . If the involutive planar algebra is spherical, then the two trace maps (and hence trace forms) are identical.

We now give a precise definition of a subfactor planar algebra.

**Definition 2.3.1.** *A subfactor planar algebra is an evaluable, spherical, positive-definite and shaded planar algebra.*

The properties of subfactor planar algebras endow each vector space  $A_{n,\pm}$  with a unique trace form (2.34) as an inner product which, together with the corresponding multiplication tangle (2.26), make each  $A_{n,\pm}$  a finite-dimensional semisimple algebra, see e.g. [25]. Consequently, each  $A_{n,\pm}$  is isomorphic, as an algebra, to a direct sum of matrix algebras, which facilitates the use of linear algebraic techniques in the analysis of subfactor planar algebras. To this end, we introduce

$$P'_{\text{tr}_{n,\pm}^{(c)}} := e \circ P_{\text{tr}_{n,\pm}^{(c)}} \quad (2.35)$$

and refer to the map

$$A_{n,\pm} \rightarrow \mathbb{R}, \quad a \mapsto \sqrt{P'_{\text{tr}_{n,\pm}^{(c)}}(a^*a)}, \quad (2.36)$$

as the *trace norm*.

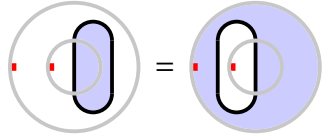
As a concrete example, we introduce here the *Temperley–Lieb subfactor planar algebra*  $(T_{n,\pm})_{n \in \mathbb{N}_0}$ , and revisit it later in Section 5.1 and again in Section 6.1. In some respects, this example is the *simplest* subfactor planar algebra as it is generated by the intrinsic properties of planar tangles and therefore requires no external input. To illustrate this point, we define the Temperley–Lieb subfactor planar algebra in a roundabout way, see Section 5.1 for the standard definition. Let  $T_{n,\pm}$  denote the span of all planar tangles  $T$  with zero input disks, and with  $\eta(D_0^T) = 2n$  and  $\zeta(D_0^T) = \pm$ . Planar tangles act on vectors in  $(T_{n,\pm})_{n \in \mathbb{N}_0}$ , as the composition of tangles, see for example (2.5) (but here shaded). Vectors in  $(T_{n,\pm})_{n \in \mathbb{N}_0}$ , satisfy additional relations making the corresponding planar algebra a subfactor planar algebra. We proceed by deriving these relations.

Evaluability requires  $\dim T_{0,\pm} = 1$ , and consequently, the empty diagram and the diagram with a closed loop are not linearly independent, so we have

$$\text{Diagram with a shaded loop} = \delta_+ \text{Diagram with an empty loop}, \quad \text{Diagram with an empty loop} = \delta_- \text{Diagram with a shaded loop}, \quad (2.37)$$

where  $\delta_{\pm} \in \mathbb{C}$  is called the *shaded loop fugacity*. Naturality implies that the appearance of a closed loop within any vector can always be removed and assigned a weight  $\delta_+$  or  $\delta_-$ . It follows that  $\dim T_{n,\pm} < \infty$

for all  $n \in \mathbb{N}$ . The spherical property follows by enforcing


(2.38)

which implies

$$\delta_+ = \delta_- \quad \text{and} \quad \text{Diagram} = \text{Diagram} . \quad (2.39)$$

To be convinced that sphericity is satisfied, observe that applying either the left or right trace does not change the number of closed loops formed. From here onward we use  $\delta$  to denote  $\delta_+$  equivalently  $\delta_-$ . It follows from the closure of shaded planar tangles under the involution  $\cdot^\dagger$ , that the Temperley–Lieb subfactor planar algebra is readily involutive. Deriving relations following from the positive-definite condition is more involved than the previous conditions. It can be shown that the trace form of the Temperley–Lieb subfactor planar algebra is positive definite for  $\delta \in \{2 \cos(\frac{\pi}{k}) \mid k = 3, 4, \dots\} \cup [2, \infty)$  [26]. For  $\delta \in \{2 \cos(\frac{\pi}{k}) \mid k = 3, 4, \dots\}$ , each  $T_{n,\pm}$  is defined such that a collection of so-called *Jones-Wenzl idempotents* are set to zero, while for  $\delta > 2$  no additional relations are imposed [27, 28]. To illustrate the case  $\delta > 2$ , each  $T_{n,\pm}$  is spanned by disks with  $2n$  nodes, such that each node is connected to another node via a non-intersecting loop segment – defined up to ambient isotopy, and a  $\pm$  checkerboard shading. Accordingly, the canonical bases of  $T_{1,+}$ ,  $T_{2,-}$  and  $T_{3,+}$  are given by

$$\left\{ \text{Diagram} \right\}, \quad \left\{ \text{Diagram}, \text{Diagram} \right\} \quad \text{and} \quad \left\{ \text{Diagram}, \text{Diagram}, \text{Diagram}, \text{Diagram}, \text{Diagram} \right\}, \quad (2.40)$$

respectively.

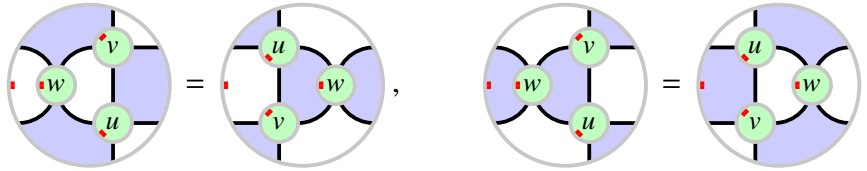
It is a remarkable fact that every subfactor planar algebra possesses the Temperley–Lieb subfactor planar algebra as a planar subalgebra [13, 26]. To define more subfactor planar algebras, it is natural to supplement the Temperley–Lieb vector spaces with additional vectors. *Singly generated planar algebras*  $(A_{n,\pm})_{n \in \mathbb{N}_0}$  are a class of subfactor planar algebras defined accordingly. Here,  $A_{0,\pm}$  and  $A_{1,\pm}$  are defined as in the Temperley–Lieb subfactor planar algebra, while  $A_{2,\pm}$  has a basis consisting of the two canonical Temperley–Lieb basis vectors and *one* additional vector. The remaining vector spaces  $A_{n,\pm}$  for  $n > 2$ , are generated by the action of the planar tangles on  $A_{2,\pm}$ . The properties of subfactor planar algebras place constraints on the interaction between the Temperley–Lieb vectors and the new element. While a general classification of singly generated planar algebras has been considered unfeasible [13], a program set about by Bisch and Jones has succeeded in classifying all singly generated planar algebras satisfying the dimensionality constraint  $\dim A_{3,\pm} \leq 14$  [29–31]. We will revisit singly generated planar algebras in Section 5.2, where we present a unified algebraic framework for unshaded singly generated planar algebras. Indeed, one can impose other constraints, apart from those on dimensionality, that give rise to new planar algebras. To one such class, we devote the next section.

## 2.4 Yang–Baxter relation planar algebras

The *Yang–Baxter equation* (YBE) [32–34] appears in many contexts in mathematics and physics, from quantum groups and low dimensional topology to high-energy particle scattering and statistical mechanics [11, 35–37]. The parameter-dependent form of the YBE is typically presented as

$$(R(u) \otimes 1)(1 \otimes R(u+v))(R(v) \otimes 1) = (1 \otimes R(v))(R(u+v) \otimes 1)(1 \otimes R(u)) \quad (2.41)$$

where  $u, v \in \Omega \subseteq \mathbb{C}$  for some suitable domain  $\Omega$ ,  $1 \in \text{End}(\mathbb{C}^2)$  is the identity matrix, and  $R(u) \in \text{End}(\mathbb{C}^2 \otimes \mathbb{C}^2)$  is referred to as the *R-matrix*. The corresponding parameter-independent version of the YBE can be established from (2.41), via a sufficiently well-defined limit, for example,  $R = \lim_{u \rightarrow 0} R(u)$  or  $R = \lim_{u \rightarrow \pm i\infty} R(u)$  [38]. The expression (2.41), together with the notation developed in Section 2.1, suggest natural counterparts to the YBE native to shaded planar algebras:



$$w = u + v \quad (2.42)$$

where  $1_{\pm} \in A_{1,\pm}$  are the identity operators, and  $R_+(u) = \text{Diagram with u in top circle}$   $\in A_{2,+}$  and  $R_-(u) = \text{Diagram with u in bottom circle}$   $\in A_{2,-}$  are referred to as *R-operators*. A solution to either YBE in (2.42) is considered *specious* if  $R_{\pm}(u) = f(u)a_{\pm}$  for some  $a_{\pm} \in A_{2,\pm}$  and some scalar function  $f$ . Specious solutions are simply a consequence of  $a_{\pm} \in A_{2,\pm}$  satisfying the parameter-independent version of the corresponding YBE. Indeed, it need not be the case that a general planar algebra possesses a non-specious solution to either YBE.

For subfactor planar algebras, there always exists a non-specious solution to both YBEs (2.42), however, this is true in a rather superficial way. To see this, note that within the Temperley–Lieb subfactor planar algebra, the following *R*-operators are solutions to the YBEs



$$\text{Diagram with u in top circle} = \sin(\lambda - u) \text{Diagram with u in top circle} + \sin(u) \text{Diagram with u in bottom circle}, \quad \text{Diagram with u in bottom circle} = \sin(\lambda - u) \text{Diagram with u in top circle} + \sin(u) \text{Diagram with u in bottom circle}, \quad \delta = 2\cos(\lambda). \quad (2.43)$$

The claim follows from the observation (2.43), together with the fact that every subfactor planar algebra contains the Temperley–Lieb subfactor planar algebra. To define subfactor planar algebras admitting *new* YBE solutions, one approach is to restrict to solutions satisfying  $\text{span}\{R_{\pm}(u) \mid u \in \Omega\} = A_{2,\pm}$ .

To this end, we may naively impose the YBEs (2.42) on subfactor planar algebras and use skein theory to classify the resulting algebras satisfying this condition. Though practical, it is not clear how one would incorporate the  $u$  and  $v$  parameter dependence. Instead, we consider a possibly larger class of subfactor planar algebras, introduced by Liu [39], satisfying necessary conditions common to those supporting YBE solutions satisfying  $\text{span}\{R_{\pm}(u) \mid u \in \Omega\} = A_{2,\pm}$ . One can then consider whether these planar algebras admit new YBE solutions.

Let  $(A_{n,\pm})_{n \in \mathbb{N}_0}$  be a shaded planar algebra, with  $B_{n,\pm}$  denoting a basis for  $A_{n,\pm}$ . Following [39], a triple  $(x, y, z) \in A_{2,-} \times A_{2,+} \times A_{2,-}$ , respectively  $(x, y, z) \in A_{2,+} \times A_{2,-} \times A_{2,+}$ , is said to satisfy a

Yang–Baxter relation (YBR) if

$$\text{Diagram 1} = \sum_{\substack{a,c \in B_{2,+} \\ b \in B_{2,-}}} C_{x,y,z}^{a,b,c} \text{Diagram 2}, \quad \text{Diagram 3} = \sum_{\substack{a,c \in B_{2,-} \\ b \in B_{2,+}}} D_{x,y,z}^{a,b,c} \text{Diagram 4}, \quad (2.44)$$

respectively, for some  $C_{x,y,z}^{a,b,c}, D_{x,y,z}^{a,b,c} \in \mathbb{C}$ .

**Definition 2.4.1.** A Yang–Baxter relation planar algebra  $(A_{n,\pm})_{n \in \mathbb{N}_0}$  is a subfactor planar algebra where every triple of vectors in  $A_{2,-} \times A_{2,+} \times A_{2,-}$  and  $A_{2,+} \times A_{2,-} \times A_{2,+}$  satisfy a Yang–Baxter relation.

**Remark.** Although a YBR planar algebra is a subfactor planar algebra, we are suppressing that qualifier, in line with the convention in [39].

While we adopt the form (2.44) of the YBRs introduced in [39], the characterisation of a planar algebra as a YBR planar algebra does not depend on the particular choices of input disk markings (and consequently shadings) in (2.44), on either side of any of the two YBRs. However, we do need a YBR for each shading of the *output* disk, as in (2.44).

In Chapter 3, we describe how one can associate a *homogeneous Yang–Baxter integrable model* to any planar algebra satisfying a particular set of sufficient conditions, including YBRs. It is thus natural to expect that YBR planar algebras play an important role in the classification of Yang–Baxter integrable models. Indeed, we find (Proposition 5.2.3 in Section 5.2.4) that a singly generated planar algebra that is *not* a YBR planar algebra *does not* encode the structure of a homogeneous Yang–Baxter integrable model.

## 2.5 Unshaded planar algebras

The *shading* of a planar algebra  $(A_{n,\pm})_{n \in \mathbb{N}_0}$  need not carry any non-trivial information. In that case, the shading can be ignored, giving rise to the corresponding *unshaded planar algebra*  $(A_n)_{n \in \mathbb{N}_0}$ . Consider the following linear maps that reverse the shading on the vectors in  $A_{n,+}$  and  $A_{n,-}$ :

$$\iota_{n,+} : A_{n,+} \rightarrow A_{n,-}, \quad \text{Diagram 1} \mapsto \text{Diagram 2}; \quad \iota_{n,-} : A_{n,-} \rightarrow A_{n,+}, \quad \text{Diagram 3} \mapsto \text{Diagram 4}, \quad (2.45)$$

here illustrated for  $n = 2$ . Following [22], there exists an unshaded planar algebra  $(A_n)_{n \in \mathbb{N}_0}$  corresponding to  $(A_{n,\pm})_{n \in \mathbb{N}_0}$  if and only if the map  $\iota_{n,\mp} \circ \iota_{n,\pm}$  acts as the identity on  $A_{n,\pm}$  for all  $n \in \mathbb{N}_0$ .

A key observation for us is that singly generated planar algebras that *do not* admit an unshaded description *cannot* encode a homogeneous Yang–Baxter integrable model within the algebraic integrability framework developed later in Chapter 3. To see this, let  $(A_{n,\pm})_{n \in \mathbb{N}_0}$  denote a singly generated planar algebra *encoding a homogeneous Yang–Baxter integrable model*, and consider the shaded  $R$ -operators of a model defined for each  $u \in \Omega$

$$R_+(u) = \text{Diagram 1} \in A_{2,+}, \quad R_-(u) = \text{Diagram 2} \in A_{2,-}. \quad (2.46)$$

By *homogeneity*, introduced in Chapter 3, these  $R$ -operators satisfy

$$\iota_{2,\pm}[R_\pm(u)] = R_\mp(u), \quad \forall u \in \Omega. \quad (2.47)$$

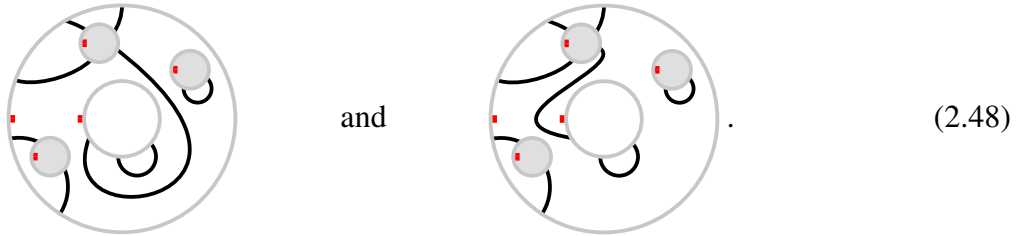
As the planar algebra *encodes* the integrability of the model,  $\{R_\pm(u) \mid u \in \Omega\}$  together with the action of planar tangles, generates the vector space  $A_{2,\pm}$  (see Section 3.1 for more details). Using (2.47), it follows that  $\iota_{2,\mp} \circ \iota_{2,\pm}$  acts as the identity on  $A_{2,\pm}$ , so the corresponding singly generated planar algebra  $(A_{n,\pm})_{n \in \mathbb{N}_0}$  admits an unshaded description.

For our homogeneous Yang–Baxter integrability purposes, it thus suffices to consider *unshaded* planar algebras only. We stress that a shaded planar algebra not admitting an unshaded description could encode the structure of an integrable model; however, the corresponding transfer operator would necessarily be *inhomogeneous*, see the Remark following (3.10).

We conclude this chapter by presenting one final planar-algebraic construction. Up to now, the action of planar tangles on themselves via composition and on the vector spaces as multilinear maps have been performed within the topology of a disk. The *affine category of a planar algebra*, provides a setting whereby planar-algebraic operations can be performed on the annulus, or equivalently, the cylinder. It is convenient to present this construction for unshaded planar algebras only, the shaded variant is a straightforward generalisation.

## 2.6 The affine category of a planar algebra

*Affine tangles* are the diagrammatic objects, defined up to *affine isotopy*, that facilitate the combination of vectors on the annulus. *Affine isotopies* are a subset of all ambient isotopies that act as the identity on the boundaries of the annulus. For example, we present two inequivalent affine tangles:



The boundaries of affine tangles can be thought of as being ‘rigid’, that is, they cannot be freely rotated relative to each other.

**Definition 2.6.1.** An (unshaded) *affine tangle*  $S$  consists of the following components in  $\mathbb{R}^2$ :

- An annulus defined by an inner disk  $D_0^S$  and an outer disk  $D_1^S$ , called the *output annulus*.
- A finite set of non-overlapping disks  $\mathcal{D}_S$  in the interior of the output annulus, called *input disk(s)*.
- A finite number of non-intersecting loop segments within the output annulus and outside of the input disk(s), connecting pair-wise, distinct points on the boundary of the disks in  $\{D_0^S, D_1^S\} \cup \mathcal{D}_S$  called *nodes*, or closing on themselves forming loops. Denote by  $\eta(D)$  the number of nodes

on the boundary of  $D \in \{D_0^S, D_1^S\} \cup \mathcal{D}_S$ . The boundary of each disk is thus composed of nodes and boundary intervals: the open intervals between the nodes or if there are no nodes, a whole circle.

- For each disk in  $\{D_0^S, D_1^S\} \cup \mathcal{D}_T$  a choice of boundary interval, here marked graphically by a red rectangle.

Each affine tangle  $S$  is defined up to affine isotopy of  $D_1^S \setminus D_0^S \subset \mathbb{R}^2$ .

**Remark.** As with planar tangles, one can consider variants of affine tangles that have additional structure, for example, by imposing a checker-board shading.

*Annular tangles* are affine tangles defined up to ambient isotopy. Accordingly, annular tangles share all the features of affine tangles. Unlike affine tangles, two annular tangles that differ by a relative rotation of one's boundary disks are equivalent. Accordingly, the two tangles in (2.48) are equivalent as annular tangles.

**Remark.** As both annular tangles and planar tangles are defined up to ambient isotopy, annular tangles can be defined as a planar tangle with a distinguished internal disk. This is the definition of annular tangles presented in [40].

We proceed by presenting the affine case only and note that the annular case can be obtained as a quotient. An  *$m$ -tangle* is a planar tangle  $T$  such that  $\eta(D_0^T) = m$ , while an  *$(m, n)$ -affine tangle* is an affine tangle  $T$  such that  $\eta(D_0^T) = m$  and  $\eta(D_1^T) = n$ . An  $(m, n)$ -affine tangle  $T$  can be composed with an  $(l, m)$ -affine tangle  $S$  by replacing the inner disk of  $T$  with  $S$ , removing the shared boundary and marked interval, and identifying the image, which we denote by  $T \circ S$ , with an  $(l, n)$ -affine tangle. A tangle, affine or otherwise, is called  *$P$ -labelled* if each input disk  $D$  is filled with a vector in  $P_{\eta(D)}$ .

**Remark.** While similar, we highlight that a  $P$ -labelled  $m$ -tangle  $T$  is distinct from the image of the multilinear map  $P_T(v_1, \dots, v_t)$  where  $v_1, \dots, v_t$  are the vectors corresponding to the  $P$ -labelling. The image  $P_T(v_1, \dots, v_t)$  is the identification of the  $P$ -labelled tangle  $T$  as an element of the vector space  $P_m$ , given the action of  $T$ . This motivates the following map.

Let  $\mathcal{T}_m(P)$  denote the vector space spanned by the set of all  $P$ -labelled  $m$ -tangles. For each  $m \in \mathbb{N}_0$ , define the linear map

$$\mathsf{T}_m : \mathcal{T}_m(P) \rightarrow P_m, \quad (2.49)$$

that acts as by identifying each  $P$ -labelled  $m$ -tangle  $T$  with the image of the map  $P_T(v_1, \dots, v_t)$  where  $v_1, \dots, v_t$  are the vectors corresponding to the  $P$ -labelling. Let  $\mathcal{A}_{m,n}(P)$  denote the vector space spanned by the set of all  $P$ -labelled  $(m, n)$ -affine tangles, and for each  $m, n, o \in \mathbb{N}_0$ , define the linear

map

$$\Psi_{m,n}^{(o)} : \mathcal{T}_{m+n+2o}(P) \rightarrow \mathcal{A}_{m,n}(P), \quad o \left\{ \overbrace{\dots}^n \right\} o \mapsto \text{Diagram} \quad (2.50)$$

For any  $S \in \mathcal{A}_{m,n}(P)$  there exists an  $o \in \mathbb{N}_0$  and a  $T \in \mathcal{T}_{m+n+2o}(A)$  such that  $S = \Psi_{m,n}^{(o)}(T)$ , where the  $o$  and the  $T$  are not necessarily unique [41].

We are now in a position to define a vector space, spanned by  $P$ -labelled  $(m,n)$ -affine tangles, that satisfies the relations within the planar algebra  $P$ . In preparation, we define

$$\mathcal{W}_{m,n} := \{a \in \mathcal{A}_{m,n}(P) \mid a = \Psi_{m,n}^{(o)}(b), b \in \text{Ker}(\mathcal{T}_{m+n+2o})\} \quad (2.51)$$

and note that  $\mathcal{W}_{m,n}$  is a vector subspace of  $\mathcal{A}_{m,n}(P)$ . For each  $m,n \in \mathbb{N}_0$ , we define

$$QP_{m,n} := \mathcal{A}_{m,n}(P)/\mathcal{W}_{m,n}, \quad (2.52)$$

and identify  $QP_{m,n}$  with the vector space of interest.

To each affine tangle  $T$ , we associate the linear  $|\mathcal{D}_T|$ -ary operator

$$\mathsf{P}_T : \bigtimes_{D \in \mathcal{D}_T} P_{\eta(D)} \rightarrow QP_{\eta(D_0^T), \eta(D_1^T)}, \quad (2.53)$$

which acts by replacing each of the input disks  $D$  of  $T$  with elements from the vector space  $P_{\eta(D)}$  in such a way that the nodes and the marking of both are aligned, for example:

$$T = \text{Diagram with 3 nodes labeled 1, 2, 3}, \quad \mathsf{P}_T(v_1, v_2, v_3) = \text{Diagram with nodes v1, v2, v3} \in QP_{4,8}. \quad (2.54)$$

Analogous to the partial trace tangles (2.24), for each  $n \in \mathbb{N}_0$ , we introduce the *affine partial trace* tangle

$$\tau_n^{(a)} := \text{Diagram with a central node and two red dots on the boundary}, \quad \mathsf{P}_{\tau_n^{(a)}} : P_{2n} \rightarrow QP_{n-1,n-1}. \quad (2.55)$$

We proceed by defining some categories of interest.

**Definition 2.6.2.** Denote by  $\text{Aff}(P)$  the affine category of a planar algebra  $P$  where

$$\text{Obj}_{\text{Aff}(P)} = \mathbb{N}_0, \quad \text{Mor}_{\text{Aff}(P)}(m, n) = QP_{m,n}, \quad (2.56)$$

for each  $m, n \in \mathbb{N}_0$ , and the composition of morphisms is defined as the composition of affine tangles.

Denote by  $\text{Vect}$  the category of vector spaces.

**Definition 2.6.3.** An affine representation of a planar algebra  $P$  is a collection of vector spaces  $(V_n)_{n \in \mathbb{N}_0}$  and a functor

$$F : \text{Aff}(P) \rightarrow \text{Vect}, \quad (2.57)$$

such that  $F_0(n) = V_n$  for all  $n \in \mathbb{N}_0$ , and  $F_1(x) \in \text{Mor}_{\text{Vect}}(V_m, V_n)$  is a linear map for all  $x \in QP_{m,n}$  and all  $m, n \in \mathbb{N}_0$ .

Each planar algebra  $P$  admits a ‘trivial’ affine representation induced by itself, where  $V_n = P_n$  for all  $n \in \mathbb{N}_0$ , and where

$$F_1(x) : V_m \rightarrow V_n, \quad (2.58)$$

acts by treating the central disk of  $x$  as an input disk, inputting vectors from  $V_m$  and identifying the image in  $V_n$ , for all  $x \in QP_{m,n}$  and all  $m, n \in \mathbb{N}_0$ . To demonstrate the action of the affine tangles as linear maps, we present the example

$$F_1(x)(v) = \begin{array}{c} \text{Diagram of } F_1(x)(v) \text{ with 4 input ports } v_1, v_2, v_3, v_4 \text{ and 4 output ports } v_1, v_2, v_3, v_4. \end{array} = \begin{array}{c} \text{Diagram of } F_1(x)(v) \text{ with 4 input ports } v_1, v_2, v_3, v_4 \text{ and 4 output ports } v_1, v_2, v_3, v_4. \end{array}, \quad x = \begin{array}{c} \text{Diagram of } x \text{ with 4 input ports } v_1, v_2, v_3, v_4 \text{ and 4 output ports } v_1, v_2, v_3, v_4. \end{array}, \quad v = \begin{array}{c} \text{Diagram of } v \text{ with 4 input ports } v_1, v_2, v_3, v_4 \text{ and 4 output ports } v_1, v_2, v_3, v_4. \end{array} \quad (2.59)$$

where  $x \in QP_{4,8}$  and  $v \in V_4$ . Another representation is induced by the affine tangles themselves. Define  $QP_n := \bigcup_{m \in \mathbb{N}_0} QP_{m,n}$ , set  $V_n = QP_n$  for all  $n \in \mathbb{N}_0$ , and let  $F_1(x)$  act on vectors in  $V_m$  via the composition of affine tangles for all  $x \in QP_{m,n}$ . The action of affine tangles as linear maps is inherited by the composition of tangles, for example

$$F_1(x)(v) = \begin{array}{c} \text{Diagram of } F_1(x)(v) \text{ with 4 input ports } v_1, v_2, v_3, v_4 \text{ and 4 output ports } v_1, v_2, v_3, v_4. \end{array} = \delta \begin{array}{c} \text{Diagram of } F_1(x)(v) \text{ with 4 input ports } v_1, v_2, v_3, v_4 \text{ and 4 output ports } v_1, v_2, v_3, v_4. \end{array}, \quad x = \begin{array}{c} \text{Diagram of } x \text{ with 4 input ports } v_1, v_2, v_3, v_4 \text{ and 4 output ports } v_1, v_2, v_3, v_4. \end{array}, \quad v = \begin{array}{c} \text{Diagram of } v \text{ with 4 input ports } v_1, v_2, v_3, v_4 \text{ and 4 output ports } v_1, v_2, v_3, v_4. \end{array} \quad (2.60)$$

where  $x \in QP_{4,4}$  and  $v \in V_4$ .

Define the following  $(n, n)$ -affine tangles

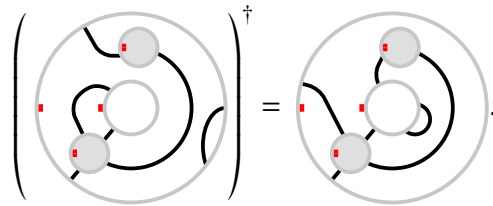
$$\Omega_n := \begin{array}{c} \text{Diagram of } \Omega_n \text{ with } n \text{ input ports and } n \text{ output ports.} \end{array}, \quad \Omega_n^0 := \begin{array}{c} \text{Diagram of } \Omega_n^0 \text{ with } n \text{ input ports and } n \text{ output ports.} \end{array}, \quad \Omega_n^{-1} := \begin{array}{c} \text{Diagram of } \Omega_n^{-1} \text{ with } n \text{ input ports and } n \text{ output ports.} \end{array}, \quad (2.61)$$

each having  $n$  ‘spokes’, and let  $\Omega_n^{\pm k}$  denote the composition of  $\Omega_n^{\pm 1}$  with itself  $k$  times, with  $k \in \mathbb{N}$ , it follows that

$$\Omega_n^k \circ \Omega_n^l = \Omega_n^{k+l}, \quad \forall k, l \in \mathbb{Z}. \quad (2.62)$$

Note that  $\Omega_n^{k \bmod n}$  and  $\Omega_n^k$  are equivalent as *annular tangles*. An affine representation of  $P$  is called *annular* if the linear map  $F_1(\Omega_n^n)$  acts as the identity for all  $n \in \mathbb{N}$ . Affine tangles within an annular representation act *as if* they are annular tangles. It follows from the ambient isotopy of planar algebras that the trivial representation is annular, while the representation induced by affine tangles is not.

Let  $P$  be an involutive planar algebra, and denote by  $\cdot^\dagger$  the involution that acts on planar tangles, and by  $\cdot^*$  the involution that acts on vectors. An equivalent to  $\cdot^\dagger$  for affine tangles (which we also denote by  $\cdot^\dagger$ ) is defined by reflecting the affine tangle about a circle with the same centre as the annulus but with a larger radius, for example:



$$\left( \text{Diagram} \right)^\dagger = \text{Diagram'}. \quad (2.63)$$

The involutions  $\cdot^\dagger$  and  $\cdot^*$ , induce the involution  $\star : \mathcal{A}_{m,n}(P) \rightarrow \mathcal{A}_{n,m}(P)$  that acts by  $\cdot^\dagger$  on the affine tangle and by  $\cdot^*$  on the  $P$ -labels. As  $P$  is involutive, we have  $(\mathcal{W}_{m,n})^\star = \mathcal{W}_{n,m}$ , the involution passes to the quotient  $\star : QP_{m,n} \rightarrow QP_{n,m}(P)$ , and it follows that  $\text{Aff}(P)$  is a  $*$ -category [41]. By construction, we have

$$P_T(v_1, \dots, v_{|\mathcal{D}_T|})^\star = P_{T^\dagger}(v_1^*, \dots, v_{|\mathcal{D}_T|}^*), \quad (2.64)$$

for all affine tangles  $T$ , and for all  $(v_1, \dots, v_{|\mathcal{D}_T|}) \in \bigtimes_{D \in \mathcal{D}_T} P_{\eta(D)}$ . Denote by  $\text{Hilb}$  the category of Hilbert spaces.

**Definition 2.6.4.** A *Hilbert representation of an involutive planar algebra  $P$*  is a collection of Hilbert spaces  $(V_n)_{n \in \mathbb{N}_0}$  and a functor

$$F : \text{Aff}(P) \rightarrow \text{Hilb}, \quad (2.65)$$

such that  $F_0(n) = V_n$  for all  $n \in \mathbb{N}_0$ , and  $F_1(x) \in \text{Mor}_{\text{Hilb}}(V_m, V_n)$  is a linear map satisfying

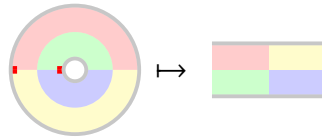
$$\langle v, F_1(x)(w) \rangle_n = \langle F_1(x)^*(v), w \rangle_m, \quad (2.66)$$

for all  $x \in QP_{m,n}$ , all  $v \in V_n$  and  $w \in V_m$ , and all  $m, n \in \mathbb{N}_0$ .

We note that the trivial representation of a subfactor planar algebra is a Hilbert representation [40, 41].

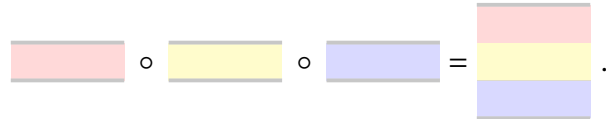
It will be convenient, when expressing affine tangles diagrammatically, to view them as existing within the plane. To this end, we define the following procedure to be applied to each affine tangle: cut from the inner disk marking to the outer disk marking, and orient the diagram such that the inner and

outer edges are horizontal, remain perpendicular to the cut edges (which are identified), and become the upper and lower edges respectively. This procedure is best illustrated diagrammatically:



(2.67)

The composition of affine tangles expressed within the plane amounts to the stacking of diagrams, for example



(2.68)

Having defined many of the planar-algebraic prerequisites, the following chapter develops the so-called homogeneous Yang–Baxter integrability framework.



Components of the following publications have been incorporated into Chapter 3.

- [2] X. Poncini, J. Rasmussen, *Integrability of planar-algebraic models*, J. Stat. Mech. (2023) 073101, arXiv:2206.14462 [math-ph].
- [3] X. Poncini, J. Rasmussen, *A classification of integrable planar-algebraic models*, arXiv:2302.11712 [math-ph].

# Chapter 3

---

## Integrable models

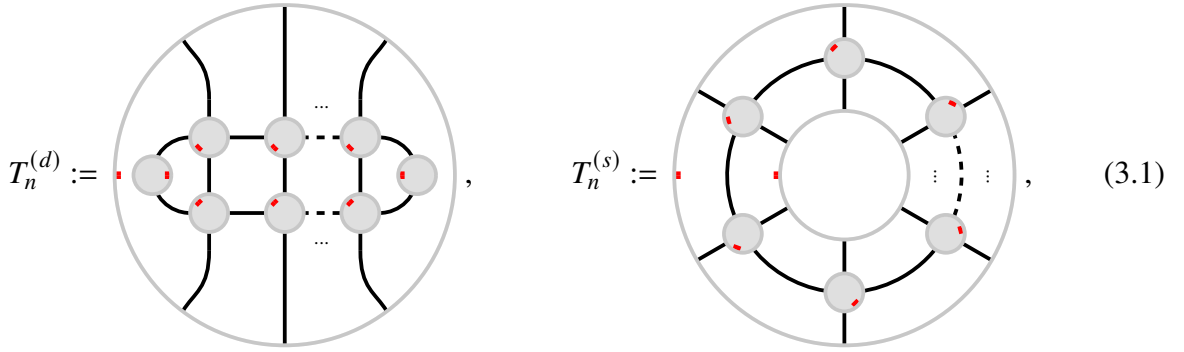
---

In this chapter, we develop a planar-algebraic framework for two-dimensional integrable models described by a *transfer operator*. Given the observations of Section 2.5, it suffices to present the framework for unshaded planar algebras. We begin by defining two types of transfer operators; one that generates a model on the strip and another that generates a model on the cylinder. A model described by a transfer operator  $T(u)$  is *integrable* if it satisfies  $[T(u), T(v)] = 0$  for all  $u$  and  $v$  on a suitable domain. A finite set of sufficient conditions, including generalised Yang–Baxter equations, is then presented for each of the transfer operators which, if satisfied, implies that the corresponding model is integrable. We then introduce an *identity point* as a value of the parameter  $u$  in which the transfer operator  $T(u)$  is proportional to an invertible element of the algebra and perform a power series expansion of the transfer operator about this point to define the *Hamiltonians* of the model. Within this framework, we present a characterisation of the *integrals of motion* associated with an integrable model and distinguish these from the aforementioned Hamiltonians. We conclude this chapter by introducing the notion of *polynomial integrability*.

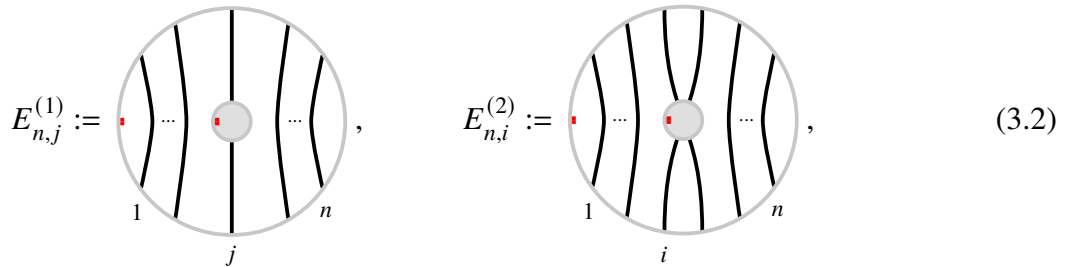
### 3.1 Transfer operators

For the planar-algebraic models considered here, the transfer operator takes a central place. It is the element of the algebra that generates each configuration of the model and assigns the appropriate weight. Accordingly, the partition function of the model is a function of the transfer operator, the details of which depend on the specific boundary conditions. Taking, for example, periodic boundary conditions, the partition function is the trace of the transfer operator raised to some power. In this case, a *solution* of the model amounts to determining the eigenvalues of the transfer operator, from which the partition function and other useful properties of the model can be determined. In this section, for each planar algebra, we define two transfer operators: one on the strip called the *homogeneous double-row* transfer operator and one on the cylinder called the *homogeneous single-row* transfer operator.

For each  $n \in \mathbb{N}$ , we define the *transfer tangle* and the *affine transfer tangle* as



respectively. We also introduce the embedding tangles



where  $j = 1, \dots, n$  and  $i = 1, \dots, n-1$ , respectively, and denote by  $B_n$  a basis for  $P_{2n}$ . Define the *K*- and *R*-operators as the parameterised elements

$$K(u) := \sum_{a \in B_1} k_a(u) a, \quad R(u) := \sum_{a \in B_2} r_a(u) a, \quad \bar{K}(u) := \sum_{a \in B_1} \bar{k}_a(u) a, \quad (3.3)$$

where  $k_a, r_a, \bar{k}_a : \Omega \rightarrow \mathbb{C}$ . We refer to  $u$  parameterising the operators in (3.3), as the corresponding *spectral parameter*.

**Remark.** The set  $\Omega$  indicates a domain over which  $R(u)$ ,  $K(u)$ , and  $\bar{K}(u)$  are well-defined. Typically,  $\Omega$  contains an open set in  $\mathbb{C}$ , allowing power-series expansions of  $R(u)$ ,  $K(u)$ , and  $\bar{K}(u)$ .

We now define the *homogeneous double-row* and *homogeneous single-row* transfer operators as

$$T_n^{(d)}(u) := P_{T_n^{(d)}}(K(u), R(u), \dots, R(u), \bar{K}(u)), \quad T_n^{(s)}(u) := P_{T_n^{(s)}}(R(u), \dots, R(u)), \quad (3.4)$$

respectively, where for the homogeneous double-row transfer operator,  $K(u)$  is placed in the left-most disk and  $\bar{K}(u)$  is placed in the right-most disk of the transfer tangle. Accordingly, we identify  $T_n^{(d)}(u)$  as an element of  $P_{2n}$ , and  $T_n^{(s)}(u)$  as an element of  $QP_{n,n}$ . Expressing the *K*- and *R*-operators diagrammatically as

$$K(u) = \text{Diagram with a central node labeled } u, \quad R(u) = \text{Diagram with a central node labeled } u \text{ and a green circle around it}, \quad \bar{K}(u) = \text{Diagram with a central node labeled } u \text{ and a yellow circle around it}, \quad (3.5)$$

the homogeneous double-row transfer operator takes the diagrammatic form

$$T_n^{(d)}(u) := \text{Diagram on the left} = \text{Diagram on the right}, \quad (3.6)$$

which is suggestive of the familiar partial-trace expression

$$T_n^{(d)}(u) = \mathbb{P}_{\tau_{n+1}^{(l)}}(R_1(u) \cdots R_n(u) \bar{K}_{n+1}(u) R_n(u) \cdots R_1(u) K_1(u)), \quad (3.7)$$

where

$$K_1(u) := \mathbb{P}_{E_{n+1,1}^{(1)}}(K(u)), \quad R_i(u) := \mathbb{P}_{E_{n+1,i}^{(2)}}(R(u)), \quad \bar{K}_{n+1}(u) := \mathbb{P}_{E_{n+1,n+1}^{(1)}}(\bar{K}(u)). \quad (3.8)$$

A similar diagrammatic expression exists for the homogeneous single-row transfer operator

$$T_n^{(s)}(u) := \text{Diagram on the left} = \text{Diagram on the right}, \quad (3.9)$$

where we have mapped to the plane using the procedure presented in (2.67), which again, suggests the familiar partial-trace expression

$$T_n^{(s)}(u) = \mathbb{P}_{\tau_{n+1}^{(a)}}(R_1(u) \cdots R_n(u)). \quad (3.10)$$

We highlight that the product of  $m$  homogeneous double-row transfer operators  $T_n^{(d)}(u)^m$  generates a  $2m \times n$  square lattice on the strip with *reflection* boundary conditions, similarly, the product of  $m$  homogeneous single-row transfer operators  $T_n^{(s)}(u)^m$  generates a  $m \times n$  square lattice on the cylinder.

**Remark.** In (3.5) and throughout, operators with different colours indicate that the associated parameterisations are distinct. More general transfer operators may be constructed, for example by including ‘inhomogeneities’ at the level of the  $R$ -operator. *Spectral inhomogeneities* are thus introduced by varying the spectral parameter of the  $R$ -operator depending on its position within the transfer tangle, while *algebraic inhomogeneities* are introduced by varying the parameterisation in the construction of the  $R$ -operator (as an element of  $A_2$ ) depending on its position within the transfer tangle, thereby introducing more than one  $R$ -operator. We refer to transfer operators with any of these features as *inhomogeneous*. However, as we will exclusively consider homogeneous transfer operators (consisting of a *single*  $u$ -parameterised  $R$ -operator), we often omit the qualifier “homogeneous”.

For each  $n \in \mathbb{N}$ , the basic *rotation tangles* are introduced as

$$r_{n,1} := \text{Diagram of a rotation tangle with } n \text{ spokes, center shaded, red dot at } \frac{1}{n} \text{ position}, \quad r_{n,-1} := \text{Diagram of a rotation tangle with } n \text{ spokes, center shaded, red dot at } \frac{1}{n} \text{ position, with dots at } \dots, \quad (3.11)$$

each having  $n$  ‘spokes’, while  $r_{n,\pm k}$  denotes the composition of  $r_{n,\pm 1}$  with itself  $k$  times, with  $k \in \mathbb{N}$ , so

$$r_{n,k} \circ r_{n,l} = r_{n,k+l}, \quad \forall k, l \in \mathbb{Z}. \quad (3.12)$$

Here,  $r_{n,0}$  denotes the unshaded identity tangle, see (2.17). We note that if  $P_n$  has no null vectors, it follows from Proposition 2.2.3 that  $P_{r_{n,0}}$  acts as the identity and that  $P_{r_{n,\pm k}}$  is invertible for all  $k \in \mathbb{N}$ . Using (3.11), the  $R$ - and  $K$ -operators (3.3) are said to be *crossing symmetric* if

$$P_{r_{2,1}}(K(u)) = \tilde{c}_K(u)K(c_K(u)), \quad P_{r_{4,1}}(R(u)) = \tilde{c}_R(u)R(c_R(u)), \quad P_{r_{2,1}}(\bar{K}(u)) = \tilde{c}_{\bar{K}}(u)\bar{K}(c_{\bar{K}}(u)) \quad (3.13)$$

for some scalar functions  $\tilde{c}_K, c_K, \tilde{c}_R, c_R, \tilde{c}_{\bar{K}}, c_{\bar{K}} : \Omega \rightarrow \mathbb{C}$  such that  $P_{r_{2,2}}(K(u)) = K(u)$ ,  $P_{r_{4,4}}(R(u)) = R(u)$  and  $P_{r_{2,2}}(\bar{K}(u)) = \bar{K}(u)$ . The point  $u_{iso} \in \Omega$  is an *isotropic point* if

$$P_{r_{2,1}}(K(u_{iso})) = K(u_{iso}), \quad P_{r_{4,1}}(R(u_{iso})) = R(u_{iso}), \quad P_{r_{2,1}}(\bar{K}(u_{iso})) = \bar{K}(u_{iso}). \quad (3.14)$$

In the following, suppose that  $(P_n)_{n \in \mathbb{N}_0}$  is an involutive planar algebra with  $\cdot^\dagger$  and  $\cdot^*$  defined as in Section 2.3. The  $K$ - and  $R$ -operators are *self-adjoint* if

$$K(u)^* = K(u), \quad R(u)^* = R(u), \quad \bar{K}(u)^* = \bar{K}(u). \quad (3.15)$$

The self-adjointness of the constituent  $K$ - and  $R$ -operators extends to the double-row transfer operator itself, as detailed in the following.

**Proposition 3.1.1.** *If the  $R$ - and  $K$ -operators are self-adjoint with respect to the involution  $\cdot^*$ , then so is the transfer operator  $T_n^{(d)}(u)$  for each  $n \in \mathbb{N}$ .*

*Proof.* Using (2.30), we have

$$T_n^{(d)}(u)^* = P_{(T_n^{(d)})^\dagger}(K(u)^*, R(u)^*, \dots, R(u)^*, \bar{K}(u)^*) = T_n^{(d)}(u), \quad (3.16)$$

where the second equality follows from  $(T_n^{(d)})^\dagger = T_n^{(d)}$  and the self-adjointness of the  $R$ - and  $K$ -operators.  $\square$

We denote the regular representation of  $P_{2n}$  by

$$\rho_n : P_{2n} \rightarrow \text{End}(P_{2n}). \quad (3.17)$$

**Corollary 3.1.2.** *Let  $(P_n)_{n \in \mathbb{N}_0}$  be an unshaded subfactor planar algebra, and suppose the  $R$ - and  $K$ -operators are self-adjoint with respect to the involution  $\cdot^*$ . Then,  $\rho_n(T_n^{(d)}(u))$  is diagonalisable for all  $n \in \mathbb{N}$ .*

*Proof.* Proposition 3.1.1 and the self-adjointness of the  $R$ - and  $K$ -operators imply that  $T_n^{(d)}(u)$  is self-adjoint. By the spectral theorem,  $\rho_n(T_n^{(d)}(u))$  is therefore diagonalisable.  $\square$

A similar argument can be made for the single-row transfer operator by requiring the  $R$ -operator to be *both* self-adjoint and possess a particular form of crossing symmetry.

**Proposition 3.1.3.** *If the  $R$ -operator is self-adjoint and satisfies  $P_{r_{4,1}}(R(u)) = R(u)$ , then  $T_n^{(s)}(u)$  is self-adjoint for all  $n \in \mathbb{N}$ .*

*Proof.* Using (2.64), we have

$$T_n^{(s)}(u)^\star = P_{(T_n^{(s)})^\dagger}(R(u)^*, \dots, R(u)^*) = P_{(T_n^{(s)})^\dagger}(R(u), \dots, R(u)) = \text{---} \circlearrowleft u \text{---} \circlearrowleft u \text{---} \circlearrowleft u \text{---} \quad (3.18)$$

where the second equality follows from the self-adjointness of the  $R$ -operator. Applying the crossing symmetry, we have

$$T_n^{(s)}(u)^\star = \text{---} \circlearrowleft u \text{---} \circlearrowleft u \text{---} \circlearrowleft u \text{---} = T_n^{(s)}(u). \quad (3.19)$$

$\square$

We denote the regular representation of  $V_n$  by

$$\rho_n : V_n \rightarrow \text{End}(V_n). \quad (3.20)$$

**Corollary 3.1.4.** *Let  $(V_n)_{n \in \mathbb{N}_0}$  be a Hilbert representation of an involutive planar algebra, and suppose the  $R$ -operator is self-adjoint and satisfies  $P_{r_{4,1}}(R(u)) = R(u)$ . Then,  $\rho_n(T_n^{(s)}(u))$  is diagonalisable for all  $n \in \mathbb{N}$ .*

**Remark.** When referring to a transfer operator in general i.e. not specifically  $T_n^{(d)}(u)$  or  $T_n^{(s)}(u)$ , we will omit the superscript and simply write  $T_n(u)$ .

## 3.2 Baxterisation and integrability

Having introduced planar-algebraic models generally, the remainder of this chapter is devoted to analysing models whose transfer operator is an element of a unital associative algebra. In light of Proposition 2.2.3, we restrict to planar algebras  $(P_n)_{n \in \mathbb{N}_0}$  where  $P_{2n-1} = \{0\}$  for all  $n \in \mathbb{N}$ , and where  $P_{2n}$  has no null vectors for all  $n \in \mathbb{N}_0$ . To distinguish such a planar algebra from the general discussion above, we will use the notation  $(A_n)_{n \in \mathbb{N}_0}$ , where  $A_n \equiv P_{2n}$ . Denote by  $B_n$  a basis for  $A_n$ , without loss of generality, we may assume that  $\mathbb{1}_n \in B_n$  (which is the unshaded version of (2.27)), and for later convenience we introduce

$$B'_n := B_n \setminus \{\mathbb{1}_n\}. \quad (3.21)$$

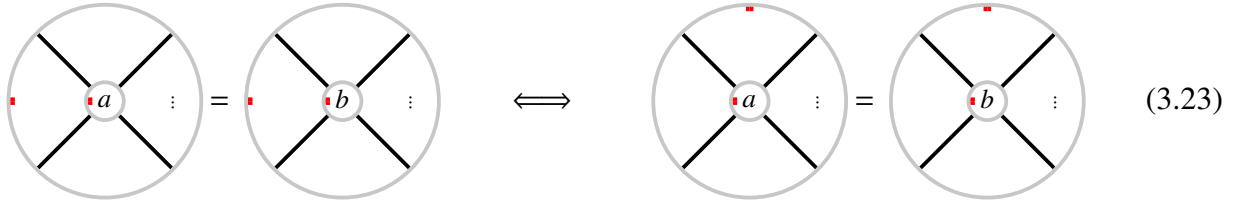
A model described by the transfer operator  $T_n(u)$  is integrable on  $\Omega$  if

$$[T_n(u), T_n(v)] = 0, \quad \forall u, v \in \Omega, \quad (3.22)$$

where  $\Omega \subseteq \mathbb{C}$  is a suitable domain. A common strategy in endowing a model with integrability is to parameterise the corresponding transfer operator to satisfy a set of *local* relations that imply (3.22). For the case of the transfer operators  $T_n^{(d)}(u)$  and  $T_n^{(s)}(u)$ , this involves fixing the parameterisations of the constituent  $R$ - and  $K$ -operators such that a set of sufficient conditions is satisfied, which in some instances, include a Yang–Baxter equation (YBE).

For the set of sufficient conditions considered below, the set implying the commutativity of  $T_n^{(s)}(u)$  is often a subset of those implying the commutativity of  $T_n^{(d)}(u)$ . In either case, we allow for the  $R$ -operator in the centre of the YBE to be parameterised differently from the two peripheral  $R$ -operators. This is more general than what is typically presented in the literature, where the peripheral  $R$ -operators  $R(u)$  and  $R(v)$ , have the same parameterisation as the central operator  $R(u+v)$ , see for example (2.41) and (2.42). We will refer to the central  $R$ -operator in a Yang–Baxter equation as the *auxiliary* operator.

The relations in Proposition 3.2.1 and Proposition 3.2.2 are formulated diagrammatically, but are readily recast in the language of planar algebras. Importantly, each of the relations in (3.25)–(3.26) and (3.30)–(3.32) is *local* in the sense that there exists an ambient disk with a suitable marking, relative to which it holds. In fact, the invertibility of the linear maps  $P_{r_{n,\pm k}}$  associated with the rotation tangles (3.11), implies that the specific marking of the ambient planar tangle is immaterial. To illustrate



$$(3.23)$$

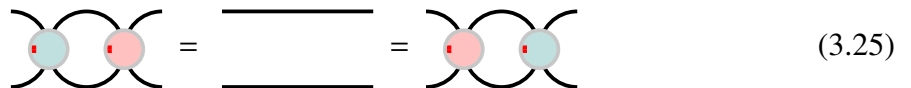
where  $a, b \in A_n$ , with the equalities statements in  $A_n$ .

**Proposition 3.2.1.** *Let the  $R$ -operator parameterisation in (3.3) be given, and suppose there exist*

$$\begin{aligned} \text{---} \text{---} \text{---} &:= \sum_{a \in B_2} y_a(u, v) a, & \text{---} \text{---} \text{---} &:= \sum_{a \in B_2} \bar{y}_a(u, v) a, \end{aligned} \quad (3.24)$$

where  $y_a$  and  $\bar{y}_a$  are scalar functions defined for all  $u, v \in \Omega \subseteq \mathbb{C}$ , such that the following two sets of relations are satisfied:

- *Inversion identities (Inv)*



$$(3.25)$$

- *Yang–Baxter equation (YBE)*



$$(3.26)$$

Then,  $[T_n^{(s)}(u), T_n^{(s)}(v)] = 0$  for all  $u, v \in \Omega$ .

*Proof.* Using the following diagrammatic relations

$$T_n^{(s)}(u)T_n^{(s)}(v) \stackrel{\text{(Inv)}}{=} \text{Diagram 1} \stackrel{\text{(YBE)}}{=} \text{Diagram 2} \quad (3.27)$$

$$= \text{Diagram 3} \stackrel{\text{(Inv)}}{=} \text{Diagram 4} = T_n^{(s)}(v)T_n^{(s)}(u), \quad (3.28)$$

we arrive at the desired result.  $\square$

Now, the corresponding result for the double-row transfer operator.

**Proposition 3.2.2.** *Let the parameterisations in (3.3) be given, and suppose there exist*

$$\text{Diagram 5} := \sum_{a \in B_2} y_a^{(i)}(u, v) a, \quad \text{Diagram 6} := \sum_{a \in B_2} \bar{y}_a^{(i)}(u, v) a, \quad (3.29)$$

where  $y_a^{(i)}$  and  $\bar{y}_a^{(i)}$ ,  $i = 1, 2, 3$ , are scalar functions defined for all  $u, v \in \Omega \subseteq \mathbb{C}$ , such that the following three sets of relations are satisfied:

- Inversion identities (Inv1 - Inv3)

$$\text{Diagram 7} = \text{Diagram 8} \quad (i = 1, 2, 3) \quad (3.30)$$

- Yang–Baxter equations (YBE1 - YBE3)

$$\text{Diagram 9} = \text{Diagram 10} \quad \text{Diagram 11} = \text{Diagram 12} \quad \text{Diagram 13} = \text{Diagram 14} \quad (3.31)$$

- Boundary Yang–Baxter equations (BYBEs)

$$\text{Diagram 15} = \text{Diagram 16} \quad \text{Diagram 17} = \text{Diagram 18} \quad (3.32)$$

where

$$\text{Diagram 19} = \sum_{a \in B_2} y_a^{(1)}(v, u) a, \quad \text{Diagram 20} = \sum_{a \in B_2} \bar{y}_a^{(1)}(v, u) a. \quad (3.33)$$

Then,  $[T_n^{(d)}(u), T_n^{(d)}(v)] = 0$  for all  $u, v \in \Omega$ .

*Proof.* Using the following familiar manipulations [42],

$$\begin{aligned}
 T_n^{(d)}(u)T_n^{(d)}(v) &= \text{(Inv1)} = \text{Diagram 2} \\
 &\quad \text{Diagram 2: } \text{Red '1' in top-left, red 'bar{1}' in bottom-right} \\
 &\quad \text{Diagram 3: } \text{(YBE1)} = \text{Diagram 4} \\
 &\quad \text{Diagram 4: } \text{Red '1' in top-left, red 'bar{1}' in bottom-right} \\
 \\
 &\text{(Inv2)} = \text{Diagram 2} \quad \text{(YBE2)} = \text{Diagram 4} \\
 &\quad \text{Diagram 2: } \text{Red '1' in top-left, red '2' in bottom-left, red 'bar{2}' in bottom-right} \\
 &\quad \text{Diagram 4: } \text{Red '1' in top-left, red '2' in bottom-left, red 'bar{2}' in bottom-right} \\
 \\
 &\text{(BYBEs)} = \text{Diagram 2} \quad \text{(YBE3)} = \text{Diagram 4} \\
 &\quad \text{Diagram 2: } \text{Red '3' in top-left, red '4' in bottom-left, red 'bar{3}' in bottom-right} \\
 &\quad \text{Diagram 4: } \text{Red '3' in top-left, red '4' in bottom-left, red 'bar{4}' in bottom-right} \\
 \\
 &\text{(Inv3+YBE4)} = \text{Diagram 2} \quad \text{(Inv4)} = \text{Diagram 4} \\
 &\quad \text{Diagram 2: } \text{Red '4' in top-left, red 'bar{4}' in bottom-left, red 'u' in bottom-right} \\
 &\quad \text{Diagram 4: } \text{Red 'v' in top-left, red 'v' in bottom-left, red 'v' in bottom-right}
 \end{aligned} \tag{3.34}$$

we arrive at the desired result. In (3.34), YBE4 and Inv4 refer respectively to YBE1 and Inv1 with  $u$  and  $v$  interchanged and 1 replaced by 4, c.f. (3.33).  $\square$

**Remark.** We denote the ‘auxiliary’  $R$ -operators in (3.29) by

$$Y_i(u, v) = \sum_{a \in B_2} y_a^{(i)}(u, v) a, \quad \bar{Y}_i(u, v) = \sum_{a \in B_2} \bar{y}_a^{(i)}(u, v) a, \tag{3.35}$$

and refer to them as *Y-operators*, as short for ‘YBE operators’. The *Y*-operators in (3.24) are identified with  $Y_2(u, v)$  and  $\bar{Y}_2(u, v)$ , respectively. Since the *Y*-operators need not be expressible in terms of the  $R$ -operators themselves, we refer to the YBEs (3.26) and (3.31), and boundary YBEs (3.32) as *generalised*. Moreover, we stress that the auxiliary operators do not necessarily appear in either of

the transfer operators. In many ways, the auxiliary operators are a means to an end in establishing commutativity. We refer to YBE1 under the specialisation  $\bar{Y}_1(u, v) = R(uv)$  as the *standard* YBE.

Traditionally, a model is *Yang–Baxter integrable* if the  $R$ - and  $K$ -operators satisfy a set of local relations, including a YBE, that imply (3.22). Proposition 3.2.1 and Proposition 3.2.2 offer a prototypical set of such relations for the homogeneous single-row transfer operator and the homogeneous double-row transfer operator, respectively. We accordingly refer to the ensuing integrability as *homogeneous Yang–Baxter integrability*. Generalising a notion introduced in [38], the  $R$ - and  $K$ -operators are said to provide a *Baxterisation* if they give rise to a Yang–Baxter integrable model. In our case, we refer to a *homogeneous Baxterisation* as one in which the  $R$ - and  $K$ -operators satisfy the local relations in Proposition 3.2.2. Under mild conditions, a homogeneous Baxterisation will also satisfy the local relations of Proposition 3.2.1, and the corresponding parameterisations of the  $R$ - and  $K$ -operators give rise to two integrable models, one described by  $T_n^{(d)}(u)$  and another by  $T_n^{(s)}(u)$ .

We view a Baxterisation as *specious* if

$$K(u) = k(u)a_1, \quad R(u) = r(u)a_2, \quad \bar{K}(u) = \bar{k}(u)\bar{a}_1, \quad (3.36)$$

where  $a_1, \bar{a}_1 \in A_1$ ,  $a_2 \in A_2$  and  $k, r, \bar{k} : \Omega \rightarrow \mathbb{C}$ , because, in that case, we have

$$T_n^{(d)}(u) = k(u)\bar{k}(u)r^{2n}(u)a, \quad a = P_{T_n^{(d)}}(a_1, a_2, \dots, a_2, \bar{a}_1) \in A_n, \quad (3.37)$$

$$T_n^{(s)}(u) = r^n(u)a, \quad a = P_{T_n^{(s)}}(a_2, \dots, a_2) \in QA_{n,n}, \quad (3.38)$$

from which (3.22) trivially follows for both  $T_n^{(d)}(u)$  and  $T_n^{(s)}(u)$ . In the following, we will disregard specious Baxterisations. We also say that a planar algebra  $(A_n)_{n \in \mathbb{N}_0}$  encodes the Yang–Baxter integrability if no proper planar subalgebra can take its place.

We say that a planar algebra  $(A_n)_{n \in \mathbb{N}_0}$  encodes the homogeneous Yang–Baxter integrability of (i) a model described by the double-row transfer operator if  $\{K(u), \bar{K}(u) \mid u \in \Omega\}$  and  $\{R(u) \mid u \in \Omega\}$  together with the action of planar tangles generate the *full* vector spaces  $A_1$  and  $A_2$ , respectively, and (ii) a model described by the single-row transfer operator if  $\{R(u) \mid u \in \Omega\}$  together with the action of planar tangles generate the *full* vector space  $A_2$ .

### 3.3 Sklyanin's formulation

The partial traces in (3.7) and (3.10) are diagrammatic in origin, accordingly, there is not necessarily a vector space over which the trace is being performed. This is contrasted with the standard formulation of both single-row and double-row transfer operators [43–45], whereby there is a natural tensorial decomposition of the constituent  $R$ -operators, which facilitates the identification of an auxiliary space over which the trace acts. Under particular circumstances, one *can* identify the auxiliary vector space.

For each  $m, n \in \mathbb{N}_0$ , the quadratic tangle

$$K_{m,n} := \text{Diagram of a quadratic tangle with two points labeled 1 and 2 inside a circle, with strands connecting them to the boundary.}, \quad \mathsf{P}_{K_{m,n}} : A_m \times A_n \rightarrow A_{m+n}, \quad (3.39)$$

induces a *tensor product* between  $A_m$  and  $A_n$  within  $A_{m+n}$ . For ease of notation, for  $u \in A_m$  and  $v \in A_n$ , we write  $u \otimes v = \mathsf{P}_{K_{m,n}}(u, v) \in A_{m+n}$ . An  $R$ -operator is called *separable* if it can be decomposed as an element of  $A_1 \otimes A_1$ , diagrammatically, we have

$$R(u) = \text{Diagram of an R-operator with a green circle containing 'u' and two strands entering and exiting.} = \sum_{a_1, a_2 \in B_1} R_{a_1, a_2}(u) \text{Diagram of an R-operator with two strands labeled 'a1' and 'a2' entering and exiting.} \quad (3.40)$$

In this case, the auxiliary vector space of the double-row transfer operator is thus given by the left-most channel, here coloured blue

$$T_n^{(d)}(u) = \text{Diagram of a double-row transfer operator with blue strands labeled 'u' and green strands labeled 'u' in the middle row, with dashed lines connecting them.} \quad (3.41)$$

For the single-row transfer operator with  $R$ -operator as in (3.40), there exists no such identification of the auxiliary channel.

A planar algebra is called *braided*, respectively *symmetric* if each vector space  $A_n$  admits of a representation of the  $n$ -strand braid, respectively symmetric, group algebra. Specialising to the symmetric case and applying the permutation operator to the  $R$ -operator, we define

$$\check{R}(u) = \text{Diagram of an R-operator with a green circle containing 'u' and two strands entering and exiting.} := \sum_{a_1, a_2 \in B_1} R_{a_1, a_2}(u) \text{Diagram of an R-operator with two strands labeled 'a1' and 'a2' entering and exiting.} \quad (3.42)$$

Taking  $\check{R}(u)$  as the  $R$ -operator for both transfer operators, we have

$$\check{T}_n^{(d)}(u) = \text{Diagram of a double-row transfer operator with blue strands labeled 'u' and green strands labeled 'u' in the middle row, with dashed lines connecting them.}, \quad \check{T}_n^{(s)}(u) = \text{Diagram of a single-row transfer operator with blue strands labeled 'u' and green strands labeled 'u' in the middle row, with dashed lines connecting them.}, \quad (3.43)$$

where the auxiliary vector space is threaded through the transfer operator in each case – reminiscent of the standard formulation [43, 44]. In fact, for the double-row transfer operator, by combining both (3.40) and (3.42), the auxiliary space can be threaded through any of the intermediate channels

$$\text{Diagram of a double-row transfer operator with blue strands labeled 'u' and green strands labeled 'u' in the middle row, with dashed lines connecting them.}, \dots, \text{Diagram of a double-row transfer operator with blue strands labeled 'u' and green strands labeled 'u' in the middle row, with dashed lines connecting them.} \quad (3.44)$$

Note that the commutativity of the operator in (3.41), likewise of the double-row transfer operator in (3.43), do not necessarily imply the commutativity of any of the intermediate operators in (3.44).

## 3.4 Hamiltonian limits

A point  $u_* \in \mathbb{C}$  is called an *identity point* of  $T_n(u)$  if  $T_n(u_*)$  is proportional to a left- or right-invertible element in  $A_n$ . About each identity point for which the proportionality is nonzero, we perform a power series expansion of the transfer operator to define the associated *Hamiltonian operators*. As will be clear in the following, two distinct identity points from the same transfer operator may give rise to two different sets of Hamiltonian operators.

Here, we present two sets of sufficient conditions to identify identity points, one for each of the transfer operators  $T_n^{(d)}(u)$  and  $T_n^{(s)}(u)$ . In preparation, we define

$$g: \Omega \rightarrow A_0, \quad u \mapsto \text{Diagram } (3.45), \quad (3.45)$$

where  $\Omega \subseteq \mathbb{C}$  is a suitable domain, and we have expressed the image in our standard diagrammatic representation cf. (3.5). Equivalently, we may write

$$g(u) = P_{\text{tr}_1 \circ M_1}(K(u), \bar{K}(u)) = P_{\text{tr}_1 \circ M_1}(\bar{K}(u), K(u)). \quad (3.46)$$

Composing  $g$  with the evaluation map (2.20), we define the scalar function

$$\hat{g} := e \circ g: \Omega \rightarrow \mathbb{C}. \quad (3.47)$$

We now present sufficient conditions for the double-row transfer operator.

**Proposition 3.4.1.** *Let  $u_* \in \Omega$  and suppose there exist  $l_{u_*}, r_{u_*} \in \mathbb{C}$  such that*

$$\text{Diagram } (3.48) \quad \left| \begin{array}{c} \text{Diagram } (3.48) \\ \text{or} \\ \text{Diagram } (3.48) \end{array} \right| \quad (3.48)$$

*Then,  $u_*$  is an identity point, with  $T_n^{(d)}(u_*) = l_{u_*}^n \hat{g}(u_*) \mathbb{1}_n$  or  $T_n^{(d)}(u_*) = r_{u_*}^n \hat{g}(u_*) \mathbb{1}_n$ , respectively.*

*Proof.* Suppose the left relation in (3.48) holds, then

$$T_n^{(d)}(u_*) = \text{Diagram } (3.49) = l_{u_*}^n \quad \left| \begin{array}{c} \text{Diagram } (3.49) \\ \dots \\ \text{Diagram } (3.49) \end{array} \right| = l_{u_*}^n \quad \dots \quad \left| \begin{array}{c} \text{Diagram } (3.49) \\ \dots \\ \text{Diagram } (3.49) \end{array} \right| = l_{u_*}^n \hat{g}(u_*) \mathbb{1}_n. \quad (3.49)$$

A similar argument applies if the right relation holds.  $\square$

**Remark.** If both relations in (3.48) are true and if  $\hat{g}(u_*) \neq 0$ , then  $l_{u_*}^{n-k} r_{u_*}^k = l_{u_*}^{n-k'} r_{u_*}^{k'}$  for all  $k, k' \in \{0, 1, \dots, n\}$ , hence  $l_{u_*} = r_{u_*}$ .

The sufficient conditions for the single-row transfer operator are as follows.

**Proposition 3.4.2.** Let  $u_* \in \Omega$  and suppose there exist  $m_{u_*}, p_{u_*} \in \mathbb{C}$  such that

$$\begin{array}{c} \text{---} \bullet u_* \text{---} \\ | \quad | \end{array} = m_{u_*} \begin{array}{c} \nearrow \\ \curvearrowright \end{array} \quad \text{or} \quad \begin{array}{c} \text{---} \bullet u_* \text{---} \\ | \quad | \end{array} = p_{u_*} \begin{array}{c} \nearrow \\ \curvearrowright \end{array}. \quad (3.50)$$

Then,  $u_*$  is an identity point, with  $T_n^{(s)}(u_*) = m_{u_*}^n \Omega_n^{-1}$  or  $T_n^{(s)}(u_*) = p_{u_*}^n \Omega_n$ , respectively.

*Proof.* Suppose the left relation in (3.50) holds, then

$$T_n^{(s)}(u_*) = \begin{array}{c} \text{---} \bullet u_* \text{---} \bullet u_* \text{---} \bullet u_* \text{---} \\ | \quad | \quad | \quad | \end{array} = m_{u_*}^n \begin{array}{c} \nearrow \\ \curvearrowright \\ \cdots \\ \nearrow \\ \curvearrowright \end{array} = m_{u_*}^n \Omega_n^{-1}. \quad (3.51)$$

Similar arguments apply if the right relation holds.  $\square$

Now suppose  $u_*$  is an identity point of the transfer operator  $T_n(u)$  where  $T_n(u) \notin \mathbb{C}\mathbb{1}_n$ , and that  $\Omega$  contains an open subset of  $\mathbb{C}$  containing  $u_*$ . It follows that there exists a  $k \in \mathbb{N}$  and a  $H_{n,u_*} \notin \mathbb{C}\mathbb{1}_n$  such that

$$T_n(u_* + \epsilon) = T_n(u_*) \left( p_{k-1}(\epsilon) \mathbb{1}_n + \epsilon^k H_{n,u_*} + O(\epsilon^{k+1}) \right), \quad (3.52)$$

where  $p_{k-1}$  is a polynomial of degree at most  $k-1$  with  $p_{k-1}(0) = 1$ , and we have assumed  $T_n(u_*)$  has a right-inverse, if  $T_n(u_*)$  has a left-inverse only, we can rewrite (3.52) by factoring  $T_n(u_*)$  from the right. The element  $H_{n,u_*}$  is considered a *Hamiltonian* associated with the identity point  $u_*$  and the corresponding transfer operator. We note that this Hamiltonian can be expressed alternatively as

$$H_{n,u_*} = \frac{1}{T_n(u)} \frac{1}{k!} \frac{\partial^k}{\partial u^k} T_n(u) \Big|_{u=u_*} \quad (3.53)$$

where again, we have assumed that  $T_n(u_*)$  has a right-inverse if this is not valid, write (3.53) with the inverse transfer operator to the right of the derivative. In any case, there exists a  $s_k \in \mathbb{C}$  and a nonzero  $h_{n,u_*} \in \text{span}_{\mathbb{C}}(B'_n)$  such that

$$H_{n,u_*} := s_k \mathbb{1}_n + h_{n,u_*}. \quad (3.54)$$

Absorbing the identity term of the Hamiltonian in (3.52), we define

$$\tilde{p}_k(\epsilon) := p_{k-1}(\epsilon) + s_k \epsilon^k, \quad (3.55)$$

and can write (3.52) as

$$T_n(u_* + \epsilon) = T_n(u_*) \left( \tilde{p}_k(\epsilon) \mathbb{1}_n + \epsilon^k h_{n,u_*} + O(\epsilon^{k+1}) \right), \quad (3.56)$$

where  $\tilde{p}_k$  is a polynomial with degree at most  $k$ . Up to rescaling, we refer to the element  $h_{n,u_*}$  as the *principal Hamiltonian* associated with the identity point  $u_*$  and the corresponding transfer operator. When unlikely to cause confusion, we may choose to omit one of the subscripts and write  $h_n$  or  $h_{u_*}$  instead of  $h_{n,u_*}$ . Note that distinct identity points of the same transfer operator may completely change the terms appearing in the power series expansion, which in turn, may give rise to distinct principal

Hamiltonians. Likewise, transfer operators parameterised by different  $R$ -operators may also give rise to distinct identity points and principal Hamiltonians.

**Remark.** In the case of the double-row transfer operator, if either relation in (3.48) holds and  $T_n^{(d)}(u_*) = 0$ , the original transfer operator may be renormalised such that the limit  $u \rightarrow u_*$  yields a nonzero scalar multiple of the identity. This was illustrated in [46] and will be revisited in Section 6.1.

If the transfer operator  $T_n(u)$  describes an integrable model for  $u \in \Omega$ , then we have the familiar commutation relations

$$[h_{n,u_*}, T_n(u)] = [H_{n,u_*}, T_n(u)] = 0, \quad \forall u_*, u \in \Omega. \quad (3.57)$$

## 3.5 Hamiltonians and integrals of motion

Consider a model whose underlying algebraic structure is given by an associative algebra  $\mathcal{A}$  with a basis  $\mathcal{B}$ , and denote by  $T(u) \in \mathcal{A}$  the transfer operator describing a model for all  $u \in \Omega$  where  $\Omega \subseteq \mathbb{C}$  is a suitable domain. Expressing the transfer operator in terms of elements in the basis  $\mathcal{B}$ , we have

$$T(u) = \sum_{a \in \mathcal{B}} t_a(u) a, \quad (3.58)$$

where  $t_a : \Omega \rightarrow \mathbb{C}$  for each  $a \in \mathcal{B}$ . Define the space of scalar functions

$$\mathcal{F} := \text{span}_{\mathbb{C}}\{t_a : \Omega \rightarrow \mathbb{C} \mid a \in \mathcal{B}\} \quad (3.59)$$

and denote by  $\mathcal{B}_T$  a basis for  $\mathcal{F}$ . As an alternative to (3.58), we can express the transfer operator in terms of elements from the basis  $\mathcal{B}_T$

$$T(u) = \sum_{f \in \mathcal{B}_T} f(u) a_f, \quad (3.60)$$

where  $a_f \in \mathcal{A}$  for each  $f \in \mathcal{B}_T$ . Introducing the space of Hamiltonians and corresponding the  $\mathcal{A}$ -subalgebra

$$\mathcal{H}_T := \text{span}_{\mathbb{C}}\{a_f \mid f \in \mathcal{B}_T\}, \quad \mathcal{A}_T := \langle \mathcal{H}_T \rangle_{\mathcal{A}}, \quad (3.61)$$

where we note that  $\dim \mathcal{H}_T \leq \dim \mathcal{F}$  and  $T(u)^n \in \mathcal{A}_T$  for all  $n \in \mathbb{N}$ .

Each nonzero element  $h \in \mathcal{H}_T$  that is not simply proportional to the identity (for  $\mathcal{A}$  unital) could conceivably be considered as the Hamiltonian of the model, while physical considerations may guide the selection. Accordingly, we refer to elements of  $\mathcal{H}_T$  as *Hamiltonians* and preferred choices, for example,  $h_{n,u_*}$  in (3.54), as *principal Hamiltonians*.

In general, we denote the centraliser of  $a$  in  $\mathcal{A}$  by  $C_{\mathcal{A}}(a)$ . For a Hamiltonian  $h \in \mathcal{H}_T$ , we view  $C_{\mathcal{A}}(h)$  as the subalgebra of all  *$h$ -conserved quantities* of the model. If the model is integrable in the sense that

$$[T(u), T(v)] = 0, \quad \forall u, v \in \Omega, \quad (3.62)$$

it follows that  $\mathcal{A}_T$  is commutative, and given a choice of  $h$ , every Hamiltonian is a  $h$ -conserved quantity. In general, the space of all  $h$ -conserved quantities is larger than the space of Hamiltonians as we have the inclusion  $\mathcal{H}_T \subseteq \mathcal{C}_{\mathcal{A}}(h)$ . Finally, we consider the centre of  $\mathcal{C}_{\mathcal{A}}(\mathcal{H}_T)$ , which we denote by  $\mathcal{Z}(\mathcal{C}_{\mathcal{A}}(\mathcal{H}_T))$ , and refer to it as the subalgebra of the *integrals of motion* (IOM) of the model. To summarise, we have the following sequence of algebras relevant to the integrable model

$$\mathcal{A}_T \subseteq \mathcal{Z}(\mathcal{C}_{\mathcal{A}}(\mathcal{H}_T)) \subseteq \mathcal{C}_{\mathcal{A}}(\mathcal{H}_T) \subseteq \mathcal{C}_{\mathcal{A}}(h) \subseteq \mathcal{A}. \quad (3.63)$$

Let us take a moment to unpack the terminology of IOM. Typically the transfer operator corresponding to an integrable model is considered the generating function of the IOM of the model. In this case, the space of IOM is restricted to  $\mathcal{H}_T$ . In our construction, the algebra  $\mathcal{A}$  endows the model with algebraic structure, it is thus natural to extend the notion of IOM beyond those generated by the transfer operator, to all elements of the algebra  $\mathcal{A}$  commuting with all of the Hamiltonians  $\mathcal{H}_T$ , that themselves all mutually commute. In the following, we consider a situation where there exists a single, algebraically independent Hamiltonian.

## 3.6 Polynomial integrability

Let  $\mathcal{A}$  denote an associative algebra and  $\{T(u) \in \mathcal{A} \mid u \in \Omega\}$  a one parameter family of operators, where  $\Omega \subseteq \mathbb{C}$ . If there exists a  $b \in \mathcal{A}$  such that

$$T(u) \in \mathbb{C}[b], \quad \forall u \in \Omega, \quad (3.64)$$

then  $[T(u), T(v)] = 0$  trivially follows for all  $u, v \in \Omega$ . Suppose the family corresponds to the transfer operator of a model, for example,  $\{T_n(u) \in A_n \mid u \in \Omega\}$  in the planar-algebraic setting defined above. If there exists some  $b_n \in A_n$  such that  $T_n(u)$  satisfies (3.64), we say that the transfer operator is *polynomialisable*, the model is *polynomially integrable* and that  $b_n$  generates the polynomial integrability. From an algebraic perspective, a polynomially integrable model may thus be considered as *trivially integrable*.

It may seem unreasonable to suppose that there exist physically relevant models exhibiting polynomial integrability. However, this is exactly what we find. In fact, for the models that we analyse see Chapter 6, it is the Hamiltonian elements defined in Section 3.4 that play the role of  $b$ , in which case the transfer operator is polynomial in the Hamiltonian.

In preparation for this analysis, we devote the following chapter. The main result (Proposition 4.2.2) is a classification of commuting one parameter families  $\{T(u) \in \mathcal{A} \mid u \in \Omega\}$  that satisfy (3.64) with  $\mathcal{A}$  a semisimple algebra. A simple corollary of this classification (Corollary 4.2.3) serves to indicate the ubiquity of polynomial integrability among integrable models.



Components of the following publication have been incorporated into Chapter 4.

[2] X. Poncini, J. Rasmussen, *Integrability of planar-algebraic models*, J. Stat. Mech. (2023) 073101, arXiv:2206.14462 [math-ph].

# Chapter 4

---

## Algebraic integrability

---

In this chapter, we characterise polynomial integrability in a general algebraic setting. We begin by presenting necessary and sufficient conditions for a parameter-dependent element of a matrix algebra to be expressible as a polynomial in another parameter-*independent* element. This result is then extended to elements within semisimple algebras. We then consider spectral properties of parameter-dependent linear operators, in particular, we introduce a notion of *spurious* degeneracies and show that there can only exist finitely many of these. Finally, we review some basic properties of cellular algebras, which we cast in a diagrammatic representation.

### 4.1 Block Toeplitz

We begin this section by introducing some notations. Denote by  $\mathcal{M}_n(\mathcal{R})$  the set of all  $n \times n$  matrices whose entries are elements of the set  $\mathcal{R}$ . For  $z \in \mathcal{M}_n(\mathbb{C})$ , the centraliser of  $z$  in  $\mathcal{M}_n(\mathbb{C})$  is denoted by  $C(z)$ . We denote by  $\mathcal{R}[x]$  the set of polynomials in  $x$  with coefficients in the set  $\mathcal{R}$ , similarly, we denote by  $\mathcal{R}(x)$  the set of rational functions in  $x$ . For us,  $x$  may be an indeterminate or an algebraic element, for example,  $x \in \mathcal{M}_n(\mathbb{C})$  implies that  $\mathbb{C}[x]$  and  $\mathbb{C}(x)$  are algebras that admit a finite-dimensional basis. Let  $c_z$  and  $m_z$  denote the characteristic and minimal polynomials of  $z \in \mathcal{M}_n(\mathbb{C})$  respectively, and note that [47]

$$c_z = m_z \iff C(z) = \mathbb{C}[z]. \quad (4.1)$$

A  $z \in \mathcal{M}_n(\mathbb{C})$  is called *non-derogatory* if it satisfies the equivalent conditions above. Each of the equivalent statements (4.1) is basis independent, it follows that any matrix similar to a non-derogatory matrix is itself non-derogatory. This notion naturally extends to linear operators on  $\mathbb{C}^n$ , such an operator is non-derogatory if there exists a basis with respect to which the corresponding matrix representation is non-derogatory.

A matrix  $J$  is in *Jordan canonical form* (JCF) if it is block-diagonal with *Jordan blocks* along the

diagonal, i.e.  $J = \text{diag}(J_{r_1}(\lambda_1), \dots, J_{r_s}(\lambda_s))$ , where a Jordan block is given by

$$J_r(\lambda) := \begin{bmatrix} \lambda & 1 & 0 & \dots & 0 \\ 0 & \lambda & 1 & \ddots & \vdots \\ \vdots & \ddots & \ddots & \ddots & 0 \\ 0 & \dots & 0 & \lambda & 1 \\ 0 & \dots & 0 & 0 & \lambda \end{bmatrix} \in \mathcal{M}_r(\mathcal{R}). \quad (4.2)$$

For an analytic function  $f$ , taking  $J$  as the argument, we have  $f(J) = \text{diag}(f(J_{r_1}(\lambda_1)), \dots, f(J_{r_s}(\lambda_s)))$ , where

$$f(J_r(\lambda)) = \begin{bmatrix} f(\lambda) & f'(\lambda) & \frac{f''(\lambda)}{2} & \dots & \frac{f^{(r-1)}(\lambda)}{(r-1)!} \\ 0 & f(\lambda) & f'(\lambda) & \ddots & \vdots \\ \vdots & \ddots & \ddots & \ddots & \frac{f''(\lambda)}{2} \\ 0 & \dots & 0 & f(\lambda) & f'(\lambda) \\ 0 & \dots & 0 & 0 & f(\lambda) \end{bmatrix}. \quad (4.3)$$

An *upper-triangular Toeplitz matrix* can be characterised by the tuple  $\mathbf{a}_r = (a_1, a_2, \dots, a_r)$  in  $\mathcal{R}^{\times r}$ , and is given by

$$T(\mathbf{a}_r) = \begin{bmatrix} a_1 & a_2 & \dots & a_r \\ 0 & a_1 & \ddots & \vdots \\ \vdots & \ddots & \ddots & a_2 \\ 0 & \dots & 0 & a_1 \end{bmatrix}. \quad (4.4)$$

Accordingly, a *block-diagonal upper-triangular Toeplitz matrix* (BT), it given by  $\text{diag}(T(\mathbf{a}_{r_1}^{[1]}), \dots, T(\mathbf{a}_{r_s}^{[s]}))$ , and we say that it has a block partitioning of  $r_1, \dots, r_s$ . Indeed, the block partitioning of a given BT matrix is not unique, for our purposes it is often sufficient that there exists a block partitioning.

**Lemma 4.1.1.** *There exists a  $b \in \mathcal{M}_n(\mathbb{C})$  in JCF such that  $B(x) \in \mathbb{C}(x)[b]$  if and only if  $B(x) \in \mathcal{M}_n(\mathbb{C}(x))$  is BT.*

*Proof.* First “ $\Rightarrow$ ”. There exists an  $x$ -dependent polynomial  $p_x$ , such that  $B(x) = p_x(b)$ . As  $b$  is in JCF it follows from (4.3) that  $B(x)$  is BT.

Now “ $\Leftarrow$ ”. Suppose a block partitioning of  $B(x)$  is given by  $r_1, \dots, r_s$ , let

$$b = \text{diag}(J_{r_1}(\lambda_1), \dots, J_{r_s}(\lambda_s)) \quad (4.5)$$

where  $\lambda_1, \dots, \lambda_s \in \mathbb{C}$  are all distinct. By construction  $b$  is non-derogatory and satisfies  $[b, B(x)] = 0$ . It follows from (4.1) that  $B(x) \in \mathbb{C}(x)[b]$ .  $\square$

**Proposition 4.1.2.** *Suppose  $B(x) \in \mathcal{M}_n(\mathbb{C}(x))$ . There exists a  $b \in \mathcal{M}_n(\mathbb{C})$  such that  $B(x) \in \mathbb{C}(x)[b]$  if and only if there exists a  $S \in \mathcal{M}_n(\mathbb{C})$  such that  $S^{-1}B(x)S$  is BT.*

*Proof.* First “ $\Rightarrow$ ”. There exists an  $x$ -dependent polynomial  $p_x$  such that  $B(x) = p_x(b)$ . Denote by  $S \in \mathcal{M}_n(\mathbb{C})$  the similarity matrix such that  $S^{-1}bS$  is in JCF. Then  $S^{-1}B(x)S = S^{-1}p_x(b)S = p_x(S^{-1}bS)$ , and it follows from Lemma 4.1.1 that  $S^{-1}B(x)S$  is BT.

Now “ $\Leftarrow$ ”. We have  $S^{-1}B(x)S$  BT. From Lemma 4.1.1,  $S^{-1}B(x)S \in \mathbb{C}(x)[\bar{b}]$  for some  $\bar{b}$  in JCF. Then  $B(x) \in \mathbb{C}(x)[b]$ , where  $b = S\bar{b}S^{-1}$ .  $\square$

**Corollary 4.1.3.** *Let  $\Omega \subseteq \mathbb{C}$  and suppose  $\{C(x) \in \mathcal{M}_n(\mathbb{C}) \mid x \in \Omega\}$  is a commutative subset of  $\mathcal{M}_n(\mathbb{C})$ , where each element is diagonalisable. There exists a  $b \in \mathcal{M}_n(\mathbb{C})$  such that  $C(x) \in \mathbb{C}[b]$  for all  $x \in \Omega$ .*

*Proof.* As each  $C(x)$  is diagonalisable and pairwise commuting, there exists an  $x$ -independent basis in  $\mathbb{C}^n$  with respect to which all  $C(x)$  are diagonal, see for example [48]. As diagonal matrices are BT, the result follows from Proposition 4.1.2.  $\square$

**Remark.** Corollary 4.1.3 implies that *any* integrable model described by a family of pairwise commuting and diagonalisable matrices is *polynomially integrable*.

This result illustrates the ubiquity of polynomial integrability among integrable models. For the reader in a hurry, we present a self-contained proof of Corollary 4.1.3, independent of the details of this chapter: As each  $C(x)$  is diagonalisable and pairwise commuting, there exists an  $x$ -independent  $S \in \mathcal{M}_n(\mathbb{C})$  such that  $S^{-1}C(x)S = \text{diag}(\gamma_1(x), \dots, \gamma_n(x))$ . Construct a  $\bar{b} = \text{diag}(\lambda_1, \dots, \lambda_n)$  where each  $\lambda_1, \dots, \lambda_n \in \mathbb{C}$  are distinct, and fix the coefficients  $a_0(x), \dots, a_{n-1}(x) \in \mathbb{C}$  of the polynomial

$$p_x(y) = \sum_{j=0}^{n-1} a_j(x)y^j, \quad (4.6)$$

such that  $p_x(\lambda_i) = \gamma_i(x)$  for all  $i = 0, \dots, n-1$  and  $x \in \Omega$ . As  $\lambda_1, \dots, \lambda_n$  are all distinct, one can always do this. It follows that  $C(x) = p_x(b)$  where  $b = S\bar{b}S^{-1}$ .

The following section is devoted to elevating Proposition 4.1.2 and Corollary 4.1.3 such that they apply to elements of *semisimple* algebras.

## 4.2 Semisimple algebras

Let  $\mathcal{A}$  be a finite-dimensional unital associative algebra over  $\mathbb{C}$ . Motivated by the discussion of matrices presented in Section 4.1, we generalise the notion of *non-derogatory* elements to those  $b \in \mathcal{A}$  satisfying

$$C_{\mathcal{A}}(b) = \mathbb{C}[b]. \quad (4.7)$$

In this case, we say that  $b$  generates its own centraliser. For  $b$  non-derogatory it follows that each  $c \in C_{\mathcal{A}}(b)$  can be expressed as a polynomial in  $b$ , that is

$$c = \sum_{i=0}^{d-1} c_i b^i, \quad d = \dim \mathbb{C}[b] \quad (4.8)$$

where  $c_0, \dots, c_{d-1} \in \mathbb{C}$ .

Let us now recall some general results about the structure of  $\mathcal{A}$ . Up to isomorphism,  $\mathcal{A}$  has finitely many irreducible modules here denoted by  $L_1, \dots, L_r$ , each of which are finite-dimensional and satisfy

$$\mathcal{A}/\text{rad}(\mathcal{A}) \cong \bigoplus_{i=1}^r \text{End}(L_i), \quad (4.9)$$

where  $\text{rad}(\mathcal{A})$  denotes the Jacobson radical [49]. Letting  $\rho_i$  denote the representation corresponding to the module  $L_i$  for each  $i = 1, \dots, r$ , the homomorphism

$$\rho := \bigoplus_{i=1}^r \rho_i : \mathcal{A} \rightarrow \bigoplus_{i=1}^r \text{End}(L_i) \quad (4.10)$$

is surjective with kernel given by  $\text{rad}(\mathcal{A})$ .

An algebra  $\mathcal{A}$  is *semisimple* if its regular representation is completely reducible [49]. Equivalently,  $\mathcal{A}$  is semisimple under the following statements

$$\text{rad}(\mathcal{A}) = \{0\} \iff \mathcal{A} \cong \bigoplus_{i=1}^r (\dim L_i) L_i \iff \dim \mathcal{A} = \sum_{i=1}^r (\dim L_i)^2. \quad (4.11)$$

It follows that for  $\mathcal{A}$  semisimple,  $\rho$  is an isomorphism.

**Lemma 4.2.1.** *Let  $\mathcal{A}$  be a semisimple algebra, and suppose  $b \in \mathcal{A}$ . Then,  $b$  is non-derogatory if and only if  $\rho(b)$  is non-derogatory.*

*Proof.* First “ $\Rightarrow$ ”. We have  $b \in \mathcal{A}$  non-derogatory. Consider  $\psi \in \text{End}(L)$  satisfying  $\psi \circ \rho(b) = \rho(b) \circ \psi$ . As  $\mathcal{A}$  is semisimple,  $\rho$  is an isomorphism, and we can therefore write  $\rho^{-1}(\psi)b = b\rho^{-1}(\psi)$ . It follows from  $b$  being non-derogatory that  $\rho^{-1}(\psi) \in \mathbb{C}[b]$  hence  $\psi \in \mathbb{C}[\rho(b)]$ , so  $\rho(b)$  is non-derogatory.

Now “ $\Leftarrow$ ”. We have  $\rho(b) \in \text{End}(L)$  non-derogatory. Consider  $c \in \mathcal{A}$  satisfying  $cb = bc$ . As  $\rho$  is a homomorphism, we have  $\rho(c)\rho(b) = \rho(b)\rho(c)$ . It follows from  $\rho(b)$  being non-derogatory that  $\rho(c) \in \mathbb{C}[\rho(b)]$  hence  $c \in \mathbb{C}[b]$ , so  $b$  is non-derogatory.  $\square$

The following is an algebraic version of Proposition 4.1.2.

**Proposition 4.2.2.** *Let  $\mathcal{A}$  be a semisimple algebra, and suppose  $U(x) \in \mathcal{A}$ . There exists an  $x$ -independent  $b \in \mathcal{A}$  such that  $U(x) \in \mathbb{C}(x)[b]$  if and only if there exists a  $x$ -independent  $L$ -basis such that the matrix representation of  $\rho(U(x))$  is BT.*

*Proof.* First “ $\Rightarrow$ ”. We have  $U(x) \in \mathbb{C}(x)[b]$  where  $b \in \mathcal{A}$  is  $x$ -independent. As  $\rho$  is a homomorphism, we have  $\rho(U(x)) \in \mathbb{C}(x)[\rho(b)]$ . As  $\rho(b)$  is  $x$ -independent, there exists an  $x$ -independent  $L$ -basis with respect to which the corresponding matrix representation of  $\rho(b)$  is in JCF. It follows from Lemma 4.1.1 that the matrix representation of  $\rho(U(x))$  with respect to this basis is BT.

Now “ $\Leftarrow$ ”. Denote by  $B$  the  $L$ -basis with respect to which the matrix representation,  $U(x)$ , of  $\rho(U(x))$  is BT. Construct a  $\psi \in \text{End}(L)$  such that the matrix representation,  $P$ , with respect to  $B$  is in JCF with a block partitioning matching  $U(x)$ , and with each block having a unique eigenvalue. By

construction  $P$  is non-derogatory and by Lemma 4.2.1, so to is  $b := \rho^{-1}(\psi)$ . We also note that  $U(x)P = PU(x)$ , hence  $\rho(U(x)) \circ \psi = \psi \circ \rho(U(x))$ . As  $\rho$  is an isomorphism, we arrive at  $U(x)b = bU(x)$  from which it follows that  $U(x) \in \mathbb{C}(x)[b]$ .  $\square$

We also have the algebraic counterpart to Corollary 4.1.3.

**Corollary 4.2.3.** *Let  $\mathcal{A}$  be a semisimple algebra,  $\Omega \subseteq \mathbb{C}$ , and suppose  $\{C(x) \in \mathcal{A} \mid x \in \Omega\}$  is a commutative subset of  $\mathcal{A}$  such that there exists an  $L$ -basis relative to which the matrix representation  $\rho(C(x))$  is diagonal. There exists  $b \in \mathcal{A}$  such that  $C(x) \in \mathbb{C}[b]$  for every  $x \in \Omega$ .*

**Remark.** Yang–Baxter relation subfactor planar algebras offer themselves as prototypical algebras endowing models with polynomial integrable structure. They are (i) semisimple and therefore admit to the previous classification, (ii) possess an inner product, with respect to which the diagonalisability of the transfer operator can be established, and (iii) have a natural Yang–Baxter integrable structure. These features together translate the *global* property of polynomial integrability into *local* properties satisfied by the constituent  $K$ - and  $R$ -operators of a given transfer operator. For  $T_n^{(d)}(u)$  these are YBEs, BYBEs, inversion identities, and self-adjointness. While for  $T_n^{(s)}(u)$  the BYBEs are replaced by  $R$ -operator crossing symmetry. We return to these observations in Chapter 5.

## 4.3 Spectral degeneracies

Let  $A(x) : \mathbb{C}^n \rightarrow \mathbb{C}^n[x]$  be an  $x$ -dependent linear map such that, with respect to a particular basis, each element of the corresponding matrix representation is polynomial in  $x$ . Denote the corresponding characteristic polynomial by

$$c(x, \lambda) := \det(\lambda \text{id} - A(x)), \quad (4.12)$$

where  $\text{id}$  denotes the identity matrix. By construction  $c(x, \lambda)$  is a polynomial in both  $x$  and  $\lambda$ , whose degree in  $\lambda$  is  $n$ . Indeed, determining the zeros of (4.12) in terms of  $\lambda$  gives the  $n$  eigenvalues of  $A(x)$ , which, in general, will depend on  $x$ . If, for  $x$  an indeterminate, there are less than  $n$  distinct eigenvalues, we say there exists *permanent degeneracies* in the spectrum of  $A(x)$ . Suppose the spectrum of  $A(x)$  possesses  $l$  distinct eigenvalues for  $x$  an indeterminate (where of course  $l \leq n$ ). If, for a given  $x_0 \in \mathbb{C}$ , the spectrum of  $A(x_0)$  possesses less than  $l$  distinct eigenvalues, we say there exist *spurious degeneracies* in the spectrum of  $A(x)$  at the point  $x_0$ . As we will see in Proposition 4.3.1 below, for our particular operator  $A(x)$ , there are finitely many  $x_0$ -values for which spurious degeneracies arise.

To this end, we note that a polynomial  $f(x, y)$  is *irreducible* if it cannot be written as a product of two non-constant polynomial factors. The function  $y(x)$  that satisfies  $f(x, y(x)) = 0$ , is called an *algebraic function*, and we recall that these functions possess finitely many branch points and at most algebraic singularities [50]. Also, two polynomials  $f(x, y)$  and  $g(x, y)$  are *relatively prime* if they share no non-constant factors. In this case, there are finitely many  $x_0 \in \mathbb{C}$  for which  $f(x_0, y)$  and  $g(x_0, y)$  share the same root  $y(x_0)$ , see for example Theorem 3 on page 300 of [50].

**Proposition 4.3.1.** *The spectrum of  $A(x)$  is spurious for finitely many  $x$ -values in  $\mathbb{C}$ .*

*Proof.* The characteristic polynomial of  $A(x)$  admits the following decomposition

$$c(x, \lambda) := \prod_{i=1}^t c_i(x, \lambda), \quad (4.13)$$

where  $c_i(x, \lambda) \in \mathbb{C}[x, \lambda]$  is irreducible for all  $i = 1, \dots, t$  and  $1 \leq t \leq n$ . There are two possible sources of spurious degeneracies, the first are those arising from each individual  $c_i(x, \lambda)$ . As  $c_i(x, \lambda)$  is an irreducible polynomial, it only contributes spurious degeneracies at values  $x_0 \in \mathbb{C}$  for which  $c_i(x_0, \lambda) \in \mathbb{C}[\lambda]$  becomes reducible, there are finitely many such  $x$ -values. The second possible source is from each pair  $c_i(x, \lambda)$  and  $c_j(x, \lambda)$  such that  $i \neq j$ , which are either relatively prime or equal up to a scalar multiple. In the latter case, the pair contributes permanent degeneracies to the spectrum of  $A(x)$ , while in the former case, the pair contributes spurious degeneracies for finitely many  $x$ -values. Together with the previous observations and the fact that there are finitely many irreducible factors in (4.13), the result follows.  $\square$

## 4.4 Cellular algebras

In this section, we define cellular algebras, their simple modules and give a criterion for semisimplicity. Before establishing these results explicitly, we outline key aspects with reference to their appearance below. A cellular algebra  $\mathcal{A}$  is defined with respect to a collection of *cell datum*  $(\Lambda, M, C, *)$ , where  $\Lambda$  is partially ordered set,  $M(\lambda)$  for each  $\lambda \in \Lambda$  is a finite set,  $C$  is an injective map and  $*$  is an anti-involution. This data, presented in Definition 4.4.1, equip the algebra with the following features: **(C1)** the existence of a basis, endowed from  $C$ , whose elements can be split into two components each sharing a common label  $\lambda \in \Lambda$ ; **(C2)** an anti-involution  $*$ , that facilitates the exchange of the two components; **(C3)** a product between an element of the algebra and a basis element with an index  $\lambda$ , such that the result is a linear combination of elements, each with an index less than or equal to  $\lambda$ .

The partitioning of basis elements into two components, endowed from **(C1)**, suggests a diagrammatic representation whereby each basis element is expressed as a rectangle with a distinct bottom and top component accompanied by an index  $\lambda$ , see (4.16). In this representation, the product **(C3)** amounts to stacking diagrams where  $ab$  corresponds to  $b$  atop  $a$ , and suggests a natural collection of left modules  $W(\lambda)$  for each  $\lambda \in \Lambda$ , with a basis consisting of the lower component of the algebraic basis elements labelled by  $\lambda$ , see equations (4.21) and (4.22). Similarly one can construct a right module  $W(\lambda)^*$  whose basis consists of the upper component of the algebraic elements labelled by  $\lambda$ . Each  $W(\lambda)$  is equipped with a natural bilinear form  $\phi_\lambda$ , endowed from the product **(C3)**, see (4.24) and (4.25). This bilinear form is shown, in Proposition 4.4.2, to encode the irreducibility of the module  $W(\lambda)$ , i.e., when the radical of  $\phi_\lambda$  is trivial the module is simple. Finally, if the collection of radicals of  $\phi_\lambda$  for all  $\lambda \in \Lambda$  is trivial, it follows that the algebra decomposes as a direct sum of simple modules.

We now proceed in greater detail, the presentation closely resembles the original [51]. Most proofs are omitted. Care is taken to cast key results in the aforementioned diagrammatic representation. Let  $\mathcal{R}$  denote a commutative ring with identity.

**Definition 4.4.1.** A cellular algebra over  $\mathcal{R}$  is an associative unital algebra  $\mathcal{A}$ , together with cell datum  $(\Lambda, M, C, *)$  where

(C1)  $\Lambda$  is a partially ordered set and for each  $\lambda \in \Lambda$ ,  $M(\lambda)$  is a finite set such that

$$C : \bigsqcup_{\lambda \in \Lambda} M(\lambda) \times M(\lambda) \rightarrow \mathcal{A}, \quad (4.14)$$

is an injective map with image an  $\mathcal{R}$ -basis of  $\mathcal{A}$ .

(C2) If  $\lambda \in \Lambda$  and  $S, T \in M(\lambda)$ , write  $C(S, T) = C_{S,T}^\lambda \in \mathcal{A}$ . Then  $*$  is an  $\mathcal{R}$ -linear anti-involution of  $\mathcal{A}$  such that  $(C_{S,T}^\lambda)^* = C_{T,S}^\lambda$ .

(C3) If  $\lambda \in \Lambda$  and  $S, T \in M(\lambda)$  then for any element  $a \in \mathcal{A}$  we have

$$a C_{S,T}^\lambda \equiv \sum_{S' \in M(\lambda)} r_a(S', S) C_{S',T}^\lambda \pmod{\mathcal{A}(< \lambda)}, \quad (4.15)$$

where  $r_a(S', S) \in \mathcal{R}$  is independent of  $T$  and where  $\mathcal{A}(< \lambda)$  is the  $\mathcal{R}$ -submodule of  $\mathcal{A}$  generated by  $\{C_{S'',T''}^\mu \mid \mu < \lambda; S'', T'' \in M(\mu)\}$ .

The image under the map defined in (C1) here denoted  $C_{S,T}^\lambda$ , and its image under the anti-involution  $*$  defined in (C2) admit the diagrammatic representations

$$C_{S,T}^\lambda = \begin{array}{c} T \\ \hline S \end{array} \lambda, \quad (C_{S,T}^\lambda)^* = \begin{array}{c} S \\ \hline T \end{array} \lambda, \quad (4.16)$$

respectively. Similarly, casting the product (C3) diagrammatically, we have

$$\begin{array}{c} T \\ \hline S \\ \hline a \end{array} \lambda = \sum_{\substack{\lambda' \in \Lambda \\ S', T' \in M(\lambda)}} k_{\lambda'}(S', T') \begin{array}{c} T \\ \hline S \\ \hline T' \\ \hline S' \end{array} \lambda' \equiv \sum_{S' \in M(\lambda)} r_a(S', S) \begin{array}{c} T \\ \hline S' \end{array} \lambda \pmod{\mathcal{A}(< \lambda)}, \quad (4.17)$$

where  $a$ , expressed in terms of the basis afforded by (C1), and  $r_a(S', S)$  are given by

$$\begin{array}{c} a \\ \hline \end{array} = \sum_{\substack{\lambda' \in \Lambda \\ S', T' \in M(\lambda)}} k_{\lambda'}(S', T') \begin{array}{c} T' \\ \hline S' \end{array} \lambda', \quad r_a(S', S) = \sum_{T' \in M(\lambda)} k_\lambda(S', T') \begin{array}{c} S \\ \hline T' \end{array} \lambda. \quad (4.18)$$

For each  $\lambda \in \Lambda$ , define

$$\mathcal{A}(\{\lambda\}) := \langle C_{S,T}^\lambda \mid S, T \in M(\lambda) \rangle_{\mathcal{R}} \quad (4.19)$$

and note that  $\mathcal{A} \cong \bigoplus_{\lambda \in \Lambda} \mathcal{A}(\{\lambda\})$  as  $\mathcal{R}$ -modules. It follows from **(C3)** that for each  $S_1, S_2, T_1, T_2 \in M(\lambda)$ , we have

$$C_{S_1, T_1}^\lambda C_{S_2, T_2}^\lambda \equiv \psi(T_1, S_2) C_{S_1, T_2}^\lambda \pmod{\mathcal{A}(< \lambda)}, \quad (4.20)$$

where  $\psi(T_1, S_2) \in \mathcal{R}$ , readily extends to the bilinear map  $\psi : M(\lambda) \times M(\lambda) \rightarrow \mathcal{R}$ .

Let the left, respectively right,  $\mathcal{A}$ -modules  $W(\lambda)$  and  $W(\lambda)^*$  be defined as the free  $\mathcal{R}$ -modules with the common basis  $\{C_S \mid S \in M(\lambda)\}$ , yet distinct  $\mathcal{A}$ -actions

$$aC_S = \sum_{S' \in M(\lambda)} r_a(S', S) C_{S'}, \quad C_S a = \sum_{S' \in M(\lambda)} r_{a^*}(S', S) C_{S'}, \quad a \in \mathcal{A}. \quad (4.21)$$

The corresponding diagrammatic representation of a left, respectively right, module basis element is given by

$$C_S = \boxed{\begin{array}{c} \text{---} \\ S \end{array}}^\lambda, \quad C_T = \boxed{\begin{array}{c} T \\ \text{---} \end{array}}_\lambda, \quad (4.22)$$

where  $C_S \in W(\lambda)$  and  $C_T \in W(\lambda)^*$ , and whose action (4.21) interpreted diagrammatically is consistent with (4.17). We have the natural  $\mathcal{R}$ -module isomorphism

$$C^\lambda : W(\lambda) \otimes_{\mathcal{R}} W(\lambda) \rightarrow A(\{\lambda\}), \quad C_S \otimes C_T \mapsto C_{S, T}^\lambda, \quad (4.23)$$

and the bilinear form

$$\phi_\lambda : W(\lambda) \times W(\lambda) \rightarrow \mathcal{R}, \quad (C_S, C_T) \mapsto \psi(S, T), \quad (4.24)$$

both of which can be expressed diagrammatically as

$$C^\lambda(C_S \otimes C_T) = \boxed{\begin{array}{c} T \\ \text{---} \\ S \end{array}}^\lambda, \quad \phi_\lambda(C_S, C_T) = \boxed{\begin{array}{c} T \\ \text{---} \\ S \end{array}}_\lambda. \quad (4.25)$$

We note that the form  $\phi_\lambda$  is *symmetric*  $\phi_\lambda(u, v) = \phi_\lambda(v, u)$ , *invariant* under the involution  $\phi_\lambda(a^*u, v) = \phi_\lambda(u, av)$ , and satisfies  $C^\lambda(u \otimes v)w = \phi_\lambda(v, w)u$  for all  $u, v, w \in W(\lambda)$  and all  $a \in \mathcal{A}(\{\lambda\})$ .

The *radical* of  $\phi_\lambda$  is defined

$$\text{rad } \phi_\lambda := \{u \in W(\lambda) \mid \phi_\lambda(u, v) = 0 \text{ for all } v \in W(\lambda)\}. \quad (4.26)$$

Letting  $\{C_{S_1}, \dots, C_{S_{d_\lambda}}\}$  be an ordered basis for  $W(\lambda)$ , such that  $S_1, \dots, S_{d_\lambda} \in M(\lambda)$ . Then the matrix

$$G_\lambda := \begin{bmatrix} \phi_\lambda(C_{S_1}, C_{S_1}) & \phi_\lambda(C_{S_1}, C_{S_2}) & \dots & \phi_\lambda(C_{S_1}, C_{S_{d_\lambda}}) \\ \phi_\lambda(C_{S_2}, C_{S_1}) & \phi_\lambda(C_{S_2}, C_{S_2}) & \dots & \phi_\lambda(C_{S_2}, C_{S_{d_\lambda}}) \\ \vdots & \vdots & \ddots & \vdots \\ \phi_\lambda(C_{S_{d_\lambda}}, C_{S_1}) & \phi_\lambda(C_{S_{d_\lambda}}, C_{S_2}) & \dots & \phi_\lambda(C_{S_{d_\lambda}}, C_{S_{d_\lambda}}) \end{bmatrix} \quad (4.27)$$

is symmetric, and is referred to as the *Gram matrix*. We conclude by establishing the following.

**Proposition 4.4.2.** *The following statement holds*

$$\det G_\lambda \neq 0 \iff \text{rad } \phi_\lambda = \{0\} \iff \{a_\lambda \in \mathcal{A}(\{\lambda\}) \mid a_\lambda v = 0 \text{ for all } v \in W(\lambda)\} = \{0\}. \quad (4.28)$$

*Proof.* First “1  $\Leftrightarrow$  2”. Observe  $\ker G_\lambda = \text{rad } \phi_\lambda$ , and note  $\ker G_\lambda = \{0\} \Leftrightarrow \det G_\lambda \neq 0$ .

Now “1  $\Leftrightarrow$  3”. As above, let  $\{C_{S_1}, \dots, C_{S_{d_\lambda}}\}$  be an ordered basis for  $W(\lambda)$ , and construct an arbitrary element of  $\mathcal{A}(\{\lambda\})$  via the isomorphism (4.23)

$$a_\lambda = \sum_{i,j=1}^{d_\lambda} c_{ij}^{(\lambda)} C^\lambda(S_i \otimes_R S_j) = \sum_{i,j=1}^{d_\lambda} c_{ij}^{(\lambda)} C_{S_i, S_j}^\lambda, \quad (4.29)$$

where each  $c_{ij}^{(\lambda)} \in \mathcal{R}$ . Acting an arbitrary basis vector  $C_{S_k} \in W(\lambda)$  on  $a_\lambda$ , we have

$$a_\lambda C_{S_k} = \left( \sum_{i,j=1}^{d_\lambda} c_{ij}^{(\lambda)} C_{S_i, S_j}^\lambda \right) C_{S_k} = \sum_{i,j=1}^{d_\lambda} c_{ij}^{(\lambda)} \phi_\lambda(C_{S_j}, C_{S_k}) C_{S_i} = \sum_{i=1}^{d_\lambda} \left( \sum_{j=1}^{d_\lambda} c_{ij}^{(\lambda)} \phi_\lambda(C_{S_j}, C_{S_k}) \right) C_{S_i}. \quad (4.30)$$

As each  $C_{S_i}$  are linearly independent, the statement  $a_\lambda C_{S_k} = 0$  for all  $k = 1, \dots, d_\lambda$ , is equivalent to

$$\sum_{j=1}^{d_\lambda} c_{ij}^{(\lambda)} \phi_\lambda(C_{S_j}, C_{S_k}) = 0. \quad (4.31)$$

This set of homogeneous equations can be expressed as the matrix equation

$$G_\lambda \mathbf{c}_i^{(\lambda)} = 0, \quad \mathbf{c}_i^{(\lambda)} = \begin{bmatrix} c_{i1}^{(\lambda)} \\ c_{i2}^{(\lambda)} \\ \vdots \\ c_{id_\lambda}^{(\lambda)} \end{bmatrix}, \quad (4.32)$$

for  $i = 1, \dots, d_\lambda$ . The set of homogeneous matrix equations (4.32) have a non-trivial solution if and only if  $\det G_\lambda = 0$ .  $\square$

It follows that the representation

$$\rho := \bigoplus_{\lambda \in \Lambda} \rho_\lambda: \mathcal{A} \rightarrow \bigoplus_{\lambda \in \Lambda} \text{End}(W(\lambda)) \quad (4.33)$$

is faithful if and only if  $\det G_\lambda \neq 0$  for all  $\lambda \in \Lambda$ .

The following publication has been incorporated as Chapter 5.

[3] X. Poncini, J. Rasmussen, *A classification of integrable planar-algebraic models*, arXiv:2302.11712 [math-ph].

# Chapter 5

---

## Yang–Baxter relation planar algebras

---

In this chapter, we apply the algebraic integrability framework to subfactor planar algebras. We begin with the simplest algebra of this class – the Temperley–Lieb subfactor planar algebra and recover the well-known Baxterisation within our framework. We then consider singly generated planar algebras and find that the only such planar algebras underlying homogeneous Yang–Baxter integrable models are the so-called Yang–Baxter relation planar algebras. According to a result of Liu, there are three such planar algebras: the well-known Fuss–Catalan and Birman–Wenzl–Murakami planar algebras, in addition to one more which we refer to as the Liu planar algebra. The Fuss–Catalan and Birman–Wenzl–Murakami algebras are known to underlie homogeneous Yang–Baxter integrable models, and we show that the Liu algebra likewise admit a Baxterisation. We also show that the double-row transfer operator describing a homogeneous Yang–Baxter integrable model underlied by the Temperley–Lieb subfactor planar algebra or one of the singly generated Yang–Baxter relation (YBR) planar algebras is polynomialisable. Using terminology established in Chapter 3, our findings for singly generated planar algebras may now be summarised as follows.

**Theorem 5.0.1.** *Let  $A$  be a singly generated planar algebra. Then, there exists (i) a single-row transfer operator and (ii) a double-row transfer operator; each describing a homogeneous Yang–Baxter integrable model encoded by  $A$  if and only if  $A$  is a Yang–Baxter relation planar algebra.*

**Theorem 5.0.2.** *Let the homogeneous Yang–Baxter integrability of a model be encoded by a singly generated Yang–Baxter relation planar algebra. Then, there exist algebra-parameter choices and a suitable  $u$ -domain such that the corresponding double-row transfer operator is polynomialisable.*

As a unifying framework for describing the singly generated YBR planar algebras, inspired by the series of works [29–31, 39], we find it convenient to introduce the (unshaded) *proto-singly-generated* planar algebra  $(PS_n)_{n \in \mathbb{N}_0}$ . Although  $PS_n$  is infinite-dimensional for  $n \geq 3$  and does not encode a homogeneous Yang–Baxter integrable model, we demonstrate that it serves as an ‘ambient’ algebra admitting quotients isomorphic to the FC, BMW, and Liu algebras.

Given our focus on the Temperley–Lieb planar algebra and singly generated planar algebras, where  $\dim A_1 = |B_1| = 1$ , we may accordingly normalise the  $K$ -operators in (3.3) so that they equal the identity

element,

$$K(u) = \overline{K}(u) = \mathbb{1}_1. \quad (5.1)$$

We also note that for the Temperley–Lieb planar algebra and singly generated planar algebras,  $A_2$  is commutative. It follows that the set of local relations in Proposition 3.2.1 is a subset of those in Proposition 3.2.2. Accordingly, for these algebras, a homogeneous Baxterisation gives rise to two homogeneous Yang–Baxter integrable models; one described by the double-row transfer operator  $T_n^{(d)}(u)$  and another described by the single-row transfer operator  $T_n^{(s)}(u)$ .

## 5.1 Temperley–Lieb planar algebra

### 5.1.1 Planar algebra

Let  $T_{n,\pm}$  denote the complex vector space spanned by disks with  $2n$  nodes such that each node is connected to another node via a non-intersecting loop segment – defined up to ambient isotopy, and a  $\pm$  checker-board shading (see Section 2.2). Examples of *Temperley–Lieb disks* are

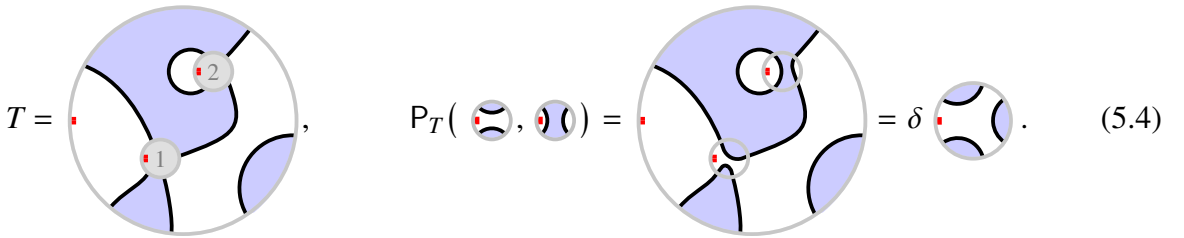


$$\in T_{2,-}, \quad \in T_{3,+}, \quad \in T_{5,-}. \quad (5.2)$$

The dimension of  $T_{n,\pm}$  is given by a Catalan number

$$\dim T_{n,\pm} = \frac{1}{n+1} \binom{2n}{n}. \quad (5.3)$$

The *Temperley–Lieb (TL) planar algebra*  $TL(\delta)$  is the graded vector space  $(T_{n,\pm})_{n \in \mathbb{N}_0}$ , together with the natural diagrammatic action of shaded planar tangles, with each loop replaced by a factor of the parameter  $\delta \in \mathbb{C}$ . To illustrate, we present the example



$$T = \text{ (disk with 2 nodes, shaded region)}, \quad P_T(\text{ (disk with 2 nodes, shaded region)}) = \text{ (disk with 3 nodes, shaded region, with a factor of } \delta \text{ from the loop segment}). \quad (5.4)$$

From [13], we know that  $TL(\delta)$  is spherical and involutive, with the involution  $\cdot^*$  defined as the conjugate-linear map that acts by reflecting every disk about a line perpendicular to its marked boundary interval.

Let  $\mathcal{T}$  denote the set of all  $\delta$ -values such that the planar algebra  $TL(\delta)$  is positive semi-definite. For each  $\delta \in \mathcal{T}$ , the *TL subfactor planar algebra*  $TL(\delta)$  is then defined as the quotient of  $TL(\delta)$  by the kernel of the trace norm (2.36). The complete details of the set  $\mathcal{T}$  were established in [26], where

$$\mathcal{T} = \{ 2 \cos \left( \frac{\pi}{k} \right) \mid k = 3, 4, \dots \} \cup [2, \infty). \quad (5.5)$$

For  $\delta$  in  $\{ 2 \cos \left( \frac{\pi}{k} \right) \mid k = 3, 4, \dots \}$ , the kernel of the traces norm is non-trivial hence  $TL(\delta)$  and  $TL(\delta)$  are not isomorphic, while for  $\delta > 2$ ,  $TL(\delta)$  is positive definite, in which case  $TL(\delta) \cong TL(\delta)$ .

**Remark.** Here and throughout, the sans-serif font distinguishes a subfactor planar algebra, such as  $\text{TL}(\delta)$ , from the corresponding (not necessarily subfactor) planar algebra, here  $\text{TL}(\delta)$ .

**Remark.** Recall the collection of vector spaces  $(\mathbf{T}_{n,\pm})_{n,\pm}$  defined in Section 2.3. For  $\delta > 2$ , we note that  $\mathbf{T}_{n,\pm} = \mathbf{T}_{n,\pm}$  for all  $n \in \mathbb{N}_0$ .

It follows from Section 2.5 that planar algebras giving rise to Yang–Baxter integrable models admit an unshaded description. For the remainder of this section, we will therefore consider the corresponding *unshaded* TL planar algebra  $(\mathbf{T}_n)_{n \in \mathbb{N}_0}$  where we ignore the shading on both vectors and tangles. For brevity, we omit the ‘unshaded’ qualifier and refer to this planar algebra as TL.

### 5.1.2 Presentation

For each  $n \in \mathbb{N}$ , the *TL algebra*  $\text{TL}_n(\delta)$  is defined by endowing the vector space  $\mathbf{T}_n$  with the multiplication induced by the unshaded planar tangle  $M_n$  following from (2.26). We note that the TL algebra is both unital (with unit denoted by  $\mathbb{1}$ ) and associative, and that it is a  $*$ -algebra with involution inherited from the TL planar algebra. As is well-known [15], the generators of  $\text{TL}_n(\delta)$  can be expressed diagrammatically as

$$\mathbb{1} \leftrightarrow \begin{array}{c} \text{---} \\ | \quad | \\ \text{---} \end{array} \quad , \quad e_i \leftrightarrow \begin{array}{c} \text{---} \\ | \quad | \\ \text{---} \end{array} \quad (i = 1, \dots, n-1). \quad (5.6)$$

The TL algebra  $\text{TL}_n(\delta)$  admits a presentation

$$\text{TL}_n(\delta) \cong \langle e_1, \dots, e_{n-1} \rangle, \quad (5.7)$$

with the relations

$$e_i^2 = \delta e_i, \quad (5.8)$$

$$e_j e_i e_j = e_j, \quad |i - j| = 1, \quad (5.9)$$

$$e_i e_j = e_j e_i, \quad |i - j| > 1. \quad (5.10)$$

For each  $n \in \mathbb{N}$ , there exists a unique  $w_n \in \text{TL}_n(\delta)$  such that

$$w_n^2 = w_n, \quad e_i w_n = w_n e_i = 0, \quad i = 1, \dots, n-1. \quad (5.11)$$

We will have more to say about this *Jones–Wenzl idempotent* [52] in Section 6.1.4.

Let  $\mathcal{T}_n$  denote the set of all  $\delta$  such that the trace form (2.34) is positive semi-definite on  $\mathbf{T}_n$ , noting that  $\mathcal{T} \subseteq \mathcal{T}_n$  for all  $n \in \mathbb{N}_0$ . For each  $\delta \in \mathcal{T}_n$ , the *TL subfactor algebra*  $\text{TL}_n(\delta)$  is then defined as the quotient of  $\text{TL}_n(\delta)$  by the kernel of the trace norm. As for the corresponding planar algebras, we have  $\text{TL}_n(\delta) \cong \text{TL}_n(\delta)$  for  $\delta$  generic i.e. for  $\delta > 2$ .

### 5.1.3 Baxterisation

Relative to the canonical  $T_2$ -basis  $\{\mathbb{1}_2, e\}$ , we introduce the parameterised  $R$ -operator as

$$R(u) = r_{\mathbb{1}}(u)\mathbb{1}_2 + r_e(u)e, \quad \text{Diagram: } \begin{array}{c} \text{A green circle with } u \text{ inside, connected to two lines that cross each other.} \end{array} = r_{\mathbb{1}}(u) \begin{array}{c} \text{Diagram: A green circle with } u \text{ inside, connected to two lines that cross each other.} \end{array} + r_e(u) \begin{array}{c} \text{Diagram: A green circle with } u \text{ inside, connected to two lines that cross each other.} \end{array}, \quad (5.12)$$

with  $r_{\mathbb{1}}, r_e : \Omega \rightarrow \mathbb{C}$ .

**Remark.** For the  $R$ -operator to be non-specious, the functions  $r_{\mathbb{1}}$  and  $r_e$  are required to be nonzero when exploring homogeneous integrability encoded by  $\text{TL}_n(\delta)$ .

It is known [11], that  $\text{TL}_n(\delta)$  admits a Baxterisation of the form (5.12). Within the integrability framework developed in Chapter 3, we have the following.

**Proposition 5.1.1.** *The  $R$ -operator*

$$R(u) = \mathbb{1}_2 + u e \quad (5.13)$$

provides a homogeneous Baxterisation of  $\text{TL}_n(\delta)$ , with

$$\bar{Y}_1(u, v) = R\left(\frac{u+v+\delta uv}{1-uv}\right), \quad Y_1(u, v) = \frac{-(1-uv)^2}{(u+v+\delta)(u+v+\delta uv)} R\left(\frac{u+v+\delta}{uv-1}\right), \quad (5.14)$$

and (for  $i = 2, 3$ )

$$\bar{Y}_i(u, v) = \bar{Y}_1\left(\frac{1}{u}, v\right), \quad Y_i(u, v) = Y_1\left(\frac{1}{u}, v\right). \quad (5.15)$$

*Proof.* We first observe that the  $R$ -operator (5.13) satisfies the following crossing symmetries

$$\begin{array}{c} \text{Diagram: A green circle with } u \text{ inside, connected to two lines that cross each other.} \end{array} = u \begin{array}{c} \text{Diagram: A green circle with } u \text{ inside, connected to two lines that cross each other.} \end{array}, \quad \begin{array}{c} \text{Diagram: A green circle with } u \text{ inside, connected to two lines that cross each other.} \end{array} = \begin{array}{c} \text{Diagram: A green circle with } u \text{ inside, connected to two lines that cross each other.} \end{array}. \quad (5.16)$$

The BYBEs (3.32) are satisfied by applying the crossing symmetries, observing that  $\text{TL}_2$  is a commutative algebra, and noting that  $\bar{Y}_1(u, v)$  and  $Y_1(u, v)$  are symmetric in  $u$  and  $v$ .

Applying the crossing symmetries (5.16) for  $u \neq 0$ , we can express the YBEs (3.31) as

$$\begin{array}{c} \text{Diagram: Two red circles with } \bar{1} \text{ and } u \text{ inside, connected to two lines that cross each other.} \end{array} = \begin{array}{c} \text{Diagram: Two red circles with } \bar{1} \text{ and } u \text{ inside, connected to two lines that cross each other.} \end{array}, \quad \begin{array}{c} \text{Diagram: Two red circles with } \bar{2} \text{ and } 1/u \text{ inside, connected to two lines that cross each other.} \end{array} = \begin{array}{c} \text{Diagram: Two red circles with } \bar{2} \text{ and } 1/u \text{ inside, connected to two lines that cross each other.} \end{array}, \quad \begin{array}{c} \text{Diagram: Two red circles with } \bar{3} \text{ and } v \text{ inside, connected to two lines that cross each other.} \end{array} = \begin{array}{c} \text{Diagram: Two red circles with } \bar{3} \text{ and } v \text{ inside, connected to two lines that cross each other.} \end{array}. \quad (5.17)$$

It follows that  $\bar{Y}_i(u, v)$  and  $Y_i(u, v)$  for each  $i = 2, 3$  can be expressed in terms of  $\bar{Y}_1(u, v)$  and  $Y_1(u, v)$  respectively, as

$$\bar{Y}_2(u, v) = \bar{Y}_1\left(\frac{1}{u}, v\right), \quad \bar{Y}_3(u, v) = \bar{Y}_1\left(v, \frac{1}{u}\right), \quad Y_2(u, v) = Y_1\left(\frac{1}{u}, v\right), \quad Y_3(u, v) = Y_1\left(v, \frac{1}{u}\right). \quad (5.18)$$

It remains to verify that (5.13) and (5.14) provide a solution to Inv1 (3.30) and YBE1 (3.31), see Appendix A.1 for details.  $\square$

Relative to the involution  $\cdot^*$  on the TL algebra, the  $R$ -operator (5.13) is self-adjoint for all  $u \in \mathbb{R}$ .

**Remark.** We have verified that, up to a normalising factor, the generalised Yang–Baxter framework of Proposition 3.2.2 does not admit any other non-specious solution of the form (5.12), than the one presented in Proposition 5.1.1.

Note that by setting  $\delta = 2\cos(\lambda)$ , and by rescaling and reparameterising the  $R$ -operator (5.13) as

$$\tilde{R}(u) = \sin(\lambda - u) \mathbb{1}_2 + \sin(u) e = \sin(\lambda - u) R(\phi(u)), \quad \phi(u) := \frac{\sin(u)}{\sin(\lambda - u)}, \quad (5.19)$$

we recover the familiar Baxterisation of  $\text{TL}_n(\delta)$  presented in (2.43).

## 5.2 Proto-singly-generated algebra

Every subfactor planar algebra has a planar subalgebra isomorphic to the Temperley–Lieb subfactor planar algebra, see e.g. [29]. Accordingly,  $A_{2,\pm}$  of a subfactor planar algebra  $(A_{n,\pm})_{n \in \mathbb{N}_0}$  contains the two Temperley–Lieb vectors

$$\mathbb{1}_{2,\pm} = P_{Id_{2,\pm}}(), \quad e_{\pm} := P_{\mathcal{E}_{\pm}}(), \quad (5.20)$$

where

$$\text{Id}_{2,+} = \text{Id}_{2,-} = \text{Id}_2, \quad \mathcal{E}_+ := \text{Id}_2, \quad \mathcal{E}_- := \text{Id}_2, \quad (5.21)$$

with  $\text{Id}_{2,\pm}$  a special case of (2.27). In all but the degenerate case (see Remark after (5.28)), which we exclude in the following, the vectors in (5.20) are linearly independent so  $\dim A_{2,\pm} \geq 2$ , while the Temperley–Lieb subfactor planar algebra itself has  $\dim A_{2,\pm} = 2$ .

For a *singly generated* subfactor planar algebra,  $\dim A_{1,\pm} = 1$  and  $\dim A_{2,\pm} = 3$ , so  $A_{2,\pm}$  has a basis consisting of the two Temperley–Lieb vectors (5.20) and *one* additional vector, hence the terminology. Moreover, the vector spaces  $A_{n,\pm}$  for  $n > 2$  are generated by the action of planar tangles on vectors in  $A_{2,\pm}$ .

**Remark.** Although a singly generated planar algebra is a *subfactor* planar algebra, we are suppressing that qualifier, in line with the convention in [29].

It follows from Section 2.5 that a singly generated planar algebra giving rise to a Yang–Baxter integrable model can be replaced by the corresponding unshaded planar algebra. Accordingly, we will henceforth restrict to the class of *unshaded* singly generated planar algebras. About these, we have the following key result involving the *proto-singly-generated planar algebra*  $PS^{(\epsilon)}(\alpha, \delta)$  constructed in Section 5.2.1 and Section 5.2.2 below.

**Proposition 5.2.1.** *An unshaded singly generated planar algebra is a quotient of  $\text{PS}^{(\epsilon)}(\alpha, \delta)$  for some  $\epsilon, \alpha, \delta$ .*

Indeed,  $\text{PS}^{(\epsilon)}(\alpha, \delta)$  is defined in terms of relations that, for some  $\epsilon, \alpha, \delta$ , are satisfied by any given unshaded singly generated planar algebra. Here,  $\delta$  is the loop weight arising in

$$e^2 = \delta e, \quad (5.22)$$

where

$$e := \mathsf{P}_{\mathcal{E}}(), \quad \mathcal{E} := \text{Diagram of a Temperley–Lieb generator}, \quad (5.23)$$

is the unshaded Temperley–Lieb generator. We note that  $e^* = e$ .

### 5.2.1 Planar algebra

We now introduce a planar algebra whose vector spaces are spanned by planar tangles with labelled disks, and where planar tangles act on these vector spaces in the natural diagrammatic way. For each  $n \in \mathbb{N}_0$ , let  $S_n$  denote a set whose elements label disks with  $2n$  nodes. With  $S := \bigsqcup_{n \in \mathbb{N}_0} S_n$ , an *S-labelled tangle* is thus a planar tangle whose input disks each have been labelled by an element of  $S$ . For such a label set  $S$ , the *unshaded universal planar algebra* consists of the vector spaces  $(A_n(S))_{n \in \mathbb{N}_0}$  where, for each  $n$ ,  $A_n(S)$  is spanned by all  $S$ -labelled tangles with  $2n$  nodes on their output disk, together with the planar-tangle action colloquially named ‘what you see is what you get’, illustrated in (5.50) below, see also [13, 53]. We note that the elements of  $S$  have no additional structure. Accordingly, the list of cardinalities,  $|S_0|, |S_1|, |S_2|, \dots$ , characterises a universal planar algebra.

A universal planar algebra is infinite-dimensional. Indeed, even if  $S_k = \emptyset$  for all  $k \in \mathbb{N}_0$ , then each  $A_n(S)$  is spanned by the corresponding set of Temperley–Lieb vectors, together with those same vectors but with all possible combinations of closed loops. To tame the dimensionality of a universal planar algebra, relations are imposed on  $(A_n(S))_{n \in \mathbb{N}_0}$ . For any set  $C$  of vectors in  $(A_n(S))_{n \in \mathbb{N}_0}$ , we thus let  $I(C)$  denote the planar ideal generated by  $C$ , and  $(A_n(S, C))_{n \in \mathbb{N}_0}$  the corresponding *quotient planar algebra*.

We refer to a (universal) quotient planar algebra  $(A_n(S, C))_{n \in \mathbb{N}_0}$  as a *proto-singly-generated (PSG) planar algebra* if  $S$  and  $C$  satisfy

$$\dim A_0(S, C) = \dim A_1(S, C) = 1, \quad \dim A_2(S, C) = 3, \quad |S_n| = \delta_{n,2}, \quad (5.24)$$

and such that  $A_0(S, C)$ ,  $A_1(S, C)$ , and  $A_2(S, C)$  are as in an unshaded singly generated planar algebra. Accordingly, these vector spaces are (i) ‘spherical’: satisfying (2.23) for  $n = 0, 1, 2$ ; (ii) ‘involutive’: closed under  $\cdot^*$ , satisfying (2.30) for all planar tangles  $T$  with  $\eta(D) \in \{0, 2, 4\}$  for all  $D \in \mathcal{D}_T \cup \{D_0^T\}$ ; and (iii) ‘positive-definite’: the trace form (2.34) being positive-definite for  $n = 0, 1, 2$ . The PSG planar algebra is otherwise generated by the action of the planar tangles, with no further relations imposed.

**Remark.** A PSG planar algebra is not evaluable (since  $\dim A_n(S, C) = \infty$  for  $n > 2$ ) nor necessarily having a positive-definite trace form for each  $n$ . It follows that additional structure must be imposed on  $A_n(S, C)$  for  $n > 2$  to obtain a singly generated planar algebra.

Since  $A_1(S, C)$  is positive-definite, we have

$$0 < \mathsf{P}'_{\text{tr}_1}(\mathbb{1}_1^* \mathbb{1}_1) = \delta. \quad (5.25)$$

With that, the positive-definiteness of  $A_2(S, C)$  similarly implies that

$$0 < P'_{\text{tr}_2}([\mathbb{1}_2 - \frac{1}{\delta}e]^* [\mathbb{1}_2 - \frac{1}{\delta}e]) = \delta^2 - 1, \quad (5.26)$$

from which it then follows that

$$\delta > 1. \quad (5.27)$$

The evaluations in (5.25) and (5.26) involve the Jones-Wenzl idempotent  $\omega_n$  [52] for  $n = 1$  and  $n = 2$ , respectively. For general  $n \in \mathbb{N}$ , we have  $\omega_n^* = \omega_n$  and

$$P'_{\text{tr}_n}(\omega_n^* \omega_n) = P'_{\text{tr}_n}(\omega_n) = U_n\left(\frac{\delta}{2}\right) = \prod_{k=1}^n \left(\delta - 2 \cos \frac{k\pi}{n+1}\right), \quad (5.28)$$

where  $U_n$  is the  $n^{\text{th}}$  Chebyshev polynomial of the second kind.

**Remark.** If  $A_2(S, C)$  is positive semi-definite for a given value of  $\delta$ , then one obtains a well-defined subfactor planar algebra by quotienting out the ideal generated by all the vectors  $a \in A_2(S, C)$  for which  $P'_{\text{tr}_2}(a^* a) = 0$ . In the degenerate case  $\delta = 1$ , for example, the Temperley–Lieb planar subalgebra is trivialised by quotienting out the ideal generated by  $\mathbb{1}_2 - \frac{1}{\delta}e$  appearing in (5.26), whereby  $\dim A_2(S, C)$  reduces to 2, c.f. (5.24).

The conditions  $C$  are determined in Section 5.2.2 below, where we find that the PSG planar algebra is unique, up to the specification of parameters, including the loop weight  $\delta$ . From here onward, we accordingly opt for the abridged notation  $\text{PS}_n \equiv A_n(S, C)$ ,  $n \in \mathbb{N}_0$ , with  $S$  and  $C$  as above.

## 5.2.2 Defining relations

Here, we determine the relations satisfied by the vectors in a distinguished  $\text{PS}_2$ -basis of the form  $\{\mathbb{1}_2, e, s\}$ . Taking inspiration from the classification approach in [39], selecting  $s$  as conveniently as possible is key in the following. For later convenience, we establish the result below.

**Lemma 5.2.2.** *Let  $(A_{n,\pm})_{n \in \mathbb{N}_0}$  be a subfactor planar algebra and  $\{p_1, \dots, p_k\}$  a basis for  $A_{n,\pm}$  for some  $n$  and shading  $+/ -$ , and suppose  $\{p_1, \dots, p_k\}$  is a complete set of mutually orthogonal idempotents. Then,  $P'_{\text{tr}_{n,\pm}}(p_i) > 0$  and  $p_i^* = p_i$  for all  $i = 1, \dots, k$ .*

*Proof.* By construction,

$$p_i^* = \sum_{j=1}^k c_{ij} p_j, \quad i = 1, \dots, k, \quad (5.29)$$

for some scalars  $c_{ij}$ , where, by (2.32),

$$c_{ij} \in \{0, 1\}, \quad \forall i, j \in \{1, \dots, k\}, \quad (5.30)$$

while the positive-definiteness implies that

$$0 < P'_{\text{tr}_{n,\pm}}(p_i^* p_i) = c_{ii} P'_{\text{tr}_{n,\pm}}(p_i), \quad i = 1, \dots, k, \quad (5.31)$$

so  $c_{11} = \dots = c_{kk} = 1$  and

$$P'_{\text{tr}_{n,\pm}}(p_i) > 0, \quad i = 1, \dots, k. \quad (5.32)$$

From

$$0 = \mathbb{1}_{n,\pm}^* - \mathbb{1}_{n,\pm} = \sum_{i,j=1}^k c_{ij} p_j - \sum_{j=1}^k p_j, \quad (5.33)$$

it then follows that  $c_{ij} = \delta_{ij}$ , hence  $p_i^* = p_i$  for all  $i = 1, \dots, k$ .  $\square$

First, let  $\text{PS}_2$  be endowed with the multiplication induced by the unshaded companion to (2.26). Since  $\dim \text{PS}_0 = 1$ , the idempotent  $\mathcal{P}_0 := \frac{1}{\delta}e$  satisfies  $\dim(\mathcal{P}_0 \text{PS}_2 \mathcal{P}_0) = 1$  and is therefore primitive. By assumption,  $\text{PS}_2$  is positive-definite, hence semisimple, and because  $\{\mathbb{1}_2, \mathcal{P}_0\} \subset \text{PS}_2$  and  $\dim \text{PS}_1 = 1$ , it follows that  $\text{PS}_2$  is commutative, see e.g. [23]. The set  $\{\mathcal{P}_0\} \subset \text{PS}_2$  can thus be extended to a  $\text{PS}_2$ -basis,  $\{\mathcal{P}_0, \mathcal{P}_1, \mathcal{P}_2\}$ , consisting of a complete set of mutually orthogonal (and primitive) idempotents, where we note that

$$\delta^2 = P'_{\text{tr}_2}(\mathbb{1}_2) = 1 + P'_{\text{tr}_2}(\mathcal{P}_1) + P'_{\text{tr}_2}(\mathcal{P}_2). \quad (5.34)$$

By Lemma 5.2.2, the positive-definiteness of  $\text{PS}_2$  implies that

$$0 < P'_{\text{tr}_2}(\mathcal{P}_\ell^* \mathcal{P}_\ell) = P'_{\text{tr}_2}(\mathcal{P}_\ell), \quad \ell = 1, 2. \quad (5.35)$$

We now introduce

$$s := p_1 \mathcal{P}_1 + p_2 \mathcal{P}_2, \quad (5.36)$$

where  $p_1, p_2 \in \mathbb{C}$ , and for  $\{\mathbb{1}_2, e, s\}$  to be a basis for  $\text{PS}_2$ , it must hold that  $p_1 \neq p_2$ . It follows that

$$es = 0 = se, \quad s^2 = (p_1 + p_2)s - p_1 p_2 (\mathbb{1}_2 - \frac{1}{\delta}e), \quad (5.37)$$

hence  $P_{r_{4,1}}^2(s)e = 0$ , and that

$$P_{\text{tr}_2}(s) = p_1 P_{\text{tr}_2}(\mathcal{P}_1) + p_2 P_{\text{tr}_2}(\mathcal{P}_2). \quad (5.38)$$

For convenience, we choose  $p_1, p_2$  such that

$$P_{\text{tr}_2}(s) = 0, \quad (5.39)$$

noting that (5.35) then ensures that  $p_1 \neq p_2$  (as required) and implies that  $p_1, p_2 \neq 0$ . Without loss of generality, we may further choose the normalisation of  $s$  such that  $p_1 p_2 = -1$ , thereby obtaining

$$s^2 = \mathbb{1}_2 - \frac{1}{\delta}e + \alpha s, \quad (5.40)$$

where  $\alpha := p_1 + p_2$ , noting that  $\alpha$  can take any value in  $\mathbb{C} \setminus \{-2i, 2i\}$ .

By construction

$$P_{r_{4,1}}(s) = \epsilon_1 \mathbb{1}_2 + \epsilon_e e + \epsilon s, \quad (5.41)$$

for some  $\epsilon_1, \epsilon_s, \epsilon \in \mathbb{C}$ , while (5.39) implies that

$$P_{r_{4,1}}(s)e = 0 \quad (5.42)$$

(since  $\delta \neq 0$ ) and, by sphericity, that  $P_{r_{4,1}}^3(s)e = 0$ . Using  $P_{r_{4,1}}^4 = \text{id}$  and  $\delta^2 \neq 1$ , it follows that

$$\epsilon_1 = \epsilon_e = 0, \quad \epsilon^4 = 1. \quad (5.43)$$

Subsequently, recalling that  $P_{r_{4,2}} = P_{r_{4,1}}^2$ , the relations  $P_{r_{4,2}}(\mathbb{1}_2) = \mathbb{1}_2$  and  $P_{r_{4,2}}(e) = e$  imply that

$$0 = P_{r_{4,2}}(s^2) - P_{r_{4,2}}(s)P_{r_{4,2}}(s) = \alpha(\epsilon^2 - 1)s, \quad (5.44)$$

so we must have  $\alpha = 0$  if  $\epsilon^2 = -1$ . This requirement may be implemented by setting

$$\alpha = (1 + \epsilon^2)\hat{\alpha}, \quad (5.45)$$

where  $\hat{\alpha} \in \mathbb{C} \setminus \{-i, i\}$ .

Under the conjugate-linear involution  $\cdot^*$ , we have

$$\mathbb{1}_2^* = \mathbb{1}_2, \quad e^* = e, \quad s^* = \frac{p_1 \bar{p}_2 - \bar{p}_1 p_2}{p_1 - p_2} \left( \mathbb{1}_2 - \frac{1}{\delta} e \right) + \frac{\bar{p}_1 - \bar{p}_2}{p_1 - p_2} s, \quad (5.46)$$

where  $\bar{p}$  denotes the complex conjugate to the scalar  $p$ . Using  $p_1 p_2 = -1$ , it follows that, for  $\alpha \in \mathbb{R}$ , we have  $p_1, p_2 \in \mathbb{R}$ , hence  $s^* = s$ .

Expressing  $s$  diagrammatically as

$$s = \text{Diagram } (5.47)$$

the analysis above implies that

$$\text{Diagram } = \text{Diagram} - \frac{1}{\delta} \text{Diagram} + \alpha \text{Diagram}, \quad \text{Diagram} = \epsilon \text{Diagram}, \quad \epsilon \in \{-1, 1, -i, i\}. \quad (5.48)$$

For each  $(\alpha, \epsilon)$  and  $\delta > 1$ , where  $(\alpha, \epsilon) \in (\mathbb{C} \setminus \{-2i, 2i\}) \times \{-1, 1\}$  or  $(\alpha, \epsilon) \in \{0\} \times \{-i, i\}$ , we thus have a PSG planar algebra  $(\text{PS}_n)_{n \in \mathbb{N}_0}$ , where a basis for  $\text{PS}_2$  is given diagrammatically by

$$B_2 = \left\{ \text{Diagram}, \text{Diagram}, \text{Diagram} \right\}. \quad (5.49)$$

To illustrate the corresponding action of planar tangles, we have

$$T = \text{Diagram}, \quad P_T(\text{Diagram}, \text{Diagram}, \text{Diagram}) = \text{Diagram} = \delta \text{Diagram}. \quad (5.50)$$

We note that the conditions

$$P_{r_{4,1}}^\ell(s)e = 0, \quad \ell = 0, 1, 2, 3, \quad (5.51)$$

where  $P_{r_{4,1}}^0$  is the identity map on  $\text{PS}_2$ , correspond to the diagrammatic relations

$$\text{Diagram 1} = \text{Diagram 2} = \text{Diagram 3} = \text{Diagram 4} = 0. \quad (5.52)$$

In fact, this ‘uncapability’ of  $s$  was a motivating factor behind imposing (5.39). Moreover, the tracelessness of  $s$  allows us to represent the trace-form inner product relative to the ordered basis  $\{\mathbb{1}_2, e, s\}$  as

$$\begin{pmatrix} \delta^2 & \delta & 0 \\ \delta & \delta^2 & 0 \\ 0 & 0 & \delta^2 - 1 \end{pmatrix}, \quad (5.53)$$

confirming the positive-definiteness of  $\text{PS}_2$  for  $\delta > 1$ , c.f. (5.27).

To summarise, the PSG planar algebra  $\text{PS}^{(\epsilon)}(\alpha, \delta)$  is the quotient planar algebra  $(A_n(S, C^{(\epsilon)}(\alpha, \delta)))_{n \in \mathbb{N}_0}$ , where

$$S = \bigsqcup_{n \in \mathbb{N}_0} S_n, \quad S_2 = \{\text{Diagram 1}\}, \quad S_k = \emptyset, \quad \forall k \neq 2, \quad (5.54)$$

and

$$C^{(\epsilon)}(\alpha, \delta) = \left\{ \text{Diagram 1} - \delta \text{Diagram 2}, \text{Diagram 2}, \text{Diagram 3} - \epsilon \text{Diagram 4}, \text{Diagram 4} - \text{Diagram 1} + \frac{1}{\delta} \text{Diagram 2} - \alpha \text{Diagram 3} \right\}, \quad (5.55)$$

with  $\delta > 1$ , and  $(\alpha, \epsilon) \in (\mathbb{C} \setminus \{-2i, 2i\}) \times \{-1, 1\}$  or  $(\alpha, \epsilon) \in \{0\} \times \{-i, i\}$ .

With the parameters as above,  $\text{PS}^{(\epsilon)}(\alpha, \delta)$  is the unique planar algebra satisfying the conditions outlined in the paragraph containing (5.24). It follows that any unshaded singly generated planar algebra can be obtained by specialising the parameters  $\epsilon, \alpha, \delta$  and by taking a quotient in such a way that each  $\text{PS}_n$ ,  $n \in \{3, 4, \dots\}$ , is spherical, involutive and positive-definite. These observations conclude the proof of Proposition 5.2.1.

### 5.2.3 Presentation

We proceed to describe the algebra that arises when endowing the vector space  $\text{PS}_n$  with the multiplication induced by the unshaded companion to (2.26). For each  $n \in \mathbb{N}$ ,  $\delta > 1$ , and each pair  $(\alpha, \epsilon) \in (\mathbb{C} \setminus \{-2i, 2i\}) \times \{-1, 1\}$  or  $(\alpha, \epsilon) \in \{0\} \times \{-i, i\}$ , the *PSG algebra*  $\text{PS}_n^{(\epsilon)}(\alpha, \delta)$  is thus defined as the unital associative algebra  $\langle e_i, s_i \mid i = 1, \dots, n-1 \rangle$  subject to the relations

$$\begin{aligned} s_i^2 &= \mathbb{1} - \frac{1}{\delta} e_i + \alpha s_i, & e_i s_i &= s_i e_i = 0, & s_i s_j &= s_j s_i, & |i - j| &> 1, \\ e_i e_{i \pm 1} e_i &= e_i, & e_i e_{i \pm 1} s_i &= \epsilon^{\pm 1} e_i s_{i \pm 1}, & s_i e_{i \pm 1} e_i &= \epsilon^{\mp 1} s_{i \pm 1} e_i, \end{aligned} \quad (5.56)$$

with  $\mathbb{1}$  denoting the unit. Following from (5.56), we also have the relations

$$e_i^2 = \delta e_i, \quad e_i e_j = e_j e_i, \quad e_i s_j = s_j e_i, \quad |i - j| > 1, \quad (5.57)$$

$$e_i s_{i \pm 1} s_i = e_i (\epsilon^{\mp 1} (e_{i \pm 1} - \frac{1}{\delta} \mathbb{1}) + \alpha s_{i \pm 1}), \quad s_i s_{i \pm 1} e_i = (\epsilon^{\pm 1} (e_{i \pm 1} - \frac{1}{\delta} \mathbb{1}) + \alpha s_{i \pm 1}) e_i, \quad (5.58)$$

and

$$e_i s_{i \pm 1} e_i = 0, \quad s_i e_{i+1} s_i = s_{i+1} e_i s_{i+1}. \quad (5.59)$$

We note that it suffices to list one of the two relations  $e_i s_i = 0$  or  $s_i e_i = 0$  in (5.56).

The generators of  $\text{PS}_n^{(\epsilon)}(\alpha, \delta)$  are represented diagrammatically as

$$1 \leftrightarrow \begin{array}{|c|c|} \hline \cdots & \\ \hline 1 & n \\ \hline \end{array}, \quad e_i \leftrightarrow \begin{array}{|c|c|c|c|} \hline \cdots & & & \\ \hline 1 & & i & i+1 & n \\ \hline \end{array}, \quad s_i \leftrightarrow \begin{array}{|c|c|c|c|} \hline \cdots & & & \\ \hline 1 & & i & i+1 & n \\ \hline \end{array}, \quad (5.60)$$

with the marked boundary interval linking the two horizontal edges via an invisible arc on the left. Multiplication is then implemented by vertical concatenation, where the diagram representing the product  $ab$  is obtained by placing the diagram representing  $b$  atop the one representing  $a$ .

**Remark.** The PSG planar algebra ‘includes’ the PSG algebras but not the other way around. A planar algebra  $(A_n)_{n \in \mathbb{N}_0}$  offers a consistent way to define operations that are not accessible to the individual algebras  $A_n$  themselves, such as (unshaded versions of) the traces (2.21) and rotations (3.11).

We stress that there are no non-trivial relations involving  $s_i s_{i \pm 1} s_i$  without also involving terms with four or more  $s$ -factors. Accordingly, for  $n = 3$ , there are infinitely many linearly independent vectors of the form  $(s_1 s_2)^k$ , hence  $\dim \text{PS}_3 = \infty$ , manifesting the non-evaluability of the planar algebra.

## 5.2.4 Baxterisability

Concerning the notion of homogeneous Yang–Baxter integrability outlined in Section 3.2, including the definition of homogeneous double- and single-row transfer operators and non-specious Baxterisations, we have the following result.

**Proposition 5.2.3.** *Singly generated planar algebras that encode homogeneous Yang–Baxter integrable models on the strip or on the cylinder must be YBR.*

*Proof.* Since singly generated planar algebras that do not admit an unshaded description cannot encode a homogeneous Yang–Baxter integrable model within our algebraic integrability framework (see Section 2.5), Proposition 5.2.1 allows us to focus on the PSG planar algebra and its quotients. It thus suffices to show that if one does not impose conditions turning the PSG planar algebra into a YBR planar algebra, then there exist no  $R$ - and  $Y$ -operators such that (i) the YBE

$$\begin{array}{c} \text{Diagram with two green circles labeled } u \text{ and } v, \text{ and two red circles labeled } u \text{ and } v. \text{ The top red circle } u \text{ is on the left, and the bottom red circle } v \text{ is on the right. The top green circle } u \text{ is on the right, and the bottom green circle } v \text{ is on the left. They are connected by a vertical line and two diagonal lines forming a Y-shaped junction.} \\ = \\ \text{Diagram with two green circles labeled } u \text{ and } v, \text{ and two red circles labeled } u \text{ and } v. \text{ The top red circle } u \text{ is on the right, and the bottom red circle } v \text{ is on the left. The top green circle } u \text{ is on the left, and the bottom green circle } v \text{ is on the right. They are connected by a vertical line and two diagonal lines forming a Y-shaped junction.} \end{array} \quad (5.61)$$

is satisfied, and (ii) the  $Y$ -operator is ‘horizontally invertible’, i.e. it satisfies (3.30) with some companion element of  $A_2$ . Note that we have selected (i) and (ii) as they are common to the sets of homogeneous Yang–Baxter integrability sufficient conditions for models on the cylinder (Proposition 3.2.1) and models on the strip (Proposition 3.2.2).

Relative to the  $A_2$ -basis  $\{1, e, s\}$ , we introduce

$$R(u) = r_{11}(u)1 + r_e(u)e + r_s(u)s, \quad \bar{Y}(u, v) = \bar{y}_{11}(u, v)1 + \bar{y}_e(u, v)e + \bar{y}_s(u, v)s, \quad (5.62)$$

which can be expressed diagrammatically as

$$\begin{array}{c} \text{Diagram 1} \\ \text{Diagram 2} \end{array} = r_{\mathbb{1}}(u) \begin{array}{c} \text{Diagram 3} \\ \text{Diagram 4} \end{array} + r_e(u) \begin{array}{c} \text{Diagram 5} \\ \text{Diagram 6} \end{array} + r_s(u) \begin{array}{c} \text{Diagram 7} \\ \text{Diagram 8} \end{array}, \quad \begin{array}{c} \text{Diagram 9} \\ \text{Diagram 10} \end{array} = \bar{y}_{\mathbb{1}}(u, v) \begin{array}{c} \text{Diagram 11} \\ \text{Diagram 12} \end{array} + \bar{y}_e(u, v) \begin{array}{c} \text{Diagram 13} \\ \text{Diagram 14} \end{array} + \bar{y}_s(u, v) \begin{array}{c} \text{Diagram 15} \\ \text{Diagram 16} \end{array}, \quad (5.63)$$

where  $r_{\mathbb{1}}, r_e, r_s : \Omega \rightarrow \mathbb{C}$  and  $\bar{y}_{\mathbb{1}}, \bar{y}_e, \bar{y}_s : \Omega \times \Omega \rightarrow \mathbb{C}$ .

**Remark.** If  $r_s$  is the zero function, then the attempted Baxterisation is, in fact, encoded by the Temperley–Lieb planar algebra, and not by a singly generated planar algebra, hence it is not of relevance here.

From (5.61), we get

$$0 = \begin{array}{c} \text{Diagram 17} \\ \text{Diagram 18} \end{array} - \begin{array}{c} \text{Diagram 19} \\ \text{Diagram 20} \end{array}$$

$$\begin{aligned} &= \left\{ [r_e(u)r_e(v) + r_{\mathbb{1}}(u)r_{\mathbb{1}}(v) + \delta r_{\mathbb{1}}(u)r_e(v) - \frac{1}{\delta\epsilon}r_s(u)r_s(v)]\bar{y}_{\mathbb{1}}(u, v) \right. \\ &\quad \left. - [r_e(u)r_{\mathbb{1}}(v) - r_{\mathbb{1}}(u)r_e(v)]\bar{y}_e(u, v) - \frac{1}{\delta}[\epsilon r_{\mathbb{1}}(u)r_s(v) + \frac{1}{\epsilon^2}r_s(u)r_e(v)]\bar{y}_s(u, v) \right\} (e_1 - e_2) \\ &\quad + \left\{ [r_e(u)r_s(v) + \frac{1}{\epsilon}r_s(u)r_{\mathbb{1}}(v) + \frac{\alpha}{\epsilon}r_s(u)r_s(v)]\bar{y}_{\mathbb{1}}(u, v) - r_e(u)r_{\mathbb{1}}(v)\bar{y}_s(u, v) \right\} (s_1 - s_2) \\ &\quad + \left\{ [r_e(u)r_s(v) - r_s(u)r_e(v)]\bar{y}_e(u, v) - [r_e(u)r_e(v) + \frac{\alpha}{\epsilon}r_s(u)r_e(v)]\bar{y}_s(u, v) \right\} (s_1e_2 - e_1s_2) \\ &\quad + \left\{ \frac{1}{\epsilon}[r_{\mathbb{1}}(u)r_s(v) - r_s(u)r_{\mathbb{1}}(v)]\bar{y}_e(u, v) + [r_{\mathbb{1}}(u)r_{\mathbb{1}}(v) + \alpha r_{\mathbb{1}}(u)r_s(v)]\bar{y}_s(u, v) \right\} (s_2e_1 - e_2s_1) \\ &\quad \left. + \left\{ \frac{1}{\epsilon}r_s(u)r_s(v)\bar{y}_s(u, v) \right\} (s_1s_2s_1 - s_2s_1s_2), \right. \end{aligned} \quad (5.64)$$

where

$$e_1 = \begin{array}{c} \text{Diagram 21} \end{array}, \quad s_1 = \begin{array}{c} \text{Diagram 22} \end{array}, \quad e_2 = \begin{array}{c} \text{Diagram 23} \end{array}, \quad s_2 = \begin{array}{c} \text{Diagram 24} \end{array}. \quad (5.65)$$

First, suppose  $(s_1s_2s_1 - s_2s_1s_2)$  is linearly independent of the other algebra elements in (5.64). Then, for the corresponding term to vanish,  $r_s$  or  $\bar{y}_s$  must be zero, with the observation following (5.63) subsequently implying that the function  $\bar{y}_s$  must be zero. As  $r_s \neq 0$  and  $\bar{y}_s = 0$ , the vanishing of the  $(s_1e_2 - e_1s_2)$ -term and the  $(s_2e_1 - e_2s_1)$ -term in (5.64) implies that

$$[r_e(u)r_s(v) - r_s(u)r_e(v)]\bar{y}_e(u, v) = 0 \quad \text{and} \quad [r_{\mathbb{1}}(u)r_s(v) - r_s(u)r_{\mathbb{1}}(v)]\bar{y}_e(u, v) = 0. \quad (5.66)$$

Since  $\bar{y}_s = 0$ , the horizontal invertibility of the  $Y$ -operator implies that  $\bar{y}_e \neq 0$ , so

$$\frac{r_e(u)}{r_s(u)} = \frac{r_e(v)}{r_s(v)} \quad \text{and} \quad \frac{r_{\mathbb{1}}(u)}{r_s(u)} = \frac{r_{\mathbb{1}}(v)}{r_s(v)}, \quad (5.67)$$

correspond to two  $u, v$ -independent constants. It follows that the  $R$ -operator is of the form in (3.36), so the Baxterisation is specious.

Finally, if  $(s_1s_2s_1 - s_2s_1s_2)$  can be expressed as a linear combination of other terms in (5.64), then we are in a quotient of the PSG planar algebra that is YBR.  $\square$

Section 5.3, Section 5.4, and Section 5.5 offer concrete examples of YBR planar algebras encoding homogeneous Yang–Baxter integrability, thereby establishing the *existence* of planar algebras satisfying the necessary condition provided by Proposition 5.2.3. Indeed, we use Liu’s classification in Theorem 5.2.4 below to show that, for *every* singly generated YBR planar algebra, there exists a corresponding homogeneous Baxterisation, which gives rise to a homogeneous Yang–Baxter integrable model on the strip and on the cylinder.

**Theorem 5.2.4** (Liu [39]). *A singly generated YBR planar algebra is isomorphic to a quotient of an FC, BMW, or Liu planar algebra.*

The planar algebras listed in Theorem 5.2.4 are recalled in Section 5.3, Section 5.4, and Section 5.5, respectively. In Section 5.6, we supplement these findings by showing that each model defined on the strip is also *polynomially integrable*. Theorem 5.0.1 and Theorem 5.0.2 summarise these key findings.

**Remark.** If the FC, BMW, or Liu planar algebra in Theorem 5.2.4 is positive semi-definite, then its quotient by the kernel of the trace norm (that is, the quotient by the ideal generated by all  $v$  for which  $P_{\text{tr}_n}(v^*v) = 0$  for some  $n$ ) is isomorphic to the corresponding YBR planar algebra. However, to keep  $\dim A_2(S, C) = 3$  in (5.24), we will only apply this quotient operation for  $n > 2$ , c.f. the Remark following (5.28).

## 5.3 Fuss–Catalan algebra

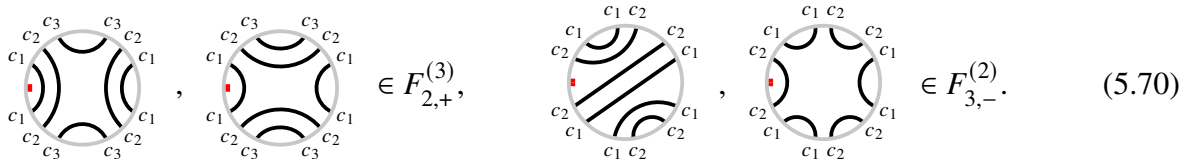
### 5.3.1 Planar algebra

Let  $F_{n,\pm}^{(k)}$  denote the complex vector space spanned by disks with  $2kn$  nodes such that (i) each node is labelled by one of the  $k$  colours  $c_1, \dots, c_k$ , (ii) clockwise from the marked interval, nodes are assigned colours according to

$$\underbrace{(c_1, \dots, c_k), (c_k, \dots, c_1), (c_1, \dots, c_k), \dots, (c_k, \dots, c_1)}_{\#(\dots)=2n} \quad \text{for disks in } F_{n,+}^{(k)}, \quad (5.68)$$

$$\underbrace{(c_k, \dots, c_1), (c_1, \dots, c_k), (c_k, \dots, c_1), \dots, (c_1, \dots, c_k)}_{\#(\dots)=2n} \quad \text{for disks in } F_{n,-}^{(k)}, \quad (5.69)$$

and (iii) every node is connected to another node with the same colour, using a non-intersecting loop segment defined up to ambient isotopy. Examples of such *Fuss–Catalan disks* are



$$\in F_{2,+}^{(3)}, \quad \in F_{3,-}^{(2)}. \quad (5.70)$$

The vector-space dimensions are given by Fuss–Catalan numbers, as

$$\dim F_{n,\pm}^{(k)} = \frac{1}{kn+1} \binom{kn+n}{n}. \quad (5.71)$$

The  $k$ -coloured Fuss–Catalan planar algebra  $\text{FC}^{(k)}(\gamma_1, \dots, \gamma_k)$  is the collection of vector spaces  $(F_{n,\pm}^{(k)})_{n \in \mathbb{N}_0}$  together with the following action of shaded planar tangles [23]: (i) for each string within a shaded planar tangle, draw  $k - 1$  parallel strings in the adjacent unshaded region and assign each a label  $c_k, \dots, c_1$  starting from the original string (for  $k > 1$ , the tangle shading is thus encoded in the string labels and can thereafter be omitted), (ii) if a loop is formed with the colour  $c_l$ , it is removed and replaced by the scalar weight  $\gamma_l$ , and (iii) the output vector is given by the output disk with the given colour labels and ensuing string connections. To illustrate, we have

$$T = \text{ (shaded disk with two marked points 1 and 2) } , \quad P_T(\text{ (two input disks) }) = \text{ (shaded disk with output disk) } = \gamma_1 \text{ (output disk) } , \quad (5.72)$$

where  $c_1$  and  $c_2$  correspond to the colours cyan and black, respectively. If  $\gamma_1 = \dots = \gamma_m$ , then the colours of the strings are immaterial and the corresponding planar algebra admits an unshaded description.

As we are concerned with unshaded singly generated planar algebras, we denote by  $\text{FC}(\gamma)$  the unshaded planar algebra corresponding to  $\text{FC}^{(2)}(\gamma, \gamma)$ , and refer to it simply as *Fuss–Catalan* (FC). From [54], we know that  $\text{FC}(\gamma)$  is spherical and involutive, with the involution  $*$  defined as the conjugate-linear map that acts by reflecting every disk about a line perpendicular to its marked boundary interval.

Let  $\mathcal{F}$  denote the set of all  $\gamma$  such that  $\text{FC}(\gamma)$  is positive semi-definite. For each  $\gamma \in \mathcal{F}$ , the *FC subfactor planar algebra*  $\text{FC}(\gamma)$  is then defined as the quotient of  $\text{FC}(\gamma)$  by the kernel of the trace norm. Details of the set  $\mathcal{F}$  are presented in [54], including  $\{2 \cos(\frac{\pi}{k}) \mid k = 3, 4, \dots\} \subset \mathcal{F}$ . For  $\gamma$  in that discrete subset,  $\text{FC}(\gamma)$  is positive semi-definite, while for  $\gamma > 2$ ,  $\text{FC}(\gamma)$  is positive-definite, in which case  $\text{FC}(\gamma) \cong \text{FC}(\gamma)$ .

### 5.3.2 Presentation

For each  $n \in \mathbb{N}$ , the *FC algebra*  $\text{FC}_n(\gamma)$  is defined by endowing the (unshaded) vector space  $F_n^{(2)}$  with the multiplication induced by the unshaded planar tangle  $M_n$  following from (2.26). We note that the FC algebra is both unital (with unit denoted by  $\mathbb{1}$ ) and associative, and that it is a  $*$ -algebra with involution inherited from the FC planar algebra. Using a diagrammatic representation similar to the one in (5.60),  $\text{FC}_n(\gamma)$  is generated by the following algebra elements:

$$\mathbb{1} \leftrightarrow \begin{array}{c} \text{ (two vertical lines) } \\ | \quad | \\ 1 \quad n \end{array} , \quad P_i \leftrightarrow \begin{array}{c} \text{ (two vertical lines with a crossing) } \\ | \quad | \\ 1 \quad i \quad i+1 \quad n \end{array} , \quad E_i \leftrightarrow \begin{array}{c} \text{ (two vertical lines with a crossing) } \\ | \quad | \\ 1 \quad i \quad i+1 \quad n \end{array} \quad (5.73)$$

where each label below a diagram labels a *pair* of string endpoints.

For  $\gamma \neq 0$ , the FC algebra admits [54] a presentation

$$\text{FC}_n(\gamma) \cong \langle E_i, P_i \mid i = 1, \dots, n-1 \rangle , \quad (5.74)$$

with relations

$$\begin{aligned} E_i^2 &= \gamma^2 E_i, & P_i E_i &= E_i P_i = \gamma E_i, & P_i^2 &= \gamma P_i, \\ E_i E_{i\pm 1} E_i &= E_i, & P_i E_{i\pm 1} P_i &= P_i P_{i\pm 1} = P_{i\pm 1} P_i, & E_i P_{i\pm 1} E_i &= \gamma E_i, \\ E_i E_j &= E_j E_i, & E_i P_j &= P_j E_i, & P_i P_j &= P_j P_i, & |i - j| > 1. \end{aligned} \quad (5.75)$$

Following from (5.75), we also have the relations

$$P_i P_{i\pm 1} E_i = \gamma P_{i\pm 1} E_i, \quad E_i P_{i\pm 1} P_i = \gamma E_i P_{i\pm 1}, \quad P_i P_{i\pm 1} P_i = \gamma P_i P_{i\pm 1}, \quad (5.76)$$

and

$$E_i E_{i\pm 1} P_i = E_i P_{i\pm 1}, \quad P_i E_{i\pm 1} E_i = P_{i\pm 1} E_i. \quad (5.77)$$

For  $\gamma = 0$ , the relations (5.75), (5.76) and (5.77) still hold, but the relations in (5.77) do not all follow from the relations in (5.75), and should be imposed separately.

**Remark.** The Temperley–Lieb subalgebra  $\langle E_1, \dots, E_{n-1} \rangle \subset \text{FC}_n(\gamma)$  has loop fugacity  $\delta = \gamma^2$ .

We let  $\mathcal{F}_n$  denote the set of all  $\gamma$  such that the trace form (2.34) is positive semi-definite on  $F_n^{(2)}$ , noting that  $\mathcal{F} \subseteq \mathcal{F}_n$  for all  $n \in \mathbb{N}_0$ . For each  $\gamma \in \mathcal{F}_n$ ,  $\text{FC}_n(\gamma)$  is then defined as the quotient of  $\text{FC}_n(\gamma)$  by the kernel of the trace norm. As for the corresponding planar algebras, we have  $\text{FC}_n(\gamma) \cong \text{FC}_n(\gamma)$  for  $\gamma$  generic i.e. for  $\gamma > 2$ .

### 5.3.3 Quotient description

**Proposition 5.3.1.** *For  $\gamma^2 > 1$  and each  $\mu \in \{-1, 1\}$ , we have*

$$\text{FC}_n(\gamma) \cong \text{PS}_n^{(1)}(\mu(\gamma - \gamma^{-1}), \gamma^2) / \langle \iota_{i,j} \mid |i - j| = 1; i, j \in \{1, \dots, n-1\} \rangle, \quad (5.78)$$

where

$$\iota_{i,j} = \hat{s}_i e_j \hat{s}_i - \hat{s}_i \hat{s}_j + \hat{s}_j e_i + e_j \hat{s}_i + e_j e_i - \hat{s}_i - \hat{s}_j - \mathbb{1}, \quad (5.79)$$

with  $\hat{s}_i = \mu \gamma s_i$ .

*Proof.* The proposed algebra isomorphism sets

$$E_i = e_i, \quad P_i = \frac{1}{\gamma + \gamma^{-1}} (\mathbb{1} + e_i + \hat{s}_i), \quad (5.80)$$

or equivalently,

$$e_i = E_i, \quad \hat{s}_i = -\mathbb{1} - E_i + (\gamma + \gamma^{-1}) P_i. \quad (5.81)$$

With this, one verifies that the relations (5.75) imply the relations (5.56) and the vanishing of (5.79), and that the relations (5.56) together with the vanishing of (5.79) imply the relations (5.75).  $\square$

**Remark.** By renormalising the  $P_i$  generators, introducing  $\hat{P}_i := P_i / \gamma$ , the relations (5.75)–(5.77) only depend on the loop weight through  $\delta = \gamma^2$ , as we then have

$$\begin{aligned} E_i^2 &= \delta E_i, & \hat{P}_i E_i &= E_i \hat{P}_i = E_i, & \hat{P}_i^2 &= \hat{P}_i, \\ E_i E_{i\pm 1} E_i &= E_i, & \hat{P}_i E_{i\pm 1} \hat{P}_i &= \hat{P}_i \hat{P}_{i\pm 1} = \hat{P}_{i\pm 1} \hat{P}_i, & E_i \hat{P}_{i\pm 1} E_i &= E_i, \\ E_i E_j &= E_j E_i, & E_i \hat{P}_j &= \hat{P}_j E_i, & \hat{P}_i \hat{P}_j &= \hat{P}_j \hat{P}_i, & |i - j| > 1, \end{aligned} \quad (5.82)$$

and

$$\hat{P}_i \hat{P}_{i\pm 1} E_i = \hat{P}_{i\pm 1} E_i, \quad E_i \hat{P}_{i\pm 1} \hat{P}_i = E_i \hat{P}_{i\pm 1}, \quad \hat{P}_i \hat{P}_{i\pm 1} \hat{P}_i = \hat{P}_i \hat{P}_{i\pm 1}, \quad (5.83)$$

$$E_i E_{i\pm 1} \hat{P}_i = E_i \hat{P}_{i\pm 1}, \quad \hat{P}_i E_{i\pm 1} E_i = \hat{P}_{i\pm 1} E_i. \quad (5.84)$$

### 5.3.4 Baxterisation

Relative to the canonical  $F_2^{(2)}$ -basis  $\{\mathbb{1}_2, E, P\}$ , we introduce the parameterised  $R$ -operator as

$$R(u) = r_{\mathbb{1}}(u) \mathbb{1}_2 + r_E(u) E + r_P(u) P, \quad \text{Diagram: } \begin{array}{c} \text{Two vertical lines} \\ \text{Top line: red dot at top, green circle with } u \text{ at bottom} \\ \text{Bottom line: green circle with } u \text{ at top, red dot at bottom} \end{array} = r_{\mathbb{1}}(u) \text{Diagram: } \begin{array}{c} \text{Two vertical lines} \\ \text{Top line: red dot at top, red circle at bottom} \\ \text{Bottom line: red circle at top, red dot at bottom} \end{array} + r_E(u) \text{Diagram: } \begin{array}{c} \text{Two vertical lines} \\ \text{Top line: red dot at top, red circle at bottom} \\ \text{Bottom line: green circle with } u \text{ at top, red dot at bottom} \end{array} + r_P(u) \text{Diagram: } \begin{array}{c} \text{Two vertical lines} \\ \text{Top line: red dot at top, red circle at bottom} \\ \text{Bottom line: green circle with } u \text{ at top, green circle with } u \text{ at bottom} \end{array}, \quad (5.85)$$

with  $r_{\mathbb{1}}, r_E, r_P : \Omega \rightarrow \mathbb{C}$ .

**Remark.** Although  $\langle E_1, \dots, E_{n-1} \rangle$  and  $\langle P_1, \dots, P_{n-1} \rangle$  are subalgebras of  $\text{FC}_n(\gamma)$ , the  $P$  generators do not form a *planar* subalgebra of  $\text{FC}(\gamma)$ . It follows that only  $r_P$  is required to be nonzero when exploring homogeneous integrability encoded by  $\text{FC}_n(\gamma)$ .

It is known [55] that  $\text{FC}_n(\gamma)$  admits a Baxterisation. Within the integrability framework developed in Section 3.2, we have the following.

**Proposition 5.3.2.** *The  $R$ -operator*

$$R(u) = \mathbb{1}_2 + \frac{u(u-1)}{\delta - 1 - u} E + (u-1) \hat{P}, \quad (5.86)$$

provides a homogeneous Baxterisation of  $\text{FC}_n(\gamma)$ , with

$$\bar{Y}_1(u, v) = R(uv), \quad Y_1(u, v) = -\frac{(\delta - 1 - uv)^2}{(\delta - 1)(uv - 1)((\delta - 1)^2 - uv)} R\left(\frac{(\delta - 1)^2}{uv}\right), \quad (5.87)$$

and (for  $i = 2, 3$ )

$$\bar{Y}_i(u, v) = \bar{Y}_1\left(\frac{\delta-1}{u}, v\right), \quad Y_i(u, v) = Y_1\left(\frac{\delta-1}{u}, v\right). \quad (5.88)$$

*Proof.* We first observe that the  $R$ -operator (5.13) satisfies the following crossing symmetries

$$\text{Diagram: } \begin{array}{c} \text{Two vertical lines} \\ \text{Top line: red dot at top, green circle with } u \text{ at bottom} \\ \text{Bottom line: green circle with } u \text{ at top, red dot at bottom} \end{array} = \frac{u(u-1)}{\delta - 1 - u} \text{Diagram: } \begin{array}{c} \text{Two vertical lines} \\ \text{Top line: red dot at top, red circle at bottom} \\ \text{Bottom line: red circle at top, red dot at bottom} \end{array}, \quad \text{Diagram: } \begin{array}{c} \text{Two vertical lines} \\ \text{Top line: red dot at top, green circle with } u \text{ at bottom} \\ \text{Bottom line: green circle with } u \text{ at top, red dot at bottom} \end{array} = \text{Diagram: } \begin{array}{c} \text{Two vertical lines} \\ \text{Top line: red dot at top, red circle at bottom} \\ \text{Bottom line: green circle with } u \text{ at top, green circle with } u \text{ at bottom} \end{array}. \quad (5.89)$$

The BYBEs (3.32) are satisfied by applying the crossing symmetries, observing  $\text{FC}_2$  is a commutative algebra, and noting that  $\bar{Y}_1(u, v)$  and  $Y_1(u, v)$  are symmetric in  $u$  and  $v$ .

Applying the crossing symmetries (5.89) for  $u \neq 0$ , it follows, as in Proposition 5.1.1, that the  $Y$ -operators can be expressed as

$$\bar{Y}_2(u, v) = \bar{Y}_1\left(\frac{\delta-1}{u}, v\right), \quad \bar{Y}_3(u, v) = \bar{Y}_1\left(v, \frac{\delta-1}{u}\right), \quad Y_2(u, v) = Y_1\left(\frac{\delta-1}{u}, v\right), \quad Y_3(u, v) = Y_1\left(v, \frac{\delta-1}{u}\right). \quad (5.90)$$

It remains to verify that (5.86) and (5.87) provide a solution to Inv1 (3.30) and YBE1 (3.31), see Appendix A.2 for details.  $\square$

It follows from the crossing symmetries (5.89) that conditions (3.30) and (3.31) reduce to the single inversion identity and the single *standard* YBE

$$\begin{array}{c} \text{Diagram 1: Two strands crossing, with labels } w \text{ and } \overline{w} \text{ on the strands.} \\ \text{Diagram 2: Two strands crossing, with labels } u \text{ and } \overline{u} \text{ on the strands.} \end{array} = \begin{array}{c} \text{Diagram 3: Two strands crossing, with labels } w \text{ and } \overline{w} \text{ on the strands.} \\ \text{Diagram 4: Two strands crossing, with labels } u \text{ and } \overline{u} \text{ on the strands.} \end{array} \quad (5.91)$$

Relative to the involution  $\cdot^*$  on the FC algebra, the  $R$ -operator (5.86) is self-adjoint for all  $u \in \mathbb{R} \setminus \{\delta - 1\}$ .

**Remark.** We have verified that, up to a normalising factor, the generalised Yang–Baxter framework of Proposition 3.2.2 does not admit any other non-specious solution of the form (5.85), with  $r_P$  nonzero, than the one presented in Proposition 5.3.2.

## 5.4 Birman–Wenzl–Murakami algebra

### 5.4.1 Planar algebra

Let  $W_n$  denote the complex vector space spanned by disks with  $2n$  nodes such that, within each disk, (i) the nodes are connected pairwise by strings, defined up to regular isotopy, (ii) strings may intersect but not self-intersect, (iii) two strings cannot intersect one another more than once, and (iv) strings cannot form closed loops. To illustrate, we present the following examples and non-examples:

$$\begin{array}{c} \text{Diagram 1: Two strands crossing, with labels } w \text{ and } \overline{w} \text{ on the strands.} \\ \text{Diagram 2: Two strands crossing, with labels } u \text{ and } \overline{u} \text{ on the strands.} \\ \text{Diagram 3: Two strands crossing, with labels } v \text{ and } \overline{v} \text{ on the strands.} \end{array} \quad \text{and} \quad \begin{array}{c} \text{Diagram 4: Two strands crossing, with labels } w \text{ and } \overline{w} \text{ on the strands.} \\ \text{Diagram 5: Two strands crossing, with labels } u \text{ and } \overline{u} \text{ on the strands.} \\ \text{Diagram 6: Two strands crossing, with labels } v \text{ and } \overline{v} \text{ on the strands.} \end{array} \quad (5.92)$$

The dimension of  $W_n$  is given by

$$\dim W_n = (2n - 1)!! \quad (5.93)$$

For each pair of scalars  $\tau \neq 0$  and  $q \notin \{-1, 0, 1\}$ , the *Birman–Wenzl–Murakami (BMW) planar algebra*  $\text{BMW}(\tau, q)$  is the collection of vector spaces  $(W_n)_{n \in \mathbb{N}_0}$  together with the natural diagrammatic action of planar tangles, defined up to regular isotopy and subject to the relations

$$\text{Diagram 1: } \text{Diagram 1} = \delta \text{ Diagram 2}, \quad \text{Diagram 2: } \text{Diagram 2} = \tau \text{ Diagram 3}, \quad \text{Diagram 3: } \text{Diagram 3} = \tau^{-1} \text{ Diagram 4}, \quad (5.94)$$

$$\text{Diagram 5: } \text{Diagram 5} - \text{Diagram 6} = Q \left[ \text{Diagram 6} - \text{Diagram 7} \right], \quad (5.95)$$

where

$$\delta = 1 + \frac{\tau - \tau^{-1}}{Q}, \quad Q = q - q^{-1} \quad (5.96)$$

**Remark.** Self-intersecting or loop-forming strings may arise as the result of a planar tangle acting on vectors in  $(W_n)_{n \in \mathbb{N}_0}$ , hence the relevance of relations like (5.94).

The planar algebra  $\text{BMW}(\tau, q)$  is spherical and, for  $|\tau| = |q| = 1$  or  $\tau, q \in \mathbb{R}$ , involutive [31, 56]. In these cases, the involution  $\cdot^*$  is defined as the conjugate-linear map that acts by ‘reflecting’ respectively

‘flipping’ every disk about a line perpendicular to its marked boundary interval, as indicated by

$$\left(\begin{array}{c} \text{disk} \\ \text{disk} \end{array}\right)^* = \left(\begin{array}{c} \text{disk} \\ \text{disk} \end{array}\right), \quad \left(\begin{array}{c} \text{disk} \\ \text{disk} \end{array}\right)^* = \left(\begin{array}{c} \text{disk} \\ \text{disk} \end{array}\right), \quad \left(\begin{array}{c} \text{disk} \\ \text{disk} \end{array}\right)^* = \begin{cases} \left(\begin{array}{c} \text{disk} \\ \text{disk} \end{array}\right), & |\tau| = |q| = 1, \\ \left(\begin{array}{c} \text{disk} \\ \text{disk} \end{array}\right), & \tau, q \in \mathbb{R}, \end{cases} \quad (5.97)$$

recalling that  $q \neq \pm 1$ .

We let  $\mathcal{B}$  denote the set of all  $(\tau, q)$  such that  $\text{BMW}(\tau, q)$  is positive semi-definite. For each  $(\tau, q) \in \mathcal{B}$ , the *BMW subfactor planar algebra*  $\text{BMW}(\tau, q)$  is then defined as the quotient of  $\text{BMW}(\tau, q)$  by the kernel of the trace norm. Details of the set  $\mathcal{B}$  are presented in [31].

### 5.4.2 Presentation

For each  $n \in \mathbb{N}$ , the *BMW algebra*  $\text{BMW}_n(\tau, q)$  is defined by endowing the vector space  $W_n$  with the multiplication induced by the unshaded planar tangle  $M_n$  following from (2.26). We note that the BMW algebra is both unital (with unit denoted by  $\mathbb{1}$ ) and associative, and that, for  $|\tau| = |q| = 1$  or  $\tau, q \in \mathbb{R}$ , it is a  $*$ -algebra with involution inherited from the BMW planar algebra. As is well-known [15, 57, 58], the generators of  $\text{BMW}_n(\tau, q)$  can be represented diagrammatically as

$$1 \leftrightarrow \begin{array}{|c|c|} \hline \dots & \\ \hline 1 & n \\ \hline \end{array}, \quad g_i \leftrightarrow \begin{array}{|c|c|c|c|} \hline \dots & & & \dots \\ \hline & i & i+1 & \\ \hline \end{array}, \quad g_i^{-1} \leftrightarrow \begin{array}{|c|c|c|c|} \hline \dots & & & \dots \\ \hline & i & i+1 & \\ \hline \end{array}, \quad e_i \leftrightarrow \begin{array}{|c|c|c|c|} \hline \dots & & & \dots \\ \hline & i & i+1 & n \\ \hline \end{array}. \quad (5.98)$$

The algebra  $\text{BMW}_n(\tau, q)$  admits [56] a presentation

$$\text{BMW}_n(\tau, q) \cong \langle e_i, g_i, g_i^{-1} \mid i = 1, \dots, n-1 \rangle, \quad (5.99)$$

with relations

$$\begin{aligned} g_i g_{i \pm 1} g_i &= g_{i \pm 1} g_i g_{i \pm 1}, & g_i - g_i^{-1} &= Q(\mathbb{1} - e_i), \\ g_i e_{i \pm 1} g_i &= g_{i \pm 1}^{-1} e_i g_{i \pm 1}^{-1}, & g_i e_i &= e_i g_i = \tau^{-1} e_i, \\ e_i g_{i \pm 1} g_i &= g_{i \pm 1} g_i e_{i \pm 1} = e_i e_{i \pm 1}, & g_i g_j &= g_j g_i, \quad |i - j| > 1. \end{aligned} \quad (5.100)$$

It follows from these relations that

$$e_i^2 = \delta e_i, \quad e_i e_{i \pm 1} e_i = e_i, \quad g_i e_j = e_j g_i, \quad e_i e_j = e_j e_i, \quad |i - j| > 1, \quad (5.101)$$

with  $\delta$  as in (5.96), and that

$$g_i e_{i \pm 1} e_i = g_{i \pm 1}^{-1} e_i, \quad e_i e_{i \pm 1} g_i = e_i g_{i \pm 1}^{-1}, \quad e_i g_{i \pm 1} e_i = \tau e_i. \quad (5.102)$$

We note that it suffices to list one of the two relations  $g_i e_i = \tau^{-1} e_i$  or  $e_i g_i = \tau^{-1} e_i$  in (5.100).

We let  $\mathcal{B}_n$  denote the set of all  $(\tau, q)$  such that the trace form (2.34) is positive semi-definite on  $W_n$ , noting that  $\mathcal{B} \subseteq \mathcal{B}_n$  for all  $n \in \mathbb{N}_0$ . For each  $(\tau, q) \in \mathcal{B}_n$ , the *BMW subfactor algebra*  $\text{BMW}_n(\tau, q)$  is then defined as the quotient of  $\text{BMW}_n(\tau, q)$  by the kernel of the trace norm.

### 5.4.3 Quotient description

Let

$$\Gamma := (\tau^2 + Q\tau - 1)(\tau^2 + Q(Q^2 + 3)\tau - 1) = (\tau + q)(\tau - q^{-1})(\tau + q^3)(\tau - q^{-3}), \quad (5.103)$$

where the rewriting uses (5.96).

**Proposition 5.4.1.** *For  $\delta > 1$ , with  $\delta$  parametrised as in (5.96), and for each  $\mu \in \{-1, 1\}$ , we have*

$$\text{BMW}_n(\tau, q) \cong \text{PS}_n^{(1)}\left(\frac{\mu Q(\tau^2 + 1)}{\sqrt{\Gamma}}, 1 + \frac{\tau - \tau^{-1}}{Q}\right) / \langle \iota_1, \dots, \iota_{n-2} \rangle, \quad (5.104)$$

where

$$\begin{aligned} \iota_i = \hat{s}_i \hat{s}_{i+1} \hat{s}_i - \hat{s}_{i+1} \hat{s}_i \hat{s}_{i+1} + Q^2 \tau \{ & (\tau^2 + 1)(\tau^2 + Q(Q^2 + 3)\tau - 1)[e_i - e_{i+1}] \\ & - (Q + \tau)(1 - Q\tau)[\hat{s}_i - \hat{s}_{i+1} + e_i \hat{s}_{i+1} - e_{i+1} \hat{s}_i + \hat{s}_{i+1} e_i - \hat{s}_i e_{i+1}] \} \end{aligned} \quad (5.105)$$

with  $\hat{s}_i = \mu \sqrt{\Gamma} s_i$ .

*Proof.* The proposed algebra isomorphism uses the same notation,  $e_i$ , for the Temperley–Lieb generators, and sets

$$s_i = \frac{\mu}{\sqrt{\Gamma}} [Q\tau(Q + \tau)\mathbb{1} + Q(1 - Q\tau)e_i - (\tau^2 + 2Q\tau - 1)g_i], \quad (5.106)$$

or equivalently,

$$g_i = \frac{1}{\tau^2 + 2Q\tau - 1} [Q\tau(Q + \tau)\mathbb{1} + Q(1 - Q\tau)e_i - \mu \sqrt{\Gamma} s_i]. \quad (5.107)$$

With this, one verifies that the relations (5.100) imply the relations (5.56) and the vanishing of (5.105). Likewise, the relations (5.56) together with the vanishing of (5.105) are seen to imply the relations (5.100).  $\square$

**Remark.** For  $\epsilon = 1$ ,  $s \in W_2$  is invariant under  $\mathsf{P}_{r_{4,1}}$ , as becomes evident when rewriting (5.106) as

$$s_i = \frac{\mu Q(\tau^2 + 1)}{2\sqrt{\Gamma}} (\mathbb{1} + e_i) - \frac{\mu(\tau^2 + 2Q\tau - 1)}{2\sqrt{\Gamma}} (g_i + g_i^{-1}), \quad (5.108)$$

since

$$\mathsf{P}_{r_{4,1}}(\mathbb{1}_2) = e, \quad \mathsf{P}_{r_{4,1}}(e) = \mathbb{1}_2, \quad \mathsf{P}_{r_{4,1}}(g^{\pm 1}) = g^{\mp 1}. \quad (5.109)$$

**Remark.** The algebra  $\text{BMW}_n(\tau, q)$  is occasionally referred to as *Kauffman’s Dubrovnik version* [58]. It differs from the one in [59], which is based on

$$g_i + g_i^{-1} = Q_0(\mathbb{1} + e_i), \quad e_i^2 = \delta_0 e_i, \quad \delta_0 = -1 + \frac{\tau + \tau^{-1}}{Q_0}, \quad Q_0 = q + q^{-1}, \quad (5.110)$$

and consequently admits a description as a quotient of  $\text{PS}_n^{(\epsilon)}$  similar to the one in Proposition 5.4.1, but for  $\epsilon = -1$ . The two possible imaginary values,  $\epsilon = i$  and  $\epsilon = -i$ , enter similar quotient descriptions of the Liu algebra in Section 5.5.2.

### 5.4.4 Baxterisation

Relative to the canonical  $W_2$ -basis  $\{\mathbb{1}_2, e, g\}$ , we introduce the parameterised  $R$ -operator as

$$R(u) = r_{\mathbb{1}}(u)\mathbb{1}_2 + r_e(u)e + r_g(u)g, \quad \text{with } r_{\mathbb{1}}, r_e, r_g : \Omega \rightarrow \mathbb{C}, \quad (5.111)$$

with  $r_{\mathbb{1}}, r_e, r_g : \Omega \rightarrow \mathbb{C}$ .

**Remark.** Since  $e_i$  is quadratic in  $g_i$ , the function  $r_g$  is required to be nonzero when exploring homogeneous integrability encoded by  $\text{BMW}_n(\tau, q)$ .

It is known [60], see also [61], that  $\text{BMW}_n(\tau, q)$  admits a Baxterisation. Within the integrability framework developed in Section 3.2, we have the following.

**Proposition 5.4.2.** *Let  $Q = q - q^{-1}$  and  $\omega \in \{-\tau q, \tau q^{-1}\}$ , the  $R$ -operator*

$$R(u) = \frac{q^2 - 1}{q^2 - u} \left[ \mathbb{1}_2 + \frac{1 - u}{u - \omega} e + \frac{1 - u}{Qu} g \right] \quad (5.112)$$

*provides a homogeneous Baxterisation of  $\text{BMW}_n(\tau, q)$ , with*

$$\bar{Y}_1(u, v) = R(uv), \quad Y_1(u, v) = \frac{Q^2 \omega^2 uv (uv - \omega)^2}{(1 - uv)(uv - \omega^2)(uv - \omega q^2)(uv - \omega q^{-2})} R\left(\frac{\omega^2}{uv}\right), \quad (5.113)$$

and (for  $i = 2, 3$ )

$$\bar{Y}_i(u, v) = \bar{Y}_1\left(\frac{\omega}{u}, v\right), \quad Y_i(u, v) = Y_1\left(\frac{\omega}{u}, v\right). \quad (5.114)$$

*Proof.* We first observe that the  $R$ -operator (5.13) satisfies the following crossing symmetries

$$\text{Diagram} = \frac{\omega(1-u)(q^2 - \omega/u)}{u(u-\omega)(q^2 - u)} \text{Diagram}, \quad \text{Diagram} = \text{Diagram}. \quad (5.115)$$

The BYBEs (3.32) are satisfied by applying the crossing symmetries, observing  $\text{BMW}_2$  is a commutative algebra, and noting that  $\bar{Y}_1(u, v)$  and  $Y_1(u, v)$  are symmetric in  $u$  and  $v$ .

Applying the crossing symmetries (5.115) for  $u \neq 0$ , it follows, as in Proposition 5.1.1, that the  $Y$ -operators can be expressed as

$$\bar{Y}_2(u, v) = \bar{Y}_1\left(\frac{\omega}{u}, v\right), \quad \bar{Y}_3(u, v) = \bar{Y}_1\left(v, \frac{\omega}{u}\right), \quad Y_2(u, v) = Y_1\left(\frac{\omega}{u}, v\right), \quad Y_3(u, v) = Y_1\left(v, \frac{\omega}{u}\right). \quad (5.116)$$

It remains to verify that (5.112) and (5.113) provide a solution to Inv1 (3.30) and YBE1 (3.31), see Appendix A.3 for details.  $\square$

It follows from the crossing symmetries (5.115) that conditions (3.30) and (3.31) reduce to the single inversion identity and the single *standard* YBE

$$\text{Diagram} = \text{Diagram}, \quad \text{Diagram} = \text{Diagram}. \quad (5.117)$$

Relative to the involution  $\cdot^*$  on the BMW algebra with  $\tau, q \in \mathbb{R}$ , the  $R$ -operator (5.112) is self-adjoint for all  $u \in \mathbb{R} \setminus \{q^2, \omega\}$ .

**Remark.** We have verified that, up to a normalising factor, the generalised Yang–Baxter framework of Proposition 3.2.2 does not admit any other non-specious solution of the form (5.111), with  $r_g$  nonzero, than the one presented in Proposition 5.4.2.

## 5.5 Liu algebra

### 5.5.1 Planar algebra

The *Liu planar algebra* is naturally defined as a quotient planar algebra much akin to the PSG planar algebra in Section 5.2. With  $C^{(\epsilon)}(\alpha, \delta)$  as in (5.55), we thus introduce

$$C_L^{(\epsilon)}(\delta) := C^{(\epsilon)}(0, \delta) \cup \left\{ \text{diagram } 1 - \text{diagram } 2 - \frac{1}{\delta^2} \left[ \text{diagram } 3 - \text{diagram } 4 - \epsilon \left( \text{diagram } 5 - \text{diagram } 6 + \text{diagram } 7 - \text{diagram } 8 \right) \right] \right\}, \quad (5.118)$$

where  $\delta \neq 0$  and  $\epsilon \in \{-i, i\}$ . Following [39], the *Liu planar algebra*  $L^{(\epsilon)}(\delta)$  is then defined as the quotient planar algebra  $(A_n(S, C_L^{(\epsilon)}(\delta)))_{n \in \mathbb{N}_0}$ , where  $S$  is as in (5.54).

**Remark.** In the PSG planar algebra in Section 5.2, for  $PS_1$  and  $PS_2$  to be positive-definite, we have  $\delta > 1$ , see (5.27). Here, in our definition of the Liu planar algebra, we relax this condition to  $\delta \neq 0$ .

From here onward, we opt for the abridged notation  $L_n \equiv A_n(S, C_L^{(\epsilon)}(\delta))$ ,  $n \in \mathbb{N}_0$ . Imposing the relations  $C_L^{(\epsilon)}(\delta)$  tames the dimensionality of the universal planar algebra, resulting in the dimension formula

$$\dim L_n = (2n - 1)!!.. \quad (5.119)$$

The Liu planar algebra  $L^{(\epsilon)}(\delta)$  is spherical and involutive [39], with the involution  $\cdot^*$  defined as the conjugate-linear map that acts by reflecting every disk about a line perpendicular to its marked boundary interval, as

$$\left( \text{diagram } 1 \right)^* = \text{diagram } 1, \quad \left( \text{diagram } 2 \right)^* = \text{diagram } 2, \quad \left( \text{diagram } 3 \right)^* = \text{diagram } 3, \quad (5.120)$$

recalling that  $s^* = s$  for  $\alpha = 0$ , see comment following (5.46).

We let  $\mathcal{L}^{(\epsilon)}$  denote the set of all  $\delta$  such that  $L^{(\epsilon)}(\delta)$  is positive semi-definite. For each  $\delta \in \mathcal{L}^{(\epsilon)}$  and  $\epsilon \in \{-i, i\}$ , the *Liu subfactor planar algebra*  $L^{(\epsilon)}(\delta)$  is then defined as the quotient of  $L^{(\epsilon)}(\delta)$  by the kernel of the trace norm. Details of the set  $\mathcal{L}^{(\epsilon)}$  are presented in [39], including  $\left\{ i \frac{q_m + q_m^{-1}}{q_m - q_m^{-1}} \mid m \in \mathbb{N} \right\} \subseteq \mathcal{L}^{(\epsilon)}$ , where  $q_m = q^{\frac{i\pi}{2m+2}}$ .

### 5.5.2 Presentation and quotient description

For each  $n \in \mathbb{N}$ ,  $\epsilon \in \{-i, i\}$  and  $\delta \neq 0$ , the *Liu algebra*  $L_n^{(\epsilon)}(\delta)$  is defined by endowing the vector space  $L_n$  with the multiplication induced by the unshaded planar tangle  $M_n$  following from (2.26). We note that the Liu algebra is both unital (with unit denoted by  $\mathbb{1}$ ) and associative, and that it is a  $^*$ -algebra with involution inherited from the Liu planar algebra. The generators can be represented diagrammatically as in (5.60), and the algebra admits a presentation  $\langle e_i, s_i \mid i = 1, \dots, n-1 \rangle$  subject to the relations

$$\begin{aligned} s_i^2 &= \mathbb{1} - \frac{1}{\delta} e_i, & e_i s_i &= s_i e_i = 0, & s_i s_j &= s_j s_i, & |i - j| &> 1, \\ e_i e_{i \pm 1} e_i &= e_i, & e_i e_{i \pm 1} s_i &= \epsilon^{\pm 1} e_i s_{i \pm 1}, & s_i e_{i \pm 1} e_i &= \epsilon^{\mp 1} s_{i \pm 1} e_i, \end{aligned} \quad (5.121)$$

and

$$s_i s_{i+1} s_i - s_{i+1} s_i s_{i+1} = \frac{1}{\delta^2} [s_i - s_{i+1} - \epsilon (e_i s_{i+1} - s_{i+1} e_i + e_{i+1} s_i - s_i e_{i+1})], \quad (5.122)$$

with  $\mathbb{1}$  denoting the unit. Following from (5.121), we also have the relations

$$e_i^2 = \delta e_i, \quad e_i e_j = e_j e_i, \quad e_i s_j = s_j e_i, \quad |i - j| > 1, \quad (5.123)$$

$$e_i s_{i \pm 1} s_i = \epsilon^{\mp 1} (e_i e_{i \pm 1} - \frac{1}{\delta} e_i), \quad s_i s_{i \pm 1} e_i = \epsilon^{\pm 1} (e_{i \pm 1} e_i - \frac{1}{\delta} e_i), \quad (5.124)$$

and

$$e_i s_{i \pm 1} e_i = 0, \quad s_i e_{i+1} s_i = s_{i+1} e_i s_{i+1}. \quad (5.125)$$

We note that it suffices to list one of the two relations  $e_i s_i = 0$  or  $s_i e_i = 0$  in (5.121).

**Remark.** It follows from the presentation above that the minimal vanishing polynomial in  $s_i$  is  $s_i^3 - s_i$ , so  $s_i$  is not invertible.

The Liu algebra differs from the FC and BMW algebras in that there is no known basis for  $L_n^{(\epsilon)}(\delta)$  in terms of which the relations (5.121)–(5.125) admit a natural diagrammatic representation. In Section 5.5.4, we consider a basis which includes a braid [39], and where (5.122) can be interpreted as a type-III Reidemeister move. However, in this basis, some of the other relations fail to have a natural diagrammatic interpretation.

By comparing the presentation above with the one of  $PS_n^{(\epsilon)}(\alpha, \delta)$  in Section 5.2.3, we obtain the following result, recalling that  $\alpha = 0$  for  $\epsilon \in \{-i, i\}$ .

**Proposition 5.5.1.** *For each  $n \in \mathbb{N}$ ,  $\epsilon \in \{-i, i\}$ , and  $\delta > 1$ , we have*

$$L_n^{(\epsilon)}(\delta) \cong PS_n^{(\epsilon)}(0, \delta) / \langle \iota_1, \dots, \iota_{n-2} \rangle, \quad (5.126)$$

where

$$\iota_i = s_i s_{i+1} s_i - s_{i+1} s_i s_{i+1} - \frac{1}{\delta^2} [s_i - s_{i+1} - \epsilon (e_i s_{i+1} - s_{i+1} e_i + e_{i+1} s_i - s_i e_{i+1})]. \quad (5.127)$$

We let  $\mathcal{L}_n^{(\epsilon)}$  denote the set of all  $\delta$  such that the trace form (2.34) is positive semi-definite on  $L_n$ , noting that  $\mathcal{L}^{(\epsilon)} \subseteq \mathcal{L}_n^{(\epsilon)}$  for all  $n \in \mathbb{N}_0$ . For each  $\delta \in \mathcal{L}_n^{(\epsilon)}$ ,  $L_n^{(\epsilon)}(\delta)$  is defined as the *Liu subfactor algebra* constructed as the quotient of  $L_n^{(\epsilon)}(\delta)$  by the kernel of the trace norm.

### 5.5.3 Baxterisation

Relative to the canonical  $L_2$ -basis  $\{\mathbb{1}_2, e, s\}$ , we introduce the parameterised  $R$ -operator as

$$R(u) = r_{\mathbb{1}}(u) \mathbb{1}_2 + r_e(u) e + r_s(u) s, \quad \text{with } \mathbb{1}_2 = r_{\mathbb{1}}(u) \text{ and } e = r_e(u) \text{ and } s = r_s(u), \quad (5.128)$$

with  $r_{\mathbb{1}}, r_e, r_s : \Omega \rightarrow \mathbb{C}$ .

**Remark.** Since  $e_i$  is quadratic in  $s_i$ , the function  $r_s$  is required to be nonzero when exploring homogeneous integrability encoded by  $L_n^{(\epsilon)}(\delta)$ .

Unlike the TL, FC and BMW algebras, the Liu algebra  $L_n^{(\epsilon)}(\delta)$ , is not known to admit a Baxterisation. A distinct feature of the Liu algebra is the absence of symmetries of the unparameterised  $R$ -operator, which is not invariant under rotation by  $\pi$  (unless  $r_s(u) = 0$ ),

$$\begin{array}{c} \text{Diagram 1} \\ \text{Diagram 2} \end{array} \neq \begin{array}{c} \text{Diagram 2} \\ \text{Diagram 1} \end{array}. \quad (5.129)$$

Despite this fact, we show in Proposition 5.5.2 below, that the Liu algebra admits a homogeneous Baxterisation. To describe it, we find it useful to introduce the function

$$\phi : (u, v) \mapsto \frac{u+v}{1-uv}. \quad (5.130)$$

**Proposition 5.5.2.** *For each  $\mu \in \{-1, 1\}$ ,*

$$R^{(\mu)}(u) = \mathbb{1}_2 + ue + \mu\delta us \quad (5.131)$$

*provides a homogeneous Baxterisation of  $L_n^{(\epsilon)}(\delta)$ , with*

$$\bar{Y}_1(u, v) = R^{(\mu)}(x), \quad Y_1(u, v) = \frac{\delta x - 1}{(\delta^2 + 1)x(x + \delta)} R^{(-\mu)}\left(\frac{x + \delta}{\delta x - 1}\right), \quad x := \phi(u, v), \quad (5.132)$$

and (for  $i = 2, 3$ )

$$\bar{Y}_i(u, v) = \mathbb{1}_2 + ye - (-1)^i \mu\delta\epsilon s, \quad Y_i(u, v) = \frac{1}{\delta^2 - y^2} \bar{Y}_i(v, u), \quad y := \frac{1}{\phi(u, -v)}. \quad (5.133)$$

*Proof.* The BYBEs (3.32) are satisfied by observing  $\mathbb{L}_2$  is a commutative algebra, and noting that

$$\bar{Y}_1(u, v) = \bar{Y}_4(u, v), \quad \bar{Y}_2(u, v) = P_{r_{4,2}}(\bar{Y}_3(u, v)), \quad Y_1(u, v) = Y_4(u, v), \quad Y_2(u, v) = P_{r_{4,2}}(Y_3(u, v)). \quad (5.134)$$

It remains to verify that (5.131)–(5.133) provide a solution to Inv1–Inv3 (3.30), and YBE1–YBE3 (3.31), see Appendix A.4 for details.  $\square$

Relative to the involution  $\cdot^*$  on the Liu algebra, the  $R$ -operator (5.131) is self-adjoint for all  $u \in \mathbb{R}$ . On the other hand, unlike the  $R$ -operators in the FC and BMW algebras, the  $R$ -operator (5.131) is not crossing symmetric, not even partially crossing symmetric, that is, there do not exist scalar functions  $\tilde{c}$  and  $c$  such that

$$P_{r_{4,1}}(R^{(\mu)}(u)) = \tilde{c}(u)R^{(\mu)}(c(u)) \quad \text{or} \quad P_{r_{4,2}}(R^{(\mu)}(u)) = \tilde{c}(u)R^{(\mu)}(c(u)). \quad (5.135)$$

This explains why the  $Y$ -operators are not expressible in terms of the  $R$ -operator itself, as is the situation in the TL, FC and BMW cases, c.f. (5.1.1)–(5.1.4), (5.87)–(5.88) and (5.113)–(5.114), respectively.

**Remark.** We have verified that, up to a normalising factor, the generalised Yang–Baxter framework of Proposition 3.2.2 does not admit any other non-specious solution of the form (5.128), with  $r_s$  nonzero, than the one presented in Proposition 5.5.2.

### 5.5.4 Braid limits

For each  $\mu \in \{-1, 1\}$ , the  $R$ -operator (5.131) yields well-defined  $L_2$ -elements under the specialisations  $u = -i$  and  $u = i$ ,

$$R^{(\mu)}(-i) = \mathbb{1}_2 - ie - i\mu\delta s, \quad R^{(\mu)}(i) = \mathbb{1}_2 + ie + i\mu\delta s, \quad (5.136)$$

and we collect the ensuing four elements in the set

$$\mathcal{B} = \{\mathbb{1}_2 + \epsilon_1 e + \epsilon_2 \delta s \mid \epsilon_1, \epsilon_2 \in \{-i, i\}\}. \quad (5.137)$$

For each  $b \in \mathcal{B}$ , we have

$$b^2 = 2b - (\delta^2 + 1)\mathbb{1}_2, \quad (5.138)$$

so, for  $\delta^2 \neq -1$ ,  $b$  is invertible, with inverse given by

$$b^{-1} = \frac{1}{\delta^2 + 1}(2\mathbb{1}_2 - b). \quad (5.139)$$

Although not obtained as limits of our  $R$ -operator, the elements of  $\mathcal{B}$  also feature in [39], where it is shown that for each  $b \in \mathcal{B}$ , the generators  $\{b_1, \dots, b_{n-1}\} \subset L_n$  satisfy

$$b_i b_{i\pm 1} b_i = b_{i\pm 1} b_i b_{i\pm 1}, \quad b_i b_j = b_j b_i, \quad |i - j| > 1. \quad (5.140)$$

Here,  $b_i \in L_n$  denotes the element ‘acting’ as  $b$  on the  $i$ th and  $(i+1)$ th nodes and as the identity elsewhere. This justifies referring to (5.136) as *braid limits*.

## 5.6 Polynomial integrability

For the TL algebra and each of the singly generated algebras FC, BMW, and Liu, we refer to the homogeneous double-row transfer operator built using the  $R$ -operator parameterised in (5.13), (5.86), (5.112), and (5.131), respectively, as the *canonical transfer operator* on  $\Omega$ , with  $\Omega \subseteq \mathbb{C}$  a suitable domain (that depends on the underlying algebra). In each case, this transfer operator is the unique (up to renormalisations and reparameterisations) algebra element encoding homogeneous Yang–Baxter integrability on the strip.

Using Liu’s Theorem 5.2.4, the Remark following Corollary 4.2.3, and results obtained in the previous three sections, we can now account for the *polynomialisability* of the double-row transfer operator in Theorem 5.0.2. With notation as in Section 5.1, Section 5.3, Section 5.4, and Section 5.5, the following result thus gives conditions on the various algebra-defining parameters, ensuring that the respective canonical transfer operator is polynomialisable.

**Proposition 5.6.1.**

(TL) : Let  $n \in \mathbb{N}$  and  $\delta \in \mathcal{T}_n$ , and suppose  $T_n^{(d)}(u) \in \text{TL}_n(\delta)$  is the corresponding canonical transfer operator, with  $u \in \mathbb{R}$ . Then,  $T_n^{(d)}(u)$  is polynomialisable.

(FC) : Let  $n \in \mathbb{N}$  and  $\gamma \in \mathcal{F}_n$ , and suppose  $T_n^{(d)}(u) \in \text{FC}_n(\gamma)$  is the corresponding canonical transfer operator, with  $u \in \mathbb{R} \setminus \{\gamma^2 - 1\}$ . Then,  $T_n^{(d)}(u)$  is polynomialisable.

(BMW) : Let  $n \in \mathbb{N}$  and  $(\tau, q) \in \mathcal{B}_n \cap \mathbb{R}^2$ , and suppose  $T_n^{(d)}(u) \in \text{BMW}_n(\tau, q)$  is the corresponding canonical transfer operator, with  $u \in \mathbb{R} \setminus \{q^2, \omega\}$ . Then,  $T_n^{(d)}(u)$  is polynomialisable.

(Liu) : Let  $n \in \mathbb{N}$ ,  $\epsilon \in \{-i, i\}$ , and  $\delta \in \mathcal{L}_n^{(\epsilon)}$ , and suppose  $T_n^{(d)}(u) \in \mathcal{L}_n^{(\epsilon)}(\delta)$  is the corresponding canonical transfer operator, with  $u \in \mathbb{R}$ . Then,  $T_n^{(d)}(u)$  is polynomialisable.

**Remark.** As the TL subfactor planar algebra is a planar subalgebra of every subfactor planar algebra, we have  $\delta \in \mathcal{T} \subset \mathbb{R}$  for any subfactor planar algebra, see (5.5). In the Liu case, in particular, it thus holds that  $\mathcal{L}_n^{(\epsilon)} \cap \mathbb{R} = \mathcal{L}_n^{(\epsilon)}$  for all  $n \in \mathbb{N}$  and  $\epsilon \in \{-i, i\}$ .

Here, we have established that the double-row transfer operator encoding homogeneous Yang–Baxter integrability for the TL planar algebra and each of the singly generated YBR planar algebras is polynomialisable. The following chapter is devoted to explicitly determining the form of such polynomials for two well-known models on the strip.

Components of the following publication have been incorporated into Chapter 6.

[2] X. Poncini, J. Rasmussen, *Integrability of planar-algebraic models*, J. Stat. Mech. (2023) 073101, arXiv:2206.14462 [math-ph].

# Chapter 6

---

## Hamiltonians and polynomial integrability

---

In this chapter, we explicitly determine algebraic elements giving rise to the polynomial integrability of two models on the strip: a Temperley–Lieb model and an eight-vertex model. By construction, the principal Hamiltonians and transfer operator share similar spectral features, at least to linear order in  $u$ . It is therefore natural to consider these elements as candidates for the polynomial integrability generator. We begin with the Temperley–Lieb model by establishing some facts about the double-row transfer operator parameterised as in Section 5.1 which are then used to derive the principal Hamiltonians of the model. Analysis of two principal Hamiltonians for small  $n$  reveals, in a faithful representation, that they possess a non-degenerate spectrum. This, together with the fact that Hamiltonians commute with the transfer operator, establishes that the transfer operator is polynomial in the principal Hamiltonians. We conclude by determining explicit polynomial expressions of the transfer operator in terms of these Hamiltonians and find that, for all  $\delta \in \mathbb{C}$  and small  $n$ , at least one of the polynomials is well-defined.

We proceed by constructing an eight-vertex model with an underlying tensor planar-algebraic structure and recover the familiar quantum inverse scattering framework discussed in Section 3.3. We show that the corresponding double-row transfer operator is diagonalisable and present explicit expressions for all of its eigenvalues and corresponding eigenvectors. We then exploit similarities in the spectral properties of the transfer operator and a principal Hamiltonian to establish that the transfer operator is polynomial in this Hamiltonian. Moreover, we determine explicit polynomial expressions of the transfer operator in terms of this principal Hamiltonian for all  $n \in \mathbb{N}$ .

**Remark.** As this chapter is concerned exclusively with the double-row transfer operator  $T_n^{(d)}(u)$ , we omit the superscript and refer to it simply as  $T_n(u)$ .

### 6.1 Revisiting the Temperley–Lieb planar algebra

Proposition 5.6.1 implies that for  $\delta > 2$ , there exists a  $u$ -independent integral of motion  $b_n \in \text{TL}_n(\delta)$ , such that the double-row transfer operator  $T_n(u)$  can be expressed as a polynomial in  $b_n$ . For a faithful representation  $\varrho_n$  defined in Section 6.1.1, it follows from Section 4.2, that  $\varrho_n(b_n)$  and  $\varrho_n(T_n(u))$  will have closely related Jordan decompositions. In the following, we derive the principal Hamiltonians

associated with  $T_n(u)$ , see (6.45) and (6.50), and use spectral analysis to argue that both of these  $\text{TL}_n(\delta)$ -elements can indeed play the role of  $b_n$ , at least for small  $n$ . We supplement this result by determining an explicit polynomial expression for  $T_n(u)$  in terms of each of the Hamiltonian elements, and find that they are well-defined for all  $u \in \mathbb{C}$  and all but finitely many  $\delta$ -values in  $\mathbb{C}$ . The restrictions on  $u$  and  $\delta$  in Proposition 5.6.1 can thus be relaxed accordingly, at least for small  $n$ . Moreover, we find that, for small  $n$ ,  $T_n(u)$  is polynomial in at least one of the two principal Hamiltonians for all  $\delta, u \in \mathbb{C}$ , see the discussion following (6.78).

**Remark.** Our focus in the following is on probing the naturally arising principal Hamiltonians as candidates for the integral of motion  $b_n$ . In fact, one could also explore whether any given specialisation of  $T_n(u)$ , where  $u$  is fixed to some value, could play the role of  $b_n$ . We have indeed examined several such candidates, but the standard Hamiltonian (6.45) has so far had the fewest number of *exceptional points*, see the discussion in Section 6.1.5.

### 6.1.1 Standard modules and cellularity

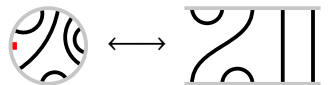
For each  $n \in \mathbb{N}$ , let

$$D_n := \{n - 2k \mid k = 0, \dots, \lfloor \frac{n}{2} \rfloor\}, \quad (6.1)$$

which is a naturally ordered set with  $\min(D_n) = \frac{1}{2}(1 - (-1)^n)$ . Recall that  $B_n$  denotes the basis for  $\text{T}_n$  consisting of Temperley–Lieb disks, which we refer to as *n-diagrams*, and define the following set

$$B'_n := B_n \setminus \{1_n\}. \quad (6.2)$$

It is common to represent *n-diagrams* as rectangular diagrams as in Section 5.1, here drawn such that the marked boundary interval corresponds to the left-most vertical side, as illustrated by



$$(6.3)$$

We introduce the linear involution

$${}^\circledast: \text{T}_n \rightarrow \text{T}_n, \quad x \mapsto x^\circledast, \quad (6.4)$$

that acts by reflecting *n-diagrams* about a line perpendicular to the marked boundary interval, and if  $x$  is expressed as a rectangular diagram, this is simply the horizontal. On the algebra  $\text{TL}_n(\delta)$ , this yields an anti-involution.

**Remark.** We highlight that  $\cdot^\circledast$  is linear and is therefore distinct from the *conjugate*-linear involution  $\cdot^*$  introduced in Section 5.1.

For each  $d \in D_n$ , let  $B_{n,d} \subseteq B_n$  denote the set of *n-diagrams* with exactly  $d$  nodes on the lower edge connected to nodes on the upper edge. The  $d$  loop segments connecting these  $2d$  nodes are referred to as *through-lines*. We now let  $S_{n,d}$  denote the set of all *n-diagrams* with  $d$  through-lines, whose upper

edge has been discarded along with any loop segments having both endpoints on the upper edge. The elements of  $S_{n,d}$  are referred to as  $(n,d)$ -link states and the elements of

$$S_n := \bigcup_{d \in D_n} S_{n,d} \quad (6.5)$$

are referred to as  $n$ -link states. To illustrate,



$$\text{Diagram (6.6): } \text{Left: } \text{Diagram with two strands and four loops. Right: Diagram with two strands and four loops. Both are mapped to: Diagram with two strands and four loops.} \quad (6.6)$$

give rise to the same  $(6,2)$ -link state. In fact, the  $(n,d)$ -link states may be viewed as equivalence classes of  $n$ -diagrams. From that perspective, the two 6-diagrams in (6.6) are seen as representatives of the same  $(6,2)$ -link state.

The vector space

$$V_{n,d} := \text{span}_{\mathbb{C}}(S_{n,d}), \quad \dim V_{n,d} = |S_{n,d}| = \binom{n}{\frac{n-d}{2}} - \binom{n}{\frac{n-d}{2} - 1}, \quad (6.7)$$

becomes a  $\text{TL}_n(\delta)$ -module by defining an action of the algebra generators on the link states such that  $a_2(a_1 v) = (a_2 a_1) v$  for all  $a_1, a_2 \in \text{TL}_n(\delta)$  and  $v \in V_{n,d}$ . The action defining the familiar *standard module*,  $V_{n,d}$ , is first given diagrammatically for  $n$ -diagrams acting on  $(n,d)$ -link states in the ‘natural way’, see e.g. [62], and then extended linearly to all of  $\text{TL}_n(\delta)$  and all of  $V_{n,d}$ .

For each pair  $x, y \in S_{n,d}$ , let  $(x, y)_{n,d}$  be constructed by reflecting the link state  $x$  about the horizontal, placing it below the link state  $y$ , connecting the strands in the natural way, and replacing any loop by a factor of  $\delta$ , see e.g. [62] for details. This extends to a bilinear map

$$(\cdot, \cdot)_{n,d}: V_{n,d} \times V_{n,d} \rightarrow \mathbb{C}[\delta], \quad (x, y) \mapsto (x, y)_{n,d}. \quad (6.8)$$

Relative to the  $(n,d)$ -link state basis  $S_{n,d}$ , the nonzero elements of the corresponding Gram matrix  $G_{n,d}$  are all monomials in  $\delta$ . The Gram determinant is thus polynomial in  $\delta$ , and following [63], it can be expressed as

$$\det G_{n,d} = \prod_{j=1}^{\frac{n-d}{2}} \left( \frac{U_{d+j}(\frac{\delta}{2})}{U_{j-1}(\frac{\delta}{2})} \right)^{\dim V_{n,d+2j}}, \quad (6.9)$$

where  $U_k(x)$  is the  $k^{\text{th}}$  Chebyshev polynomial of the second kind.

For each pair  $x, y \in S_{n,d}$ , let  $|x y|_{n,d}$  be constructed by reflecting the link state  $y$  about the horizontal, placing it above the link state  $x$  and connecting the  $d$  defects non-intersectingly. This extends to a bilinear map

$$|\cdot \cdot|_{n,d}: V_{n,d} \times V_{n,d} \rightarrow \text{TL}_{n,d}(\delta), \quad (x, y) \mapsto |x y|_{n,d}. \quad (6.10)$$

where  $\text{TL}_{n,d}(\delta)$  is the subset of  $\text{TL}_n(\delta)$  whose elements have exactly  $d$  through-lines. It follows that

$$|x y|_{n,d} z = (y, z)_{n,d} x, \quad \forall x, y, z \in V_{n,d}. \quad (6.11)$$

When clear, the subscripts of  $(\cdot, \cdot)_{n,d}$  and  $|\cdot \cdot|_{n,d}$  will be suppressed, writing  $(\cdot, \cdot)$  and  $|\cdot \cdot|$ , respectively.

It follows from Section 4.4 that  $\text{TL}_n(\delta)$  is cellular with cell datum  $(D_n, S_n, |\cdot \cdot|, \circledast)$ . We note that the involution  $\circledast$  provides an adjoint operation relative to the bilinear form  $(\cdot, \cdot)$  on  $V_{n,d}$ :

$$(x, ay) = (a^\circledast x, y), \quad a \in \text{TL}_n(\delta), x, y \in V_{n,d}. \quad (6.12)$$

In preparation for the discussion in Section 6.1.4, let

$$V_n := \text{span}_{\mathbb{C}}(S_n), \quad (6.13)$$

and note that, as vector spaces,

$$V_n = \bigoplus_{d \in D_n} V_{n,d}, \quad (6.14)$$

hence

$$\dim V_n = \sum_{d \in D_n} \dim V_{n,d} = \binom{n}{\lfloor \frac{n}{2} \rfloor}. \quad (6.15)$$

We also let  $\varrho_{n,d}$  denote the representation corresponding to the standard module  $V_{n,d}$ , and let

$$\varrho_n := \bigoplus_{d \in D_n} \varrho_{n,d}. \quad (6.16)$$

Relative to an ordered  $V_n$ -basis of the form

$$S_{n,s_n} \cup S_{n,s_n+2} \cup \dots \cup S_{n,n}, \quad s_n := \frac{1}{2}(1 - (-1)^n), \quad (6.17)$$

the matrix representation of  $\varrho_n$  is block-diagonal. Moreover, from Section 4.4, we have that  $\varrho_n$  is faithful for all  $\delta \in \mathbb{C}$  for which  $\prod_{d \in D_n} \det G_{n,d} \neq 0$ . In particular,  $\varrho_n$  is faithful for  $\delta$  an indeterminate and fails to be faithful for at most finitely many  $\delta$ -values in  $\mathbb{C}$ .

## 6.1.2 Transfer operators

Recalling the form of the  $R$ - and  $K$ -elements giving rise to a homogeneous Baxterisation presented in Section 5.1, we have

$$R(u) = \mathbb{1}_2 + ue, \quad K(u) = \overline{K}(u) = \mathbb{1}_1, \quad (6.18)$$

where  $u \in \mathbb{C}$ . Diagrammatically, this  $R$ -element is given by

$$R(u) = \text{Diagram} = \text{Diagram} + u \text{Diagram}, \quad (6.19)$$

and the transfer operator can be expressed in its familiar (see e.g. [21]) diagrammatic form

$$T_n(u) = \text{Diagram} \dots \text{Diagram} \quad (6.20)$$

To emphasise its dependence on  $\delta$ , we occasionally write  $T_n(u, \delta)$  instead.

**Remark.** The parameterisation in (6.18) ensures that  $R(u) \neq 0$  for all  $u$ , and this would similarly have been achieved had we chosen to work with  $\hat{R}(\hat{u}) = \hat{u} \mathbb{1}_2 + e$ , where  $\hat{R}(\hat{u}) \neq 0$  for all  $\hat{u} \in \mathbb{C}$ . Viewing  $u$

and  $\hat{u}$  as coordinates on the Riemann sphere, we see that, for all  $u \in \mathbb{C} \cup \{\infty\}$ ,  $R(u) \mapsto R(\hat{u}) = \frac{1}{u} \hat{R}(u)$  as  $u \mapsto \hat{u} \equiv \frac{1}{u}$ .

With (6.19), we have the decompositions

$$\begin{array}{c} \text{Diagram with } v \text{ and } u \text{ in green circles} \\ = uv \end{array} \Bigg| \begin{array}{c} \text{Diagram with } u+v+\delta \text{ in green circle} \\ + (u+v+\delta) \end{array} , \quad \begin{array}{c} \text{Diagram with } v \text{ and } u \text{ in green circles} \\ = \text{Diagram with } u+v+\delta uv \text{ in green circle} \end{array} \Bigg| \begin{array}{c} \text{Diagram with } u+v+\delta uv \text{ in green circle} \\ + (u+v+\delta uv) \end{array} , \quad (6.21)$$

$$\begin{array}{c} \text{Diagram with } v \text{ and } u \text{ in green circles} \\ = \text{Diagram with } u+v+\delta uv \text{ in green circle} \end{array} , \quad \begin{array}{c} \text{Diagram with } v \text{ and } u \text{ in green circles} \\ = uv \end{array} \Bigg| \begin{array}{c} \text{Diagram with } u+v+\delta \text{ in green circle} \\ + (u+v+\delta) \end{array} . \quad (6.22)$$

Equations (6.21) and (6.22), reduce to the so-called “drop-down” relations [64] under a specialisation, see also Proposition 3.4.1.

**Proposition 6.1.1.** *We have*

$$T_n(u)|_{\delta+2u=0} = \delta u^{2n} \mathbb{1}_n, \quad T_n(u)|_{u(2+\delta u)=0} = \delta \mathbb{1}_n. \quad (6.23)$$

*Proof.* The results follow from repeated application of (6.21) with  $v = u$ , to (6.20).  $\square$

**Proposition 6.1.2.** *We have*

$$T_n(u) = \text{Diagram with } u \text{ in green circles} \dots \text{Diagram with } u \text{ in green circles} . \quad (6.24)$$

*Proof.* For  $u(2+\delta u)(\delta+2u) = 0$ , apply (6.22) with  $v = u$  to the right-hand side of (6.24). Comparing with Proposition 6.1.1, we arrive at (6.24). If  $u(2+\delta u)(\delta+2u) \neq 0$ , the operators

$$\text{Diagram with } u \text{ in red circle} = \frac{1-u^2}{u(2+\delta u)} \text{Diagram with } u \text{ in red circle} + \text{Diagram with } u \text{ in green circle} , \quad \text{Diagram with } u \text{ in red circle} = \frac{u^2-1}{2u+\delta} \text{Diagram with } u \text{ in red circle} + \text{Diagram with } u \text{ in green circle} , \quad (6.25)$$

satisfy

$$\text{Diagram with } u \text{ in red circle} = \text{Diagram with } u \text{ in red circle} , \quad \text{Diagram with } u \text{ in green circle} = \text{Diagram with } u \text{ in green circle} , \quad (6.26)$$

and

$$\text{Diagram with } u \text{ in green circle} = \frac{u(2+\delta u)}{\delta+2u} \text{Diagram with } u \text{ in red circle} , \quad \text{Diagram with } u \text{ in red circle} = \frac{\delta+2u}{u(2+\delta u)} \text{Diagram with } u \text{ in green circle} . \quad (6.27)$$

It follows that

$$T_n(u) = \text{Diagram with } u \text{ in green circles} \dots \text{Diagram with } u \text{ in green circles} = \text{Diagram with } u \text{ in green circles} \dots \text{Diagram with } u \text{ in green circles} \text{Diagram with } u \text{ in red circle} \text{Diagram with } u \text{ in red circle} , \quad (6.28)$$

and we arrive at the desired result.  $\square$

Recall that the  $R$ -operator satisfies the following crossing symmetries

$$\begin{array}{c} \text{Diagram with } u \text{ in green circle} \\ \text{Diagram with } 1/u \text{ in red circle} \end{array} = u \quad \begin{array}{c} \text{Diagram with } 1/u \text{ in green circle} \\ \text{Diagram with } u \text{ in red circle} \end{array}, \quad (6.29)$$

with  $u = 1$  an isotropic point. By Proposition 6.1.2,

$$T_n(u) = u^{2n} T_n(1/u), \quad (6.30)$$

so  $u^{-n} T_n(u)$  is invariant under  $u \mapsto 1/u$ . Since  $T_n(u)$  is polynomial in  $u$  of degree at most  $2n$ , it follows that there exists  $\tilde{T}_n(x) \in \text{TL}_n(\delta)[x]$  such that

$$T_n(u) = u^n \tilde{T}_n(u + \frac{1}{u}). \quad (6.31)$$

Moreover, there exist  $a_0, \dots, a_{2n} \in \text{TL}_n(\delta)$  such that

$$T_n(u) = \sum_{i=0}^{2n} a_i u^i, \quad (6.32)$$

and using (6.30), it follows that  $a_{2n-i} = a_i$ ,  $i = 0, \dots, n-1$ , so

$$\tilde{T}_n(x) = a_n + 2 \sum_{i=1}^n a_{n-i} T_i^{(c)}\left(\frac{x}{2}\right), \quad (6.33)$$

where  $T_k^{(c)}$  is the  $k^{\text{th}}$  Chebyshev polynomial of the first kind. In establishing (6.33), we have used the familiar relation

$$T_k^{(c)}(\cosh \theta) = \cosh(k\theta), \quad \theta \in \mathbb{C}. \quad (6.34)$$

To shine further light on the structure of  $T_n(u, \delta)$ , we introduce the following parameterised elements of  $\text{TL}_n(\delta)$ . For  $n \in \mathbb{N}$  and each pair  $j, k \in \mathbb{N}_0$  such that  $j + k \leq n - 2$ , let

$$S_{j,k}^{(n)}(u) := \left[ \underbrace{\dots}_{j} \quad \underbrace{\begin{array}{c} \text{Diagram with } u \text{ in green circle} \\ \text{Diagram with } u \text{ in red circle} \end{array} \dots} \quad \underbrace{\dots}_{k} \right], \quad (6.35)$$

which reduces to  $S_{j, n-j-2}^{(n)}(u) = e_{j+1}$  for  $k = n - j - 2$ . To emphasise its dependence on  $\delta$ , we occasionally write  $S_{j,k}^{(n)}(u, \delta)$ . Note that  $S_{j,k}^{(n)}(u) \in \text{span}_{\mathbb{C}}(B'_n)$ .

**Lemma 6.1.3.** *For  $n \in \mathbb{N}$ , we have*

$$\underbrace{\begin{array}{c} \text{Diagram with } u \text{ in green circle} \\ \text{Diagram with } u \text{ in red circle} \end{array} \dots \begin{array}{c} \text{Diagram with } u \text{ in green circle} \\ \text{Diagram with } u \text{ in red circle} \end{array}}_n = u^{2n-2} \mathbb{1}_n + (\delta + 2u) \sum_{k=0}^{n-2} u^{2k} S_{0,k}^{(n)}(u) \quad (6.36)$$

and

$$\underbrace{\begin{array}{c} \text{Diagram with } u \text{ in green circle} \\ \text{Diagram with } u \text{ in red circle} \end{array} \dots \begin{array}{c} \text{Diagram with } u \text{ in green circle} \\ \text{Diagram with } u \text{ in red circle} \end{array}}_n = \mathbb{1}_n + u(2 + \delta u) \sum_{j=0}^{n-2} S_{j,0}^{(n)}(u). \quad (6.37)$$

*Proof.* The result (6.36) follows by induction on  $n$ , decomposing the two right-most  $R$ -operators as in (6.22) with  $v = u$  and using that both sides of (6.36) reduce to  $\mathbb{1}_1$  for  $n = 1$ . The result (6.37) follows similarly.  $\square$

For  $k \in \mathbb{N}_0$  and  $x \in \mathbb{C}$ , we let

$$[k]_x := 1 + x + \cdots + x^{k-1} \quad (k > 1), \quad [1]_x := 1, \quad [0]_x := 0. \quad (6.38)$$

**Proposition 6.1.4.** *The transfer operator decomposes as*

$$T_n(u, \delta) = (\delta[n+1]_{u^2} + 2u[n]_{u^2})\mathbb{1}_n + u(\delta + 2u)(2 + \delta u) \sum_{j=0}^{n-2} \sum_{k=0}^{n-2-j} u^{2k} S_{j,k}^{(n)}(u). \quad (6.39)$$

*Proof.* By (6.22) with  $v = u$ , we have

$$T_n(u) = u(2 + \delta u) \quad \text{Diagram: } \begin{array}{c} \text{A horizontal chain of } n \text{ green circles, each with a red dot and labeled } u. \text{ The first circle is connected to the second by a vertical line, and the last circle is connected to the second circle from the left by a vertical line.} \end{array} + \quad \text{Diagram: } \begin{array}{c} \text{A horizontal chain of } n \text{ green circles, each with a red dot and labeled } u. \text{ The first circle is connected to the second by a vertical line, and the last circle is connected to the second circle from the left by a vertical line. A curly brace is placed to the right of the first two circles, indicating a sum of terms.} \end{array} \quad (6.40)$$

The result now follows by induction on  $n$ , applying (6.36) to the first term on the right in (6.40) and the induction hypothesis to the second term.  $\square$

**Corollary 6.1.5.** *For  $u(\delta + 2u)(2 + \delta u) \neq 0$ , we have*

$$\frac{1}{u^{n-2}} \sum_{j=0}^{n-2} \sum_{k=0}^{n-2-j} u^{2k} S_{j,k}^{(n)}(u) = u^{n-2} \sum_{j=0}^{n-2} \sum_{k=0}^{n-2-j} \frac{1}{u^{2k}} S_{j,k}^{(n)}\left(\frac{1}{u}\right). \quad (6.41)$$

*Proof.* The result follows from (6.30) and Proposition 6.1.4.  $\square$

**Corollary 6.1.6.** *The transfer operator decomposes uniquely as*

$$T_n(u, \delta) = (\delta[n+1]_{u^2} + 2u[n]_{u^2})\mathbb{1}_n + u(\delta + 2u)(2 + \delta u) \sum_{a \in B'_n} \Gamma_a^{(n)}(u, \delta) a, \quad (6.42)$$

where  $\Gamma_a^{(n)}(u, \delta)$  is polynomial in  $u, \delta$  for every  $a \in B'_n$ .

*Proof.* With the parameterisation (6.18), the decomposition of  $T_n(u, \delta)$  into connectivity diagrams (elements of  $B_n$ ) involves only coefficients that are polynomial in  $u, \delta$ , and since  $B_n$  is a linearly independent set, the decomposition is unique. The restriction to a summation over  $B'_n$  is permitted (and required for uniqueness) because  $S_{j,k}^{(n)}(u) \in \text{span}_{\mathbb{C}}(B'_n)$ .  $\square$

**Remark.** The expression (6.20) for  $T_n(u, \delta)$  may be formally extended to  $n = 0$ , yielding  $T_0(u, \delta) = \delta \mathbb{1}_0$ . With  $\mathbb{1}_0 \equiv 1$ , this becomes  $T_0(u, \delta) = \delta$ .

### 6.1.3 Hamiltonian limits

Proposition 6.1.1 gives sufficient conditions for the determination of identity points. We now classify the identity points for  $T_n(u, \delta)$ ,  $n \geq 2$ .

**Proposition 6.1.7.** *Let  $n \in \mathbb{N}_{\geq 2}$ . For  $\delta \notin \{-2, 0, 2\}$ , the set of identity points for  $T_n(u, \delta)$  is given by  $\{0, -\frac{\delta}{2}, -\frac{2}{\delta}\}$ . For  $T_n(u, \pm 2)$ , the set of identity points is given by  $\{0, \mp 1\}$ . For  $T_n(u, 0)$ , the only identity point is  $u_* = 0$ .*

*Proof.* It follows from (6.35) that the connectivity diagram corresponding to  $e_1 \cdots e_{n-1}$  only appears in  $S_{j,k}^{(n)}$  for  $j = k = 0$ , with coefficient  $u^{n-2}$ . By Proposition 6.1.4, the element thus appears in  $T_n(u, \delta)$  with coefficient  $u^{n-1}(\delta + 2u)(2 + \delta u)$ . This expression vanishes exactly for the indicated values of  $u$ .  $\square$

To determine the Hamiltonian associated with the identity point  $u_* = 0$ , we use Proposition 6.1.4 to compute

$$T_n(\epsilon, \delta)|_{\delta \neq 0} = (\delta + 2\epsilon)\mathbb{1}_n + 2\epsilon\delta \sum_{j=1}^{n-1} e_j + O(\epsilon^2), \quad (6.43)$$

$$\frac{1}{2\epsilon}T_n(\epsilon, 0) = \mathbb{1}_n + 2\epsilon \sum_{j=1}^{n-1} e_j + O(\epsilon^2). \quad (6.44)$$

For  $n \geq 2$  and all  $\delta$ , we may thus choose the familiar (see e.g. [21, 46, 65])

$$h_0 := - \sum_{i=1}^{n-1} e_i \quad (6.45)$$

as the principal Hamiltonian associated with  $u_* = 0$ .

**Remark.** There is also a ‘hidden’ identity point at infinity, see the Remark, following (6.20), that addresses the extension of the domain for  $u$  from  $\mathbb{C}$  to the Riemann sphere. The corresponding principal Hamiltonian is proportional to  $h_0$ .

Hamiltonians associated with the identity points  $u_* = -\frac{\delta}{2} \neq 0$  and  $u_* = -\frac{2}{\delta}$  do not seem to have been discussed before in the literature. To determine the corresponding principal Hamiltonians,  $h_{-\frac{\delta}{2}}$  and  $h_{-\frac{2}{\delta}}$ , we expand as

$$T_n(-\frac{\delta}{2} + \epsilon, \delta)|_{\delta \neq 0, \pm 2} = \left( \frac{\delta^{2n+1}}{4^n} + \epsilon \left( 2[n]_{\frac{\delta^2}{4}} - \frac{n\delta^{2n}}{4^{n-1}} \right) \right) \mathbb{1}_n + \epsilon(\delta^2 - 4) \sum_{j=0}^{n-2} \sum_{k=0}^{n-2-j} \left( \frac{\delta}{2} \right)^{2k+1} S_{j,k}^{(n)}(-\frac{\delta}{2}) + O(\epsilon^2), \quad (6.46)$$

$$T_n(-\frac{2}{\delta} + \epsilon, \delta)|_{\delta \neq 0, \pm 2} = \left( \delta - 2\epsilon[n]_{\frac{4}{\delta^2}} \right) \mathbb{1}_n - \epsilon(\delta^2 - 4) \sum_{j=0}^{n-2} \sum_{k=0}^{n-2-j} \left( \frac{2}{\delta} \right)^{2k+1} S_{j,k}^{(n)}(-\frac{2}{\delta}) + O(\epsilon^2), \quad (6.47)$$

and

$$T_n(-1+\epsilon, 2) = 2(1-\epsilon n + \epsilon^2 n^2) \mathbb{1}_n - 4\epsilon^2 \sum_{j=0}^{n-2} \sum_{k=0}^{n-2-j} S_{j,k}^{(n)}(-1, 2) + O(\epsilon^3), \quad (6.48)$$

$$T_n(1+\epsilon, -2) = -2(1+\epsilon n + \epsilon^2 n^2) \mathbb{1}_n - 4\epsilon^2 \sum_{j=0}^{n-2} \sum_{k=0}^{n-2-j} S_{j,k}^{(n)}(1, -2) + O(\epsilon^3). \quad (6.49)$$

**Proposition 6.1.8.** *For  $n \in \mathbb{N}_{\geq 2}$ ,  $\delta \neq 0$ , and up to rescaling, the principal Hamiltonian for  $u_* \in \{-\frac{\delta}{2}, -\frac{2}{\delta}\}$  is given by*

$$h_{u_*} = \frac{1}{u_*^{n-2}} \sum_{j=0}^{n-2} \sum_{k=0}^{n-2-j} u_*^{2k} S_{j,k}^{(n)}(u_*). \quad (6.50)$$

With the chosen normalisation, it holds that  $h_{-\frac{\delta}{2}} = h_{-\frac{2}{\delta}}$ .

*Proof.* The expression (6.50) follows from (3.56) and the expansions (6.46)–(6.49). The relation  $h_{-\frac{\delta}{2}} = h_{-\frac{2}{\delta}}$  follows from Corollary 6.1.5.  $\square$

Although  $h_{n, -\frac{\delta}{2}}$  and  $h_{n, -\frac{2}{\delta}}$  are linearly dependent,  $h_{n, -\frac{\delta}{2}}$  and  $h_{n, 0}$  are not. We also note that

$$h_{u_*} \in \text{span}_{\mathbb{C}[\delta]}(B'_n), \quad u_* \in \{0, -\frac{2}{\delta}\}. \quad (6.51)$$

For  $n = 2, 3, 4, 5$ , the principal Hamiltonian  $h_{n, -\frac{\delta}{2}}$  is given in Appendix A.5.2.

At the isotropic point  $u = 1$ , Proposition 6.1.4 implies that

$$T_n(1, \delta) = ((n+1)\delta + 2n) \mathbb{1}_n + (\delta + 2)^2 \sum_{j=0}^{n-2} \sum_{k=0}^{n-2-j} S_{j,k}^{(n)}(1, \delta), \quad (6.52)$$

and we note that  $T_n(1, -2) = -2\mathbb{1}_n$ , in accordance with (6.49).

#### 6.1.4 Minimal Hamiltonian polynomials

Since  $\text{TL}_n(\delta)$  is finite-dimensional, corresponding to each  $a \in \text{TL}_n(\delta)$ , there exists a unique monic polynomial, of least positive degree, that annihilates  $a$  – the so-called *minimal polynomial* of  $a$ . Let  $m_{u_*}^{(n)}$  denote the minimal polynomial of  $h_{n, u_*}$  for  $\delta$  an indeterminate, and let  $m_{u_*, \delta}^{(n)}$  denote the minimal polynomial of  $h_{n, u_*}$  for  $\delta \in \mathbb{C}$ . Examples are provided in Appendix A.5.1 and Appendix A.5.2. We denote the degrees of the *minimal Hamiltonian polynomials*,  $m_{u_*}^{(n)}$  and  $m_{u_*, \delta}^{(n)}$ , by

$$l_{u_*}^{(n)} := \deg(m_{u_*}^{(n)}), \quad l_{u_*, \delta}^{(n)} := \deg(m_{u_*, \delta}^{(n)}). \quad (6.53)$$

For ease of presentation, we let

$$\mathfrak{c}_n := \binom{n}{\lfloor \frac{n}{2} \rfloor}. \quad (6.54)$$

**Proposition 6.1.9.** *For each  $n \in \mathbb{N}_{\geq 2}$  and  $u_* \in \{0, -\frac{2}{\delta}\}$ , we have*

$$l_{u_*, \delta}^{(n)} \leq l_{u_*}^{(n)} \leq \mathfrak{c}_n. \quad (6.55)$$

*Proof.* For  $\varrho_n$  faithful, the minimal polynomial of  $\varrho_n(h_{u_*})$  is the same as that of  $h_{u_*}$ , irrespective of  $\delta$  being an indeterminate or taking on a complex value. Specialising  $\delta$  to a complex value may introduce spurious (see Section 4.3 and the remark following (6.58)) degeneracies in the spectrum of  $\varrho_n(h_{u_*})$ , and such degeneracies could reduce the degree of the minimal polynomial of  $\varrho_n(h_{u_*})$ . This explains the first inequality. The second inequality follows from the existence of a  $\mathfrak{c}_n$ -dimensional representation,  $\varrho_n$ , that is faithful for  $\delta$  an indeterminate.  $\square$

**Remark.** To appreciate the inequality  $l_{u_*,\delta}^{(n)} \leq \mathfrak{c}_n$  directly, note that  $\varrho_n$  is a  $\mathfrak{c}_n$ -dimensional representation that is faithful for all but finitely many  $\delta$ -values. The degree of the minimal polynomial for  $\delta$  complex and generic is thus bounded by  $\mathfrak{c}_n$ , and, possibly rescaled to remain well-defined, the corresponding minimal polynomial will remain annihilating when specialising  $\delta$  to one of these values. Such a rescaling can be chosen such that the rescaled polynomial is nonzero when specialising  $\delta$ , and the degree of this rescaled polynomial may decrease upon specialisation (this happens if and only if the rescaling multiplies the leading monomial by a factor that is zero when specialised) but cannot increase.

**Proposition 6.1.10.** *Let  $n \in \mathbb{N}_{\geq 2}$ ,  $u_* \in \{0, -\frac{2}{\delta}\}$ , and  $\delta$  an indeterminate. Then,  $h_{n,u_*}$  is non-derogatory if and only if  $l_{u_*}^{(n)} = \mathfrak{c}_n$ .*

*Proof.* For  $\varrho_n$  faithful, the minimal polynomial of  $h_{u_*}$  is the same as that of  $\varrho_n(h_{u_*})$ , and  $h_{u_*}$  is non-derogatory if and only if  $\varrho_n(h_{u_*})$  is non-derogatory. The latter is also equivalent to  $m_{\varrho_n(h_{u_*})} = c_{\varrho_n(h_{u_*})}$ , hence to  $\deg(m_{\varrho_n(h_{u_*})}) = \mathfrak{c}_n$ . Since  $\varrho_n$  is faithful for  $\delta$  an indeterminate, the result follows.  $\square$

Through direct computation, we have found that the spectrum of  $\varrho_n(h_0)$  for  $\delta = -2$  is non-degenerate for  $n = 2, \dots, 17$ . It follows that

$$l_{0,-2}^{(n)} = \mathfrak{c}_n, \quad n = 2, \dots, 17. \quad (6.56)$$

We likewise find that the spectrum of  $\varrho_n(h_{n,-\frac{2}{\delta}})$  for  $\delta = \pi + \pi^{-1}$  is non-degenerate for  $n = 2, \dots, 6$ , hence

$$l_{-\frac{2}{\delta},\pi+\pi^{-1}}^{(n)} = \mathfrak{c}_n, \quad n = 2, \dots, 6. \quad (6.57)$$

The specific  $\delta$ -values in these computations are immaterial, as long as they are ‘sufficiently generic’.

**Conjecture 6.1.11.** *For every  $n \in \mathbb{N}_{\geq 2}$ , each  $u_* \in \{0, -\frac{2}{\delta}\}$ , and  $\delta$  an indeterminate, the spectrum of  $\varrho_n(h_{u_*})$  is non-degenerate.*

This conjecture implies that, for every  $n \in \mathbb{N}_{\geq 2}$  and  $u_* \in \{0, -\frac{2}{\delta}\}$ , we have

$$l_{u_*}^{(n)} = \mathfrak{c}_n. \quad (6.58)$$

**Remark.** Necessary conditions for *strict* inequalities in (6.55) are the existence of spurious respectively permanent degeneracies in the spectrum of  $\varrho_n(h_{u_*})$ . However, these are not *sufficient* conditions as the Jordan-block structure may ‘prevent’ a corresponding reduction in the degree of the minimal polynomials.

**Proposition 6.1.12.** *Let  $n \in \mathbb{N}_{\geq 2}$  and  $u_* \in \{0, -\frac{2}{\delta}\}$ . Then, there exist at most finitely many values  $\delta \in \mathbb{C}$  for which the spectrum of  $\varrho_n(h_{u_*})$  possesses spurious degeneracies.*

*Proof.* Since the matrix elements of  $\varrho_n(h_{u_*})$  are polynomial in  $\delta$ , the result follows from Proposition 4.3.1.  $\square$

**Corollary 6.1.13.** *Let  $n \in \mathbb{N}_{\geq 2}$  and  $u_* \in \{0, -\frac{2}{\delta}\}$ . Then, there exist at most finitely many  $\delta$ -values for which*

$$l_{u_*, \delta}^{(n)} < l_{u_*}^{(n)}. \quad (6.59)$$

*Proof.* The result follows from Proposition 6.1.9 and Proposition 6.1.12.  $\square$

About the Jones–Wenzl idempotent,  $w_n$ , we note that (5.11) and (6.51) imply  $w_n h_{u_*} = h_{u_*} w_n = 0$ , hence  $w_n \in C_{\text{TL}_n(\delta)}(h_{u_*})$ . Assuming (6.58) holds, Proposition 6.1.10 then implies that  $w_n \in \langle h_{u_*} \rangle_{\text{TL}_n(\delta)}$  for  $\delta$  an indeterminate. It follows that, for every  $n \in \mathbb{N}_{\geq 2}$  and each  $u_* \in \{0, -\frac{2}{\delta}\}$ , there exists a polynomial  $p_{u_*}^{(n)}$  such that  $p_{u_*}^{(n)}(0) = \mathbb{1}_n$  and

$$w_n = p_{u_*}^{(n)}(h_{u_*}), \quad m_{u_*}^{(n)}(h_{u_*}) = h_{u_*} w_n. \quad (6.60)$$

Its degree is thus given by

$$\deg(p_{u_*}^{(n)}) = l_{u_*}^{(n)} - 1 = c_n - 1. \quad (6.61)$$

By (6.56) and (6.57), the relations (6.60) and (6.61) do indeed hold for  $n = 2, \dots, 17$  in the case  $u_* = 0$ , and for  $n = 2, \dots, 6$  in the case  $u_* = -\frac{2}{\delta}$ .

## 6.1.5 Transfer-operator Hamiltonian polynomials

The above spectral analysis of the principal Hamiltonians  $h_{n, u_*}$  for small  $n$ , together with Proposition 6.1.14 below, indicates that these elements are viable candidates in terms of which the Temperley–Lieb transfer operator  $T_n(u, \delta)$  is polynomial. We proceed by presenting explicit polynomial expressions of  $T_n(u, \delta)$  in terms of the principal Hamiltonians for small  $n$ , and by offering conjectures about the form of such polynomials for general  $n$ .

**Proposition 6.1.14.** *Let  $n \in \mathbb{N}_{\geq 2}$ ,  $u_* \in \{0, -\frac{2}{\delta}\}$ , and  $\psi$  denote a faithful representation of  $\text{TL}_n(\delta)$ . If the spectrum of  $\psi(h_{u_*})$  is non-degenerate, then  $T_n(u, \delta)$  is polynomial in  $h_{u_*}$ .*

*Proof.* Let the spectrum of  $\psi(h_{u_*})$  be non-degenerate. Then, the characteristic and minimal polynomials of  $\psi(h_{u_*})$  agree, so  $\psi(h_{u_*})$  is non-derogatory. Since  $\psi$  is faithful, it follows that  $h_{u_*}$  is non-derogatory, and since  $T_n(u, \delta)$  commutes with  $h_{u_*}$ , we have  $T_n(u, \delta) \in \langle h_{u_*} \rangle_{\text{TL}_n(\delta)}$ .  $\square$

**Remark.** In the following, we will use that  $\varrho_n$  is faithful for  $\delta$  an indeterminate and for all but finitely many  $\delta \in \mathbb{C}$ .

Because the matrix elements of  $\varrho_n(T_n(u, \delta))$  are polynomial in  $\delta$ , Proposition 4.3.1 implies that there are at most finitely many  $\delta$ -values in  $\mathbb{C}$  for which the spectrum of  $\varrho_n(T_n(u, \delta))$  possesses spurious

degeneracies. Combined with the non-degeneracy observations implying (6.56) and (6.57), it follows from Proposition 6.1.14 that for every  $n = 2, \dots, 17$ ,  $T_n(u, \delta)$  is polynomial in  $h_0$  for all but finitely many  $\delta$ -values, and that for every  $n = 2, \dots, 6$ ,  $T_n(u, \delta)$  is polynomial in  $h_{-\frac{2}{\delta}}$  for all but finitely many  $\delta$ -values. For  $n = 2$ , for example, we have  $h_{-\frac{2}{\delta}} = -h_0$  for  $\delta \neq 0$ , and

$$T_2(u, \delta) = (\delta[3]_{u^2} + 2u[2]_{u^2})\mathbb{1}_2 - u(\delta + 2u)(2 + \delta u)h_0, \quad (6.62)$$

valid for all  $\delta \in \mathbb{C}$ . In the following, we will argue that  $T_n(u, \delta) \in \mathbb{C}[u][h_{u_*}]$ ,  $u_* \in \{0, -\frac{2}{\delta}\}$ , for every  $n \in \mathbb{N}_{\geq 2}$  and all but finitely many  $\delta$ -values. We refer to these values as  $h_{n,u_*}$ -exceptional and note that the number of them, and their value will depend on  $n$  and  $u_*$ .

**Conjecture 6.1.15.** *Let  $n \in \mathbb{N}_{\geq 3}$  and  $\delta$  an indeterminate. For each  $u_* \in \{0, -\frac{2}{\delta}\}$ ,  $T_n(u, \delta)$  admits a unique decomposition of the form*

$$T_n(u, \delta) = (\delta[n+1]_{u^2} + 2u[n]_{u^2})\mathbb{1}_n + \frac{u(\delta + 2u)(2 + \delta u)}{f_{n,u_*}(\delta)} \sum_{i=1}^{l_{u_*}^{(n)}-1} a_i^{n,u_*}(u, \delta) h_{u_*}^i, \quad (6.63)$$

where  $f_{n,u_*}(\delta)$  is a monic polynomial and  $a_i^{n,u_*}(u, \delta)$  are polynomials such that no root of  $f_{n,u_*}(\delta)$  is a root of  $a_i^{n,u_*}(u, \delta)$  for all  $i = 1, \dots, l_{u_*}^{(n)} - 1$ .

For  $u_* = 0$ , we have verified Conjecture 6.1.15 for  $n = 3, 4, 5, 6$ , finding

$$f_{3,0}(\delta) = f_{4,0}(\delta) = 1, \quad f_{5,0}(\delta) = (\delta^2 + 4)(\delta^2 - \frac{1}{2})(\delta^4 - 27\delta^2 + 121), \quad (6.64)$$

and

$$\begin{aligned} f_{6,0}(\delta) = & \delta^2(\delta^2 + 2)(\delta^2 - \frac{1}{6})(\delta^2 - \frac{1}{4})(\delta^2 - \frac{5}{4})(\delta^2 - 3)(\delta^2 - \frac{16}{3})(\delta^2 - \frac{121}{12}) \\ & (\delta^4 - 14\delta^2 + \frac{121}{9})(\delta^4 - 25\delta^2 - \frac{121}{2})(\delta^6 - \frac{41}{4}\delta^4 + \frac{53}{2}\delta^2 - \frac{9}{4})(\delta^6 - 18\delta^4 + 81\delta^2 - 16) \\ & (\delta^6 + 11\delta^4 + \frac{185}{4}\delta^2 + \frac{121}{2})(\delta^8 + \frac{19}{9}\delta^6 + \frac{467}{18}\delta^4 + \frac{320}{9}\delta^2 - \frac{512}{9}), \end{aligned} \quad (6.65)$$

while for  $u_* = -\frac{2}{\delta}$ , we have verified it for  $n = 3, 4, 5$ , finding

$$f_{3,-\frac{2}{\delta}}(\delta) = \delta^6 - 64, \quad (6.66)$$

$$\begin{aligned} f_{4,-\frac{2}{\delta}}(\delta) = & (\delta^8 - 256)^2(\delta^8 + 8\delta^6 + 32\delta^4 + 256)(\delta^8 + \frac{8}{3}\delta^6 - 32\delta^4 + \frac{256}{3}\delta^2 - \frac{256}{3}) \\ & (\delta^{16} - 8\delta^{14} - 64\delta^{12} + 640\delta^{10} + 512\delta^8 - 26624\delta^6 + 98304\delta^4 - 131072\delta^2 + 65536), \end{aligned} \quad (6.67)$$

$$f_{5,-\frac{2}{\delta}}(\delta) = (\delta^{10} - 1024)^3 p_5(\delta), \quad (6.68)$$

where  $p_5(\delta)$  is a non-degenerate even polynomial of degree 198. Explicit expressions for the associated polynomials  $a_i^{n,u_*}(u, \delta)$  are not presented here. Instead, explicit expressions for similar polynomials are provided in a refined formulation, see Conjecture A.5.3 in Appendix A.5.3.

**Conjecture 6.1.16.** *Let  $n \in \mathbb{N}_{\geq 3}$  and  $\delta$  an indeterminate. Then,*

$$f_{n,-\frac{2}{\delta}}(\delta) = (\delta^{2n} - 4^n)^{n-2} p_n(\delta), \quad (6.69)$$

where  $p_n(\delta)$  is a non-degenerate even polynomial.

If Conjecture 6.1.15 holds, then every  $h_{n,u_*}$ -exceptional  $\delta$ -value will be a root of  $f_{n,u_*}(\delta)$ . The converse need not be true since  $T_n(u, \delta)$  could be polynomial in  $h_{n,u_*}$  even if  $\delta$  is a root of  $f_{n,u_*}(\delta)$ , see below. Letting  $E_{n,u_*}$  denote the set of  $h_{n,u_*}$ -exceptional  $\delta$ -values and  $Z_{n,u_*}$  the set of roots (or zeros) of  $f_{n,u_*}(\delta)$ , we thus have

$$E_{n,u_*} \subseteq Z_{n,u_*}. \quad (6.70)$$

To appreciate what happens if this is not an equality, let  $u \notin \{0, -\frac{\delta}{2}, -\frac{2}{\delta}\}$  and rewrite (6.63) as

$$\sum_{i=1}^{l_{u_*}^{(n)}-1} a_i^{n,u_*}(u, \delta) h_{u_*}^i = \frac{f_{n,u_*}(\delta)}{u(\delta+2u)(2+\delta u)} \left( T_n(u, \delta) - (\delta[n+1]_{u^2} + 2u[n]_{u^2}) \mathbb{1}_n \right). \quad (6.71)$$

Specialising  $\delta$  to a root,  $\delta_r$ , of  $f_{n,u_*}(\delta)$  then means that

$$\sum_{i=1}^{l_{u_*}^{(n)}-1} a_i^{n,u_*}(u, \delta) h_{u_*}^i \Big|_{\delta=\delta_r} = 0, \quad (6.72)$$

and since at least one of the polynomials  $a_i^{n,u_*}(u, \delta)$  is nonzero when evaluated at  $\delta = \delta_r$ , it follows that

$$l_{u_*, \delta_r}^{(n)} < l_{u_*}^{(n)}. \quad (6.73)$$

For  $\delta_r \in Z_{n,u_*} \setminus E_{n,u_*}$ , the decomposition (6.63) is replaced by

$$T_n(u, \delta_r) = (\delta_r[n+1]_{u^2} + 2u[n]_{u^2}) \mathbb{1}_n + u(\delta_r + 2u)(2 + \delta_r u) \sum_{i=1}^{l_{u_*, \delta_r}^{(n)}-1} a_{i, \delta_r}^{n,u_*}(u) h_{u_*}^i \Big|_{\delta=\delta_r}, \quad (6.74)$$

where  $a_{i, \delta_r}^{n,u_*}(u)$  is polynomial for all  $i$ . Although  $Z_{3,0} = Z_{4,0} = \emptyset$  and  $Z_{5,0} = E_{5,0}$ , we find that such a root  $\delta_r$  does indeed exist for  $n = 6$ , as

$$Z_{6,0} \setminus E_{6,0} = \{0\}. \quad (6.75)$$

Note that  $\delta_r = 0$  is the only degenerate root of  $f_{6,0}(\delta)$ . Through direct computation, we likewise find that

$$Z_{n, -\frac{2}{\delta}} = E_{n, -\frac{2}{\delta}}, \quad n = 3, 4, 5, \quad (6.76)$$

but have not managed to determine  $Z_{n, -\frac{2}{\delta}}$  and  $E_{n, -\frac{2}{\delta}}$  for  $n \geq 6$ .

For  $\delta_r \in E_{n,u_*}$ ,  $T_n(u, \delta_r)$  is *not* expressible as a polynomial in  $h_{n,u_*}$ . However, observing that

$$Z_{n,0} \cap Z_{n, -\frac{2}{\delta}} = \emptyset, \quad n = 3, 4, 5, \quad (6.77)$$

we conclude that

$$E_{n,0} \cap E_{n, -\frac{2}{\delta}} = \emptyset, \quad n = 3, 4, 5. \quad (6.78)$$

It follows that, for  $n = 3, 4, 5$  and every  $\delta \in \mathbb{C}$ ,  $T_n(u, \delta)$  is polynomial in *at least one* of the two Hamiltonians:  $h_{n,0}$  and  $h_{n, -\frac{2}{\delta}}$ .

## 6.2 Tensor planar algebra: an eight-vertex model

In this section, we specialise to *tensor planar algebras* and thereby recover the familiar quantum inverse scattering framework, in which case, the  $R$ -operators are tensorially separable, and outline how the planar-algebraic framework simplifies. To illustrate, we consider a specialisation of the zero-field eight-vertex model [66, 67] that satisfies the free-fermion condition, and whose principal Hamiltonian corresponds to the Ising model Hamiltonian. The general model was solved by Baxter in [34], see also [11], while our presentation highlights the underlying polynomial integrable structure of a particular specialisation, by analysing the spectral properties of the transfer operator and the associated Hamiltonian.

We thus show that the transfer operator of this specialised eight-vertex model is diagonablisable and present an exact solution. Although the model is Yang–Baxter integrable, its simplicity allows us to use standard techniques to obtain explicit expressions for all eigenvalues and corresponding eigenvectors of the transfer operator. We then exploit similarities in the spectral properties of the transfer operator and the Ising Hamiltonian to establish that the transfer operator is polynomial in this element. Moreover, we decompose the transfer operator into an explicit linear combination of a complete set of orthogonal idempotents expressed in terms of the minimal polynomial of the Ising Hamiltonian.

### 6.2.1 Definition and cellularity

For each  $n \in \mathbb{N}_0$  and  $\ell \in \mathbb{N}$ , let  $E_n$  denote the complex  $\ell^n$ -dimensional vector space spanned by disks with  $n$  labelled boundary points where each label is taken from the set  $\{1, \dots, \ell\}$ . As the disks do not come equipped with any further (interior or otherwise) structure, we have  $E_n \cong E^{\otimes n}$ , where  $E$  is an  $\ell$ -dimensional vector space.

The *tensor planar algebra* is the graded vector space  $(E_n)_{n \in \mathbb{N}_0}$ , together with the following action of planar tangles: If a string in the planar tangle connects a pair of boundary points with different labels, then the output is the zero vector, and if not, then the labels of the output vector are given by the labels at the opposite string endpoints. If both endpoints of a string are on the exterior boundary of the planar tangle, then the output vector is a sum obtained by varying the common label of the two endpoints. Following from compatibility with the glueing of planar tangles, and using the evaluation map  $e$  (2.20), a loop is accordingly replaced by the scalar  $\ell$ . To illustrate, with  $T$  as in (2.4) and  $a, b \in \mathbb{C}$ , we have

$$\mathbb{P}_T \left( \begin{array}{c} 3 \\ 1 \end{array}, a \begin{array}{c} 2 \\ 1 \end{array}, b \begin{array}{c} 3 \\ 4 \end{array} + b \begin{array}{c} 2 \\ 3 \end{array}, \begin{array}{c} 3 \\ 2 \end{array}, \begin{array}{c} 3 \\ 1 \end{array}, \begin{array}{c} 3 \\ 4 \end{array} \right) = a \begin{array}{c} 3 \\ 1 \end{array} + b \begin{array}{c} 3 \\ 1 \end{array} = b \ell \sum_{k=1}^{\ell} \begin{array}{c} k \\ 2 \\ 4 \end{array}, \quad (6.79)$$

We now equip each  $E_{2n}$  with the multiplication induced by the unshaded planar tangle  $M_n$  following from (2.26), and identify the first  $n$  labels clockwise from the marked boundary interval as

characterising an incoming vector, with the remaining  $n$  labels characterising an outgoing vector. The vector space  $E_{2n}$  thus has the structure of an endomorphism algebra,

$$E_{2n} = \text{End}(E^{\otimes n}), \quad (6.80)$$

and is consequently cellular.

### 6.2.2 Transfer operator

Let bases for  $E_2$  and  $E_4$  be given by

$$B_1 = \{e_j^k \mid j, k \in \{1, \dots, \ell\}\}, \quad B_2 = \{e_{j,l}^{k,m} \mid j, k, l, m \in \{1, \dots, \ell\}\}, \quad (6.81)$$

respectively, such that, viewed as matrices relative to the natural basis orderings,  $e_j^k$  are  $\ell \times \ell$  matrix units with 1 in position  $(j, k)$  and zeros elsewhere. By construction,

$$E_{2n} \cong [\text{End}(E)]^{\otimes n}, \quad (6.82)$$

so every element of  $E_4$  is separable. In particular, the  $E_4$  basis vectors decompose as

$$e_{j,l}^{k,m} = e_j^k \otimes e_l^m, \quad j, k, l, m \in \{1, \dots, \ell\}. \quad (6.83)$$

As parameterised elements of  $E_2$  and  $E_4$ , respectively, the  $K$ - and  $R$ -operators (3.3) are here written as

$$K(u) = \sum_{j,k=1}^{\ell} K_j^k(u) \text{ (diagram)}, \quad R(u) = \sum_{j,k,l,m=1}^{\ell} R_{j,l}^{k,m}(u) \text{ (diagram)}, \quad \bar{K}(u) = \sum_{j,k=1}^{\ell} \bar{K}_j^k(u) \text{ (diagram)}, \quad (6.84)$$

where  $K_j^k, R_{j,l}^{k,m}, \bar{K}_j^k$  are scalar functions, and where we have attached short strings to the labelled boundary points, for illustrative purposes. The separability of  $E_4$  allows us to write

$$R(u) = \sum_{j,k,l,m=1}^{\ell} R_{j,l}^{k,m}(u) \text{ (diagram)} = \sum_{j,k,l,m=1}^{\ell} R_{j,l}^{k,m}(u) e_j^k \otimes e_l^m. \quad (6.85)$$

Using the *same* scalar functions but with the upper indices interchanged, we get

$$\check{R}(u) = \sum_{j,k,l,m=1}^{\ell} R_{j,l}^{k,m}(u) \text{ (diagram)} = \sum_{j,k,l,m=1}^{\ell} R_{j,l}^{k,m}(u) \text{ (diagram)} = \sum_{j,k,l,m=1}^{\ell} R_{j,l}^{k,m}(u) e_j^m \otimes e_l^k, \quad (6.86)$$

in terms of which we construct the Sklyanin-type transfer operator  $\check{T}_n(u) \in E_{2n}$ , as in (3.43).

Accordingly,  $\check{T}_n(u)$  can be expressed familiarly as a vector-space trace over an auxiliary copy of  $\text{End}(E)$  in  $E_{2n+2}$ . In the following, the auxiliary space is the  $(n+1)^{\text{th}}$  copy, and the corresponding trace is denoted by  $\text{tr}_{n+1}$ . For each  $i = 1, \dots, n$ , we first introduce

$$R_{i,n+1}(u) := \sum_{j,k,l,m=1}^{\ell} R_{j,l}^{k,m}(u) \mathbb{1}_{i-1} \otimes e_j^k \otimes \mathbb{1}_{n-i} \otimes e_l^m, \quad (6.87)$$

$$R_{n+1,i}(u) := \sum_{j,k,l,m=1}^{\ell} R_{j,l}^{k,m}(u) \mathbb{1}_{i-1} \otimes e_l^m \otimes \mathbb{1}_{n-i} \otimes e_j^k, \quad (6.88)$$

where the indices  $i$  and  $n+1$  denote the copies of  $E$  on which the operators act non-trivially, as well as

$$K_1(u) := \sum_{j,k=1}^{\ell} K_j^k(u) e_j^k \otimes \mathbb{1}_n, \quad \bar{K}_{n+1}(u) := \sum_{j,k=1}^{\ell} \bar{K}_j^k(u) \mathbb{1}_n \otimes e_j^k. \quad (6.89)$$

The transfer operator can then be expressed in terms of the ‘pre-trace’ transfer operator

$$L_{n+1}(u) := R_{n,n+1}(u) \cdots R_{1,n+1}(u) K_1(u) R_{n+1,1}(u) \cdots R_{n+1,n}(u) \bar{K}_{n+1}(u) \quad (6.90)$$

as

$$\check{T}_n(u) = \text{tr}_{n+1}(L_{n+1}(u)). \quad (6.91)$$

### 6.2.3 Eight-vertex model

For the remainder of this chapter, we let

$$\dim(E) = 2 \quad (6.92)$$

and fix the parameterisation to an eight-vertex model, characterised by

$$R_{j,l}^{k,m}(u) = \begin{cases} 1, & j = m, l = k, \\ u, & j = l, k = m, j \neq k, \\ u, & j = k, l = m, j \neq l, \\ 0, & \text{otherwise,} \end{cases} \quad K_j^k(u) = \bar{K}_j^k(u) = \begin{cases} 1, & j = k, \\ 0, & j \neq k. \end{cases} \quad (6.93)$$

Working in the natural matrix representation where  $e_j^k$  are matrix units, and where  $\mathbb{1}$  denotes the  $2 \times 2$  identity matrix, the  $R$ - and  $K$ -operators can be expressed in terms of Pauli matrices as

$$R(u) = \frac{1}{2} \left[ (1+u)(\mathbb{1} \otimes \mathbb{1} + \sigma^x \otimes \sigma^x) + (1-u)(\sigma^y \otimes \sigma^y + \sigma^z \otimes \sigma^z) \right], \quad K(u) = \bar{K}(u) = \mathbb{1}. \quad (6.94)$$

It follows that

$$R^2(u) = (1+u^2) \mathbb{1} \otimes \mathbb{1} + 2u \sigma^x \otimes \sigma^x, \quad (6.95)$$

$$R(u)(\mathbb{1} \otimes \sigma^x)R(u) = (1+u^2) \sigma^x \otimes \mathbb{1} + 2u \mathbb{1} \otimes \sigma^x, \quad (6.96)$$

and using the standard notation

$$\sigma_{m,i}^{\alpha} := \mathbb{1}_{i-1} \otimes \sigma^{\alpha} \otimes \mathbb{1}_{m-i}, \quad \alpha \in \{x, y, z\}, \quad i \in \{1, \dots, m\}, \quad m \in \mathbb{N}, \quad (6.97)$$

we then have the following result.

**Lemma 6.2.1.**  $L_{n+1}(u)$  is polynomial in  $\sigma_{n+1,1}^x, \dots, \sigma_{n+1,n+1}^x$ .

It follows that

$$L_{n+1}(u) = L_n^{(0)}(u) \otimes \mathbb{1} + L_n^{(1)}(u) \otimes \sigma^x, \quad (6.98)$$

for some  $L_n^{(0)}(u), L_n^{(1)}(u) \in E_{2n}$ , and consequently that

$$\check{T}_n(u) = 2L_n^{(0)}(u) \quad (6.99)$$

and

$$[\check{T}_n(u), \check{T}_n(v)] = 0, \quad \forall u, v \in \mathbb{C}. \quad (6.100)$$

The next result allows us to determine the polynomial structures of  $L_{n+1}(u)$  and  $\check{T}_n(u)$ .

**Proposition 6.2.2.** *With  $L_1(u) \equiv \mathbb{1}$  and  $\check{T}_1(u) = 2(1+u^2)\mathbb{1}$ , the matrices  $L_{n+1}(u)$  and  $\check{T}_n(u)$  are determined recursively by*

$$L_{n+1}(u) = ((1+u^2)\mathbb{1}_{n+1} + 2u\sigma^x \otimes \sigma^x \otimes \mathbb{1}_{n-1})(\mathbb{1} \otimes L_n(u)), \quad (6.101)$$

$$\check{T}_n(u) = ((1+u^2)\mathbb{1}_n + 2u\sigma^x \otimes \sigma^x \otimes \mathbb{1}_{n-2})(\mathbb{1} \otimes \check{T}_{n-1}(u)). \quad (6.102)$$

*Proof.* Using  $K(u) = \bar{K}(u) = \mathbb{1}$  and that  $R_{n+1,i}(u) = R_{i,n+1}(u)$  for all  $i$ , the relation (6.101) follows from

$$\begin{aligned} L_{n+1}(u) &= R_{n,n+1}(u) \cdots R_{1,n+1}(u) R_{1,n+1}(u) \cdots R_{n,n+1}(u) \\ &= R_{n,n+1}(u) \cdots R_{2,n+1}(u) [(1+u^2)\mathbb{1}_{n+1} + 2u\sigma^x \otimes \mathbb{1}_{n-1} \otimes \sigma^x] R_{2,n+1}(u) \cdots R_{n,n+1}(u) \\ &= (1+u^2)\mathbb{1} \otimes L_n(u) + 2u\sigma^x \otimes (R_{n-1,n}(u) \cdots R_{1,n}(u) [\mathbb{1}_{n-1} \otimes \sigma^x] R_{1,n}(u) \cdots R_{n-1,n}(u)) \\ &= ((1+u^2)\mathbb{1}_{n+1})(\mathbb{1} \otimes L_n(u)) \\ &\quad + 2u\sigma^x \otimes (R_{n-1,n}(u) \cdots R_{2,n}(u) [\sigma^x \otimes \mathbb{1}_{n-1}] R_{1,n}(u) R_{1,n}(u) \cdots R_{n-1,n}(u)) \\ &= ((1+u^2)\mathbb{1}_{n+1})(\mathbb{1} \otimes L_n(u)) + 2u(\sigma^x \otimes \sigma^x \otimes \mathbb{1}_{n-1})(\mathbb{1} \otimes L_n(u)), \end{aligned} \quad (6.103)$$

where the fourth equality is a consequence of

$$R(u)(\mathbb{1} \otimes \sigma^x)R(u) = (\sigma^x \otimes \mathbb{1})R^2(u). \quad (6.104)$$

The relation (6.102) is an immediate consequence of (6.101).  $\square$

In preparation for giving explicit expressions for  $\check{T}_n(u)$ , let

$$I_{n,k} := \{(i_1, \dots, i_{2k}) \in \mathbb{N}^{2k} \mid 1 \leq i_1 < \dots < i_{2k} \leq n\}, \quad k = 1, \dots, \lfloor \frac{n}{2} \rfloor, \quad (6.105)$$

and define

$$\kappa_{n,k}: I_{n,k} \rightarrow \mathbb{Z}, \quad (i_1, \dots, i_{2k}) \mapsto \sum_{l=1}^{2k} (-1)^l i_l. \quad (6.106)$$

Note that  $\kappa_{n,k}(\iota) \in \{1, \dots, n-1\}$  for all  $\iota \in I_{n,k}$ .

**Proposition 6.2.3.** *The transfer operator admits the multiplicative expression*

$$\check{T}_n(u) = 2(1+u^2) \prod_{i=1}^{n-1} \left[ (1+u^2) \mathbb{1}_n + 2u \sigma_{n,i}^x \sigma_{n,i+1}^x \right] \quad (6.107)$$

and the additive expression

$$\check{T}_n(u) = 2(1+u^2)^n \mathbb{1}_n + 2(1+u^2) \sum_{k=1}^{\lfloor \frac{n}{2} \rfloor} \sum_{\iota=(i_1, \dots, i_{2k}) \in I_{n,k}} (1+u^2)^{n-\kappa_{n,k}(\iota)} (2u)^{\kappa_{n,k}(\iota)} \sigma_{n,i_1}^x \cdots \sigma_{n,i_{2k}}^x. \quad (6.108)$$

*Proof.* The multiplicative expression is readily seen to satisfy the recursion relation (6.102), including the initial condition for  $n = 1$ . The additive expression follows by expanding the multiplicative expression.  $\square$

We let  $|\pm\rangle$  denote eigenvectors of  $\sigma^x$ ,

$$\sigma^x |\pm\rangle = \pm |\pm\rangle, \quad |\pm\rangle := \begin{bmatrix} 1 \\ \pm 1 \end{bmatrix}, \quad (6.109)$$

and let

$$K_n: \{\pm\}^n \rightarrow \{0, 1, \dots, n-1\}, \quad (s_1, \dots, s_n) \mapsto \sum_{i=1}^{n-1} |s_i - s_{i+1}|, \quad (6.110)$$

denote the function that counts the number of sign changes present in  $(s_1, \dots, s_n) \in \{\pm\}^n$ . The pre-images

$$\mathcal{V}_{n,k} := \text{span}_{\mathbb{C}} \{ |K_n^{-1}(k)\rangle \}, \quad k = 0, 1, \dots, n-1, \quad (6.111)$$

have dimension

$$\dim \mathcal{V}_{n,k} = 2 \binom{n-1}{k}, \quad (6.112)$$

consistent with

$$\dim(E^{\otimes n}) = |\{\pm\}^n| = 2^n = \sum_{k=0}^{n-1} \dim \mathcal{V}_{n,k}. \quad (6.113)$$

**Proposition 6.2.4.** *The transfer operator  $\check{T}_n(u)$  is diagonalisable, with eigenvectors*

$$|\mathbf{s}\rangle = |s_1\rangle \otimes \cdots \otimes |s_n\rangle, \quad \mathbf{s} = (s_1, \dots, s_n) \in \{\pm\}^n, \quad (6.114)$$

and corresponding eigenvalues

$$\lambda_{\mathbf{s}}(u) = 2(1+u^2)(1-u)^{2K_n(\mathbf{s})}(1+u)^{2(n-1-K_n(\mathbf{s}))}. \quad (6.115)$$

*Proof.* The result follows from the multiplicative expression (6.107).  $\square$

The following result readily follows from Proposition 6.2.4.

**Corollary 6.2.5.** *For each  $k = 0, 1, \dots, n-1$ ,  $\mathcal{V}_{n,k}$  is the  $\check{T}_n(u)$ -eigenspace corresponding to the eigenvalue  $2(1+u^2)(1-u)^{2k}(1+u)^{2(n-1-k)}$ , and we have the eigenspace decomposition*

$$E^{\otimes n} = \bigoplus_{k=0}^{n-1} \mathcal{V}_{n,k}. \quad (6.116)$$

### 6.2.4 Polynomial integrability

Since  $\check{T}_n(u)$  is diagonalisable and satisfies (6.100), the corresponding eight-vertex model is polynomially integrable. As we show in the following, the transfer operator is polynomial in the principal Hamiltonian given in (6.118).

It follows from Proposition 6.2.3 that  $u_* = 0$  is the only identity point, with

$$\check{T}_n(\epsilon) = 2\mathbb{1}_n + 4\epsilon \sum_{i=1}^{n-1} \sigma_{n,i}^x \sigma_{n,i+1}^x + O(\epsilon^2). \quad (6.117)$$

The corresponding (renormalised) principal Hamiltonian is given by

$$h_n = \sum_{i=1}^{n-1} \sigma_{n,i}^x \sigma_{n,i+1}^x. \quad (6.118)$$

**Proposition 6.2.6.** *The principal Hamiltonian  $h_n$  is diagonalisable, with eigenvectors*

$$|\mathbf{s}\rangle = |s_1\rangle \otimes \cdots \otimes |s_n\rangle, \quad \mathbf{s} = (s_1, \dots, s_n) \in \{\pm\}^n, \quad (6.119)$$

and corresponding eigenvalues

$$\mu_{\mathbf{s}} = n - 1 - 2K_n(\mathbf{s}). \quad (6.120)$$

Moreover, for each  $k = 0, 1, \dots, n-1$ ,  $\mathcal{V}_{n,k}$  is the  $h_n$ -eigenspace corresponding to the eigenvalue  $n - 1 - 2k$ .

*Proof.* The result follows from (6.118).  $\square$

**Remark.** The eigenvalues of  $\check{T}_n(u)$  and  $h_n$  are related as

$$\lambda_{\mathbf{s}}(\epsilon) = 2[1 + 2\epsilon\mu_{\mathbf{s}} + O(\epsilon^2)], \quad \forall \mathbf{s} \in \{\pm\}^n. \quad (6.121)$$

The form of the minimal polynomial of  $h_n$  follows from Proposition 6.2.6. To fix our notation, we define the polynomials

$$m_j(x) := \prod_{k=0}^{j-1} [x - (j-1-2k)], \quad j \in \mathbb{N}. \quad (6.122)$$

**Corollary 6.2.7.** *The minimal polynomial of  $h_n$  is  $m_n$ .*

Although  $h_n$  is not non-derogatory, it follows from Corollary 6.2.5 and Proposition 6.2.6 that

$$\check{T}_n(u) \in \mathbb{C}(u)[h_n]. \quad (6.123)$$

The next result provides details of this polynomial. In preparation, let  $\lambda_k(u)$  and  $\mu_k$  denote the eigenvalues corresponding to the (joint) eigenspaces  $\mathcal{V}_{n,k}$ ,  $k = 0, 1, \dots, n-1$ , of  $\check{T}_n(u)$  and  $h_n$ , respectively. For ease of reference, we recall their expressions,

$$\lambda_k(u) = 2(1+u^2)(1-u)^{2k}(1+u)^{2(n-1-k)}, \quad \mu_k = n - 1 - 2k, \quad (6.124)$$

and introduce the  $n \times n$  matrix

$$V_n := \begin{bmatrix} 1 & \mu_0 & \dots & \mu_0^{n-1} \\ 1 & \mu_1 & \dots & \mu_1^{n-1} \\ \vdots & \vdots & \ddots & \vdots \\ 1 & \mu_{n-1} & \dots & \mu_{n-1}^{n-1} \end{bmatrix}, \quad n \in \mathbb{N}. \quad (6.125)$$

Since this is a Vandermonde matrix with  $\mu_i \neq \mu_j$  for all  $i \neq j$ , it is invertible, and the inverse can be evaluated explicitly. For every  $n \in \mathbb{N}$ , we let  $m_0(h_n) \equiv h_n^0 \equiv \mathbb{1}_n$ .

**Proposition 6.2.8.** *For every  $n \in \mathbb{N}$  and all  $u \in \mathbb{C}$ , we have*

$$\check{T}_n(u) = \sum_{i=0}^{n-1} \tau_i(u) h_n^i, \quad (6.126)$$

where

$$\tau_i(u) = \sum_{j=0}^{n-1} [V_n^{-1}]_{i+1, j+1} \lambda_j(u), \quad i = 0, 1, \dots, n-1. \quad (6.127)$$

*Proof.* That an expression of the form (6.126) exists follows from (6.123) and Corollary 6.2.7. Using the common eigenbasis  $\{|\mathbf{s}\rangle | \mathbf{s} \in \{\pm\}^n\}$  of  $\check{T}_n(u)$  and  $h_n$  to diagonalise the expression, yields

$$\text{diag}(\lambda_0(u), \lambda_1(u), \dots, \lambda_{n-1}(u)) = \sum_{i=0}^{n-1} \text{diag}(\tau_i(u) \mu_0^i, \tau_i(u) \mu_1^i, \dots, \tau_i(u) \mu_{n-1}^i), \quad (6.128)$$

where we have omitted repeated eigenvalues. Compressing the diagonal matrices into vectors, we obtain

$$\begin{bmatrix} \lambda_0(u) \\ \lambda_1(u) \\ \vdots \\ \lambda_{n-1}(u) \end{bmatrix} = \begin{bmatrix} 1 & \mu_0 & \dots & \mu_0^{n-1} \\ 1 & \mu_1 & \dots & \mu_1^{n-1} \\ \vdots & \vdots & \ddots & \vdots \\ 1 & \mu_{n-1} & \dots & \mu_{n-1}^{n-1} \end{bmatrix} \begin{bmatrix} \tau_0(u) \\ \tau_1(u) \\ \vdots \\ \tau_{n-1}(u) \end{bmatrix}, \quad (6.129)$$

and since  $V_n$  is invertible, (6.127) follows.  $\square$

For each  $i = 0, 1, \dots, n-1$ , we let

$$m_n^{(i)}(x) := \prod_{\substack{k=0 \\ k \neq i}}^{n-1} (x - \mu_k), \quad (6.130)$$

and note that

$$m_n(x) = (x - \mu_i) m_n^{(i)}(x), \quad m_n^{(i)}(\mu_j) = \delta_{ij} (-1)^i (2n-2)!! \binom{n-1}{i}^{-1}. \quad (6.131)$$

Since  $m_n^{(i)}(\mu_i) \neq 0$  for all  $i$ , we can renormalise the polynomials (6.130) as

$$\hat{m}_n^{(i)}(x) := \frac{m_n^{(i)}(x)}{m_n^{(i)}(\mu_i)}, \quad i = 0, 1, \dots, n-1. \quad (6.132)$$

In terms of these polynomials, we now define

$$\mathbf{p}_i := \hat{m}_n^{(i)}(h_n), \quad i = 0, 1, \dots, n-1. \quad (6.133)$$

Using standard arguments, we have the following result.

**Proposition 6.2.9.**  $\{\mathbf{p}_i \mid i = 0, 1, \dots, n-1\}$  is a complete set of orthogonal idempotents:

$$\sum_{i=0}^{n-1} \mathbf{p}_i = \mathbb{1}_n, \quad \mathbf{p}_j \mathbf{p}_k = \delta_{jk} \mathbf{p}_k, \quad \forall j, k \in \{0, 1, \dots, n-1\}. \quad (6.134)$$

*Proof.* By construction, each  $\hat{m}_n^{(i)}(x)$  is a polynomial of degree  $n-1$ , so  $\sum_{i=0}^{n-1} \hat{m}_n^{(i)}(x)$  is a polynomial of degree at most  $n-1$ . Since  $\hat{m}_n^{(i)}(\mu_j) = \delta_{ij}$  for all  $i, j$ , we have  $\sum_{i=0}^{n-1} \hat{m}_n^{(i)}(\mu_j) = 1$  for every  $j \in \{0, 1, \dots, n-1\}$ , and since  $|\{\mu_0, \mu_1, \dots, \mu_{n-1}\}| = n$ , it follows that  $\sum_{i=0}^{n-1} \hat{m}_n^{(i)}(x) = 1$ , hence  $\sum_{i=0}^{n-1} \mathbf{p}_i = \mathbb{1}_n$ . For  $j \neq k$ , we have

$$\mathbf{p}_j \mathbf{p}_k = \frac{m_n(h_n)}{m_n^{(j)}(\mu_j) m_n^{(k)}(\mu_k)} \prod_{\substack{i=0 \\ i \neq j, k}}^{n-1} (h_n - \mu_i \mathbb{1}_n) = 0. \quad (6.135)$$

Finally, for each  $k = 0, 1, \dots, n-1$ , we have

$$(m_n^{(k)}(x) - m_n^{(k)}(\mu_k)) \Big|_{x=\mu_k} = 0, \quad (6.136)$$

so

$$m_n^{(k)}(x) - m_n^{(k)}(\mu_k) = (x - \mu_k) q_k(x), \quad (6.137)$$

for some polynomial  $q_k(x)$ . It follows that

$$\mathbf{p}_k \mathbf{p}_k - \mathbf{p}_k = \frac{(h_n - \mu_k \mathbb{1}_n) q_k(h_n)}{m_n^{(k)}(\mu_k)} \hat{m}_n^{(k)}(h_n) = \frac{q_k(h_n)}{(m_n^{(k)}(\mu_k))^2} m_n(h_n) = 0. \quad (6.138)$$

□

**Lemma 6.2.10.** For each  $i = 0, 1, \dots, n-1$ , we have

$$\ker(\mathbf{p}_i) = \bigoplus_{\substack{k=0 \\ k \neq i}}^{n-1} \mathcal{V}_{n,k}, \quad \text{im}(\mathbf{p}_i) = \mathcal{V}_{n,i}. \quad (6.139)$$

*Proof.* Let  $i, k \in \{0, 1, \dots, n-1\}$  and  $v \in \mathcal{V}_{n,k}$ . Then,

$$\mathbf{p}_i v = \hat{m}_n^{(i)}(\mu_k) v = \delta_{ik} v, \quad (6.140)$$

and since  $\mathbf{p}_i$  is an idempotent, the result follows. □

**Proposition 6.2.11.** For every  $n \in \mathbb{N}$  and all  $u \in \mathbb{C}$ , we have

$$\check{T}_n(u) = \sum_{i=0}^{n-1} \lambda_i(u) \mathbf{p}_i = \sum_{i=0}^{n-1} \binom{n-1}{i} \frac{(-1)^i \lambda_i(u)}{(2n-2)!!} m_n^{(i)}(h_n). \quad (6.141)$$

*Proof.* The result follows from Proposition 6.2.4, Corollary 6.2.5, Lemma 6.2.10 and (6.131).  $\square$

Alternative expressions for  $\check{T}_n(u)$  can be obtained, for example by evaluating the inverse  $V_n^{-1}$  explicitly and using

$$m_n(x) = x^n - \sum_{i,j=0}^{n-1} [V_n^{-1}]_{i-1,j-1} \mu_j^n x^i. \quad (6.142)$$

We thus conjecture that  $\check{T}_n(u)$  admits the following expression in terms of the *double factorial binomial coefficient* [68],

$$\binom{n_1}{n_2} := \frac{n_1!!}{n_2!! (n_1 - n_2)!!}. \quad (6.143)$$

**Conjecture 6.2.12.** *For every  $n \in \mathbb{N}$  and all  $u \in \mathbb{C}$ , we have*

$$\check{T}_n(u) = 2 \sum_{k=0}^{n-1} (1+u^2)^{n-k} (2u)^k \sum_{j=0}^{\lfloor \frac{k}{2} \rfloor} \binom{n-k-2+2j}{2j} \frac{(-1)^j m_{k-2j}(h_n)}{(k-2j)!}. \quad (6.144)$$

We have verified Conjecture 6.2.12 for  $n = 1, \dots, 180$ .



The following publication has been incorporated as Chapter 7.

[1] B. Durhuus, X. Poncini, J. Rasmussen, M. Ünel, *Critical behaviour of loop models on causal triangulations*, J. Stat. Mech. (2021) 113102, arXiv:2104.14176 [hep-th].

# Chapter 7

---

## Loop models on causal triangulations

---

In this chapter, we develop a planar-algebraic framework to describe and analyse statistical mechanical models on *two-dimensional causal dynamical triangulations*. We introduce a dense and a dilute loop model, each defined in terms of an underlying transfer operator (distinct from the one defined in Section 3.1), and whose underlying algebraic structure is endowed from the tensor planar algebra. Both models are characterised by a geometric coupling constant  $g$  and a loop parameter  $\alpha$  such that the purely geometric causal triangulation model is recovered for  $\alpha = 1$ . We show that the dense loop model can be mapped to a solvable planar tree model, whose partition function we compute explicitly and use to determine the critical behaviour of the loop model. The dilute loop model can likewise be mapped to a planar tree model; however, a closed-form expression for the corresponding partition function is not obtainable using the standard methods employed in the dense case. Instead, we derive bounds on the critical coupling  $g_c$  and apply transfer operator techniques to examine the critical behaviour for  $\alpha$  small.

### 7.1 Background

If a two-dimensional statistical mechanical model with a second-order phase transition is coupled to a random background, its critical exponents may change and there may be a back-reaction on the background geometry changing its Hausdorff dimension. A prominent example of this phenomenon is the Ising model on a random two-dimensional triangulation (or quadrangulation), as demonstrated in [69]. Other examples are dimer models [70], Potts models [71, 72], and multicritical models [73], see also [74] for an overview. The relation between the critical exponents, or scaling dimensions, of a matter field on a flat background and on a random curved background is given quite generally by the KPZ-formula of Liouville quantum gravity [75]. A conjectured formula for the Hausdorff dimension of the background geometry as a function of the central charge of the matter fields can be found in [76], although recent mathematical results in Liouville quantum gravity [77, 78] imply restrictions on the possible range of validity of this formula.

It is natural to ask how universal this so-called dressing of critical exponents is with respect to the

ensembles of background geometries considered. In particular, it is natural to compare the ensemble of unrestricted dynamical triangulations (DT) (see e.g. [74]) considered in the references above, with the ensemble of causal dynamical triangulations (CDT) [79]. Without coupling to a matter system, these ensembles, which we shall call *pure DT* and *pure CDT* in the following, exhibit different critical behaviours, the former having Hausdorff dimension 4 [80, 81], while the latter has Hausdorff dimension 2 [82]. Very few analytical results are available concerning matter systems coupled to CDT. A number of numerical studies have been carried out, notably for Ising type and Potts type models [83–85], but there is no clear indication of a change in the critical exponents. In [86, 87], a class of restricted dimer models are mapped to certain labelled tree models. Using this, the corresponding Hausdorff dimension is found to be affected by the dimer system, although the underlying mechanism remains unclear. In the work [88], a class of CDT models with curvature-dependent weights is found to exhibit the same scaling behaviour as pure CDT.

In statistical mechanics, one usually works with local degrees of freedom, such as spins or heights, as in the Ising and Potts models above. However, percolation and polymer systems, for example, require that one keeps track of connectivities or some other inherently nonlocal degrees of freedom and this paradigm shift has a profound effect on the physical properties of the models. Critical fully-packed loop models on regular square lattices have thus been found to give rise to *logarithmic* conformal field theories in the continuum scaling limit [21]. Using underlying Temperley–Lieb algebraic structures [13, 89], these loop models are found to be Yang–Baxter integrable and amenable to exact solutions. One of these models describes critical dense polymers and has been solved exactly on the strip [46], the cylinder [64] and the torus [90], confirming predictions about scaling dimensions made in [91–93]. Other types of loop models have also been constructed, including dilute loop models associated with the  $O(n)$  models [94, 95] where the configurations may contain spaces of variable sizes in between the loop segments. Loop models have also been coupled to random surfaces [73, 96], including random triangulations [97, 98]. However, to the best of our knowledge, loop models have yet to be coupled to CDT.

In this chapter, we introduce and study two models of loop configurations on two-dimensional causal dynamical triangulations: a *dense loop model* and a *dilute loop model*, reminiscent of the familiar fully-packed and dilute loop models, respectively. Both models are characterised by a geometric coupling constant  $g$  associated with the underlying triangulations, as in pure CDT, and a loop parameter  $\alpha$  that encodes the relative weights of the admissible loop configurations on individual elementary triangles. No weight is associated with the number of closed loops in the models considered here, effectively setting the corresponding loop fugacities to 1. We show that the known correspondence between pure CDT and planar trees [82, 99] extends to each of the loop models and a corresponding class of labelled trees. This implies simple relations between the partition functions of the loop models and those of the associated labelled tree models. In the case of the dense loop model, we solve the corresponding tree model exactly and find that its Hausdorff dimension equals that of pure CDT. The critical behaviour of the loop model is readily extracted from the closed-form expression we obtain for the partition function following our tree analysis. Although the dilute loop model can likewise be

mapped to a planar tree model, a closed-form expression for the corresponding partition function is not obtainable using the techniques employed in the dense case. Instead, we employ analyticity arguments, centred around the transfer operator, to examine the critical behaviour of the loop model for  $\alpha$  close to 0. We conclude that the critical behaviour for  $\alpha$  small is different from that of pure CDT, and provide an explanation for this difference. Based on results in [100], we argue that the Hausdorff dimension equals 1 in this phase. While these results may hold for more general values of  $\alpha$ , our analysis has not been able to confirm this. In fact, it is consistent with our findings that there exists a transition point  $\alpha_0 \in (0, 1)$  at which the scaling behaviour changes.

## 7.2 Loop models

We begin in Section 7.2.1 by recalling the properties of *two-dimensional causal dynamical triangulations*, which we refer to simply as *causal triangulations*. By considering *dual causal triangulations*, we develop a planar-algebraic framework to describe models on causal triangulations. While the underlying algebraic structure of this framework is identical to that of Chapter 3, the transfer operator used to describe models on causal triangulations is distinct. As an application of this framework, we define a pure CDT model in Section 7.2.2, a dense loop model in Section 7.2.3 and a dilute loop model in Section 7.2.4, and formulate each in a planar-algebraic setting.

### 7.2.1 Causal triangulations

A *causal triangulation* of the disk is defined by a central vertex  $x$ , a distinguished vertex  $v_1$  in  $S_1$ , and a sequence of concentric cycles (circular graphs)  $S_0 \equiv \{x\}, S_1, \dots, S_m$  where  $m \in \mathbb{N}$  is the *height*, such that for each  $k = 0, \dots, m-1$  edges connect vertices between each cycle  $S_k$  and  $S_{k+1}$  as to form a triangulation. We denote by  $A_k$  the annulus bounded by  $S_k$  and  $S_{k+1}$ , and note that  $A_0$  is simply a disk with boundary  $S_1$  and a central node  $x$ . The natural ordering on the concentric cycles is interpreted as encoding a natural time direction; with the inner-most ( $S_0$ ) and outer-most ( $S_m$ ) cycles denoting the first and last instant of time respectively. Accordingly, edges within each cycle are called *space-like* and are here coloured red, while edges connecting two cycles are called *time-like* and are here coloured black, see for example Figure 7.1c. For a given  $S_k$  we denote the number of space-like edges by  $|S_k|$  and note that  $|S_0| = 0$ , while  $|S_k| > 0$  for all  $k \in \mathbb{N}$ . Within each  $A_k$ , an *elementary triangle* is either *forward-directed* with a single node in  $S_{k+1}$  and the remaining two nodes in  $S_k$ , or *backward-directed* with a single node in  $S_k$  and the remaining two nodes in  $S_{k+1}$ .

As a means to orient causal triangulations, beginning with the distinguished vertex  $v_1$  in  $S_1$ , we introduce a procedure that assigns a distinguished vertex  $v_k$  in  $S_k$  for all  $k = 1 \dots m$ . From  $v_1$ , travel along the right-most emanating edge to a vertex in  $S_2$  that we denote by  $v_2$ . Likewise,  $v_2$  is connected to a vertex denoted by  $v_3$  in  $S_3$  by travelling along its right-most emanating edge. Repeating this procedure until we arrive at a vertex in  $S_m$ , we have a sequence of distinguished vertices  $v_0 \equiv x, v_1, \dots, v_m$  where each neighbouring pair is connected by a time-like edge:  $\{v_k, v_{k+1}\}$  for  $k = 0, \dots, m-1$ . Relative to the

distinguished vertex  $v_k$ , space-like edges in  $S_k$  are assigned a clockwise order. Accordingly, the first space-like edge within each annulus  $A_k$  corresponds to a forward-directed triangle for all  $k = 1, \dots, m$ .

Note that the above prescription can be adapted to define a causal triangulation of the *cylinder* and of the *sphere*. For the cylinder, the cycle  $S_0$  is omitted, and the first instant of time is therefore given by  $S_1$ . While for the sphere, we introduce the cycle  $S_{m+1} \equiv \{y\}$  as the pole opposite to  $S_0$  and adjoin forward-directed triangles to each of the space-like edges in  $S_m$  such that each of these triangles are connected to the unique vertex  $y$  in  $S_{m+1}$ . See Figure 7.1 for an example of a causal triangulation of each of these topologies.

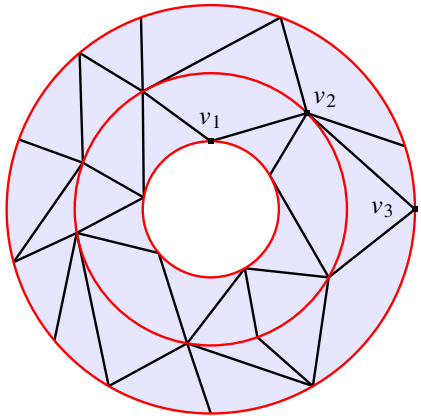
To each causal triangulation of the disk, cylinder or sphere there is a unique *dual* triangulation constructed as follows: assign a trivalent dual vertex to each of the elementary triangles such that the three emanating dual edges each intersect a unique edge of the triangle; if two elementary triangles share an edge, identify the two corresponding dual edges that intersect that given edge. Here, the dual edge inherits the colour of the edge it intersects c.f. Figures 7.1a and 7.1b. We identify the distinguished dual edge  $w_k$  as that which intersects the distinguished time-like edge  $\{v_k, v_{k+1}\}$  for  $k = 0, \dots, m-1$ . Accordingly, the dual disk has *free* edges emanating from the outer cycle, the dual cylinder has edges emanating from both the outer and inner cycle, and the dual sphere has no free edges. See Figure 7.1 for an example of a causal triangulation and the corresponding dual for each of these topologies.

From the perspective of the planar-algebraic framework presented in Chapter 3, the dual of a causal triangulation is highly suggestive. The concentric circles of dual nodes indicate a natural multiplicative structure, while the dual nodes themselves can be elevated to input disks – indicating a generality beyond pure triangulations. Moreover, the distinguished dual edges  $w_1$  respectively  $w_m$  can be translated to the marked interval of the inner disk respectively outer disk of an annular planar tangle. Despite these common features, the corresponding transfer operator of models on causal triangulations is distinct from that presented in Chapter 3; there are two main differences (i) it consists of a sum of constituent transfer operators, each not necessarily belonging to the same vector space, and (ii) the  $R$ -operators within the constituent transfer operators are not identical, and likewise, need not belong to the same vector space.

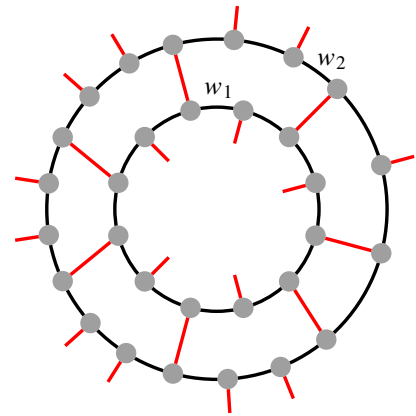
We proceed by defining the annular tangle

$$T_{\mathbf{i}}^{\mathbf{o}} := \text{Diagram} \quad (7.1)$$

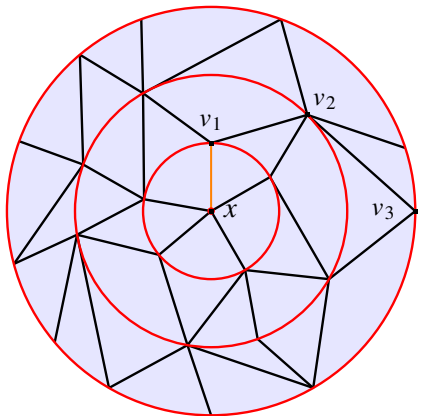
where  $\mathbf{i} := (i_1, \dots, i_n)$  is an element of  $\mathbb{N}^n$  and  $\mathbf{o} := (o_1, \dots, o_n)$  is an element of  $\mathbb{N}^{n-1} \times \mathbb{N}_0$  for  $n \in \mathbb{N}$ ,



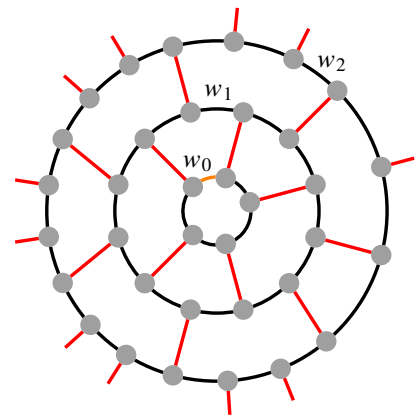
(a)



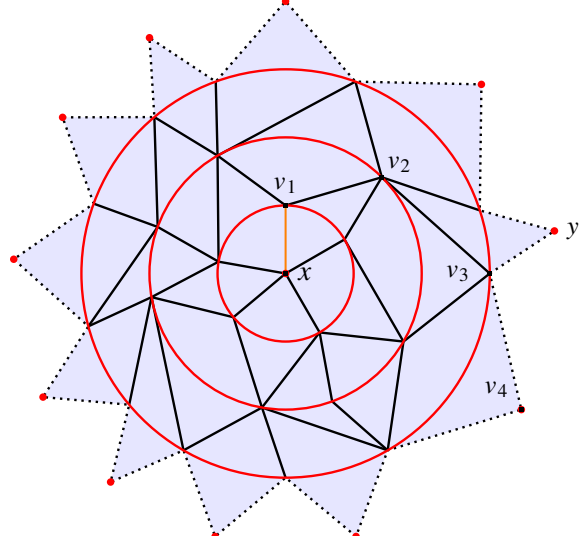
(b)



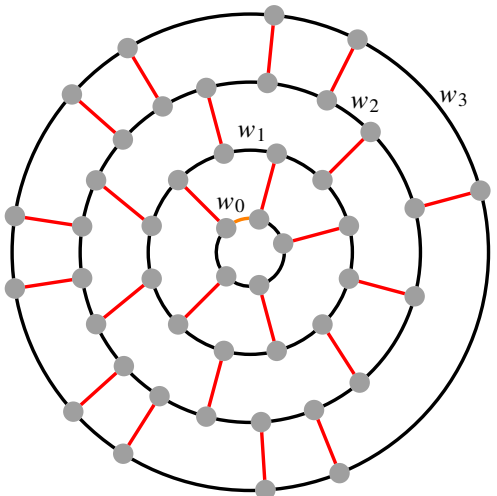
(c)



(d)



(e)



(f)

Figure 7.1: In the first column, we present a causal triangulation on three topologies; the cylinder (a) and the extension of this triangulation to the disk (c) and the sphere (e). While in the second column, we present the corresponding dual triangulation of the cylinder (b), disk (d) and sphere (f).

that indicate the distribution of inner and outer nodes respectively. Note that the inner and outer distinguished intervals are placed about the distinguished edge of the dual triangulation.

Let  $(P_n)_{n \in \mathbb{N}_0}$  denote the collection vector spaces of a general planar algebra, and let  $(QP_{m,n})_{m,n \in \mathbb{N}_0}$  denote the corresponding collection of affine vector spaces, defined in Section 2.6. The  $R$ -operators are defined as the parameterised elements

$$R_j^k(u) := \underbrace{-\cdots-}_{j} \underbrace{\overbrace{\cdots}^k}_{\cdots} \cdots \underbrace{\cdots-}_{j}, \quad (7.2)$$

with

$$\underbrace{-\cdots-}_{j} = \sum_{a \in B_3} r_a(u) \underbrace{-\cdots-}_{j}, \quad \underbrace{-\cdots-}_{j} = \sum_{a \in B_3} r_a(u) \underbrace{-\cdots-}_{j}, \quad (7.3)$$

where  $B_3$  is a basis for  $P_3$ ,  $r_a : \Omega \rightarrow \mathbb{C}$  and  $\Omega$  is a suitable domain. By construction,  $R_j^k(u)$  is an element of the vector space  $P_{j+k+2}$ . We can now define the constituent transfer operator as

$$T_{\mathbf{i}}^{\mathbf{o}}(u) := \mathsf{P}_{T_{\mathbf{i}}^{\mathbf{o}}}(R_{i_1}^{o_1}(u), \dots, R_{i_n}^{o_n}(u)), \quad (7.4)$$

which is an element  $QP_{i,o}$  where  $i = \sum_{k=1}^n i_k$  and  $o = \sum_{k=1}^n o_k$ . Applying the map to the plane introduced in Section 2.6, we can express  $T_{\mathbf{i}}^{\mathbf{o}}(u)$  diagrammatically as

$$T_{\mathbf{i}}^{\mathbf{o}}(u) := \underbrace{-\cdots-}_{i_1} \underbrace{\overbrace{\cdots}^{o_1}}_{i_2} \cdots \underbrace{\overbrace{\cdots}^{o_n}}_{i_n}, \quad R_{i_k}^{o_k}(u) = \underbrace{-\cdots-}_{i_k} \underbrace{\overbrace{\cdots}^{o_k}}_{i_k}, \quad (7.5)$$

where we identify the left-most and right-most edges, which corresponds to the distinguished edge of the dual triangulation. Finally, we define the transfer operator of a general CDT model as

$$T(u) := \sum_{n \in \mathbb{N}} \sum_{\substack{\mathbf{i} \in \mathbb{N}^n \\ \mathbf{o} \in \mathbb{N}^{n-1} \times \mathbb{N}_0}} T_{\mathbf{i}}^{\mathbf{o}}(u), \quad (7.6)$$

where we note that  $T(u)$  is an element of the graded vector space  $(QP_{n,m})_{n,m \in \mathbb{N}_0}$ .

Recall the product structure among elements of  $(QP_{n,m})_{n,m \in \mathbb{N}_0}$ , defined in Section 2.6. Let  $a \in QP_{n,m}$  and  $b \in QP_{r,s}$ , we define

$$ab := \begin{cases} b \circ a, & m = r \\ 0, & m \neq r \end{cases} \quad (7.7)$$

where  $b \circ a$  corresponds to the insertion of  $a$  inside  $b$ . To illustrate, the example dual triangulation presented in Figure 7.1b corresponds to the element

$$T_{\mathbf{i}_1}^{\mathbf{o}_1}(u) T_{\mathbf{i}_2}^{\mathbf{o}_2}(u), \quad \mathbf{o}_1 = (1, 2, 1, 2, 1), \quad \mathbf{o}_2 = (1, 2, 2, 2, 2, 2), \\ \mathbf{i}_1 = (1, 1, 1, 1, 1), \quad \mathbf{i}_2 = (1, 2, 1, 1, 1, 1). \quad (7.8)$$

With the multiplication defined in (7.7), we emphasise that many terms in the product between two transfer operators are eliminated. The particular model described by the transfer operator depends entirely on the parameterisation of the constituent  $R$ -operators (7.2)–(7.3). Given a parameterisation, the transfer operator  $T(u)^n$  generates, as a linear combination, all height  $n$  causal triangulations of the cylinder, where we note that the inner-most and outer-most edges are weighted as the ‘square root’ of the internal edges.

### 7.2.2 Pure CDT model

Let  $C_m(N)$  denote the set of all height  $m$  causal triangulations of the disk with  $N$  vertices, and let  $C_m$  denote the corresponding set where the constraint on vertex number is relaxed. We define

$$|C| := \sum_{k=0}^m |S_k|, \quad C \in C_m, \quad (7.9)$$

as the number of space-like edges in  $C$ , equivalently the number of vertices in  $C$ , excluding the central vertex. It is convenient to include the *degenerate case* where  $m = 0$ , hence  $C \equiv S_0$  and  $|C| = 0$  for the unique ‘triangulation’  $C \in C_0$ .

The *pure CDT model* weights each  $C$  in  $C_m$  by associating a factor of  $g \in \mathbb{C}$  to each space-like edge in  $C$ . Accordingly, the partition functions of the model are defined as

$$Z(g) := \sum_{m=0}^{\infty} Z_m(g), \quad Z_m(g) := \sum_{C \in C_m} g^{|C|}, \quad (7.10)$$

and we note that  $Z_0(g) = 1$ . As is clear from the expression above, the model need not be well defined for all  $g \in \mathbb{C}$ . It is understood [79], and will be shown below, that there exists a critical coupling  $g_c > 0$  such that  $Z(g)$  is analytic for  $g < |g_c|$ , while  $Z(g)$  is divergent for  $g > g_c$ , and therefore is singular at the point  $g = g_c$ .

**Remark.** As each causal triangulation of the disk has a unique equivalent on the sphere and on the cylinder, and these triangulations have the same number of space-like edges, configurations of the pure CDT model can be considered as belonging to either of these topologies.

There is not a unique algebraic structure underlying the pure CDT model. As our goal is to understand the critical behaviour of the partition function (7.10), we opt for the simplest planar algebra such that the partition function of the model can be expressed as a function of the transfer operator. Accordingly, we specialise to the tensor planar algebra  $(E_n)_{n \in \mathbb{N}_0}$  where  $E_n \cong E^{\otimes n}$  and  $\dim E = 1$ , see Section 6.2.1 for the definition. As there is a single label for the nodes of each disk in  $E_n$  for  $n \in \mathbb{N}$ , we will omit it entirely.

For the pure CDT model, the elementary operators must simply account for the weight associated with each space-like edge, as such, we introduce the following parameterisation

$$\begin{array}{c} \text{Diagram: a vertical line with a green circle labeled } g \text{ at the top, followed by a horizontal line segment.} \\ \text{Diagram: a vertical line with a green circle labeled } g \text{ at the top, followed by a horizontal line segment with a red dot at the top.} \end{array} = g^{\frac{1}{2}} \begin{array}{c} \text{Diagram: a vertical line with a green circle at the top, followed by a horizontal line segment with a black dot at the top.} \\ \text{Diagram: a vertical line with a green circle at the top, followed by a horizontal line segment with a black dot at the top.} \end{array}, \quad (7.11)$$

where the combination of two dual space-like edges under the product assigns the appropriate weight  $g$ . Given this parameterisation, we write the  $R$ -operator as

$$R_j^k(g) = g^{\frac{1}{2}(j+k)} \text{---} \underbrace{\dots}_{j} \text{---} \underbrace{\dots}_{k} \text{---} . \quad (7.12)$$

Recall that if two elements in the tensor planar algebra have the same number of external nodes with the same labels, they are equal, independent of their internal structure. Accordingly, by collecting terms in the transfer operator, we have

$$T(g) = \sum_{r,s \in \mathbb{N}} \binom{r+s-1}{r} g^{\frac{r+s}{2}} \text{---} \underbrace{\dots}_{s} \text{---} \underbrace{\dots}_{r} \text{---} , \quad (7.13)$$

where the combinatorial factor counts the number of ways  $r$  outward (up) pointing edges and  $(s-1)$  inward (down) pointing edges can be distributed to the right (viewed outwardly) of the first inward pointing edge.

It will be convenient, when analysing the transfer operator  $T(g)$ , to instead work with a representation of this algebraic element here denoted by  $\mathsf{T}(g)$ , that acts on the Hilbert space of square summable sequences

$$l_2(\mathbb{N}) := \{(x_n)_{n \in \mathbb{N}} \mid \sum_{n=1}^{\infty} |x_n|^2 < \infty; x_i \in \mathbb{C}, i \in \mathbb{N}\}, \quad (7.14)$$

where  $n$  labels the number of edges. Accordingly, the matrix elements of  $\mathsf{T}(g)$  with respect to the standard orthonormal basis of  $l_2(\mathbb{N})$  are given by

$$\mathsf{T}_{r,s}(g) = \binom{r+s-1}{r} g^{\frac{r+s}{2}}. \quad (7.15)$$

To distinguish our terminology, we will refer to  $\mathsf{T}(g)$  as the *transfer matrix* corresponding to the transfer operator  $T(g)$ . In the following, we use Dirac notation  $|w\rangle$  to denote a sequence in  $l_2(\mathbb{N})$  with coordinates  $w_n$ , we similarly let  $\langle w|$  denote the corresponding conjugated sequence. Geometrically,  $|w\rangle$  is acted upon by the outer (top) edges, while  $\langle w|$  is acted upon by the lower (bottom) edges.

Finally, we define the sequence  $|v(g)\rangle \in l_2(\mathbb{N})$ , where

$$v_n(g) := g^{\frac{n}{2}}, \quad n \in \mathbb{N}. \quad (7.16)$$

Given the definition of the partition function (7.10), the representation  $\mathsf{T}(g)$  (7.15), and the vector  $|v(g)\rangle$  (7.16), the fixed height partition function of the pure CDT model can be written

$$Z_m(g) = \langle v(g) | \mathsf{T}(g)^{m-1} | v(g) \rangle, \quad (7.17)$$

for all  $m \in \mathbb{N}$ .

### 7.2.3 Dense loop model

Each height  $m$  *dense loop configuration* on the disk with  $N$  vertices can be constructed from a given  $C \in C_m$ , by replacing each of the elementary triangles in  $C$  with one of the two similarly directed triangles in Figure 7.2 such that loop segments are only allowed to terminate on the *boundary* of the triangulation (the cycle  $S_m$ ). Consequently, one must impose a compatibility condition along each space-like edge. The elementary triangles of dense loop configurations are constructed by decorating the original triangles with blue *arc(s)*, which are non-intersecting and defined up to ambient isotopy. Arcs within a loop configuration may combine to form closed loops. One may similarly define dense loop configurations on the cylinder and on the sphere. See Figure 7.3 for an example of a dense loop configuration on the disk (Figure 7.3c) and the corresponding configuration on the cylinder (Figure 7.3a) and on the sphere (Figure 7.3e).

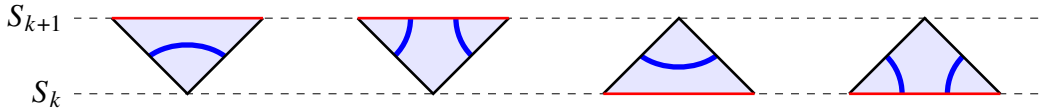


Figure 7.2: The possible decorations of elementary triangles in the dense loop model.

Let  $\mathcal{L}_m^{de}(N)$  denote the set of all height  $m$  dense loop configurations (on the disk) with  $N$  vertices, and let  $\mathcal{L}_m^{de}$  denote the corresponding set where the constraint on vertex number is relaxed. Each crossing of a space-like edge by a loop segment is called an *intersection*, and we denote by  $s(L)$  the total number of intersections in  $L \in \mathcal{L}_m^{de}(N)$ . As in Section 7.2.2, we denote by  $|L|$  the total number of space-like edges in the dense loop configuration  $L$ .

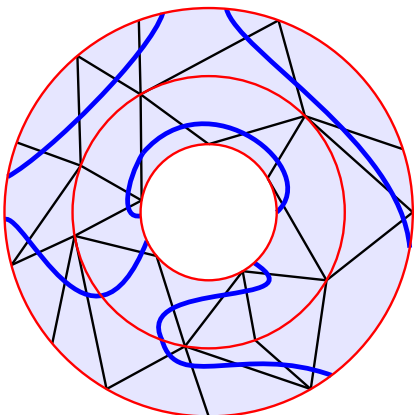
The *dense loop model* weights each  $L$  in  $\mathcal{L}_m^{de}$  by associating a factor of  $g \in \mathbb{C}$  and a factor of  $\alpha \in [0, 1]$  to each space-like edge and intersection in  $L$ , respectively. Accordingly, the partition functions of the model are defined as

$$Z^{de}(g, \alpha) := \sum_{m=0}^{\infty} Z_m^{de}(g, \alpha), \quad Z_m^{de}(g, \alpha) := \sum_{L \in \mathcal{L}_m^{de}} g^{|L|} \alpha^{s(L)}, \quad (7.18)$$

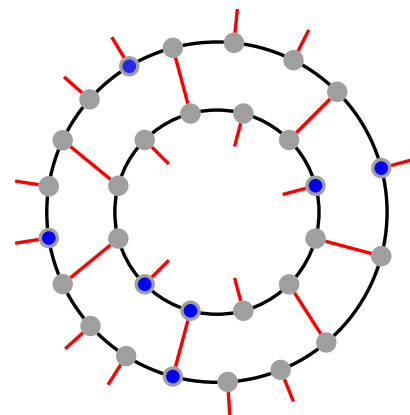
where we note that  $Z_0^{de}(g, \alpha) = 1$ , and take  $\alpha^n$ , for  $\alpha = 0$  and  $n \in \mathbb{N}_0$ , to mean  $\delta_{n,0}$ . In the following, we will show, for fixed  $\alpha$ , that there exists a critical coupling  $g_c^{de}(\alpha) > 0$  such that  $Z^{de}(g, \alpha)$  is analytic for  $|g| < g_c^{de}(\alpha)$ , while  $Z^{de}(g, \alpha)$  is divergent for  $g > g_c^{de}(\alpha)$ , and therefore is singular along the curve  $g = g_c^{de}(\alpha)$ .

**Remark.** As in the pure CDT model, each dense loop configuration on the disk has an equivalent on the sphere and on the cylinder, and each of these equivalent forms has the same number of space-like edges and intersections. It follows that the configurations of the dense loop model can be considered as belonging to either of these topologies.

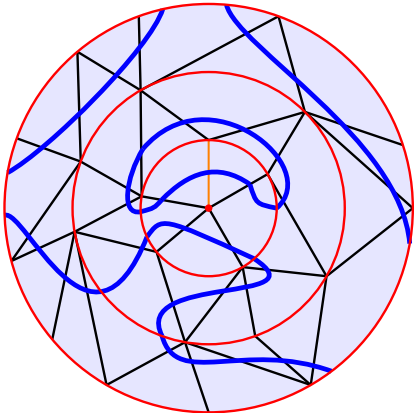
The algebraic structure underlying the dense loop model is not unique. We adopt the attitude presented in Section 7.2.2, where we opt for the simplest planar algebra such that the partition function of the model can be expressed as a function of the transfer operator. To this end, we specialise to



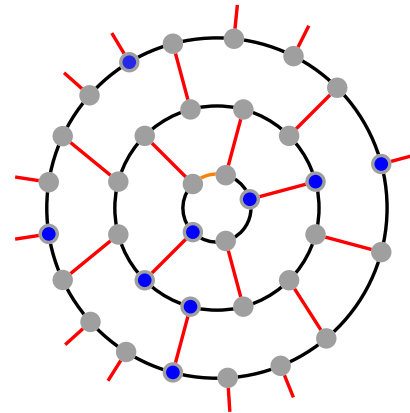
(a)



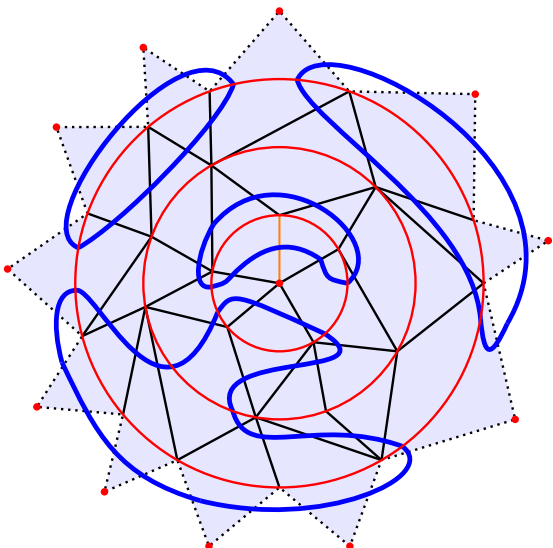
(b)



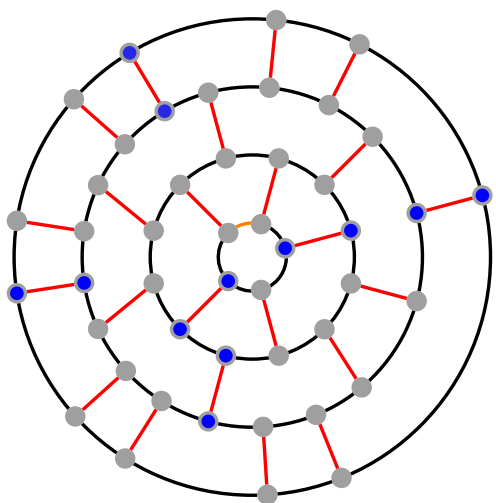
(c)



(d)



(e)



(f)

Figure 7.3: In the first column, we present a dense loop configuration on three topologies; the cylinder (a) and the extension of this configuration to the disk (c) and the sphere (e). While in the second column, we present the corresponding dual configuration of the cylinder (b), disk (d) and sphere (f).

the tensor planar algebra  $(E_n)_{n \in \mathbb{N}_0}$  where  $E_n \cong E^{\otimes n}$  and  $\dim E = 2$ . Nodes of each disk within  $E_n$  are assigned two possible labels, here represented diagrammatically by the colours black and blue.

Expressing the elementary triangles as elements of the underlying planar algebra, we have:

$$\begin{array}{c} \text{Diagram} \\ \text{with black dot} \end{array} \leftrightarrow \begin{array}{c} \text{Diagram} \\ \text{with blue dot} \end{array}, \quad \begin{array}{c} \text{Diagram} \\ \text{with black dot} \end{array} \leftrightarrow \begin{array}{c} \text{Diagram} \\ \text{with blue dot} \end{array}, \quad \begin{array}{c} \text{Diagram} \\ \text{with black dot} \end{array} \leftrightarrow \begin{array}{c} \text{Diagram} \\ \text{with blue dot} \end{array}, \quad \begin{array}{c} \text{Diagram} \\ \text{with black dot} \end{array} \leftrightarrow \begin{array}{c} \text{Diagram} \\ \text{with blue dot} \end{array}. \quad (7.19)$$

Accordingly, we parameterise the elementary operators by

$$\begin{array}{c} \text{Diagram} \\ \text{with black dot} \end{array} = g^{\frac{1}{2}} \begin{array}{c} \text{Diagram} \\ \text{with black dot} \end{array} + g^{\frac{1}{2}}\alpha \begin{array}{c} \text{Diagram} \\ \text{with blue dot} \end{array}, \quad \begin{array}{c} \text{Diagram} \\ \text{with black dot} \end{array} = g^{\frac{1}{2}} \begin{array}{c} \text{Diagram} \\ \text{with black dot} \end{array} + g^{\frac{1}{2}}\alpha \begin{array}{c} \text{Diagram} \\ \text{with blue dot} \end{array}, \quad (7.20)$$

from which the  $R$ -operators (7.2) follow. For brevity, we have not indicated the  $g$  and  $\alpha$  dependence of the green diagrams in (7.20). Given this parameterisation of the  $R$ -operators, we denote the corresponding transfer operator  $T^{de}(g, \alpha)$ , which can be expressed as

$$T^{de}(g, \alpha) = \sum_{r,s \in \mathbb{N}} \binom{r+s-1}{r} g^{\frac{r+s}{2}} \begin{array}{c} \text{Diagram} \\ \text{with black dot} \end{array}, \quad \bullet = \bullet + \alpha \bullet. \quad (7.21)$$

As our primary motivation is defining a transfer operator that reproduces the partition function of the model, we can introduce a simpler counterpart to  $T^{de}(g, \alpha)$  which, from the perspective of the partition function, is indistinguishable from the original. In particular,  $T^{de}(g, \alpha)$ , keeps track of unnecessary information about the specific positioning of intersected space-like edges, it suffices to simply ensure compatibility between space-like edges. Accordingly, the two possible elementary configurations corresponding to a single space-like edge are  $\begin{array}{c} \text{Diagram} \\ \text{with black dot} \end{array}$  and  $\begin{array}{c} \text{Diagram} \\ \text{with blue dot} \end{array}$ , which assign the weight  $g$  and  $g\alpha^2$  respectively. The correct assignment of weights can be achieved by simply considering a single elementary configuration  $\begin{array}{c} \text{Diagram} \\ \text{with black dot} \end{array}$  which is assigned the weight  $g(1+\alpha^2)$ . In light of this observation, we introduce an *effective transfer operator* corresponding to  $T^{de}(g, \alpha)$ , defined as

$$\bar{T}^{de}(g, \alpha) := \sum_{r,s \in \mathbb{N}} \binom{r+s-1}{r} [g(1+\alpha^2)]^{\frac{r+s}{2}} \begin{array}{c} \text{Diagram} \\ \text{with black dot} \end{array}, \quad (7.22)$$

where each node  $\bullet$  is considered a ‘square root’ of a space-like edge and is assigned the weight  $[g(1+\alpha^2)]^{\frac{1}{2}}$ . While the algebraic operators appearing in  $\bar{T}^{de}(g, \alpha)^m$  do not have a direct relation to the underlying loop configurations, they assign the correct weight of  $g(1+\alpha^2)$  to each *internal* space-like edge.

**Remark.** As the effective transfer operator  $\bar{T}^{de}(g, \alpha)$  is parameterised in terms of elements that only use a single node label, we consider the underlying planar algebra to be as in the pure CDT model, where  $\dim E = 1$ .

Proceeding as in the pure CDT case, we denote by  $T^{de}(g, \alpha)$  the corresponding representation of  $\bar{T}^{de}(g, \alpha)$ , that acts on the Hilbert space  $l_2(\mathbb{N})$ , whose matrix elements are given by

$$T_{r,s}^{de}(g, \alpha) = \binom{r+s-1}{r} [g(1+\alpha^2)]^{\frac{r+s}{2}}. \quad (7.23)$$

We also introduce the sequence  $|v^{de}(g, \alpha)\rangle \in l_2(\mathbb{N})$ , where

$$v_n^{de}(g, \alpha) := [g(1 + \alpha^2)]^{\frac{n}{2}}, \quad n \in \mathbb{N}. \quad (7.24)$$

Given the definition of the partition function (7.18), the representation  $T^{de}(g, \alpha)$  (7.23), and the vector  $|v^{de}(g, \alpha)\rangle$  (7.24), the fixed height partition function of the dense loop model can be written

$$Z_m^{de}(g, \alpha) = \langle v^{de}(g, \alpha) | T^{de}(g, \alpha)^{m-1} | v^{de}(g, \alpha) \rangle, \quad (7.25)$$

for all  $m \in \mathbb{N}$ .

### 7.2.4 Dilute loop model

Each height  $m$  *dilute loop configuration* on the disk with  $N$  vertices can be constructed from a given  $C \in C_m$ , by replacing each of the elementary triangles in  $C$  with one of the four similarly directed triangles in Figure 7.5, such that loop segments are only allowed to terminate on the *boundary* of the triangulation. Consequently, one must impose a compatibility condition along *both* space-like and time-like edges. The elementary triangles of dilute loop configurations are constructed by decorating the original triangles with at least one blue arc, which, as in the dense loop model, are non-intersecting, defined up to ambient isotopy and may combine to form closed loops. One may similarly define dilute loop configurations on the cylinder and on the sphere. See Figure 7.4 for an example of a dilute loop configuration on the disk (Figure 7.4c) and a corresponding configuration on the cylinder (Figure 7.4a) and on the sphere (Figure 7.4e). Unlike dense loop configurations, the extension of a disk configuration to the sphere can be performed in two *distinct* ways, each resulting in *distinct* configurations on the sphere. Moreover, the extension of a configuration on the cylinder to the disk need not be well defined, we explore this in the following.

For dense and dilute loop models, let  $s_k(L)$  denote the number of intersections of the cycle  $S_k$  associated with the loop configuration  $L$  which may be on the cylinder, disk or sphere. In the dilute loop model, the compatibility condition along space-like and time-like edges ensures that the parity of  $s_k(L)$  is the same for all  $k$ , that is

$$s_k(L) \equiv s_{k'}(L) \pmod{2}, \quad \forall k, k'. \quad (7.26)$$

Considering dilute configurations on the disk and sphere, the initial condition  $s_0(L) = 0$ , restricts the parity of the remaining cycles to be *even*. While for dilute configurations on the cylinder, both parities are allowed. It follows that only the even parity annular configurations admit extensions to the disk, in which case the extension is not unique and gives rise to two distinct configurations.

Let  $\mathcal{L}_m^{di}(N)$  denote the set of all height  $m$  dilute loop configurations (on the disk) with  $N$  vertices, and let  $\mathcal{L}_m^{di}$  denote the corresponding set where the constraint on vertex number is relaxed. We adopt the same notation as in the dense model where  $|L|$  and  $s(L)$  denote the number of space-like edges and intersections in a dilute loop configuration  $L \in \mathcal{L}_m^{di}(N)$ , respectively.

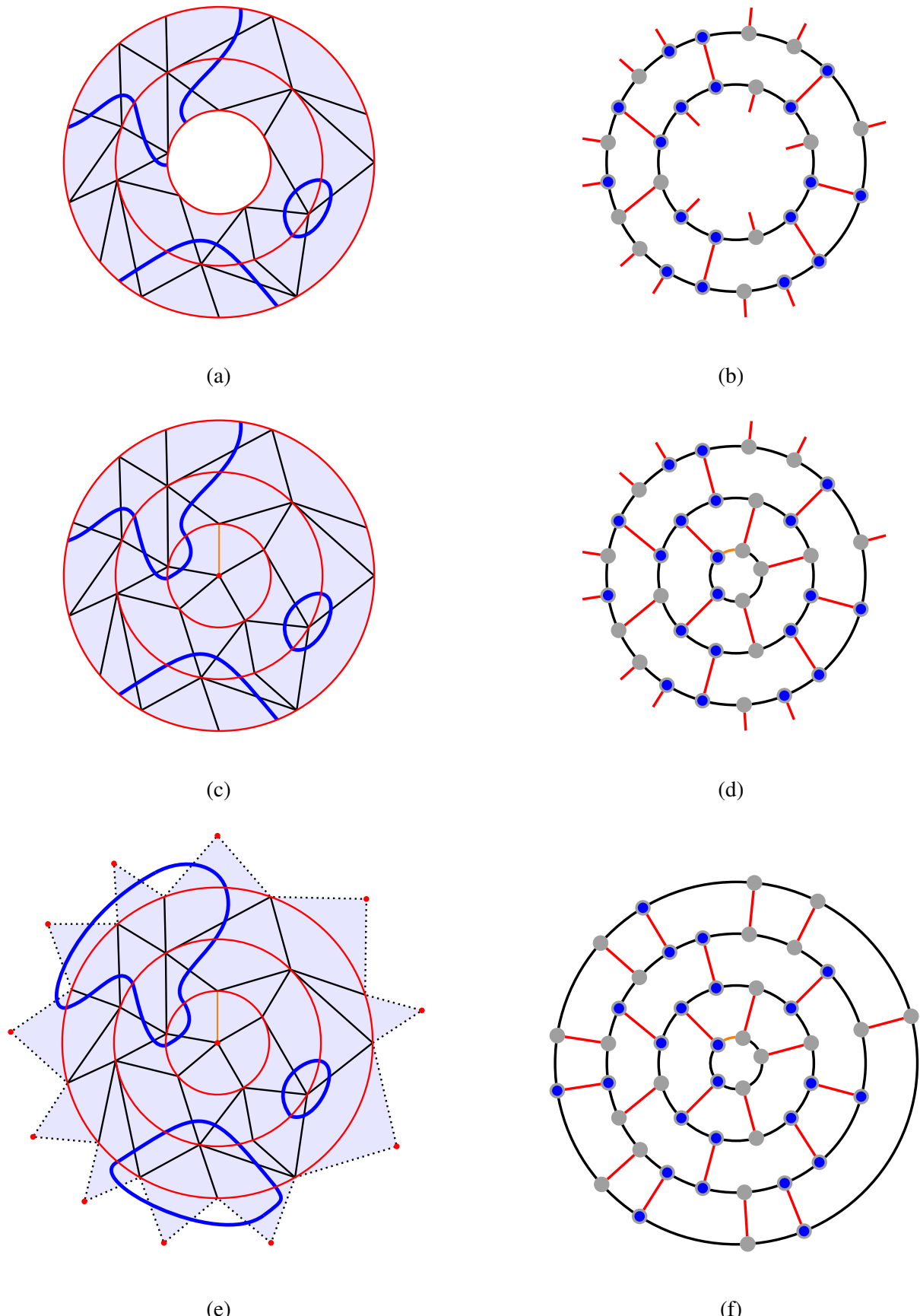


Figure 7.4: In the first column, we present a dilute loop configuration on three topologies; the cylinder (a) and an extension of this configuration to the disk (c) and the sphere (e). While in the second column, we present the corresponding dual configuration of the cylinder (b), disk (d) and sphere (f).

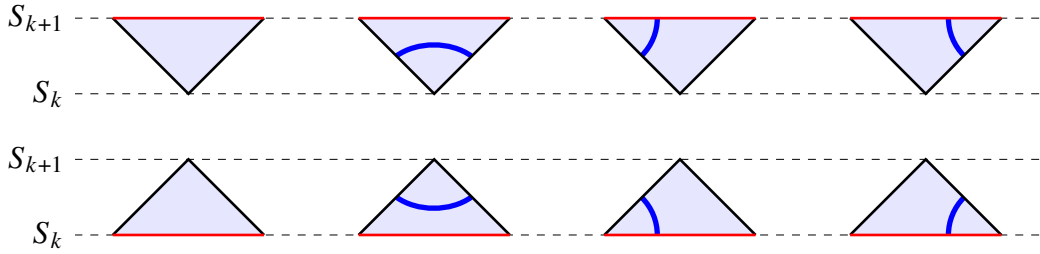


Figure 7.5: The possible decorations of elementary triangles in the dilute loop model.

The *dilute loop model* weights each  $L$  in  $\mathcal{L}_m^{di}$  by associating a factor of  $g \in \mathbb{C}$  and a factor of  $\alpha \in [0, 1]$  to each space-like edge and intersection in  $L$ , respectively. Accordingly, the partition functions of the model are defined as

$$Z^{di}(g, \alpha) := \sum_{m=0}^{\infty} Z_m^{di}(g, \alpha), \quad Z_m^{di}(g, \alpha) := \sum_{L \in \mathcal{L}_m^{di}} g^{|L|} \alpha^{s(L)}, \quad (7.27)$$

where we note that  $Z_0^{di}(g, \alpha) = 1$ , and take  $\alpha^n$ , for  $\alpha = 0$  and  $n \in \mathbb{N}_0$ , to mean  $\delta_{n,0}$ . In the following, we will show that, for fixed  $\alpha$ , there exists a critical coupling  $g_c^{di}(\alpha) > 0$  such that  $Z^{di}(g, \alpha)$  is analytic for  $|g| < g_c^{di}(\alpha)$ , while  $Z^{di}(g, \alpha)$  is divergent for  $g > g_c^{di}(\alpha)$ , and therefore is singular along the curve  $g = g_c^{di}(\alpha)$ .

**Remark.** While the parity condition of dilute loop configurations (7.26) inhibits a natural correspondence between configurations on the cylinder and the disk, there is a two-to-one correspondence between configurations on the sphere and the disk. Accordingly, configurations of the dilute loop model can be considered as belonging to either the disk or sphere, as long as one accounts for the factor of two appropriately.

As in the dense loop model, we specialise to the tensor planar algebra  $(E_n)_{n \in \mathbb{N}_0}$  where  $E_n \cong E^{\otimes n}$  and  $\dim E = 2$ , and use black and blue to represent the two node labels. Expressing the elementary triangles of the dilute loop model as elements of the underlying planar algebra, we have:

$$\begin{array}{cccc} \text{Diagram 1} & \leftrightarrow & \text{Diagram 2} & \leftrightarrow \\ \text{Diagram 3} & \leftrightarrow & \text{Diagram 4} & \leftrightarrow \end{array} \quad (7.28)$$

$$\begin{array}{cccc} \text{Diagram 5} & \leftrightarrow & \text{Diagram 6} & \leftrightarrow \\ \text{Diagram 7} & \leftrightarrow & \text{Diagram 8} & \leftrightarrow \end{array} \quad (7.29)$$

Accordingly, we parameterise the elementary operators by

$$\text{Diagram 1} = g^{\frac{1}{2}} \left( \text{Diagram 3} + \text{Diagram 4} \right) + (g\alpha)^{\frac{1}{2}} \left( \text{Diagram 5} + \text{Diagram 6} \right), \quad (7.30)$$

$$\text{Diagram 2} = g^{\frac{1}{2}} \left( \text{Diagram 3} + \text{Diagram 4} \right) + (g\alpha)^{\frac{1}{2}} \left( \text{Diagram 7} + \text{Diagram 8} \right), \quad (7.31)$$

from which the  $R$ -operators (7.2) follow. Note that we have not indicated the  $g$  and  $\alpha$  dependence of the green diagrams in (7.30). Given this parameterisation of the  $R$ -operators, we denote the corresponding transfer operator  $T^{di}(g, \alpha)$ . Unlike for the dense loop model, a simplified expression for  $T^{di}(g, \alpha)$  and an associated effective transfer operator  $\bar{T}^{di}(g, \alpha)$  cannot be immediately stated. An analogous construction for the dilute loop model exists but will be deferred until Section 7.5.3, as it relies on results established in the forthcoming section.

## 7.3 Tree correspondences

In this section, we begin by recalling the correspondence between causal triangulations and planar trees. Section 7.3.2 is devoted to extending this correspondence to relate loop models on causal triangulations and classes of labelled planar trees. In Section 7.3.3, we make use of these correspondences to relate the partition functions of the matched constructions, which ultimately facilitates the analysis of CDT partition functions using tree methods.

### 7.3.1 Pure CDT model

Let  $\mathcal{T}_m(N)$  denote the set of height  $m+1$  planar trees with  $N$  edges and a root of degree 1, similarly,  $\mathcal{T}_m$  where the constraint on vertex number is relaxed, and finally  $\mathcal{T}$  where the height constraint is relaxed. It is well-known [82, 99] that there exists a bijective correspondence between causal triangulations and planar trees

$$\psi : C_m(N) \rightarrow \mathcal{T}_m(N). \quad (7.32)$$

Let  $C \in C_m(N)$ , the map  $\psi$  is constructed as follows: first, remove all space-like edges, then for each vertex in  $S_k$  for  $1 \leq k < m$  remove the right-most outward-pointing time-like edge, finally, add a new vertex  $x_0$  and a corresponding edge  $\{x_0, x\}$  immediately to the left (viewed outwardly) of the distinguished edge  $\{x, v_1\}$ . The resulting graph, denoted by  $T = \psi(C)$ , is an element of the set  $\mathcal{T}_m(N)$ , and the map  $\psi$  is readily seen to admit an inverse. Note that the vertices of  $C$  and  $T$  are the same, except for the vertex  $x_0$ , and that the *graph distance* from  $x$  to any vertex  $v$  in  $C$  and the one between the corresponding vertices in  $T$  are the same. Given the equivalence between vertices, we will often use the same notion for equivalent vertices in  $C$  and  $T$ , that is, for  $v$  in  $C$  we will refer to the corresponding vertex in  $T$  as simply  $v$ . In Figure 7.6, we present an example of this construction.

Denote by  $d_G(x, y)$  the graph distance between two vertices  $x$  and  $y$  in the graph  $G$ . We introduce

$$V_k(T) := \{v \in T \mid d_T(x_0, v) = k+1\}, \quad (7.33)$$

as the set of vertices in  $T \in \mathcal{T}_m(N)$  with a graph distance of  $k+1$  from the root vertex  $x_0$ . Refining the notation

$$V_k(T) = \{v_{k,i} \mid i = 1, \dots, |V_k(T)|\}, \quad (7.34)$$

where  $v_{k,1} \equiv v_k$  is the distinguished vertex of the corresponding triangulation, defined in Section 7.2.1, and the remaining vertices  $v_{k,i}$  are labelled clockwise from  $v_{k,1}$ , for  $i = 2, \dots, |V_k(T)|$ . Finally, we define

$$V(T) := \bigcup_{k=1}^m V_k(T), \quad (7.35)$$

which is the vertex set of  $T$ , excluding the vertices  $x_0$  and  $x$ .

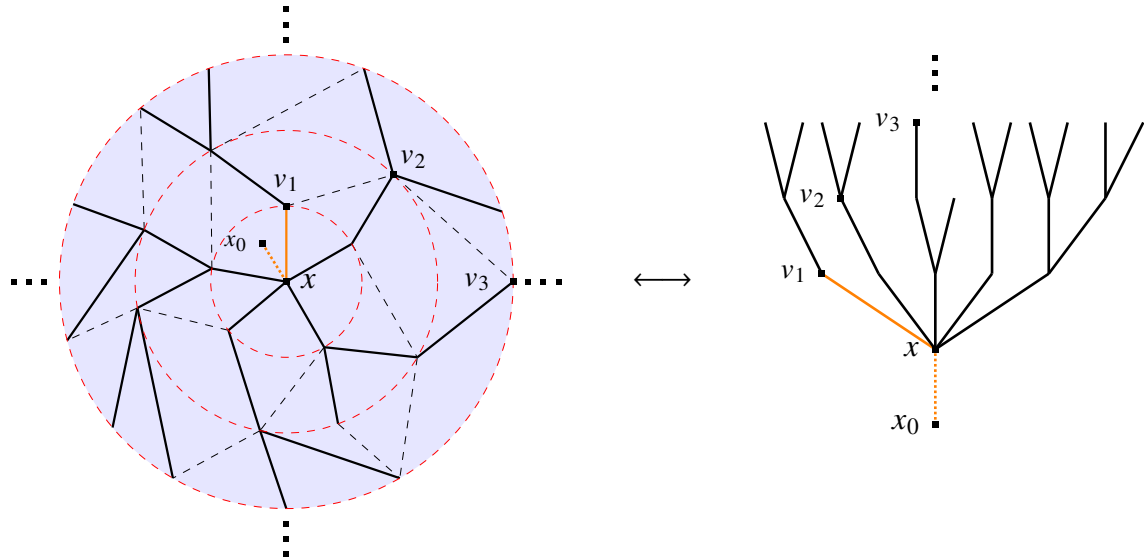


Figure 7.6: A causal triangulation of the disk  $C$  and the corresponding tree  $\psi(C)$ .

### 7.3.2 Loop models

In the following, we extend the correspondence (7.32) to a pair of correspondences applicable to the respective sets  $\mathcal{L}_m^{de}(N)$  and  $\mathcal{L}_m^{di}(N)$  of loop configurations. First, we define the sets of planar trees that correspond to the sets of loop configurations. Denote by  $\tilde{\mathcal{T}}_m(N)$  the set of height  $m+1$  planar trees with  $N$  vertices each of which, except for  $x_0$  and  $x$ , are assigned a binary label, here denoted by a 0 or 1, that is

$$\tilde{\mathcal{T}}_m(N) := \{(T, \delta) \mid T \in \mathcal{T}_m(N), \delta : V(T) \rightarrow \{0, 1\}\}, \quad (7.36)$$

and we denote by  $\tilde{\mathcal{T}}_m$  the corresponding set where we relax the constraint on the number of vertices. For each  $(T, \delta) \in \tilde{\mathcal{T}}_m(N)$ , we define the *labelling characteristics* at height  $k+1$

$$\boldsymbol{\delta}_k := (\delta(v_{k,1}), \dots, \delta(v_{k,|V_k(T)|})) \quad (7.37)$$

and the following summary statistics

$$\delta_k := \sum_{v \in V_k(T)} \delta(v), \quad |\delta| := \sum_{k=1}^m \delta_k, \quad (7.38)$$

where  $\delta_k$  counts the number of labels at each height  $k = 1, \dots, m$ , and  $|\delta|$  counts the total number of labels in  $(T, \delta) \in \tilde{\mathcal{T}}_m$ . We now define the set which is the subject of the latter correspondence

$$\tilde{\mathcal{T}}_m^{ev}(N) := \{(T, \delta) \mid T \in \mathcal{T}_m(N), \delta_k \in 2\mathbb{N}_0, k = 1, \dots, m\}, \quad (7.39)$$

and similarly, we denote by  $\tilde{\mathcal{T}}_m^{ev}$  the corresponding set where we relax the constraint on the number of vertices. In Proposition 7.3.5 below, we establish a bijective correspondence between  $\mathcal{L}_m^{de}(N)$  and  $\tilde{\mathcal{T}}_m(N)$ , while in Proposition 7.3.6, we establish a  $2^m$  to 1 correspondence between  $\mathcal{L}_m^{di}(N)$  and  $\tilde{\mathcal{T}}_m^{ev}(N)$ . In preparation for these statements, we introduce further notation and establish preliminary results about both dense and dilute loop configurations.

For each  $C \in C_m$ , we introduce the notation  $l_k \equiv |S_k|$  for  $k = 0, \dots, m$ , and refer to  $l_k$  and  $l_{k+1}$  as the *boundary lengths* of the annulus  $A_k$ . By applying a sequence of local flip operations

$$\begin{array}{c} \text{Diagram 1} \\ \leftrightarrow \\ \text{Diagram 2} \end{array} \quad (7.40)$$

one can transform an arbitrary triangulation of  $A_k$  into one of the form depicted in Figure 7.7, called a *standard triangulation*, with the same boundary lengths  $l_k$  and  $l_{k+1}$ , and distinguished vertices  $v_k$  and  $v_{k+1}$  for each  $k = 1, \dots, m$ . The details of this construction, where we restrict to  $k = 1, \dots, m$  throughout, are as follows. Any arbitrary triangulation  $T_{A_k}$  of  $A_k$  can be described as a sequence of forward- and backward-directed triangles, here denoted by  $f$ 's and  $b$ 's respectively, where the order is endowed from the distinguished vertex  $v_k$ . By construction, each sequence begins with a forward-directed triangle. Suppose the triangulation  $T_{A_k}$  is not standard, then there exists a  $bf$  in the sequence. Apply the flip operation to the first instance of  $bf$ , transforming it into an  $fb$ . Iterating this procedure, one transforms the original triangulation into a standard triangulation maintaining the same boundary lengths  $l_k$  and  $l_{k+1}$ , and distinguished vertices  $v_k$  and  $v_{k+1}$ .

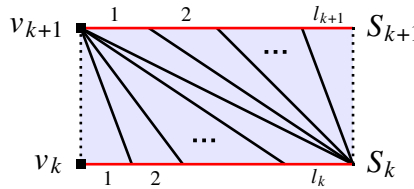


Figure 7.7: The standard triangulation of the annulus  $A_k$ . The left-most and right-most time-like edges are dashed to indicate that they are identified.

The flip operation in (7.40) is readily extended to a flip operation on the similar local components of a loop configuration on  $A_k$ . In the dense loop model, the extension is given by

$$\begin{array}{c} \text{Diagram 1} \\ \leftrightarrow \\ \text{Diagram 2} \end{array} \quad \begin{array}{c} \text{Diagram 1} \\ \leftrightarrow \\ \text{Diagram 2} \end{array} \quad \begin{array}{c} \text{Diagram 1} \\ \leftrightarrow \\ \text{Diagram 2} \end{array} \quad \begin{array}{c} \text{Diagram 1} \\ \leftrightarrow \\ \text{Diagram 2} \end{array} \quad \dots \quad (7.41)$$

In the dilute loop model, the extension is given by

$$\begin{array}{c} \text{Diagram 1} \\ \leftrightarrow \\ \text{Diagram 2} \end{array} \quad \begin{array}{c} \text{Diagram 1} \\ \leftrightarrow \\ \text{Diagram 2} \end{array} \quad \begin{array}{c} \text{Diagram 1} \\ \leftrightarrow \\ \text{Diagram 2} \end{array} \quad \begin{array}{c} \text{Diagram 1} \\ \leftrightarrow \\ \text{Diagram 2} \end{array} \quad \begin{array}{c} \text{Diagram 1} \\ \leftrightarrow \\ \text{Diagram 2} \end{array} \quad \begin{array}{c} \text{Diagram 1} \\ \leftrightarrow \\ \text{Diagram 2} \end{array} \quad \begin{array}{c} \text{Diagram 1} \\ \leftrightarrow \\ \text{Diagram 2} \end{array} \quad \begin{array}{c} \text{Diagram 1} \\ \leftrightarrow \\ \text{Diagram 2} \end{array} \quad \dots \quad (7.42)$$

We have the following result.

**Lemma 7.3.1.**

- (i) *The flip operations (7.41) and (7.42) applied to a dense, respectively dilute, loop configuration  $L$  on the disk, leave  $|L|$  and the positions of intersections invariant.*
- (ii) *The number of possible dense, respectively dilute, loop configurations on the triangulated annulus  $A_k$ , depend only on the boundary lengths  $l_k$  and  $l_{k+1}$ , not the details of the triangulation.*

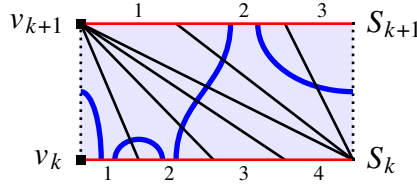


Figure 7.8: The unique dense loop configuration on the standard triangulation of  $A_k$  with intersection characteristics  $\mathbf{n}_k = (1, 1, 0, 0)$  and  $\mathbf{n}_{k+1} = (0, 1, 0)$ .

*Proof.* (i) As the flip operators (7.41) and (7.42) leave  $l_k$  and  $l_{k+1}$ , and the positions of intersections invariant at each layer, this extends to the whole loop configuration. (ii) Let  $T'$  and  $T$  be distinct disk triangulations of  $A_k$ , and enumerate all of the possible dense loop configurations on each. As the flip operations (7.41) are one-to-one, each loop configuration with an underlying triangulation  $T'$ , can be transformed into a unique loop configuration with an underlying triangulation  $T$ . Likewise with  $T$  and  $T'$  swapped. A similar procedure applies to dilute loop configurations where we instead use the flip operations (7.42).  $\square$

A dense or dilute loop configuration is not only characterised by the collection of boundary lengths  $l_k$  for  $k = 1, \dots, m$ , but also by the distribution of space-like edges which are intersected by loop segments. Accordingly, for each cycle  $S_k$  where  $k = 1, \dots, m$ , the intersection characteristics are encoded in the  $l_k$ -tuple

$$\mathbf{n}_k := (n_{k,1}, \dots, n_{k,l_k}) \in \{0, 1\}^{l_k}, \quad k = 1, \dots, m, \quad (7.43)$$

where  $n_{k,i}$  is 1 if the  $i^{\text{th}}$  space-like edge (labelled clockwise from  $v_k$ ) is intersected, and 0 otherwise. Associated with each  $\mathbf{n}_k$ , is the summary statistic

$$n_k := \sum_{i=1}^{l_k} n_{k,i}, \quad k = 1, \dots, m. \quad (7.44)$$

**Remark.** With notation as in Section 7.2, we have  $s_k(L) = 2n_k$  for  $L \in \mathcal{L}_m^{\text{de}}$ , while  $s_k(L) = n_k$  for  $L \in \mathcal{L}_m^{\text{di}}$ .

**Lemma 7.3.2.** *Let  $C_k$  be a triangulation of the annulus  $A_k$  with boundary lengths  $l_k$  and  $l_{k+1}$ , and let  $\mathbf{n}_k \in \{0, 1\}^{l_k}$  and  $\mathbf{n}_{k+1} \in \{0, 1\}^{l_{k+1}}$  denote intersection characteristics. Then,*

- (i)  *$C_k$  admits one dense loop configuration for each  $\mathbf{n}_k$  and  $\mathbf{n}_{k+1}$ ;*
- (ii)  *$C_k$  admits two, respectively zero, dilute loop configurations for each  $\mathbf{n}_k$  and  $\mathbf{n}_{k+1}$  if  $n_k + n_{k+1}$  is even, respectively odd.*

*Proof.* By Lemma 7.3.1, it suffices to consider the standard triangulation of  $A_k$ , which we proceed to do for both (i) and (ii).

(i) For the dense loop model, the entries of the intersection characteristics are in one-to-one correspondence with the loop decorations of the elementary triangles:

$$\begin{array}{c} \text{Diagram 1} \\ \text{Diagram 2} \end{array} \leftrightarrow n_{k+1,i} = 0, \quad \begin{array}{c} \text{Diagram 3} \\ \text{Diagram 4} \end{array} \leftrightarrow n_{k+1,i} = 1, \quad \begin{array}{c} \text{Diagram 5} \\ \text{Diagram 6} \end{array} \leftrightarrow n_{k,i} = 0, \quad \begin{array}{c} \text{Diagram 7} \\ \text{Diagram 8} \end{array} \leftrightarrow n_{k,i} = 1. \quad (7.45)$$

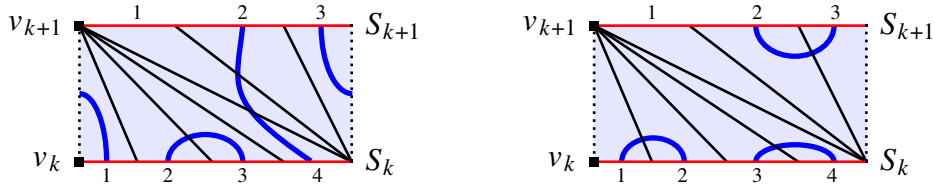


Figure 7.9: The two dilute loop configurations on the standard triangulation of  $A_k$  with intersection characteristics  $\mathbf{n}_k = (1, 1, 1, 1)$  and  $\mathbf{n}_{k+1} = (0, 1, 1)$ .

As there are no compatibility conditions along time-like edges, the claim readily follows in this case.

(ii) For the dilute loop model, the analogous correspondence is two-to-one:

$$\begin{aligned} \left\{ \begin{array}{c} \text{triangle} \\ \text{blue} \end{array}, \begin{array}{c} \text{triangle} \\ \text{red} \end{array} \right\} &\rightarrow n_{k+1,i} = 0, & \left\{ \begin{array}{c} \text{triangle} \\ \text{red} \end{array}, \begin{array}{c} \text{triangle} \\ \text{blue} \end{array} \right\} &\rightarrow n_{k+1,i} = 1, \\ \left\{ \begin{array}{c} \text{triangle} \\ \text{red} \end{array}, \begin{array}{c} \text{triangle} \\ \text{blue} \end{array} \right\} &\rightarrow n_{k,i} = 0, & \left\{ \begin{array}{c} \text{triangle} \\ \text{blue} \end{array}, \begin{array}{c} \text{triangle} \\ \text{red} \end{array} \right\} &\rightarrow n_{k,i} = 1. \end{aligned}$$

In this case, there exists a compatibility condition along time-like edges, that is, the time-like edge may be intersected or not. Consequently, there is a unique decoration for an elementary triangle for a given value of  $n_{k,i}$  or  $n_{k+1,i}$ , if the ‘intersectedness’ of the left (or right) time-like edge is known. Applying this argument successively to the standard triangulation of  $A_k$ , given the intersectedness of the left-most time-like edge connected to a forward-directed triangle (whose space-like edge is indexed by  $n_{k,1}$ ), the decorations of all forward-directed triangles are uniquely determined by the intersection characteristics  $\mathbf{n}_k$ . The intersectedness of the right-most time-like edge connected to a forward-directed triangle (whose space-like edge is indexed by  $n_{k,l_k}$ ) is the same as, respectively opposite to that of the left-most time-like edge if  $n_k$  is even, respectively odd. Repeating this argument, the decorations of all backward-directed triangles are uniquely determined by the intersection characteristics  $\mathbf{n}_{k+1}$ ; and the intersectedness of the right-most time-like edge connected to a back-directed triangle (whose space-like edge is indexed by  $n_{k+1,l_{k+1}}$ ) is the same as, respectively opposite to that of the left-most time-like edge connected to a forward-directed triangle if  $n_k + n_{k+1}$  is even, respectively odd. Given the periodic boundary conditions of the annulus, the intersectedness of the left- and right-most time-like edges must coincide, accordingly, there is no corresponding loop configuration when  $n_k + n_{k+1}$  is odd. On the other hand, for  $n_k + n_{k+1}$  even, the intersectedness of the left-most time-like edge of the annulus can take on both values, each giving rise to a distinct dilute loop configuration.  $\square$

As an example of Lemma 7.3.2, Figure 7.8 depicts the unique dense loop configuration on a standard triangulation  $A_k$  with intersection characteristics  $\mathbf{n}_k = (1, 1, 0, 0)$  and  $\mathbf{n}_{k+1} = (0, 1, 0)$ , while Figure 7.9, for the same triangulation, depicts the two dilute loop configurations with intersection characteristics  $\mathbf{n}_k = (1, 1, 1, 1)$  and  $\mathbf{n}_{k+1} = (0, 1, 1)$ .

The notion of intersection characteristics is readily extended from loop configurations on triangulated annuli to loop configurations on a triangulated disk of height  $m$  by reading off  $\mathbf{n}_k$  for each  $k = 1, \dots, m$ . Conversely, if the set of  $m$  tuples  $\mathbf{n}_k \in \{0, 1\}^{l_k}$  for each  $k = 1, \dots, m$ , correspond to at least one loop configuration on a triangulated annulus, we say that they form *admissible intersection characteristics*. It follows from Lemma 7.3.2 and the observation (7.26), that such a collection of

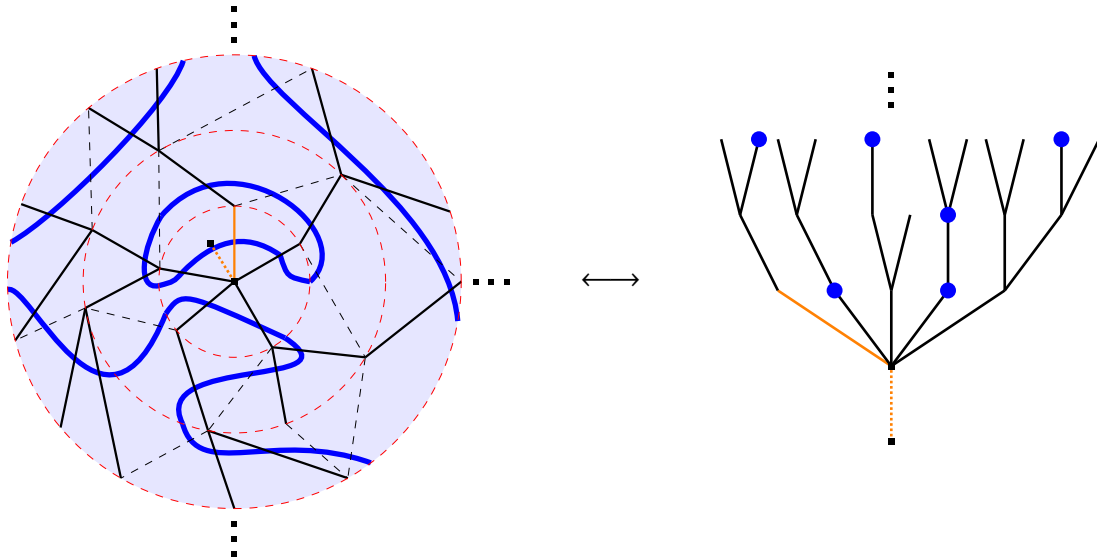


Figure 7.10: A dense loop configuration  $L$  and the corresponding labelled planar tree  $\tilde{\psi}(L)$ . Vertices labelled 1 are indicated with blue circles.

tuples always is admissible for dense loop configurations, while for dilute loop configurations, they are admissible if and only if  $n_k \in 2\mathbb{N}$  for all  $k = 1, \dots, m$ . We also note that, given a triangulation of the disk with admissible intersection characteristics, the choice of dilute loop configuration on any given triangulated annuli is independent of the choices made on the other triangulated annuli. This observation together with Lemma 7.3.2 and the proof thereof, we have the following two results.

**Lemma 7.3.3.** *A triangulation of the disk of height  $m$  with admissible intersection characteristics admits exactly one dense loop configuration and exactly  $2^m$  dilute loop configurations.*

**Corollary 7.3.4.**

- (i) *A triangulation of the cylinder with  $N$  vertices admits exactly  $2^N$  dense loop configurations, and exactly  $2^N$  dilute loop configurations.*
- (ii) *A triangulation of the disk with  $N$  vertices admits exactly  $2^{N-1}$  dense loop configurations, and exactly  $2^{N-1}$  dilute loop configurations. Thus,*

$$|\mathcal{L}_m^{de}(N)| = |\mathcal{L}_m^{di}(N)|, \quad m, N \in \mathbb{N}. \quad (7.46)$$

Remarkably, the parity constraint of dilute loop configurations is compensated by the factor of two arising at each layer in such a way that the number of dilute loop configurations coincides with the number of dense loop configurations.

The following proposition establishes the aforementioned correspondence between dense loop configurations and labelled planar trees. To illustrate, an example of this correspondence is presented in Figure 7.10, where tree vertices labelled by a 1 are indicated by a solid blue node.

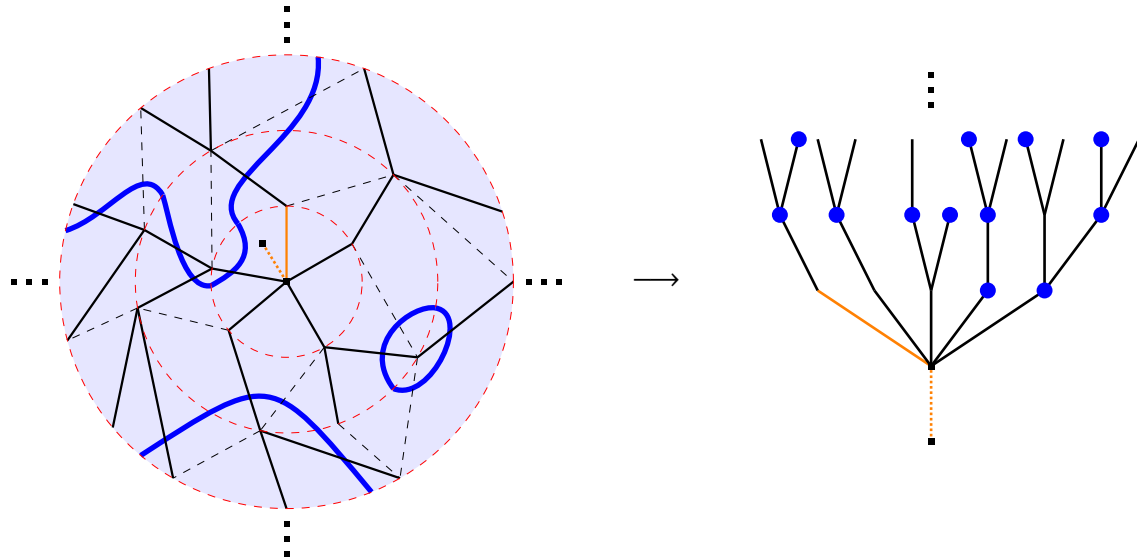


Figure 7.11: A dilute loop configuration  $L$  and the corresponding labelled planar tree  $\hat{\psi}(L)$ . Vertices labelled 1 are indicated with blue circles.

**Proposition 7.3.5.** *For each  $m \in \mathbb{N}_0$  and  $N \in \mathbb{N}$ , there is a bijective correspondence*

$$\tilde{\psi} : \mathcal{L}_m^{de}(N) \rightarrow \tilde{\mathcal{T}}_m(N) \quad (7.47)$$

*such that if  $(T, \delta) = \tilde{\psi}(L)$  then  $T = \psi(C)$ , where  $C$  is the triangulation underlying  $L$ . Moreover,  $|\delta| = s(L)/2$ .*

*Proof.* Inheriting the action of  $\psi$  from (7.32), to define the map  $\tilde{\psi}$  it suffices to define the map  $\delta$ , which acts in the following way: assign with a label 1 any vertex appearing to the left (viewed outwardly) of a space-like edge intersected by two arcs, and assign a label of 0 to all other vertices of  $V(T)$ . Here we highlight that the vertices  $x_0$  and  $x$  are not assigned any label. As the map  $\psi$  is bijective and, omitting  $x_0$ , the vertices of  $L \in \mathcal{L}_m^{de}(N)$  and  $T = \psi(C)$  coincide, the bijectivity of  $\tilde{\psi}$  follows from the fact that the intersection characteristics  $\mathbf{n}_k$  for  $k = 1, \dots, m$ , which (together with  $C$ ) uniquely describe  $L$  see Lemma 7.3.3, coincide with the labelling characteristics  $\boldsymbol{\delta}_k$  for  $k = 1, \dots, m$ , which (together with  $T$ ) uniquely describe  $(T, \delta)$  see the definition (7.36), that is  $\mathbf{n}_k = \boldsymbol{\delta}_k$  for all  $k = 1, \dots, m$ . The statement  $|\delta| = s(L)/2$  readily follows.  $\square$

The following is a counterpart to Proposition 7.3.5 for the dilute loop model, see Figure 7.11 for an example of this correspondence.

**Proposition 7.3.6.** *For each  $m \in \mathbb{N}_0$  and  $N \in \mathbb{N}$ , there is a  $2^m$  to 1 correspondence*

$$\hat{\psi} : \mathcal{L}_m^{di}(N) \rightarrow \tilde{\mathcal{T}}_m^{ev}(N) \quad (7.48)$$

*such that if  $(T, \delta) = \hat{\psi}(L)$  then  $T = \psi(C)$ , where  $C$  is the triangulation underlying  $L$ . Moreover,  $|\delta| = s(L)$ .*

*Proof.* Inheriting the action of  $\psi$  from (7.32), to define the map  $\hat{\psi}$  it suffices to define the map  $\delta$ , which acts in the following way: assign with a label 1 any vertex appearing to the left (viewed outwardly) of a space-like edge intersected by an arc, and assign a label of 0 to all other vertices of  $V(T)$ . Here we highlight that the vertices  $x_0$  and  $x$  are not assigned any label. As the map  $\psi$  is bijective and, omitting  $x_0$ , the vertices of  $L \in \mathcal{L}_m^{di}(N)$  and  $T = \psi(C)$  coincide, the  $2^m$  to 1 property of  $\hat{\psi}$  follows from the fact that the intersection characteristics  $\mathbf{n}_k$  for  $k = 1, \dots, m$ , which (together with  $C$ ) are consistent with  $2^m$  possible  $L$ 's see Lemma 7.3.3, coincide with the labelling characteristics  $\delta_k$  for  $k = 1, \dots, m$ , which (together with  $T$ ) uniquely describe  $(T, \delta)$  see the definition (7.36), that is  $\mathbf{n}_k = \delta_k$  for all  $k = 1, \dots, m$ . The statement  $|\delta| = s(L)$  readily follows.  $\square$

### 7.3.3 Partition functions

Motivated by the correspondences (7.32), (7.47) and (7.48), we define partition functions associated with the ensembles  $\mathcal{T}_m$ ,  $\tilde{\mathcal{T}}_m$  and  $\tilde{\mathcal{T}}_m^{ev}$  such that they can be related to those on causal triangulations defined in (7.10), (7.18) and (7.27) respectively. Accordingly, for a given element in each ensemble, we assign a weight of  $\alpha$  to all vertices labelled by a 1, and a weight of  $g$  to all edges except for  $\{x_0, x\}$ , and therefore have

$$W(g) := \sum_{m=0}^{\infty} W_m(g), \quad W_m(g) := \sum_{T \in \mathcal{T}_m} g^{|T|-1}, \quad (7.49)$$

$$W(g, \alpha) := \sum_{m=0}^{\infty} W_m(g, \alpha), \quad W_m(g, \alpha) := \sum_{(T, \delta) \in \tilde{\mathcal{T}}_m} g^{|T|-1} \alpha^{|\delta|}, \quad (7.50)$$

$$W^{ev}(g, \alpha) := \sum_{m=0}^{\infty} W_m^{ev}(g, \alpha), \quad W_m^{ev}(g, \alpha) := \sum_{(T, \delta) \in \tilde{\mathcal{T}}_m^{ev}} g^{|T|-1} \alpha^{|\delta|}, \quad (7.51)$$

where we highlight that  $W_0(g) = W_0(g, \alpha) = W_0^{ev}(g, \alpha) = 1$ . Following from Section 7.3.1 and the above construction, we have the relations between partition functions

$$Z(g) = W(g), \quad Z_m(g) = W_m(g). \quad (7.52)$$

Similarly, it follows from Proposition 7.3.5 and the above construction that we have the relations

$$Z^{de}(g, \alpha) = W(g, \alpha^2), \quad Z_m^{de}(g, \alpha) = W_m(g, \alpha^2). \quad (7.53)$$

Likewise, it follows from Proposition 7.3.6 that we have the relations

$$Z^{di}(g, \alpha) = \sum_{m=0}^{\infty} 2^m W_m^{ev}(g, \alpha), \quad Z_m^{di}(g, \alpha) = 2^m W_m^{ev}(g, \alpha). \quad (7.54)$$

Here we observe the  $2^m$  to 1 correspondence (7.48) manifesting in the partition functions (7.54). As we will see in the following sections, this will prove instrumental in influencing the critical behaviour of the dilute loop model.

## 7.4 Tree partition function analysis

In light of the relations (7.53) and (7.54), we analyse the partition functions  $W(g, \alpha)$  and  $W^{ev}(g, \alpha)$  as a means to determine the critical behaviour of the dense and dilute loop models. To further probe the dilute case, we consider a generalisation of the full partition function (7.51) which we refer to as the *height-coupled partition function*

$$W^{ev}(g, \alpha, k) := \sum_{m=0}^{\infty} k^m W_m^{ev}(g, \alpha), \quad (7.55)$$

where  $k > 0$  is an arbitrary height coupling, such that  $W^{ev}(g, \alpha)$  is recovered for  $k = 1$ , and  $Z^{di}(g, \alpha)$  is recovered for  $k = 2$ :

$$W^{ev}(g, \alpha) = W^{ev}(g, \alpha, 1), \quad Z^{di}(g, \alpha) = W^{ev}(g, \alpha, 2). \quad (7.56)$$

Throughout this section, we analyse  $W(g, \alpha)$ ,  $W^{ev}(g, \alpha)$  and  $W^{ev}(g, \alpha, k)$ , in Section 7.4.1 we specialise to  $\alpha = 0$  corresponding to unlabelled planar trees, while in Section 7.4.2 we relax this constraint and consider a label which takes values  $\alpha \in [0, 1)$ .

### 7.4.1 Planar trees

Under the specialisation  $\alpha = 0$ , we have the following relation between partition functions

$$W(g) = W(g, 0) = W^{ev}(g, 0) = W^{ev}(g, 0, 1). \quad (7.57)$$

In the following, using well-known arguments see e.g [101], the partition function  $W(g)$  can be determined in closed form.

**Lemma 7.4.1.** *The partition function  $W(g)$ , admits the recursion*

$$W(g) = \frac{1}{1 - gW(g)}, \quad (7.58)$$

whose solution is identified with

$$W(g) = \frac{1 - \sqrt{1 - 4g}}{2g}. \quad (7.59)$$

*Proof.* Each node of a tree in the ensemble  $\mathcal{T}$ , apart from the root, admits the possibility of arbitrarily many successive nodes. Formally,

$$\text{Diagram} = \dots + g \text{Diagram} + g^2 \text{Diagram} + g^3 \text{Diagram} + \dots \quad (7.60)$$

where the diagram  denotes the weighted ensemble of successive nodes and is equivalent to the partition function  $W(g)$ . Expressing (7.60) in terms  $W(g)$ , we have

$$W(g) = 1 + gW(g) + g^2W^2(g) + g^3W^3(g) + \dots = \sum_{k=0}^{\infty} g^k W^k(g) = \frac{1}{1 - gW(g)}. \quad (7.61)$$

Solving this recursion, we arrive at

$$W(g) = \frac{1 \pm \sqrt{1 - 4g}}{2g}. \quad (7.62)$$

Performing a power series expansion in  $g$  of (7.62), and comparing with the definition of  $W(g)$  (7.49), we disregard the positive solution and arrive at (7.59).  $\square$

We can immediately conclude that  $W(g)$  is analytic on the disk

$$\mathbb{D} := \{g \in \mathbb{C} \mid |g| < \frac{1}{4}\}, \quad (7.63)$$

with a square-root singularity at  $g_c = \frac{1}{4}$ , and we note that  $W(\frac{1}{4}) = 2$ .

Applying similar arguments, we can determine a closed-form expression for  $W_m(g)$  for all  $m \in \mathbb{N}_0$ . For each  $m \in \mathbb{N}_0$ , let  $X_m(g)$  denote the partition function for trees in  $\mathcal{T}$  of height at most  $m+1$ . By definition, it follows that

$$W_m(g) = X_m(g) - X_{m-1}(g), \quad (7.64)$$

where for convenience, we associate  $X_{-1}(g) \equiv 0$ . The following is a counterpart to Lemma 7.4.1 for  $X_m(g)$ .

**Lemma 7.4.2.** *For each  $m \in \mathbb{N}_0$ , the partition function  $X_m(g)$ , admits the recursion*

$$X_m(g) = \frac{1}{1 - gX_{m-1}(g)}, \quad (7.65)$$

whose solution is given by

$$X_m(g) = \frac{U_m(\frac{1}{2\sqrt{g}})}{\sqrt{g} U_{m+1}(\frac{1}{2\sqrt{g}})}, \quad (7.66)$$

where  $U_n(x)$  is the  $n^{\text{th}}$  Chebyshev polynomial of the section kind (with  $U_{-1}(x) \equiv 0$ ).

*Proof.* The analogous observation to (7.60) for ensembles of trees of height at most  $m$  is given by

$$\begin{array}{c} m \\ \diagdown \quad \diagup \\ \bullet \quad \bullet \end{array} = 1 + g \begin{array}{c} m-1 \\ \bullet \end{array} + g^2 \begin{array}{c} m-1 \\ \bullet \quad \bullet \\ \diagdown \quad \diagup \\ \bullet \end{array} + g^3 \begin{array}{c} m-1 \\ \bullet \quad \bullet \\ \diagdown \quad \diagup \\ \bullet \quad \bullet \\ \diagdown \quad \diagup \\ \bullet \end{array} + \dots \quad (7.67)$$

where the diagram  $\begin{array}{c} m \\ \diagdown \quad \diagup \\ \bullet \quad \bullet \end{array}$  denotes the weighted ensemble of successive nodes up to a height  $m$  and is equivalent to the partition function  $X_m(g)$ . Expressing (7.67) in terms of  $X_m(g)$  and  $X_{m-1}(g)$ , we have

$$X_m(g) = 1 + gX_{m-1}(g) + g^2X_{m-1}^2(g) + g^3X_{m-1}^3(g) + \dots = \sum_{k=0}^{\infty} g^k X_{m-1}^k(g) = \frac{1}{1 - gX_{m-1}(g)}. \quad (7.68)$$

By direct computation, we see that (7.66) solves the recursion above.  $\square$

Applying the closed-form expression of  $X_m(g)$  to (7.64), we arrive at

$$W_m(g) = \frac{1}{\sqrt{g} U_m(\frac{1}{2\sqrt{g}}) U_{m+1}(\frac{1}{2\sqrt{g}})} \quad (7.69)$$

and since

$$U_n(x) = 2^n \prod_{j=1}^n \left( x - \cos\left(\frac{j\pi}{n+1}\right) \right), \quad (7.70)$$

the partition functions  $W_m(g)$  and  $X_m(g)$  are analytic on the disk

$$\mathbb{D}_m := \{g \in \mathbb{C} \mid |g| < g_m\}, \quad g_m := \frac{1}{4} \left( 1 + \tan^2\left(\frac{\pi}{m+2}\right) \right), \quad (7.71)$$

both with a simple pole at  $g_m$ .

Under the specialisation of the height-coupled partition function where  $\alpha = 0$ , we have

$$W^{ev}(g, 0, k) := \sum_{m=0}^{\infty} k^m W_m(g) \quad (7.72)$$

and can therefore apply the above insights to analyse this partition function. As the coefficients defining  $W_m(g)$  as a power series in  $g$  are nonnegative, it follows that  $W_m(g)$  is divergent for  $g > g_m$ . Observing that  $g_m \rightarrow \frac{1}{4}$  as  $m \rightarrow \infty$ , it follows that  $W^{ev}(g, 0, k)$  diverges for all  $g > \frac{1}{4}$  and  $k > 0$ . We therefore conclude that the radius of convergence  $g_c(k)$  of  $W^{ev}(g, 0, k)$  for fixed  $k$  is at most  $\frac{1}{4}$  for any  $k > 0$ . In the following, we refine this bound, culminating in Proposition 7.4.5 below.

**Lemma 7.4.3.** *For  $g \in (0, \frac{1}{4})$  and  $m \in \mathbb{N}$ , we have*

$$\frac{\phi(W(g) - 1)^2}{W(g)} (W(g) - 1)^m < W_m(g) < (W(g) - 1)^m \quad (7.73)$$

where  $\phi$  is Euler's function.

*Proof.* When unlikely to cause confusion, we omit the arguments of a given function. Let us first establish the upper bound. Applying the recursion relation (7.65) to (7.64), we have

$$W_m = X_m - X_{m-1} = \frac{g(X_{m-1} - X_{m-2})}{(1 - gX_{m-1})(1 - gX_{m-2})} = g(X_{m-1} - X_{m-2})X_m X_{m-1}. \quad (7.74)$$

Iteratively applying this expression for  $m \in \mathbb{N}$ , we have

$$W_m = g^m X_m \prod_{i=1}^{m-1} X_i^2, \quad (7.75)$$

where we recall  $X_{-1}(g) \equiv 0$ . By definition for  $i \in \mathbb{N}$ , we have  $1 < X_i < W$ , hence  $\frac{X_i}{W} < 1$ , therefore by applying (7.58) to (7.75), we have

$$W_m = g^m W^{2m-2} X_m \prod_{i=1}^{m-1} \left( \frac{X_i}{W} \right)^2 = (W-1)^m \frac{X_m}{W^2} \prod_{i=1}^{m-1} \left( \frac{X_i}{W} \right)^2 < (W-1)^m, \quad (7.76)$$

establishing the upper bound.

Now for the lower bound, applying (7.58) we have

$$W - X_m = \frac{W - 1 - gWX_{m-1}}{1 - gX_{m-1}} = gW(W - X_{m-1})X_m. \quad (7.77)$$

Iteratively applying this expression for  $m \in \mathbb{N}$ , we have

$$W - X_m = g^m W^m (W - 1) \prod_{i=1}^m X_i. \quad (7.78)$$

Now, using  $\frac{X_i}{W} < 1$ ,  $1 < W < 2$  and (7.58), we have

$$W - X_m = g^m W^{2m} (W - 1) \prod_{i=1}^m \frac{X_i}{W} = (W - 1)^m (W - 1) \prod_{i=1}^m \frac{X_i}{W} < (W - 1)^m. \quad (7.79)$$

It follows that

$$\frac{X_i}{W} = 1 - \frac{W - X_i}{W} > 1 - \frac{(W - 1)^i}{W} > 1 - (W - 1)^i, \quad (7.80)$$

and since  $0 < W - 1 < 1$ , we have

$$\prod_{i=1}^m (1 - (W - 1)^i) > \prod_{i=1}^{\infty} (1 - (W - 1)^i) = \phi(W - 1). \quad (7.81)$$

Finally, applying (7.80) and (7.81) to (7.75), we have

$$W_m = \frac{g^m W^{2m}}{X_m} \prod_{i=1}^m \left( \frac{X_i}{W} \right)^2 = \frac{(W - 1)^m}{X_m} \prod_{i=1}^m \left( \frac{X_i}{W} \right)^2 > \frac{\phi(W - 1)^2}{W} (W - 1)^m, \quad (7.82)$$

thereby establishing the lower bound.  $\square$

The corollary immediately follows.

**Corollary 7.4.4.** *For  $k > 0$  and  $g \in (0, \frac{1}{4})$ , we have*

$$\frac{\phi(W(g) - 1)^2}{W(g)} \sum_{m=0}^{\infty} (k(W(g) - 1))^m \leq W^{ev}(g, 0, k) \leq \sum_{m=0}^{\infty} (k(W(g) - 1))^m. \quad (7.83)$$

Finally, we arrive at the proposition below.

**Proposition 7.4.5.** *The critical coupling of  $W^{ev}(g, 0, k)$  is given by*

$$g_c(k) = \begin{cases} \frac{1}{4}, & k \in (0, 1] \\ \frac{k}{(k+1)^2}, & k \in (1, \infty) \end{cases} \quad (7.84)$$

*Proof.* As identified above,  $g_c(k) \leq \frac{1}{4}$ . For  $k \in (0, 1]$ , we have  $W^{ev}(g, 0, k) \leq W(g)$ , consequently  $g_c(k) = \frac{1}{4}$ . While for  $k \in (1, \infty)$ , it follows from Corollary 7.4.4 that  $W^{ev}(g, 0, k)$  is finite if and only if

$$k(W(g) - 1) < 1. \quad (7.85)$$

Solving for  $g_c$  such that  $k(W(g_c) - 1) = 1$ , we arrive at the desired result.  $\square$

### 7.4.2 Labelled planar trees

We now consider a non-trivial labelling, with the associated coupling  $\alpha$  taking values in  $(0, 1]$ . Summing over the labels  $\delta$  of  $W_m(g, \alpha)$  in (7.50), we can express this partition function in terms of  $W_m(g)$ , as follows

$$W_m(g, \alpha) = \sum_{T \in \mathcal{T}_m} (g(1+\alpha))^{|T|-1} = W_m(g(1+\alpha)), \quad (7.86)$$

similarly for the full partition function

$$W(g, \alpha) = W(g(1+\alpha)). \quad (7.87)$$

Applying results from the previous section, we can immediately identify the critical coupling of  $W(g, \alpha)$  as  $g = \frac{1}{4(1+\alpha)}$ .

Likewise, summing over the labels  $\delta$  of  $W_m^{ev}(g, \alpha)$  in (7.51), we have

$$W_m^{ev}(g, \alpha) = \sum_{T \in \mathcal{T}_m} g^{|T|-1} \prod_{i=1}^m \frac{1}{2} [(1+\alpha)^{n_i} + (1-\alpha)^{n_i}], \quad (7.88)$$

where  $n_i(T) = |V_i(T)|$  denotes the number of vertices in  $T$  at height  $i+1$ . Unlike for the partition function  $W_m(g, \alpha)$ , we do not have an explicit closed-form expression for  $W_m^{ev}(g, \alpha)$ . To understand the critical behaviour of this partition function, we instead bound it by functions whose critical behaviour is known. We first observe that for  $\alpha \in (0, 1]$  and  $n \in \mathbb{N}$ , we have

$$(1+\alpha)^n \leq (1+\alpha)^n + (1-\alpha)^n \leq 2(1+\alpha)^{n-1}, \quad (7.89)$$

which together with

$$\sum_{i=1}^m n_i = |T| - 1, \quad T \in \mathcal{T}_m, \quad (7.90)$$

allows us to bound the partition function  $W^{ev}(g, \alpha, k)$ , as follows

$$W^{ev}(g(1+\alpha), 0, \frac{k}{2}) \leq W^{ev}(g, \alpha, k) \leq W^{ev}(g(1+\alpha), 0, \frac{k}{1+\alpha}). \quad (7.91)$$

As will be demonstrated in Section 7.5.3, this bound will prove instrumental in analysing the critical behaviour of  $Z^{di}(g, \alpha)$ .

## 7.5 Critical behaviour of loop models

In this section, we bring to bear prior analysis to determine the critical behaviour of the pure CDT model (Section 7.5.1), the dense loop model (Section 7.5.2) and the dilute loop model (Section 7.5.3). In each case, we show how the largest eigenvalue of the transfer matrix determines the critical behaviour of the model. For the dilute loop model, where a closed-form expression of the partition function is elusive, these techniques prove essential.

### 7.5.1 Pure CDT model

While much is known about the critical behaviour and large-scale structure of the pure CDT model, we begin here to outline, in the simplest case, methods that will be applied in the analysis of both loop models. These techniques naturally divide into two approaches based upon the object of study (i) the closed-form expression of the partition function  $Z(g)$ , and (ii) the transfer matrix  $T(g)$ . While (i) is indeed the most powerful, it is only applicable in the case of the dense loop model, whereas (ii) can be analysed for both loop models.

First, we recall the results [82, 99] on the analysis of the pure CDT partition function. It follows from (7.52) and (7.59) that  $Z(g)$  can be written explicitly as

$$Z(g) = \frac{1 - \sqrt{1 - 4g}}{2g}. \quad (7.92)$$

We can immediately read off the critical coupling of the pure CDT model denoted by  $g_c$ , and determine the associated value of the partition function  $Z_c := Z(g_c)$ , as

$$g_c = \frac{1}{4}, \quad Z_c = 2. \quad (7.93)$$

Furthermore, the behaviour of  $Z(g)$  near the critical point is given by

$$Z(g) \sim Z_c - 4\sqrt{g_c - g}. \quad (7.94)$$

Examining the large-scale structure of the pure CDT model, we consider a limiting distribution of infinite size (or radius) causal triangulations, the precise definition of which is given in [82], and determine the associated *Hausdorff dimension* of such configurations. For a given  $C$  in this distribution with central vertex  $x$ , the ball of radius  $R$  around  $x$  is defined as

$$B(x, R) := \{v \in V(C) \mid d_C(x, v) \leq R\}, \quad (7.95)$$

where  $d_C$  denotes the graph distance on  $C$ . We can now define the Hausdorff dimension as the polynomial growth rate of the number of vertices  $|B(x, R)|$ , as a function of  $R$ :

$$d_H(C) := \lim_{R \rightarrow \infty} \frac{\ln |B(x, R)|}{\ln R}, \quad (7.96)$$

where the limit must exist. For the pure CDT model, by making use of the closed-form expression of the partition function (7.92) and the associated behaviour about the critical point, it was shown in [82] that the Hausdorff dimension is given by

$$d_H = 2 \quad (\text{almost surely}). \quad (7.97)$$

We now pivot to analyse the transfer matrix  $T(g)$ . Here unlike above, the techniques are novel and contrast those presented in [99], as we do not rely on the explicit determination of the transfer matrix eigenvalues. First observe that the transfer matrix is *symmetrisable*, admitting a factorisation in terms of a diagonal matrix  $D$  and a symmetric matrix  $K(g)$

$$T(g) = DK(g), \quad (7.98)$$

whose elements are given by

$$D_{r,s} := \frac{\delta_{r,s}}{r}, \quad K_{r,s}(g) := \frac{(r+s-1)!}{(r-1)!(s-1)!} g^{\frac{r+s}{2}}. \quad (7.99)$$

In light of this factorisation, it is convenient to analyse the symmetric operator  $K(g)$  and translate these results to the transfer matrix.

**Proposition 7.5.1.** *The operator  $K(g)$  is trace-class for  $g \in \mathbb{D}$ , positive definite for  $g \in (0, \frac{1}{4})$ , and the operator valued function  $h \mapsto K(h^2)$  is analytic on  $\{h \in \mathbb{C} \mid |h| < \frac{1}{2}\}$ .*

*Proof.* We first note that for fixed  $s$ , we have  $(K_{r,s}(g))_{r \in \mathbb{N}} \in l_2(\mathbb{N})$  for  $|g| < 1$ . Denote by  $V$  the dense subspace of sequences with finitely many non-vanishing entries, then  $K(g)$  is well defined on  $V$  for  $|g| < 1$ . For each  $n \in \mathbb{N}$ , let  $\mathcal{P}_n$  denote the orthogonal idempotent acting on  $l_2(\mathbb{N})$  that projects onto the subspace spanned by vectors  $|w\rangle$  whose entries  $w_r$  vanish for  $r > n$ . By construction, the operator  $K_n(g) := \mathcal{P}_n K(g) \mathcal{P}_n$  is of finite rank and is bounded on  $l_2(\mathbb{N})$ , with matrix elements

$$(K_n(g))_{r,s} = \begin{cases} K_{r,s}(g), & r, s \leq n, \\ 0, & \text{otherwise.} \end{cases} \quad (7.100)$$

It is also positive semi-definite for  $g \in [0, 1)$  as

$$\frac{(r+s-1)!}{(r-1)!(s-1)!} = \sum_{k=1}^{\infty} k \binom{s}{k} \binom{r}{k} \quad \text{implies} \quad \langle w | K_n(g) | w \rangle = \sum_{k=1}^n k \left| \sum_{s=k}^n \binom{s}{k} w_s g^{\frac{s}{2}} \right|^2 \geq 0. \quad (7.101)$$

With the corresponding trace norm given by

$$\|K_n(g)\|_1 = \text{tr } K_n(g) = \sum_{s=1}^n \sum_{k=1}^s s \binom{s}{k} \binom{s-1}{k-1} g^s \leq \sum_{s=1}^{\infty} s \binom{2s-1}{s} g^s = \frac{g}{(1-4g)^{\frac{3}{2}}}, \quad (7.102)$$

where the last equality holds for  $g \in (0, \frac{1}{4})$ . It follows that the operator norms  $\|K_n(g)\|$  are uniformly bounded in  $n$  for any fixed  $g \in [0, \frac{1}{4})$ . Having established these basic results, we proceed by establishing the claims about  $K(g)$  by considering  $K_n(g)$  and the limit  $n \rightarrow \infty$ .

We first note that since  $\lim_{n \rightarrow \infty} \langle v | K_n(g) | w \rangle = \langle v | K(g) | w \rangle$  for all  $v, w \in V$ , it follows that  $K(g)$  extends to a bounded operator on  $l_2(\mathbb{N})$  equal to the weak limit of  $(K_n(g))_{n \in \mathbb{N}}$  for  $g \in [0, \frac{1}{4})$ . It follows from (7.102) and Theorem 10 in Section 2.4 of [102] that  $K(g)$  is trace-class for  $g \in (0, \frac{1}{4})$ , with trace norm

$$\|K(g)\|_1 = \text{tr } K(g) = \frac{g}{(1-4g)^{\frac{3}{2}}}. \quad (7.103)$$

Extending the trace-class domain to all of  $\mathbb{D}$ , let  $g \in \mathbb{D}$  be arbitrary and parameterise by  $g = |g|e^{i\theta}$  where  $\theta \in \mathbb{R}$ , we can therefore write

$$K(g) = U(\theta) K(|g|) U(\theta), \quad (7.104)$$

where  $U(\theta)$  is a diagonal and unitary operator with matrix elements

$$U_{r,s}(\theta) = e^{\frac{ir\theta}{2}} \delta_{r,s}. \quad (7.105)$$

It follows that  $K(g)$  is well-defined and trace-class for all  $g \in \mathbb{D}$ , with

$$\|K(g)\|_1 = \text{tr}|K(g)| = \|K(|g|)\|_1. \quad (7.106)$$

As  $g \mapsto \langle v|K(g)|w \rangle$  is analytic for  $g \in \mathbb{D}$  and all  $v, w \in V$ , the operator  $K(g)$  is also analytic on  $\mathbb{D}$  as a function of  $g^{\frac{1}{2}}$ , in the sense of Kato (see [7] Section XII.2).

Finally, we establish positivity. Taking the limit  $n \rightarrow \infty$  in (7.101), it follows that  $\langle w|K(g)|w \rangle$  is zero if and only if

$$\sum_{s=k}^{\infty} \binom{s}{k} w_s g^{\frac{s}{2}} = 0, \quad (7.107)$$

for all  $k \in \mathbb{N}$ . We note that this sum is convergent for  $|g| < 1$  and

$$\sum_{s=k}^{\infty} \binom{s}{k} w_s g^{\frac{s}{2}} = \frac{g^{\frac{k}{2}}}{k!} f^{(k)}(g^{\frac{1}{2}}), \quad f(z) := \sum_{s=1}^{\infty} w_s z^s \quad (7.108)$$

where  $f^{(k)}(z)$  denotes the  $k^{\text{th}}$  derivative of the function  $f(z)$ . Accordingly, for  $g \neq 0$  the expression  $\langle w|K(g)|w \rangle$  is zero if and only if  $f(z) = 0$ , i.e.  $w_s = 0$  for all  $s \in \mathbb{N}$ . It follows that  $K(g)$  is positive definite for  $g \in (0, \frac{1}{4})$ .  $\square$

As the diagonal operator  $D$  is bounded, it follows that the transfer operator  $T(g)$  is trace-class for  $g \in (0, \frac{1}{4})$  with trace given by

$$\text{tr}(T(g)) = \frac{1 - \sqrt{1 - 4g}}{2\sqrt{1 - 4g}}. \quad (7.109)$$

Moreover, since the matrix elements of  $K(g)$  are positive for  $g \in (0, \frac{1}{4})$ , it thus follows from the Perron–Frobenius theorem (see e.g. Theorem XIII.43 [7]) that  $K(g)$  has a positive largest eigenvalue equal to the operator norm  $\|K(g)\|$ , and the corresponding normalised eigenvector has strictly positive entries. Applying the Kato–Rellich theorem (see e.g. Theorem XII.8 [7]), this largest eigenvalue is an analytic function for  $g \in (0, \frac{1}{4})$ , and up to a phase, the entries of the corresponding normalised eigenvector are analytic functions for  $g \in (0, \frac{1}{4})$ . As  $D$  is diagonal and positive definite, these statements are also true of the positive definite operator  $D^{\frac{1}{2}}K(g)D^{\frac{1}{2}}$ .

We now define the *time-periodic partition functions* as

$$Z_m^{per}(g) := \text{tr}(T(g)^{m-1}), \quad m \geq 2, \quad (7.110)$$

which can be interpreted as summing over triangulations of a *cylinder* of height  $(m-1)$  whose boundary cycles  $S_1$  and  $S_m$  are identified (i.e.  $S_1 \equiv S_m$ ), and a weight of  $g$  is assigned to each space-like edge. Equivalently, a weight of  $g^{\frac{1}{2}}$  may be assigned to each elementary triangle.

Relating the partition functions  $Z_m(g)$  and  $Z_{m+1}^{per}(g)$ , we first observe that the trace of a positive definite trace-class operator  $O$  is equal to the sum of its eigenvalues [102], accordingly  $\text{tr}(O^n) \leq (\text{tr } O)^n$  for all  $n \in \mathbb{N}$ . As  $D^{\frac{1}{2}}K(g)D^{\frac{1}{2}}$  is positive definite, we have

$$Z_m^{per} \leq (\text{tr } T(g))^{m-1}. \quad (7.111)$$

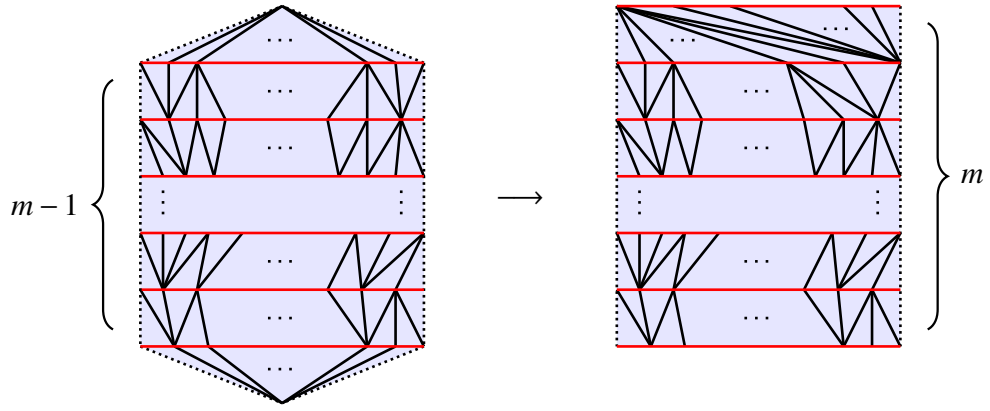


Figure 7.12: A triangulation contributing to  $Z_m(g)$  on the left, and the corresponding contribution to  $Z_{m+1}^{per}(g)$  on the right. In both diagrams, the left-most and right-most dashed edges are identified. In the right-most diagram, the bottom and top space-like edges are identified i.e.  $S_1 \equiv S_{m+1}$ .

**Lemma 7.5.2.** *For each  $m \in \mathbb{N}$  and  $g \in [0, \frac{1}{4})$ , we have*

$$Z_m(g) \leq Z_{m+1}^{per}(g). \quad (7.112)$$

*Proof.* Let  $C$  denote a causal triangulation of the sphere contributing to the partition function  $Z_m(g)$ . Each height  $m$  spherical triangulation  $C$  can be transformed into a unique *time-periodic* triangulation  $C'$  of height  $m+1$  contributing to the partition function  $Z_{m+1}^{per}(g)$ . This construction is as follows: (i) remove the  $|S_1|$  backward-directed triangles with space-like edges in  $S_1$ , (ii) place them to the right (viewed outwardly) of the  $|S_m|$  forward-directed triangles with space-like edges in  $S_m$  such that the right-most forward-directed triangle shares a time-like edge with the left-most backward-directed triangle thereby introducing a new annulus  $A_n$  with a standard triangulation between cycles  $S_n$  and  $S_{n+1}$ , and (iii) identify the new outer cycle  $S_{m+1}$  with the initial cycle  $S_1$ . See Figure 7.12 for an illustration.

As the triangle number is conserved under the map taking  $C$  to  $C'$ , both  $C$  and  $C'$  contribute the same weight to their respective partition functions. Furthermore, we note that this same map is injective but not surjective, as  $A_n$  of  $C'$  is restricted to be a standard triangulation. Together, these two facts establish the inequality.  $\square$

Exploiting the cyclicity of the trace, the partition function  $Z_m^{per}(g)$  can be expressed as

$$Z_m^{per}(g) = \text{tr}((D^{\frac{1}{2}}K(g)D^{\frac{1}{2}})^{m-1}), \quad m \geq 2. \quad (7.113)$$

Ultimately, we will use properties of the operator  $D^{\frac{1}{2}}K(g)D^{\frac{1}{2}}$  to understand the critical behaviour of  $Z_{m+1}^{per}(g)$  and hence  $Z_m(g)$ . The following proposition determines how the largest eigenvalue behaves as  $g$  approaches the critical coupling.

**Proposition 7.5.3.** *The largest eigenvalue  $\lambda_1(g)$  of  $D^{\frac{1}{2}}K(g)D^{\frac{1}{2}}$  satisfies*

$$\lambda_1(g) \nearrow 1 \quad \text{as} \quad g \nearrow \frac{1}{4}. \quad (7.114)$$

*Proof.* Note that all matrix elements of  $D^{\frac{1}{2}}K(g)D^{\frac{1}{2}}$  are strictly increasing functions of  $g$ . It follows from the variational principle (see Theorem XIII.1 in [7]), that  $\lambda_1(g)$  is strictly increasing for  $g \in (0, \frac{1}{4})$ . Again, we suppress arguments of functions when unlikely to cause confusion.

First, suppose that  $\lambda_1 \leq c_1$  where  $c_1 < 1$ . Consequently,  $(1 - kD^{\frac{1}{2}}KD^{\frac{1}{2}})^{-1}$  is a bounded operator for  $k \in [1, c_1^{-1})$  and we have

$$\sum_{m=1}^{\infty} k^m Z_{m+1}^{per}(g) = \sum_{m=1}^{\infty} \text{tr}((kD^{\frac{1}{2}}KD^{\frac{1}{2}})^m) = \text{tr}\left(\frac{kD^{\frac{1}{2}}KD^{\frac{1}{2}}}{1 - kD^{\frac{1}{2}}KD^{\frac{1}{2}}}\right) \leq k \left\| \frac{1}{1 - kD^{\frac{1}{2}}KD^{\frac{1}{2}}} \right\| \text{tr}(T) < \infty, \quad (7.115)$$

for all  $g \in (0, \frac{1}{4})$ . It follows from Lemma 7.5.2 that

$$W^{ev}(g, 0, k) = 1 + \sum_{m=1}^{\infty} k^m Z_m(g) < \infty, \quad g \in (0, \frac{1}{4}), \quad (7.116)$$

in contradiction to Proposition 7.4.5, which states that the critical coupling for  $W^{ev}(g, 0, k)$  satisfies  $g_c(k) < \frac{1}{4}$  for  $k > 1$ . Therefore  $\lim_{g \nearrow \frac{1}{4}} \lambda_1(g) \geq 1$ .

Now, suppose that  $\lambda_1 \geq c_1$  where  $c_1 > 1$ . It follows that there exists a  $g_0 < \frac{1}{4}$  such that  $\lambda_1(g_0) = 1$ . Denote by  $\lambda_1 > \lambda_2 \geq \lambda_3 \geq \dots$  the eigenvalues, and by  $\{|w^{(n)}\rangle |n \in \mathbb{N}\}$  the corresponding set of eigenvectors of the operator  $D^{\frac{1}{2}}KD^{\frac{1}{2}}$ . In particular,  $|w^{(1)}\rangle$  has been normalised such that it is analytic and has positive coordinates in an interval  $I$  about  $g_0$ . For a sufficiently small  $I$ , there exists a constant  $c > 0$ , such that

$$\langle v | D^{\frac{1}{2}} | w^{(1)} \rangle \langle w^{(1)} | D^{-\frac{1}{2}} | v \rangle \geq c, \quad (7.117)$$

for  $g \in I$ . Let us now consider  $Z(g)$  for  $g < g_0$ , we have

$$Z(g) - 1 = \sum_{m=1}^{\infty} \langle v | D^{\frac{1}{2}} (D^{\frac{1}{2}}KD^{\frac{1}{2}})^{m-1} D^{-\frac{1}{2}} | v \rangle \quad (7.118)$$

$$= \sum_{m,n=1}^{\infty} \langle v | D^{\frac{1}{2}} (D^{\frac{1}{2}}KD^{\frac{1}{2}})^{m-1} | w^{(n)} \rangle \langle w^{(n)} | D^{-\frac{1}{2}} | v \rangle \quad (7.119)$$

$$= \langle v | D^{\frac{1}{2}} | w^{(1)} \rangle \langle w^{(1)} | D^{-\frac{1}{2}} | v \rangle \sum_{m=1}^{\infty} \lambda_1^{m-1} + \sum_{m=1}^{\infty} \sum_{n=2}^{\infty} \lambda_n^{m-1} \langle v | D^{\frac{1}{2}} | w^{(n)} \rangle \langle w^{(n)} | D^{-\frac{1}{2}} | v \rangle \quad (7.120)$$

$$\geq \frac{c}{1 - \lambda_1} + \sum_{n=2}^{\infty} \frac{\langle v | D^{\frac{1}{2}} | w^{(n)} \rangle \langle w^{(n)} | D^{-\frac{1}{2}} | v \rangle}{1 - \lambda_n} \quad (7.121)$$

and it follows that

$$Z(g) \geq 1 + \frac{c}{1 - \lambda_1} - \sum_{n=2}^{\infty} \frac{|\langle v | D^{\frac{1}{2}} | w^{(n)} \rangle \langle w^{(n)} | D^{-\frac{1}{2}} | v \rangle|}{1 - \lambda_n} \geq 1 + \frac{c}{1 - \lambda_1} - \frac{\|D^{\frac{1}{2}}v\| \|D^{-\frac{1}{2}}v\|}{1 - \lambda_2}. \quad (7.122)$$

Note that while  $D^{-\frac{1}{2}}$  is unbounded,  $D^{-\frac{1}{2}}v \in l_2(\mathbb{N})$ , as the entries of  $v(g)$  decay exponentially. It follows from (7.122) that  $Z(g)$  diverges as  $g \nearrow g_0$ , which contradicts the fact that  $Z(g)$  is analytic for  $g \in \mathbb{D}$ . This contradiction, together with the previous contradiction, serves to show  $\lim_{g \nearrow \frac{1}{4}} \lambda_1(g) = 1$ .  $\square$

This concludes the analysis of the pure CDT model, in the following sections, we apply these techniques to the novel settings of the dense loop model and the dilute loop model.

### 7.5.2 Dense loop model

As we will see in this section, the critical behaviour and large-scale structure of the dense loop model are identical to the pure CDT model up to a simple shift in the coupling. Beginning with the partition function, it follows from (7.53), (7.59) and (7.87), that we have

$$Z^{de}(g, \alpha) = W(g(1+\alpha^2)) = \frac{1 - \sqrt{1 - 4g(1+\alpha^2)}}{2g(1+\alpha^2)}. \quad (7.123)$$

We can immediately read off the critical coupling of the dense loop model denoted by  $g_c^{de}(\alpha)$ , and determine the associated value of the partition function  $Z_c^{de}(\alpha) := Z^{de}(g_c^{de}(\alpha), \alpha)$ , as

$$g_c^{de}(\alpha) = \frac{1}{4(1+\alpha^2)}, \quad Z_c^{de}(\alpha) = 2. \quad (7.124)$$

Furthermore, the behaviour of  $Z^{de}(g, \alpha)$  near the critical coupling matches that of the pure CDT model, and is given by

$$Z^{de}(g, \alpha) \sim Z_c^{de}(\alpha) - c_\alpha \sqrt{g_c^{de}(\alpha) - g} \quad (7.125)$$

where  $c_\alpha = 4\sqrt{1+\alpha^2}$ .

The dense loop model and the pure CDT model share the same large-scale structure. It follows from (7.123) and (7.125), and arguments made in Section 7.5.1 that the Hausdorff dimension is given by

$$d_H^{de} = 2 \quad (\text{almost surely}). \quad (7.126)$$

Given the similarities between the critical behaviour and the large-scale structure of both pure CDT and dense loop models, the influence of coupling dense loops to CDT does not manifest in the statistical behaviour of the underlying triangulation. An analogous situation arises when coupling the Ising model to random planar trees, whereby a relation of the form (7.125) can be derived [103].

For completeness, we proceed by analysing the transfer matrix  $T^{de}(g, \alpha) = D K^{de}(g, \alpha)$ . Comparing equations (7.15) and (7.23), it is clear that we have

$$T^{de}(g, \alpha) = T(g(1+\alpha^2)), \quad K^{de}(g, \alpha) = K(g(1+\alpha^2)), \quad (7.127)$$

and consequently

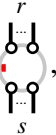
$$\text{tr}(T^{de}(g, \alpha)) = \frac{1 - \sqrt{1 - 4g(1+\alpha^2)}}{2\sqrt{1 - 4g(1+\alpha^2)}}, \quad \text{tr}(K^{de}(g, \alpha)) = \frac{g(1+\alpha^2)}{(1 - 4g(1+\alpha^2))^{\frac{3}{2}}}. \quad (7.128)$$

Accordingly, we have a counterpart to Proposition 7.5.3, where for  $\alpha \in [0, 1]$ , the largest eigenvalue  $\lambda_1(g, \alpha)$  of  $D^{\frac{1}{2}} K^{de}(g, \alpha) D^{\frac{1}{2}}$  approaches 1 from below as  $g$  approaches  $\frac{1}{4(1+\alpha^2)}$  from below. The goal of the following section is to develop a counterpart to Proposition 7.5.3 for the dilute loop model and thereby determine the critical behaviour of this model.

### 7.5.3 Dilute loop model

Unlike the dense loop model, the partition function of the dilute loop model cannot be expressed explicitly in terms of the pure CDT partition function. Accordingly, the analysis presented in the previous sections, using the closed-form expression of the partition function, is not applicable here. As will be established below, the critical behaviour and large-scale structure of the dilute loop model can be determined using transfer matrix techniques.

We begin by presenting a simplification of the transfer operator  $T^{di}(g, \alpha)$  introduced in Section 7.2.4,

$$T^{di}(g, \alpha) = \sum_{r,s \in \mathbb{N}} 2 \binom{r+s-1}{r} g^{\frac{r+s}{2}} \text{Diagram} \quad \bullet = \bullet + \alpha \bullet, \quad \#(\bullet) \in 2\mathbb{N}_0, \quad (7.129)$$


where we note that the combinatorial factor follows from Lemma 7.3.1, and both the factor of 2 and the parity constraint follow from Lemma 7.3.2. Proceeding as in the dense loop model, we define an effective transfer operator corresponding to  $T^{di}(g, \alpha)$ , that assigns the correct weight to space-like edges within a configuration. We first note that the transfer operator  $T^{di}(g, \alpha)$  generates *both* even and odd parity loop configurations, for the dilute loop model on the disk, we will restrict to even parity configurations only. Now, the two possible elementary configurations corresponding to a single space-like edge are  and , which assign the weight  $g$  and  $g\alpha$  respectively. For the dilute loop model, the correct assignment of weights can be achieved by considering a single layer configuration with  $n$  edges which, after summing over an even number of blue labels, is assigned the weight  $\frac{1}{2}g^n[(1+\alpha)^n + (1-\alpha)^n]$ . In light of this observation, we introduce an effective transfer operator corresponding to  $T^{di}(g, \alpha)$ , defined as

$$\bar{T}^{di}(g, \alpha) := \sum_{r,s \in \mathbb{N}} \binom{r+s-1}{r} g^{\frac{r+s}{2}} [(1+\alpha)^r + (1-\alpha)^r]^{\frac{1}{2}} [(1+\alpha)^s + (1-\alpha)^s]^{\frac{1}{2}} \text{Diagram}, \quad (7.130)$$


where each layer with  $n$  nodes is considered as a ‘square root’ of a layer of  $n$  space-like edges and is assigned the weight  $\frac{1}{\sqrt{2}}g^{\frac{n}{2}}[(1+\alpha)^n + (1-\alpha)^n]^{\frac{1}{2}}$ . As in the dense loop model, the algebraic operators appearing in  $\bar{T}^{di}(g, \alpha)^m$  do not have a direct relation to the underlying loop configurations, they simply assign the correct weight to each *internal* space-like edge.

Proceeding as in the pure CDT case, we denote by  $\mathsf{T}^{di}(g, \alpha)$  the corresponding representation of  $\bar{T}^{di}(g, \alpha)$ , that acts on the Hilbert space  $l_2(\mathbb{N})$ , whose matrix elements are given by

$$\mathsf{T}_{r,s}^{di}(g, \alpha) = \binom{r+s-1}{r} g^{\frac{r+s}{2}} [(1+\alpha)^r + (1-\alpha)^r]^{\frac{1}{2}} [(1+\alpha)^s + (1-\alpha)^s]^{\frac{1}{2}}. \quad (7.131)$$

We also introduce the sequence  $|v^{di}(g, \alpha)\rangle \in l_2(\mathbb{N})$ , where

$$v_n^{di}(g, \alpha) := g^{\frac{n}{2}} [(1+\alpha)^n + (1-\alpha)^n]^{\frac{1}{2}}, \quad n \in \mathbb{N}. \quad (7.132)$$

Given the definition of the partition function (7.27), the representation  $T^{di}(g, \alpha)$  (7.131), and the vector  $|v^{di}(g, \alpha)\rangle$  (7.132), the fixed height partition function of the dilute loop model can be written

$$Z_m^{di}(g, \alpha) = \langle v^{di}(g, \alpha) | T^{di}(g, \alpha)^{m-1} | v^{di}(g, \alpha) \rangle, \quad (7.133)$$

for all  $m \in \mathbb{N}$ .

Having defined the transfer matrix  $T^{di}(g, \alpha)$ , we first note that it is symmetrisable, admitting the factorisation

$$T^{di}(g, \alpha) = 2D K^{di}(g, \alpha), \quad (7.134)$$

where  $D$  is defined in (7.99), and the matrix elements of  $K^{di}(g, \alpha)$  are given by

$$K_{r,s}^{di}(g, \alpha) = \frac{1}{2} \frac{(r+s-1)!}{(r-1)!(s-1)!} g^{\frac{r+s}{2}} [(1+\alpha)^r + (1-\alpha)^r]^{\frac{1}{2}} [(1+\alpha)^s + (1-\alpha)^s]^{\frac{1}{2}}. \quad (7.135)$$

We also note that  $K^{di}(g, 0) = K(g)$ . Applying arguments developed for the pure CDT model in Section 7.5.1, we conclude that  $K^{di}(g, \alpha)$  and  $D^{\frac{1}{2}} K^{di}(g, \alpha) D^{\frac{1}{2}}$  are positive definite and trace-class operators on  $l_2(\mathbb{N})$  for  $g \in (0, \frac{1}{4(1+\alpha)})$  and  $\alpha \in [0, 1]$ , where

$$\text{tr}(K^{di}(g, \alpha)) = \frac{1}{2} [\text{tr}(K(g(1+\alpha))) + \text{tr}(K(g(1-\alpha)))] = \frac{g(1+\alpha)}{2(1-4g(1+\alpha))^{\frac{3}{2}}} + \frac{g(1-\alpha)}{2(1-4g(1-\alpha))^{\frac{3}{2}}} \quad (7.136)$$

and

$$\text{tr}(T^{di}(g, \alpha)) = \text{tr}(T(g(1+\alpha))) + \text{tr}(T(g(1-\alpha))) = \frac{1 - \sqrt{1-4g(1+\alpha)}}{2\sqrt{1-4g(1+\alpha)}} + \frac{1 - \sqrt{1-4g(1-\alpha)}}{2\sqrt{1-4g(1-\alpha)}}. \quad (7.137)$$

Examining these expressions, it is clear that for  $g > \frac{1}{4(1+\alpha)}$ , the operators  $K^{di}(g, \alpha)$  and  $T^{di}(g, \alpha)$  are not bounded. Again, arguing as in the case of  $D^{\frac{1}{2}} K(g) D^{\frac{1}{2}}$ , together with the inequality

$$|K_{r,s}^{di}(g, \alpha)| \leq K_{r,s}(|g|(1+|\alpha|)), \quad (7.138)$$

the operator  $D^{\frac{1}{2}} K^{di}(g, \alpha) D^{\frac{1}{2}}$  is analytic in the variables  $(\sqrt{g}, \alpha)$  for  $|\alpha| < 1$  and  $|g| < \frac{1}{4(1+|\alpha|)}$ . Furthermore, the Perron–Frobenius theorem applies to both  $K^{di}(g, \alpha)$  and  $D^{\frac{1}{2}} K^{di}(g, \alpha) D^{\frac{1}{2}}$  which implies that for each operator there exists a largest non-degenerate eigenvalue equal to the operator norm and that the corresponding eigenvector can be normalised such that it has positive coordinates only.

Adapting arguments made in Lemma 7.5.2, we have

$$Z_m^{di}(g, \alpha) \leq \text{tr}((T^{di}(g, \alpha))^m), \quad m \in \mathbb{N}, \quad (7.139)$$

for  $g \in (0, \frac{1}{4(1+\alpha)})$  and  $\alpha \in [0, 1]$ . In the following, we apply this result to construct a dilute model counterpart to Proposition 7.5.3.

**Proposition 7.5.4.** *For each  $\alpha \in [0, 1]$ , the largest eigenvalue  $\lambda_1^{di}(g, \alpha)$  of  $D^{\frac{1}{2}}K^{di}(g, \alpha)D^{\frac{1}{2}}$  is a strictly increasing function of  $g$ , and satisfies*

$$\lambda_1^{di}(g, \alpha) \nearrow \bar{\lambda}_1^{di}(\alpha) \quad \text{as} \quad g \nearrow \frac{1}{4(1+\alpha)}, \quad (7.140)$$

where  $\bar{\lambda}_1^{di}(\alpha) \leq 1$  for all  $\alpha$ .

*Proof.* The variational principle for eigenvalues (see e.g. Theorem XIII.1 in [7]), together with the fact that the matrix elements of  $K^{di}(g, \alpha)$  are strictly increasing functions of  $g$ , implies that  $\bar{\lambda}_1^{di}(\alpha)$  has a positive derivative with respect to  $g$ , and is therefore strictly increasing. Suppose that  $\bar{\lambda}_1^{di}(\alpha) > 1$  for some fixed  $\alpha$ , then there exists a  $g_0 < \frac{1}{4(1+\alpha)}$  such that  $\lambda_1^{di}(g_0, \alpha) = 1$ . Performing a calculation for  $g \in (0, g_0)$ , analogous to that presented in (7.122), implies that

$$W^{ev}(g, \alpha) = 1 + \sum_{m=1}^{\infty} \langle v^{di}(g, \alpha) | (\frac{1}{2} T^{di}(g, \alpha))^{m-1} | v^{di}(g, \alpha) \rangle \geq \frac{c'}{1 - \lambda_1^{di}(g, \alpha)} - B(g, \alpha), \quad (7.141)$$

where  $c' > 0$ , and  $B(g, \alpha)$  is bounded for  $g$  close to  $g_0$ . It follows from (7.141) that  $W^{ev}(g, \alpha)$  diverges as  $g$  approaches  $g_0$ , which contradicts the upper bound in (7.91) for  $k = 1$ . We therefore conclude that  $\bar{\lambda}_1^{di}(\alpha) \leq 1$ .  $\square$

Examining the limit  $\bar{\lambda}_1^{di}(\alpha)$  at the bounds of the interval  $\alpha \in [0, 1]$ , we note that  $T^{di}(g, 0) = 2T(g)$  and  $T^{di}(g, 1) = T(2g)$ , and applying Proposition 7.5.3 to these facts, we conclude

$$\bar{\lambda}_1^{di}(0) = 1, \quad \bar{\lambda}_1^{di}(1) = \frac{1}{2}. \quad (7.142)$$

Reexpressing the matrix elements of  $K^{di}(g, \alpha)$  as

$$K_{r,s}^{di}(g, \alpha) = \frac{1}{2} \frac{(r+s-1)!}{(r-1)!(s-1)!} \left[ 1 + \left( \frac{1-\alpha}{1+\alpha} \right)^r \right]^{\frac{1}{2}} \left[ 1 + \left( \frac{1-\alpha}{1+\alpha} \right)^s \right]^{\frac{1}{2}} (g(1+\alpha))^{\frac{r+s}{2}}, \quad (7.143)$$

we see, for fixed  $g(1+\alpha) \in (0, \frac{1}{4})$ , that these elements are decreasing functions in  $\alpha \in [0, 1]$ . It follows that  $\bar{\lambda}_1(\alpha)$  is a decreasing function of  $\alpha$ . With these observations in hand, we present our main result on the critical behaviour of the dilute loop model.

**Theorem 7.5.5.** *For  $\alpha$  real and sufficiently small, the critical coupling  $g_c^{di}(\alpha)$  of the partition function  $Z^{di}(g, \alpha)$  is determined by the equation*

$$\lambda_1^{di}(g_c^{di}(\alpha), \alpha) = \frac{1}{2} \quad (7.144)$$

and there exists  $C_1(\alpha), C_2(\alpha) > 0$ , such that

$$\frac{C_1(\alpha)}{g_c^{di}(\alpha) - g} \leq Z^{di}(g, \alpha) \leq \frac{C_2(\alpha)}{g_c^{di}(\alpha) - g} \quad (7.145)$$

for  $g$  close to  $g_c^{di}(\alpha)$ .

*Proof.* We first note that  $\lambda_1^{di}(g, \alpha)$  is a continuous function that is strictly increasing in  $g$ . It follows from (7.142) that for  $\alpha$  sufficiently small,  $\bar{\lambda}_1^{di}(\alpha) > \frac{1}{2}$ , and by the intermediate value theorem, the value of  $g_c^{di}(\alpha)$  satisfying (7.144) is unique and strictly smaller than  $\frac{1}{4(1+\alpha)}$ . Thus, for fixed  $\alpha$  sufficiently small,  $D^{\frac{1}{2}}K^{di}(g, \alpha)D^{\frac{1}{2}}$  is analytic in  $g$  in a neighbourhood of  $g_c^{di}(\alpha)$ .

Determining the lower bound, we perform a calculation similar to (7.122), which implies that for  $g \in (0, g_c^{di}(\alpha))$ , we have

$$Z^{di}(g, \alpha) \geq \frac{C'_1(\alpha)}{1 - 2\lambda_1^{di}(g, \alpha)} - B(g, \alpha), \quad (7.146)$$

where  $C'_1(\alpha) > 0$ , and  $B(g, \alpha)$  is bounded for  $g$  close to  $g_0$ . Recalling that for fixed  $\alpha$ ,  $\lambda_1^{di}(g, \alpha)$  is a strictly increasing analytic function of  $g \in (0, g_c^{di}(\alpha))$ , together with (7.146), the lower bound in (7.145) follows.

For the upper bound, we apply (7.139) for  $g \in (0, g_c^{di}(\alpha))$  and write

$$Z^{di}(g, \alpha) \leq 1 + \sum_{m=1}^{\infty} \text{tr}(\mathsf{T}^{di}(g, \alpha))^m = 1 + \sum_{m=1}^{\infty} 2^m \text{tr}(D^{\frac{1}{2}}K^{di}(g, \alpha)D^{\frac{1}{2}})^m = 1 + \sum_{n=1}^{\infty} \frac{2\lambda_n^{di}(g, \alpha)}{1 - 2\lambda_n^{di}(g, \alpha)}, \quad (7.147)$$

where  $\lambda_1^{di}(g, \alpha) > \lambda_2^{di}(g, \alpha) \geq \lambda_3^{di}(g, \alpha) \geq \dots$  denote the eigenvalues of  $D^{\frac{1}{2}}K^{di}(g, \alpha)D^{\frac{1}{2}}$ . Separating the first summand, the contribution from the remaining terms is bounded for  $g$  close to  $g_c^{di}(\alpha)$ , and the upper bound follows as before. From the first term in the summand of the upper bound of (7.147), one arrives at the constraint (7.144), defining  $g_c^{di}(\alpha)$ .  $\square$

Theorem 7.5.5, together with the fact that  $\bar{\lambda}_1^{di}(\alpha)$  is a decreasing function of  $\alpha$ , implies two possible outcomes for the critical behaviour of the dilute loop model:

- (i)  $\bar{\lambda}_1^{di}(\alpha) = \frac{1}{2}$  for  $\alpha = 1$  only, the constraint (7.144) holds for all  $\alpha \in [0, 1)$ ;
- (ii)  $\bar{\lambda}_1^{di}(\alpha) = \frac{1}{2}$  for  $\alpha \in [\alpha_0, 1]$  where  $0 < \alpha_0 < 1$ , constraint (7.144) holds for all  $\alpha \in [0, \alpha_0)$ .

In the case of (ii) the critical behaviour of  $Z^{di}(g, \alpha)$  for  $\alpha \in [\alpha_0, 1]$ , in particular at the transition point  $\alpha = \alpha_0$ , would be an interesting subject of study.

At least for small  $\alpha$ , the critical behaviour of the dilute loop model is distinct from that of the pure CDT model, in particular, the critical exponent characterising the singular behaviour of the pure CDT model is  $\frac{1}{2}$  and is shifted to  $-1$  in the dilute case. This change proves influential on the large-scale structure of the model where for  $\alpha = 0$ , a more detailed analysis carried out in [100], reveals that the simple pole of  $Z^{di}(g, 0)$  at  $g_c^{di}(0)$  implies that the Hausdorff dimension equals 1 in this case. It follows from Theorem 7.5.5 that for at least  $\alpha \ll 1$ , the singularity remains a simple pole, and we similarly conclude that the Hausdorff dimension is given by

$$d_H^{di}(\alpha \ll 1) = 1 \quad (\text{almost surely}). \quad (7.148)$$

## 7.6 Outlook

In this chapter, we defined a pure CDT model, a dense loop model and a dilute loop model on causal triangulations, and formulated each in a planar-algebraic setting. By developing tree correspondences in each case, we were able to apply tree techniques, together with the analysis of the transfer matrix, to study the critical behaviour of each model. The dense loop model was found to be equivalent to the pure CDT model up to a shift in the coupling, indicating no significant interaction between dense loops and causal triangulations. While the dilute loop model was found to possess a distinct critical behaviour and Hausdorff dimension, at least for small  $\alpha$ . The origin of this behaviour owes to an effective height coupling, absent in the pure CDT model. It should be noted that though the tree correspondences are invaluable in the analysis of the partition functions, they may limit non-trivial couplings between matter and geometry. To account for the absence of the tree correspondences, we envisage an analysis whereby the transfer matrix has an increased role.

In light of these comments, we consider a natural generalisation of the dilute loop model that does not readily admit a tree correspondence. Here, we assign a separate weight  $\gamma$  to arcs that intersect time-like edges only, i.e. the second diagrams of each row in Figure 7.5, and let  $t(L)$  denote the number of such arcs in  $L \in \mathcal{L}_m^{di}$ . We define the fixed height partition functions as

$$Z_m^{di}(g, \alpha, \gamma) := \sum_{L \in \mathcal{L}_m^{di}} g^{|L|} \alpha^{s(L)} \gamma^{t(L)}, \quad (7.149)$$

where for a given  $\alpha, \gamma \in [0, 1]$ , there exists a critical coupling  $g_c^{di}(\alpha, \gamma)$  such that  $Z_m^{di}(g, \alpha, \gamma)$  is finite for  $g < g_c^{di}(\alpha, \gamma)$  while divergent for  $g > g_c^{di}(\alpha, \gamma)$ . Noting the inequality  $Z_m^{di}(g, \alpha, \gamma) \leq Z_m^{di}(g, \alpha, 1) = Z_m^{di}(g, \alpha)$ , between dilute loop models, it follows that

$$g_c^{di}(\alpha, \gamma) \geq g_c^{di}(\alpha, 1) = g_c^{di}(\alpha). \quad (7.150)$$

The relation between the loop configurations and underlying triangulations ensures that one cannot perform an independent summation of loop configurations and triangulations in (7.149), as was possible for the dense and the dilute loop model partition functions. While the inseparability of matter and geometry of this new model suggests a deep connection between these structures, uncovering the details of this interaction requires the development of new techniques.





# Chapter 8

---

## Quantum field theory

---

Up to now, this thesis has focused on describing statistical mechanical models with planar algebras. In this chapter, we sketch how planar algebras can describe quantum field theories (QFTs) and where planar-algebraic models fit in. We introduce a new class of QFTs and identify Jones' semicontinuous models as ‘almost’ examples. After detailing some recent efforts to endow semicontinuous models with the properties of fully-fledged examples, we outline the applicability of the planar-algebraic framework in this context and find that the single-row transfer operator plays a central role.

### 8.1 Conformal nets

*Algebraic quantum field theory* (AQFT) provides a rigorous mathematical framework for quantum field theory (QFT) [104–106]. To each region of the spacetime manifold, one associates an algebra of observables which are subject to fundamental physical principles such as causality, relativistic covariance and energy positivity. *Conformal nets* are versions of AQFTs where the spacetime manifold is  $S^1$  and where relativistic covariance is enlarged to conformal covariance.

Let  $\text{Diff}_+(S^1)$  denote the group of orientation-preserving diffeomorphisms of the unit circle and let  $\text{Rot}(S^1)$  denote the subgroup of rotations of the unit circle. A *conformal net* consists of (i) a Hilbert space  $\mathcal{H}$ , (ii) a von Neumann algebra  $\mathcal{A}(I)$  acting on  $\mathcal{H}$  for each open interval  $I \subset S^1$ , and (iii) a continuous unitary representation  $U$  of  $\text{Diff}_+(S^1)$  on  $\mathcal{H}$ , subject to:

$$\begin{aligned} \text{Isotony: } \quad & \mathcal{A}(I) \subseteq \mathcal{A}(J), & \text{if } I \subseteq J \\ \text{Locality: } \quad & [\mathcal{A}(I), \mathcal{A}(J)] = 0, & \text{if } I \cap J = \emptyset \\ \text{Covariance: } \quad & U(\alpha)\mathcal{A}(I)U(\alpha)^* = \mathcal{A}(\alpha(I)), & \forall \alpha \in \text{Diff}_+(S^1) \\ \text{Positivity: } \quad & \text{Spec}(U(\rho)) \subset \mathbb{N}_0, & \forall \rho \in \text{Rot}(S^1) \end{aligned} \tag{8.1}$$

where  $\text{Spec}$  denotes the set of eigenvalues of an operator. See Figure 8.1 for diagrams illustrating Isotony, Locality and Covariance.

Inspired by Jones [20, 107], we define an analogue of conformal nets whereby the underlying spacetime is not a smooth manifold but instead has an ‘atomic’ structure. In preparation for this

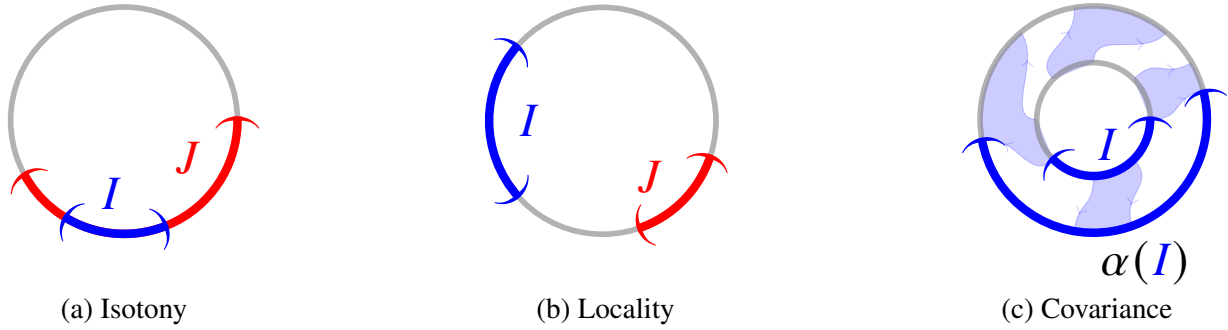


Figure 8.1: For conformal nets, we present diagrammatic representations of the properties of Isotony, Locality and Covariance.

definition, we introduce a few prerequisites. A *direct system*  $\langle A_i, f_{ij} \rangle$  consists of (i) a directed set  $\langle S, \leq \rangle$ , (ii) a vector space  $A_i$  for each  $i \in S$ , and (iii) a homomorphism  $f_{ij} : A_i \rightarrow A_j$  for each  $i \leq j$ , subject to:

$$\begin{aligned} f_{ii} &= \text{id}_i, & \forall i \in S \\ f_{ik} &= f_{ij} \circ f_{jk}, & \forall i \leq j \leq k \end{aligned} \tag{8.2}$$

where  $\text{id}_i$  denotes the identity automorphism for each  $i \in S$ . We say that the direct system  $\langle A_i, f_{ij} \rangle$  is defined *over*  $S$ . A *direct limit*  $A$ , of a direct system  $\langle A_i, f_{ij} \rangle$  over  $S$ , is defined

$$A := \bigsqcup_{i \in S} A_i / \sim, \tag{8.3}$$

where the equivalence relation  $\sim$  on  $\bigsqcup_{i \in S} A_i$  is defined as

$$(x, i) \sim (y, j) \iff f_{ik}(x) = f_{jk}(y). \tag{8.4}$$

We denote elements in  $A$  by  $[(x, i)]$ , which corresponds to the set of elements in  $\bigsqcup_{i \in S} A_i$  equivalent to  $(x, i)$  under the relation  $\sim$ .

**Remark.** Direct limits can similarly be defined when each vector space  $A_i$  comes equipped with additional structure, provided that each homomorphism respects this structure. For our purposes, we will define the direct limits of two directed systems, one of Hilbert spaces and another of von Neumann algebras.

Let  $\mathcal{D}$  denote a set of countable subsets of  $S^1$ . For each closed interval  $I \subset S^1$ , denote by  $\mathcal{D}_I$  the set of all elements in  $\mathcal{D}$ , containing the endpoints of  $I$ . A *discrete conformal net* consists of:

- (i) a directed set  $\langle \mathcal{D}, \leq \rangle$  of countable subsets of  $S^1$ ;
- (ii) a Hilbert space  $\mathcal{H}_i$  for each  $i \in \mathcal{D}$ ;
- (iii) a von Neumann algebra  $\mathcal{A}_i(I)$  acting on  $\mathcal{H}_i$ , for each closed interval  $I \subset S^1$  and each  $i \in \mathcal{D}_I$ ;
- (iv) an isometry  $f_{ij} : \mathcal{H}_i \rightarrow \mathcal{H}_j$  for each  $i \leq j$ , i.e.  $f_{ij}^* \circ f_{ij} = \text{id}_i$ ;
- (v) a discrete realisation of  $\text{Diff}_+(S^1)$  denoted  $D$ ;

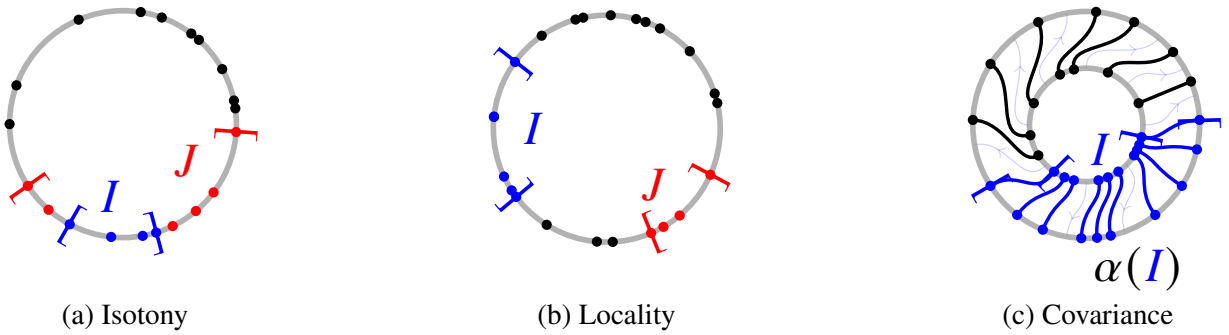


Figure 8.2: For discrete conformal nets, we present diagrammatic representations of the properties of Isotony, Locality and Covariance.

(vi) a continuous unitary representation  $U$  of  $D$  on the completion of  $\mathcal{H}$  (see below).

From these elements we define  $\mathcal{H}$  as the direct limit of the direct system  $\langle \mathcal{H}_i, f_{ij} \rangle$  over  $\mathcal{D}$ , and define  $\mathcal{A}(I)$  as the direct limit of the direct system  $\langle \mathcal{A}_i(I), g_{ij} \rangle$  over  $\mathcal{D}$ , where

$$g_{ij} : \mathcal{A}_i(I) \rightarrow \mathcal{A}_j(I), \quad x \mapsto f_{ij} \circ x \circ f_{ij}^*. \quad (8.5)$$

**Remark.** We highlight that (i)  $\mathcal{H}$  is a pre-Hilbert space, (ii)  $\mathcal{A}(I)$  is an algebra for each  $I$  where  $\mathcal{D}_I \neq \emptyset$ , and (iii) there is an action of  $\mathcal{A}(I)$  on  $\mathcal{H}$ . To illustrate the point (iii), see (8.7) below.

The algebras  $\mathcal{A}(I)$  and the pre-Hilbert space  $\mathcal{H}$  are subject to

$$\begin{aligned} \text{Isotony: } \quad & \mathcal{A}(I) \subseteq \mathcal{A}(J), & \text{if } I \subseteq J \\ \text{Locality: } \quad & [\mathcal{A}(I), \mathcal{A}(J)] = 0, & \text{if } I \cap J = \emptyset \\ \text{Covariance: } \quad & U(\alpha)\mathcal{A}(I)U(\alpha)^* = \mathcal{A}(\alpha(I)), & \forall \alpha \in D \\ \text{Positivity: } \quad & \text{Spec}(U(\rho)) \subset \mathbb{N}_0, & \forall \rho \in \text{Rot}_D \end{aligned} \quad (8.6)$$

where  $\text{Rot}_D$  denotes the rotation subgroup of  $D$ . We highlight that the conditions (8.6) are discrete analogues of the conditions (8.1). See Figure 8.2 for diagrams illustrating Isotony, Locality and Covariance.

To illustrate how the direct limits  $\mathcal{A}(I)$  and  $\mathcal{H}$  give rise to structures similar to conformal nets, we show how the action of  $\mathcal{A}(I)$  on  $\mathcal{H}$  is inherited from the corresponding direct systems over  $\mathcal{D}$ . Let  $[(a, i)] \in \mathcal{A}(I)$  and  $[(v, j)] \in \mathcal{H}$ , we have

$$[(a, i)][(v, j)] = [(g_{ik}(a), k)][(f_{jk}(v), k)] = [(f_{ik} \circ a \circ f_{ik}^*(v), k)], \quad (8.7)$$

where  $i \leq k$  and  $j \leq k$ , and where the second equality uses the action of  $\mathcal{A}_k(I)$  on  $\mathcal{H}_k$ . We proceed by showing that the action (8.7) is independent of the representatives of each equivalence class. Consider  $[(a, i)], [(a', j)] \in \mathcal{A}(I)$  and  $[(v, i)], [(v', j)] \in \mathcal{H}$ , satisfying

$$g_{ik}(a) = g_{ik}(a'), \quad f_{ik}(v) = f_{ik}(v'), \quad (8.8)$$

so  $[(a, i)] = [(a', j)]$  and  $[(v, i)] = [(v', j)]$ . Comparing the following two actions, we have

$$[(a, i)][(v, i)] = [(a(v), i)], \quad [(a', j)][(v', j)] = [(a'(v'), j)], \quad (8.9)$$

and

$$\begin{aligned}
[(a, i)]([(v, i)]) &= [(g_{ik}(a), k)]([(f_{ik}(v), k)]) \\
&= [(g_{jk}(a'), k)]([(f_{jk}(v'), k)]) \\
&= [((f_{jk} \circ a' \circ f_{jk}^* \circ f_{jk})(v'), k)] \\
&= [((f_{jk} \circ a')(v'), k)] \\
&= [(a'(v'), j)],
\end{aligned} \tag{8.10}$$

where in the second equality we have used (8.8), and in the fourth equality we have used that  $f_{jk}$  is an isometry.

Stepping back, let us briefly describe the intuition behind the features of a discrete conformal net. An element of  $\mathcal{D}$  is a ‘discretisation’ of spacetime, to which we associated a Hilbert space of states and a von Neumann algebra of observables. The direction defined on  $\mathcal{D}$  indicates a ‘resolution’ or ‘scale’ of a given discretisation. Discretisations with a ‘finer’ resolution, better approximate  $S^1$ . It follows from the injectivity of  $f_{ij}$  respectively  $g_{ij}$ , that states, respectively, observables on one resolution are present on a ‘finer’ resolution, so we have  $\mathcal{H}_i \subseteq \mathcal{H}_j$  and  $\mathcal{A}_i(I) \subseteq \mathcal{A}_j(I)$ . Two states or two observables defined on different resolutions, equivalent up to the action of the appropriate maps, are considered ‘physically indistinguishable’. Direct limits of the Hilbert spaces, respectively, von Neumann algebras, collect states respectively observables and identify those that are physically indistinguishable. Moreover, direct limits facilitate the action among observables and the action of observables on states across all scales.

To get a better feel for discrete conformal nets and their relation to planar algebras, we present so-called *semicontinuous models* in the following section. As we will see, these are *almost* examples of discrete conformal nets.

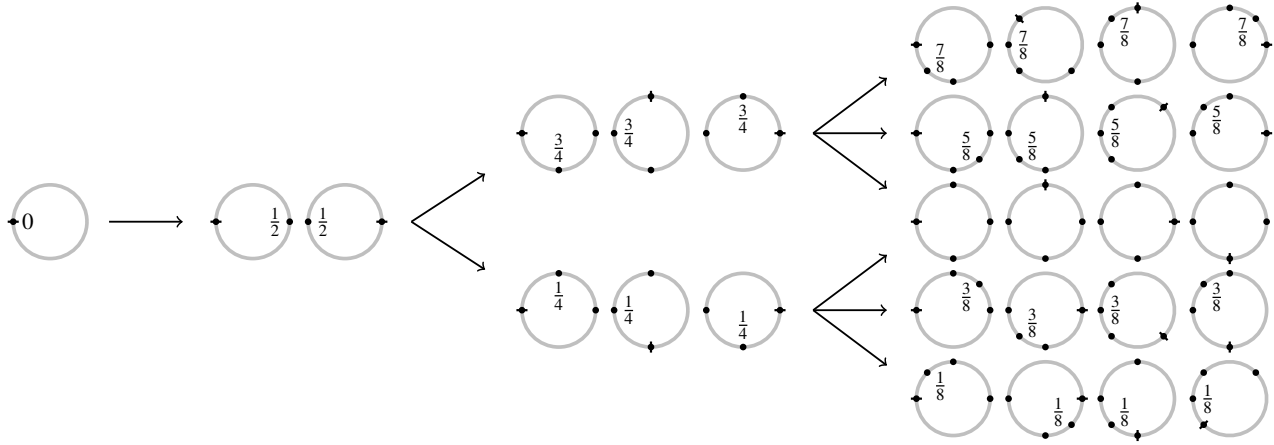
## 8.2 Semicontinuous models

### 8.2.1 Spacetimes

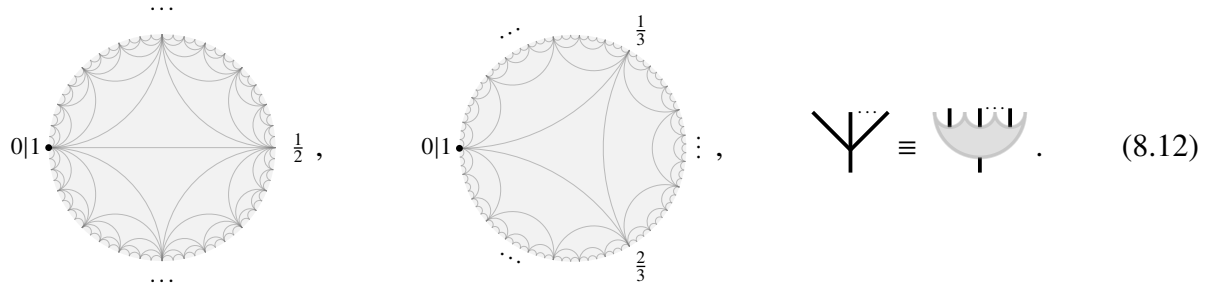
Starting with the directed set  $\mathcal{D}$ , we proceed by introducing the components of *semicontinuous models*. For  $k \in \mathbb{N}_{>1}$ , a *standard k-adic interval* is an interval of the form

$$\left[ \frac{m}{k^n}, \frac{m+1}{k^n} \right], \quad m, n \in \mathbb{N}_0. \tag{8.11}$$

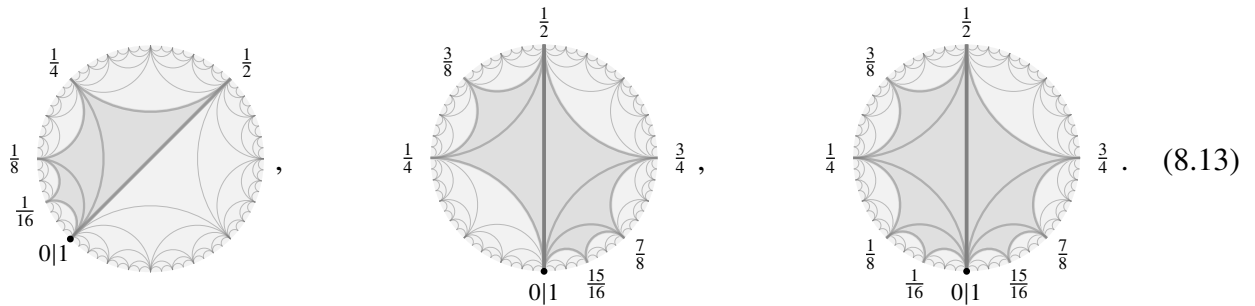
The partition of the interval  $[0, 1]$  into standard  $k$ -adic intervals is called a *k-adic subdivision of  $[0, 1]$* . Similarly, if we define the unit circle  $S^1$  as  $[0, 1]/\{0 \sim 1\}$ , the partition of  $S^1$  into standard  $k$ -adic intervals is called a *k-adic subdivision of  $S^1$* , and can be characterised by a tuple consisting of the endpoints of each interval. Rotating, equivalently, shifting the points of a  $k$ -adic subdivision of  $S^1$  by a  $k$ -adic rational will, in general, result in a distinct subdivision. See Figure 8.3 for the enumeration of dyadic subdivisions of  $S^1$  with up to four points.

Figure 8.3: The enumeration of dyadic subdivisions of  $S^1$  with up to four points.

We refer to an *annular  $k$ -tree*, as a planar tree whose root is at the centre of  $S^1$ , whose leaves lie on  $S^1$ , and where each vertex has valence  $k + 1$ . There is a one-to-one correspondence between  $k$ -adic subdivisions of  $S^1$  and annular  $k$ -trees. To illustrate this correspondence, we use the dual-tree notation [108] and present the infinite annular 2-tree and the infinite annular 3-tree



Any  $k$ -adic subdivision of  $S^1$ , equivalently, annular  $k$ -tree can be obtained by ‘filling out’ a finite region and/or rotating the infinite annular  $k$ -tree. Taking  $k = 2$ , we present some examples:



We refer to an *annular  $k$ -forest*, as a disjoint union of planar trees whose roots lie on  $S^1 \times \{0\}$ , whose leaves lie on  $S^1 \times \{1\}$ , and where each vertex has valence  $k + 1$ . An annular  $k$ -tree (equivalently  $k$ -adic subdivision of  $S^1$ ) with  $m$  leaves (equivalently points) can be ‘refined’ to one with  $n$  leaves (where  $m \leq n$ ), by filling out more of the infinite annular  $k$ -tree. This operation can be performed by ‘composing’ the corresponding annular  $k$ -tree with  $m$  leaves with the appropriate annular  $k$ -forest with

$m$  roots and  $n$  leaves. To illustrate, we present the following example:

$$i = \text{[Diagram of a shaded annular forest with 4 roots and 4 leaves]}, \quad p \circ i = \text{[Diagram of a complex annular forest with many internal components and 8 roots/leaves]}, = \text{[Diagram of a shaded annular forest with 4 roots and 4 leaves]}, \quad (8.14)$$

where  $i$  and  $p \circ i$  correspond to the first and third diagrams in (8.13) respectively. The operation (8.14) can be formalised as the composition of morphisms in the *annular forest category*  $A\mathfrak{F}_k$  where  $\text{Obj}_{A\mathfrak{F}_k} = \mathbb{N}$  and  $\text{Mor}_{A\mathfrak{F}_k}(m, n)$  is the set of all annular  $k$ -forests with  $m$  roots and  $n$  leaves, see [20] for details.

Let  $\mathcal{D}^{(k)}$  denote the set of all annular  $k$ -trees (equivalently  $k$ -adic subdivisions of  $S^1$ )

$$\mathcal{D}^{(k)} := \bigcup_{n \in \mathbb{N}} \text{Mor}_{A\mathfrak{F}_k}(1, n), \quad (8.15)$$

and define the partial order on  $\mathcal{D}^{(k)}$  as

$$i \leq j \iff j = p \circ i. \quad (8.16)$$

For each  $k \in \mathbb{N}_{\geq 2}$ , the directed set  $\langle \mathcal{D}^{(k)}, \leq \rangle$  is a valid set of spacetimes for a semicontinuous model. We proceed by introducing the relevant direct systems of Hilbert spaces and von Neumann algebras defined over  $\mathcal{D}^{(k)}$ .

## 8.2.2 Hilbert spaces

Let  $P$  denote an involutive planar algebra  $(P_n)_{n \in \mathbb{N}_0}$  and let  $(V_n)_{n \in \mathbb{N}_0}$  denote a Hilbert representation of  $P$ . Denote by  $\mathfrak{J}$  an element of  $P_{k+1}$  that satisfies

$$\text{[Diagram of a shaded annular forest with 3 roots and 3 leaves, with a red arrow pointing from the center to the boundary]} = \text{[Vertical line segment]} \quad (8.17)$$

For each annular  $k$ -forest  $p$  with  $m$  roots and  $n$  leaves, we denote by  $\Phi_{\mathfrak{J}}(p)$ , the corresponding element in  $\text{Mor}_{\text{Hilb}}(V_m, V_n)$ , where each vertex in  $p$  has been replaced by the element  $\mathfrak{J} \in P_{k+1}$ , for example:

$$p = \text{[Diagram of a shaded annular forest with 6 roots and 6 leaves]}, \quad \Phi_{\mathfrak{J}}(p) = \text{[Diagram of a similar annular forest where each vertex is replaced by the element J, indicated by red dots and red arrows]} \quad (8.18)$$

**Remark.** Courtesy of the Hilbert representation of  $P$ , we will express linear maps in  $\text{Mor}_{\text{Hilb}}(V_m, V_n)$  diagrammatically as the corresponding affine tangles in  $\text{Mor}_{\text{Aff}(P)}(m, n)$ .

By construction,  $\Phi_{\mathfrak{J}}(p)$  is an isometry for every  $p$ , that is,  $\Phi_{\mathfrak{J}}(p)^* \circ \Phi_{\mathfrak{J}}(p) = \text{id}_{V_m}$ . Define the Hilbert spaces  $\mathcal{H}_i := V_{|i|}$ , and the maps

$$f_{ij}^{(\mathfrak{J})} : \mathcal{H}_i \rightarrow \mathcal{H}_j, \quad a \mapsto \Phi_{\mathfrak{J}}(p)(a), \quad (8.19)$$

where  $j = p \circ i$ . It follows from the properties of  $\Phi_{\mathfrak{J}}(p)$ , that each  $f_{ij}^{(\mathfrak{J})}$  is an isometry and that  $\langle \mathcal{H}_i, f_{ij}^{(\mathfrak{J})} \rangle$  is a direct system over  $\mathcal{D}^{(k)}$ . Accordingly, we introduce the corresponding direct limit

$$\mathcal{H}^{(\mathfrak{J})} := \bigsqcup_{i \in S} \mathcal{H}_i / \sim, \quad (x, i) \sim (y, j) \iff f_{ik}^{(\mathfrak{J})}(x) = f_{jk}^{(\mathfrak{J})}(y). \quad (8.20)$$

Specialising to  $k = 2$  and  $V_n = P_n$ , we can view a representative of a vector in  $\mathcal{H}$  diagrammatically as

$$(x, s) = \begin{array}{c} \text{Diagram of } x \text{ in } P_7 \text{ (a circle with points and shaded region)} \\ \text{with labels: } \frac{1}{8}, \frac{1}{4}, \frac{1}{2}, \frac{5}{8}, \frac{11}{16}, \frac{3}{4}, \frac{3}{8} \end{array}, \quad x = \begin{array}{c} \text{Diagram of } x \text{ in } P_7 \text{ (a circle with points and shaded region)} \\ \text{with label: } x \end{array} \in P_7, \quad (8.21)$$

$$s = (0, \frac{1}{8}, \frac{1}{4}, \frac{1}{2}, \frac{5}{8}, \frac{11}{16}, \frac{3}{4}) \in \mathcal{D}^{(2)},$$

and highlight the following relations in  $\mathcal{H}^{(\mathfrak{J})}$

$$[(x, s)] = \begin{array}{c} \text{Diagram of } (x, s) \text{ in } P_7 \text{ (a circle with points and shaded region)} \\ \text{with labels: } \frac{1}{8}, \frac{1}{4}, \frac{1}{2}, \frac{5}{8}, \frac{11}{16}, \frac{3}{4}, \frac{3}{8} \end{array} = \begin{array}{c} \text{Diagram of } (x, s) \text{ in } P_7 \text{ (a circle with points and shaded region)} \\ \text{with labels: } \frac{1}{8}, \frac{15}{16}, \frac{7}{8}, \frac{3}{4}, \frac{3}{8}, \frac{5}{8} \end{array}. \quad (8.22)$$

### 8.2.3 von Neumann algebras

For each  $m, n \in \mathbb{N}$  such that  $m \leq n$  and each  $s = 1, \dots, n$ , we define the *inclusion map*

$$\iota_{s,n} : P_m \rightarrow \text{Hom}_{\text{Hilb}}(V_n, V_n), \quad \begin{array}{c} \text{Diagram of } \iota_{s,n} \text{ (a rectangle with points and shaded region)} \\ \text{with label: } a \end{array} \mapsto \begin{array}{c} \text{Diagram of } \iota_{s,n} \text{ (a circle with points and shaded region)} \\ \text{with labels: } s-1, 1, n, s+m \text{ mod } n \end{array}, \quad (8.23)$$

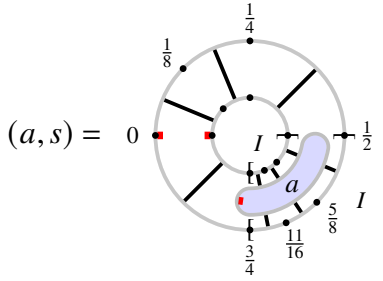
and denote by  $\iota_{s,n}(P_m)$  the subalgebra in  $\text{Hom}_{\text{Hilb}}(V_n, V_n)$  induced by the inclusion map. For each closed interval  $I \subset S^1$  and each  $i \in \mathcal{D}_I$ , denote by  $s(i, I)$  the index of the starting point of  $I$  in the tuple  $i$ . Define the von Neumann algebras  $\mathcal{A}_i(I) := \iota_{s(i, I), |i|}(P_{|i \cap I| - 1})$  and the maps

$$g_{ij}^{(\mathfrak{J})} : \mathcal{A}_i(I) \rightarrow \mathcal{A}_j(I), \quad a \mapsto f_{ij}^{(\mathfrak{J})} \circ a \circ (f_{ij}^{(\mathfrak{J})})^*. \quad (8.24)$$

It follows from properties of  $f_{ij}^{(\mathfrak{J})}$  that  $\langle \mathcal{A}_i(I), g_{ij}^{(\mathfrak{J})} \rangle$  is a direct system over  $\mathcal{D}^{(k)}$ , and we introduce the corresponding direct limit

$$\mathcal{A}^{(\mathfrak{J})}(I) := \bigsqcup_{i \in S} \mathcal{A}_i(I) / \sim, \quad (x, i) \sim (y, j) \iff g_{ik}^{(\mathfrak{J})}(x) = g_{jk}^{(\mathfrak{J})}(y). \quad (8.25)$$

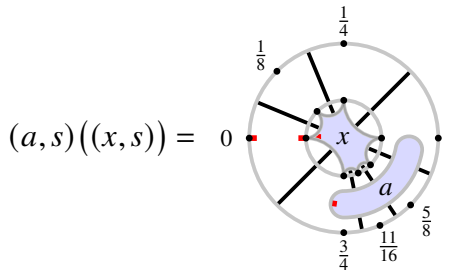
Specialising to  $k = 2$ , we can view a representative of an element in  $\mathcal{A}(I)$  diagrammatically as



$$(a, s) = 0 \quad \text{and} \quad a = \text{[diagram with purple and blue shaded regions]} \in \iota_{4,7}(P_3),$$

$$s = (0, \frac{1}{8}, \frac{1}{4}, \frac{1}{2}, \frac{5}{8}, \frac{11}{16}, \frac{3}{4}) \in \mathcal{D}^{(2)}, \quad (8.26)$$

and we note that the representative  $(a, s)$  has a natural diagrammatic action on the representative  $(x, s)$  in (8.21) as follows



$$(a, s)((x, s)) = 0 = 0 = (a(x), s). \quad (8.27)$$

By construction, this action extends to an action of  $\mathcal{A}^{(\mathfrak{I})}(I)$  on  $\mathcal{H}^{(\mathfrak{I})}$ , see (8.7)–(8.10). It readily follows from properties of planar algebras, that the algebras  $\mathcal{A}^{(\mathfrak{I})}(I)$  satisfy isotony and locality.

### 8.2.4 Groups and representations

Let  $(d, r)$  denote a pair of  $k$ -adic subdivisions of  $S^1$  with the same number of points. To  $(d, r)$ , associate a piecewise-linear homeomorphism  $f : S^1 \rightarrow S^1$  that acts by sending each subinterval of  $d$  onto the corresponding subinterval of  $r$ . We refer to  $f$  as a  *$k$ -adic rearrangement of  $S^1$* . *Thompson's group  $T_k$*  is the group of  $k$ -adic rearrangements of  $S^1$  [109, 110]. It is a remarkable fact that Thompson's groups, for each  $k \in \mathbb{N}_{\geq 2}$ , offer a discrete realisation of  $\text{Diff}_+(S^1)$  [111, 112], see also [113] for the case  $k = 2$ .

**Theorem 8.2.1.** *For each  $f \in \text{Diff}_+(S^1)$  there exists  $g \in T_k$  and  $\epsilon > 0$  such that*

$$\sup_{x \in S^1} |f(x) - g(x)| < \epsilon. \quad (8.28)$$

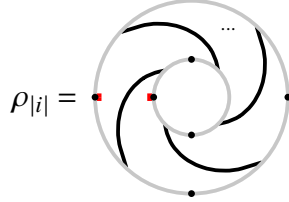
The *Jones action* [107] defines an action of  $T_k$  on  $\mathcal{H}^{(\mathfrak{I})}$ , which induces a unitary representation of  $T_k$  for each  $\mathfrak{I} \in P_{k+1}$ . While this construction ensures semicontinuous models satisfy the unitary requirement of (iv) in (8.6), it remains to show that these representations are continuous. For a semi-continuous model based on a Temperley–Lieb planar subalgebra, Jones showed that representations of the rotation subgroup are “hopelessly discontinuous” [20, 107]. This result was later extended to tensor planar algebras by Kliesch and Koenig [114], who showed that such representations are generically discontinuous. Both results [20] and [114] were established for  $k = 2$  only.

We briefly mention some recent efforts to avert these ‘no-go theorems’. Our goal is to select  $\mathfrak{I} \in P_{k+1}$  to endow the corresponding representations with continuity. We highlight that the dimension

of  $P_{k+1}$  grows at least exponentially for subfactor planar algebras. It is therefore conceivable that as we consider larger  $k \in \mathbb{N}_{\geq 2}$  there are increasingly many  $\mathfrak{J}$  giving rise to a continuous unitary representation. It remains to identify these elements. For the rotation subgroup, we have developed sufficient conditions, expressible in terms of planar-algebraic relations among  $\mathfrak{J}, \mathfrak{J}^* \in P_{k+1}$ , that endow the corresponding representations with continuity. We have found an infinite class of solutions for a semicontinuous model based on the Brauer planar algebra for each  $k = 2n+3$  where  $n \in \mathbb{N}$ .

### 8.2.5 Integrable operators on spacetime

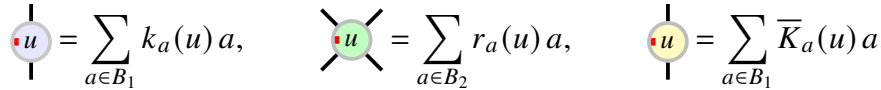
Putting the continuity issue aside, we proceed by introducing some operators that act on the spacetime of semicontinuous models. Denote by  $\mathcal{A}_i \equiv \mathcal{A}_i(S^1)$  the algebra of observables that act on all of spacetime. Of immense physical interest is the Hamiltonian – the generator of infinitesimal time-evolution. For each  $\mathcal{A}_i$ , this element simply corresponds to the rotation



$$\rho_{|i|} = \dots \quad (8.29)$$

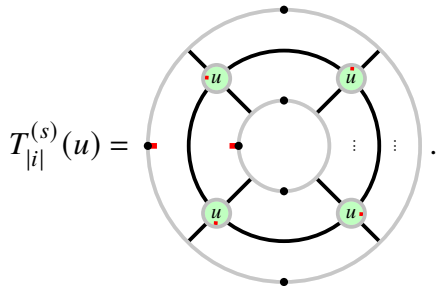
and by the positivity axiom (8.6),  $U(\rho_{|i|})$  necessarily has a positive spectrum.

A related class of operators are those with the property of *integrability*. Translating the planar-algebraic models of Chapter 3 to this setting, we introduce two classes of integrable operators acting on spacetime. Let  $(P_n)_{n \in \mathbb{N}_0}$  denote the planar algebra underlying the semicontinuous model and recall the parameterisation of the  $R$ - and  $K$ -operators:



$$\begin{aligned} \text{---} \cdot u = \sum_{a \in B_1} k_a(u) a, \quad \text{---} \cdot u \text{---} = \sum_{a \in B_2} r_a(u) a, \quad \text{---} \cdot u \text{---} = \sum_{a \in B_1} \bar{K}_a(u) a, \end{aligned} \quad (8.30)$$

where  $B_1$  and  $B_2$  denote bases for  $P_2$  and  $P_4$  respectively, and  $k_a, r_a, \bar{K}_a : \Omega \rightarrow \mathbb{C}$ . For each algebra  $\mathcal{A}_i$ , we introduce the *global transfer operator*



$$T_{|i|}^{(s)}(u) = \dots \quad (8.31)$$

It follows from Proposition 3.2.1, that if the  $R$ -operators satisfy a particular set of relations, then each of the global transfer operators are integrable. In this case, following the prescription in Section 3.5, we can associate to each  $\mathcal{A}_i$  a corresponding set of *global Hamiltonians*  $\{H_j^{(s)} \mid j \in S\}$  that satisfy

$$[T_{|i|}^{(s)}(u), H_j^{(s)}] = 0, \quad [H_j^{(s)}, H_k^{(s)}] = 0, \quad \forall j, k \in S. \quad (8.32)$$

Moreover, if the  $R$ -operator has an identity point (in the sense of Proposition 3.4.2), then  $\rho_{|i|}$  is among the global Hamiltonians derived from the transfer operator  $T_{|i|}^{(s)}(u)$ ! It follows that the transfer operator and each of the global Hamiltonians share a common set of eigenvectors with the generator of infinitesimal time-evolution. Returning to observations made in Chapter 1, a solution to a statistical mechanical model described by a transfer operator  $T_{|i|}^{(s)}(u)$ , can immediately be passed to the corresponding semicontinuous model. We, therefore, regard the global transfer operator as playing an essential role in describing the dynamics of semicontinuous models [115].

Similarly, for each  $\mathcal{A}_i(I)$ , we introduce the *local transfer operator*

$$T_{|i|}^{(d)}(u) = \text{Diagram} \quad (8.33)$$

It likewise follows from Proposition 3.2.2 that if the  $R$ - and  $K$ -operators satisfy a particular set of relations, then each of the local transfer operators are integrable. In this case, we associate to each  $\mathcal{A}_i(I)$  a set of *local Hamiltonians* analogous to those introduced (8.32).

While the results reported in this chapter are preliminary, they do indicate the applicability of planar-algebraic models beyond statistical mechanical systems. In the following chapter, we outline future projects that aim to strengthen the ties between the planar-algebraic framework and the QFTs sketched here.





# Chapter 9

---

## Conclusion

---

In this thesis, we developed a planar-algebraic framework to describe two-dimensional statistical mechanical models defined on the strip and the cylinder. In each case, we introduced a set of sufficient conditions implying integrability that are more general than is typically presented in the literature. For integrable models, we have revisited the notion of integrals of motion algebraically and considered algebraic relations among those that arise from the transfer operator, which we refer to as Hamiltonians. To characterise one extreme, where each of the Hamiltonians is polynomial in a single algebraic element, we have introduced the notion of polynomial integrability and have developed necessary and sufficient conditions for a large class of planar-algebraic models to be polynomially integrable. A simple corollary of this result is that models described by integrable and diagonalisable transfer operators are polynomially integrable – indicating the ubiquity of this property.

We then applied this framework to planar-algebraic models encoded by the class of singly generated planar algebras on both the strip and the cylinder. We showed that such models are homogeneous Yang–Baxter integrable if and only if the underlying planar algebra satisfies a Yang–Baxter relation. In establishing this result, we incorporated the well-known homogeneous Yang–Baxter integrable models encoded by the Fuss–Catalan and Birman–Wenzl–Murakami algebras into our framework and constructed a new integrable model based on the Liu planar algebra. We also showed that each of these models on the strip is polynomially integrable, although we did not determine the explicit polynomials.

As another application of our framework, we considered two planar-algebraic models defined on the strip, one underlied by the Temperley–Lieb planar algebra and the other underlied by the tensor planar algebra. In each case, we highlighted when the model is polynomially integrable and determined explicit polynomials in terms of which the transfer operator is expressible.

To demonstrate an application of the planar-algebraic framework beyond regular lattices, we introduced a dilute loop model and a dense loop model underlied by the tensor planar algebra, defined on causal triangulations of the cylinder. In each case, we showed that these models admit a description as labelled planar trees. However, only for the dense model could the corresponding tree model be solved exactly using standard methods. For the dilute loop model, we determined the critical behaviour by developing transfer operator techniques, which revealed that this model induces a change

in the Hausdorff dimension relative to the pure triangulation model. This result suggests a non-trivial interaction between the dilute ‘matter fields’ and the ‘gravitation’ of the pure triangulations.

Last of all, we demonstrated the applicability of planar-algebraic models beyond statistical mechanics by showing how these models relate to a particular class of QFTs. For this class, we introduced Jones’ semicontinuous models as ‘almost’ examples and detailed some recent efforts to make them fully-fledged examples. Within semicontinuous models, we highlighted the relevance of the planar-algebraic framework and showed that the corresponding single-row transfer operator plays a crucial role.

We conclude this thesis with a brief discussion of avenues for further research. Starting with integrable planar-algebraic models, an immediate continuation of Chapter 5 would be to develop a similar classification for *doubly generated* planar algebras. Indeed, this would require advances on two fronts (i) a classification of the algebras themselves, analogous to Liu’s classification, and (ii) a classification of those that admit solutions to the integrability sufficient conditions. An intermediate step along these lines would be to develop *singly generated extensions* of the Fuss–Catalan, Birman–Wenzl–Murakami and Liu planar algebras; and determine whether these give rise to Yang–Baxter integrable planar-algebraic models. Another avenue is to develop an *inhomogeneous* Yang–Baxter integrability framework, wherein the transfer operators are not spatially uniform. In principle, this framework would incorporate the possibility of a shaded transfer operator.

Focusing on polynomial integrability, it would be interesting to consider the physical consequences of this property. A natural approach would be to construct explicit models that are *not* polynomially integrable and compare them to related models that are. Initial indications suggest that polynomial integrability is less common on the cylinder. The reason for this is likely related to the natural tendency for rotation on the cylinder, the generation of which requires an additional operator. Another avenue of interest is to reinterpret known results in light of polynomial integrability, for example, the  $T$ -systems [116, 117] and  $Y$ -systems [118, 119], and functional relations more generally [46, 120–122].

A natural extension of the work in Chapter 7, is to consider the generalisation of the dilute loop model outlined in Section 7.6, in addition to considering dense and dilute loop models where the loop fugacity is different to one. An immediate consequence is that these models would no longer admit a natural description in terms of the tensor planar algebra. An obvious replacement would be the Temperley–Lieb planar algebra or a dilute version thereof. Why stop at Temperley–Lieb planar algebras? One may also consider other types of loop models on causal triangulations, for example, the so-called fused Temperley–Lieb loop models [61, 122, 123] based on [124, 125], and loop models with an underlying Birman–Wenzl–Murakami algebraic structure [59, 126]. Thinking beyond loop models, one may adapt vertex models [11, 34, 66, 67, 127] and RSOS models [128, 129] to the setting of causal triangulations. In all of these cases, we envisage the applicability of the planar-algebraic framework. In particular, the prominence of the transfer operator in analysing the partition functions, in addition to correlation functions more broadly.

Finally, we consider projects strengthening the connections between the planar-algebraic framework and QFTs sketched in Chapter 8. Of immediate interest is to construct semicontinuous models that are

examples of discrete conformal nets. A promising approach is to develop and solve sufficient conditions endowing continuity to representations of  $T_k$  via the Jones action. It would also be interesting to consider semicontinuous models whose symmetry group is enlarged, i.e. replacing Thompson's group  $T_k$  with one of the so-called *forest-skein groups* introduced recently by Brothier [130, 131]. Planar algebras need not be the only structures giving rise to discrete conformal nets, we envisage considering other examples and studying their properties. It would also be appealing to develop a ‘continuum limit’ that takes discrete conformal nets to conformal nets. This limit, if successfully developed, would be a systematic procedure to associate a subfactor to conformal field theory [107]. We also note that conformal nets are one example of AQFTs. It would be interesting to define *discrete algebraic quantum field theory* and consider examples beyond discrete conformal nets.



# Appendix A

---

## Appendix

---

### A.1 TL algebra Baxterisation

We begin with the YBEs (3.31), and define

$$\Delta_{Y,1} := \begin{array}{c} \text{Diagram 1} \\ \text{Diagram 2} \end{array} - \begin{array}{c} \text{Diagram 3} \\ \text{Diagram 4} \end{array} \quad (\text{A.1})$$

$$\Delta_{Y,2} := \begin{array}{c} \text{Diagram 5} \\ \text{Diagram 6} \end{array} - \begin{array}{c} \text{Diagram 7} \\ \text{Diagram 8} \end{array} \quad \Delta_{Y,3} := \begin{array}{c} \text{Diagram 9} \\ \text{Diagram 10} \end{array} - \begin{array}{c} \text{Diagram 11} \\ \text{Diagram 12} \end{array}. \quad (\text{A.2})$$

Similarly for the Invs (3.30), we define

$$\Delta_{I,i} := \begin{array}{c} \text{Diagram 13} \\ \text{Diagram 14} \end{array} - \begin{array}{c} \text{Diagram 15} \\ \text{Diagram 16} \end{array}. \quad (\text{A.3})$$

Expanding  $0 = \Delta_{Y,1}$  and collecting coefficients, we arrive at the constraint:

$$e_1 - e_2 : \quad 0 = [r_e(u)r_e(v) - r_{\mathbb{1}}(u)r_{\mathbb{1}}(v)]\bar{y}_e^{(1)} + [r_{\mathbb{1}}(u)r_e(v) + r_e(u)r_{\mathbb{1}}(v) + \delta r_e(u)r_e(v)]\bar{y}_{\mathbb{1}}^{(1)}. \quad (\text{A.4})$$

Similarly for  $0 = \Delta_{I,1}$ , we have:

$$\mathbb{1} : \quad 0 = y_e^{(1)}\bar{y}_e^{(1)} - 1 \quad (\text{A.5})$$

$$e : \quad 0 = y_{\mathbb{1}}^{(1)}\bar{y}_e^{(1)} + y_e^{(1)}\bar{y}_{\mathbb{1}}^{(1)} + \delta y_{\mathbb{1}}^{(1)}\bar{y}_{\mathbb{1}}^{(1)}. \quad (\text{A.6})$$

Applying the functions of Proposition 5.1.1 to the constraints  $0 = \Delta_{Y,1}$  and  $0 = \Delta_{I,1}$ , we indeed have a homogeneous Baxterisation.

## A.2 FC algebra Baxterisation

Expanding  $0 = \Delta_{Y,1}$  and collecting coefficients, we arrive at the constraints:

$$E_1 P_2 - P_1 E_2 : \quad 0 = [r_{\mathbb{1}}(u)r_P(v) - r_P(u)r_E(v)]\bar{y}_E^{(1)} - r_E(v)[r_{\mathbb{1}}(u) + \gamma r_P(u)]\bar{y}_P^{(1)} \quad (\text{A.7})$$

$$P_2 E_1 - E_2 P_1 : \quad 0 = [r_P(u)r_{\mathbb{1}}(v) - r_E(u)r_P(v)]\bar{y}_E^{(1)} - r_E(u)[r_{\mathbb{1}}(v) + \gamma r_P(v)]\bar{y}_P^{(1)} \quad (\text{A.8})$$

$$P_1 - P_2 : \quad 0 = r_{\mathbb{1}}(u)r_{\mathbb{1}}(v)\bar{y}_P^{(1)} - [r_P(u)r_{\mathbb{1}}(v) + r_{\mathbb{1}}(u)r_P(v) + \gamma r_P(u)r_P(v)]\bar{y}_{\mathbb{1}}^{(1)} \quad (\text{A.9})$$

$$E_1 - E_2 : \quad 0 = [r_{\mathbb{1}}(u)r_{\mathbb{1}}(v) - r_E(u)r_E(v)]\bar{y}_E^{(1)} - \gamma r_E(u)r_E(v)\bar{y}_P^{(1)} \\ - \bar{y}_{\mathbb{1}}^{(1)}[r_{\mathbb{1}}(u)r_E(v) + r_E(u)r_{\mathbb{1}}(v) + \gamma(r_P(u)r_E(v) + r_E(u)r_P(v)) + \gamma^2 r_E(u)r_E(v)]. \quad (\text{A.10})$$

Similarly for  $0 = \Delta_{I,1}$ , we have:

$$\mathbb{1} : \quad 0 = y_E^{(1)}\bar{y}_E^{(1)} - 1 \quad (\text{A.11})$$

$$P : \quad 0 = y_P^{(1)}\bar{y}_E^{(1)} + y_E^{(1)}\bar{y}_P^{(1)} + \gamma y_P^{(1)}\bar{y}_P^{(1)} \quad (\text{A.12})$$

$$E : \quad 0 = y_{\mathbb{1}}^{(1)}\bar{y}_E^{(1)} + y_E^{(1)}\bar{y}_{\mathbb{1}}^{(1)} + \gamma(y_{\mathbb{1}}^{(1)}\bar{y}_P^{(1)} + y_P^{(1)}\bar{y}_{\mathbb{1}}^{(1)}) + \gamma^2 y_{\mathbb{1}}^{(1)}\bar{y}_{\mathbb{1}}^{(1)}. \quad (\text{A.13})$$

Applying the functions of Proposition 5.3.2 to the constraints  $0 = \Delta_{Y,1}$  and  $0 = \Delta_{I,1}$ , we indeed have a homogeneous Baxterisation.

## A.3 BMW algebra Baxterisation

Expanding  $0 = \Delta_{Y,1}$  and collecting coefficients, we arrive at the constraints:

$$e_1 g_2 - g_1 e_2 : \quad 0 = [r_{\mathbb{1}}(u)r_g(v) - r_g(u)r_e(v) + Qr_g(u)r_g(v)]\bar{y}_e^{(1)} - r_{\mathbb{1}}(u)r_e(v)\bar{y}_g^{(1)} \quad (\text{A.14})$$

$$g_2 e_1 - e_2 g_1 : \quad 0 = [r_g(u)r_{\mathbb{1}}(v) - r_e(u)r_g(v) + Qr_g(u)r_g(v)]\bar{y}_e^{(1)} - r_e(u)r_{\mathbb{1}}(v)\bar{y}_g^{(1)} \quad (\text{A.15})$$

$$g_1 - g_2 : \quad 0 = r_{\mathbb{1}}(u)r_{\mathbb{1}}(v)\bar{y}_g^{(1)} - [r_g(u)r_{\mathbb{1}}(v) + r_{\mathbb{1}}(u)r_g(v) + Qr_g(u)r_g(v)]\bar{y}_{\mathbb{1}}^{(1)} \quad (\text{A.16})$$

$$e_1 - e_2 : \quad 0 = [r_e(u)r_e(v) - Q(r_g(u)r_e(v) + r_e(u)r_g(v)) + Q^2 r_g(u)r_g(v)]\bar{y}_e^{(1)} \quad (\text{A.17})$$

$$- \tau Q(r_e(u)r_e(v) + r_{\mathbb{1}}(u)r_e(v) + r_e(u)r_{\mathbb{1}}(v)) - r_e(u)r_e(v)\tau^2]\bar{y}_{\mathbb{1}}^{(1)} - \tau^2 Qr_e(u)r_e(v)\bar{y}_g^{(1)} \\ + \tau Q[r_{\mathbb{1}}(u)r_{\mathbb{1}}(v) - r_e(u)r_e(v) + Q(r_g(u)r_e(v) + r_e(u)r_g(v)) - Q^2 r_g(u)r_g(v)]\bar{y}_e^{(1)}.$$

Similarly for  $0 = \Delta_{I,1}$ , we have:

$$\mathbb{1} : \quad 0 = y_e^{(1)}\bar{y}_e^{(1)} + (1 + Q^2)y_g^{(1)}\bar{y}_g^{(1)} - Q[y_e^{(1)}\bar{y}_g^{(1)} + y_g^{(1)}\bar{y}_e^{(1)}] - 1 \quad (\text{A.18})$$

$$g : \quad 0 = y_e^{(1)}\bar{y}_g^{(1)} + y_g^{(1)}\bar{y}_e^{(1)} - Qy_g^{(1)}\bar{y}_g^{(1)} \quad (\text{A.19})$$

$$e : \quad 0 = \tau Q[y_{\mathbb{1}}^{(1)}\bar{y}_{\mathbb{1}}^{(1)} + y_e^{(1)}\bar{y}_{\mathbb{1}}^{(1)} + y_{\mathbb{1}}^{(1)}\bar{y}_e^{(1)} + Q(y_e^{(1)}\bar{y}_g^{(1)} + y_g^{(1)}\bar{y}_e^{(1)}) - Q^2 y_g^{(1)}\bar{y}_g^{(1)}] \\ + \tau^2 [y_{\mathbb{1}}^{(1)} + Qy_g^{(1)}][\bar{y}_{\mathbb{1}}^{(1)} + Q\bar{y}_g^{(1)}] - y_{\mathbb{1}}^{(1)}\bar{y}_{\mathbb{1}}^{(1)}. \quad (\text{A.20})$$

Applying the functions of Proposition 5.4.2 to the constraints  $0 = \Delta_{Y,1}$  and  $0 = \Delta_{I,1}$ , we indeed have a homogeneous Baxterisation.

## A.4 Liu algebra Baxterisation

Expanding  $0 = \Delta_{Y,i}$  for each  $i = 1, 2, 3$ , we arrive at the constraints:

$$e_1 s_2 - s_1 e_2 : 0 = \delta^2 [r_{\mathbb{1}}(u)r_s(v) - \epsilon r_s(u)r_e(v)] \bar{y}_e^{(1)} - [\delta^2 r_{\mathbb{1}}(u)r_e(v) - \epsilon r_s(u)r_s(v)] \bar{y}_s^{(1)} \quad (\text{A.21})$$

$$s_2 e_1 - e_2 s_1 : 0 = \delta^2 [\epsilon r_s(u)r_{\mathbb{1}}(v) - r_e(u)r_s(v)] \bar{y}_e^{(1)} - \epsilon [\delta^2 r_e(u)r_{\mathbb{1}}(v) + \epsilon r_s(u)r_s(v)] \bar{y}_s^{(1)} \quad (\text{A.22})$$

$$s_1 - s_2 : 0 = -\delta^2 [r_s(u)r_{\mathbb{1}}(v) + r_{\mathbb{1}}(u)r_s(v)] \bar{y}_{\mathbb{1}}^{(1)} + [\delta^2 r_{\mathbb{1}}(u)r_{\mathbb{1}}(v) - r_s(u)r_s(v)] \bar{y}_s^{(1)} \quad (\text{A.23})$$

$$e_1 - e_2 : 0 = -\delta [r_e(u)r_e(v) - r_{\mathbb{1}}(u)r_{\mathbb{1}}(v)] \bar{y}_e^{(1)} + \epsilon^{-1} [r_s(u)r_e(v) + \epsilon^2 r_e(u)r_s(v)] \bar{y}_s^{(1)} \quad (\text{A.24}) \\ + [r_s(u)r_s(v) - \delta(r_{\mathbb{1}}(u)r_e(v) + r_e(u)r_{\mathbb{1}}(v)) - \delta^2 r_e(u)r_e(v)] \bar{y}_{\mathbb{1}}^{(1)}$$

$$e_1 s_2 - s_1 e_2 : 0 = -\delta^2 [r_s(u)r_e(v) - r_e(u)r_s(v)] \bar{y}_e^{(2)} + [r_s(u)r_s(v) - \delta^2 r_e(u)r_e(v)] \bar{y}_s^{(2)} \quad (\text{A.25})$$

$$s_2 e_1 - e_2 s_1 : 0 = \delta^2 [r_s(u)r_{\mathbb{1}}(v) - r_{\mathbb{1}}(u)r_s(v)] \bar{y}_e^{(2)} - \epsilon [r_s(u)r_s(v) + \delta^2 r_{\mathbb{1}}(u)r_{\mathbb{1}}(v)] \bar{y}_s^{(2)} \quad (\text{A.26})$$

$$s_1 - s_2 : 0 = -\delta^2 [r_s(u)r_{\mathbb{1}}(v) + \epsilon r_e(u)r_s(v)] \bar{y}_{\mathbb{1}}^{(2)} + [\epsilon \delta^2 r_e(u)r_{\mathbb{1}}(v) - r_s(u)r_s(v)] \bar{y}_s^{(2)} \quad (\text{A.27})$$

$$e_1 - e_2 : 0 = -\epsilon \delta [r_{\mathbb{1}}(u)r_e(v) - r_e(u)r_{\mathbb{1}}(v)] \bar{y}_e^{(2)} + \epsilon^{-1} [r_s(u)r_e(v) + r_{\mathbb{1}}(u)r_s(v)\epsilon^3] \bar{y}_s^{(2)} \quad (\text{A.28}) \\ + [r_s(u)r_s(v) - \epsilon \delta(r_e(u)r_e(v) + r_{\mathbb{1}}(u)r_{\mathbb{1}}(v)) - \epsilon \delta^2 r_{\mathbb{1}}(u)r_e(v)] \bar{y}_{\mathbb{1}}^{(2)}$$

$$e_1 s_2 - s_1 e_2 : 0 = \epsilon \delta^2 [r_s(u)r_{\mathbb{1}}(v) - r_{\mathbb{1}}(u)r_s(v)] \bar{y}_e^{(3)} + [\epsilon^2 r_s(u)r_s(v) - \delta^2 r_{\mathbb{1}}(u)r_{\mathbb{1}}(v)] \bar{y}_s^{(3)} \quad (\text{A.29})$$

$$s_2 e_1 - e_2 s_1 : 0 = -\delta^2 [r_s(u)r_e(v) - r_e(u)r_s(v)] \bar{y}_e^{(3)} - [\delta^2 r_e(u)r_e(v) + \epsilon^2 r_s(u)r_s(v)] \bar{y}_s^{(3)} \quad (\text{A.30})$$

$$s_1 - s_2 : 0 = -\delta^2 [r_e(u)r_s(v) + \epsilon r_s(u)r_{\mathbb{1}}(v)] \bar{y}_{\mathbb{1}}^{(3)} + [\delta^2 r_e(u)r_{\mathbb{1}}(v) - \epsilon r_s(u)r_s(v)] \bar{y}_s^{(3)} \quad (\text{A.31})$$

$$e_1 - e_2 : 0 = -\delta [r_{\mathbb{1}}(u)r_e(v) - r_e(u)r_{\mathbb{1}}(v)] \bar{y}_e^{(3)} + \epsilon^{-1} [r_{\mathbb{1}}(u)r_s(v) + \epsilon^3 r_s(u)r_e(v)] \bar{y}_s^{(3)} \quad (\text{A.32}) \\ + [\epsilon r_s(u)r_s(v) - \delta(r_e(u)r_e(v) + r_{\mathbb{1}}(u)r_{\mathbb{1}}(v)) - \delta^2 r_{\mathbb{1}}(u)r_e(v)] \bar{y}_{\mathbb{1}}^{(3)}.$$

Similarly for  $0 = \Delta_{I,i}$  we have:

$$\mathbb{1} : 0 = y_e^{(i)} \bar{y}_e^{(i)} + \epsilon^{-2} y_s^{(i)} \bar{y}_s^{(i)} - 1 \quad (\text{A.33})$$

$$s : 0 = y_e^{(i)} \bar{y}_{\mathbb{1}}^{(i)} + y_{\mathbb{1}}^{(i)} \bar{y}_e^{(i)} + \delta y_{\mathbb{1}}^{(i)} \bar{y}_{\mathbb{1}}^{(i)} - \epsilon^{-2} \delta^{-1} y_s^{(i)} \bar{y}_s^{(i)} \quad (\text{A.34})$$

$$e : 0 = y_s^{(i)} \bar{y}_e^{(i)} + y_e^{(i)} \bar{y}_s^{(i)} \quad (\text{A.35})$$

for  $i = 1, 2, 3$ . Applying the functions of Proposition 5.5.2 to the constraints  $0 = \Delta_{Y,i}$  and  $0 = \Delta_{I,i}$  for each  $i = 1, 2, 3$ , we indeed have a homogeneous Baxterisation.

## A.5 $\text{TL}_n(\delta)$ polynomials

### A.5.1 Principal hamiltonian $h_0$

For  $n = 2, \dots, 7$  and  $\delta$  an indeterminate, the minimal polynomial for  $h_0$  is given by

$$m_0^{(2)}(h) = h^2 + \delta h, \quad (\text{A.36})$$

$$m_0^{(3)}(h) = h^3 + 2\delta h^2 + (\delta^2 - 1)h, \quad (\text{A.37})$$

$$m_0^{(4)}(h) = h^6 + 6\delta h^5 + 14(\delta^2 - \frac{2}{7})h^4 + 16\delta(\delta^2 - \frac{7}{8})h^3 + 9(\delta^4 - \frac{16}{9}\delta^2 + \frac{4}{9})h^2 + 2\delta(\delta^4 - 3\delta^2 + 2)h, \quad (\text{A.38})$$

$$m_0^{(5)}(h) = h^{10} + 12\delta h^9 + 63(\delta^2 - \frac{1}{7})h^8 + 190\delta(\delta^2 - \frac{41}{95})h^7 + \dots, \quad (\text{A.39})$$

$$m_0^{(6)}(h) = h^{20} + 30\delta h^{19} + 423(\delta^2 - \frac{8}{141})h^{18} + 3726\delta(\delta^2 - \frac{106}{621})h^{17} + \dots, \quad (\text{A.40})$$

$$m_0^{(7)}(h) = h^{35} + 60\delta h^{34} + 1740(\delta^2 - \frac{5}{174})h^{33} + 32488\delta(\delta^2 - \frac{701}{8122})h^{32} + \dots \quad (\text{A.41})$$

In a matrix representation of  $\rho_n(h_0)$ , the off-diagonal elements are independent of  $\delta$ , whereas the diagonal elements are of the form  $-i\delta$ ,  $i \in \{0, \dots, \lfloor \frac{n}{2} \rfloor\}$ . Since the number of elements equal to  $-i\delta$  is  $\binom{\lfloor \frac{n}{2} \rfloor}{i} \binom{\lceil \frac{n}{2} \rceil}{i}$ , and

$$\sum_{i=0}^{\lfloor \frac{n}{2} \rfloor} \binom{\lfloor \frac{n}{2} \rfloor}{i} \binom{\lceil \frac{n}{2} \rceil}{i} i = \lfloor \frac{n}{2} \rfloor c_{n-1}, \quad (\text{A.42})$$

it follows that

$$m_0^{(n)}(h) = h^{c_n} + \lfloor \frac{n}{2} \rfloor c_{n-1} \delta h^{c_n-1} + \dots \quad (\text{A.43})$$

We also note that the degree of the monic  $\delta$ -polynomial multiplying  $h^i$  in  $m_0^{(n)}(h)$  is given by  $c_n - i$ , and that this  $\delta$ -polynomial is even (respectively odd) if the degree is even (respectively odd).

For  $\delta = 0$  and  $n \geq 2$ , there are spurious degeneracies in the spectrum of  $\rho_n(h_0)$ , so  $l_{0,0}^{(n)}$  could be smaller than  $l_0^{(n)}$ . Through direct computation, we find

$$m_0^{(n)}(h)|_{\delta=0} = m_{0,0}^{(n)}(h), \quad n = 2, 3, 4, \quad (\text{A.44})$$

$$m_0^{(5)}(h)|_{\delta=0} = h m_{0,0}^{(5)}(h), \quad (\text{A.45})$$

$$m_0^{(6)}(h)|_{\delta=0} = h^2 m_{0,0}^{(6)}(h), \quad (\text{A.46})$$

$$m_0^{(7)}(h)|_{\delta=0} = h^2 U_6(\frac{h}{2}) m_{0,0}^{(7)}(h). \quad (\text{A.47})$$

We thus have

$n$	2	3	4	5	6	7
$l_{0,0}^{(n)}$	2	3	6	9	18	27
$l_0^{(n)}$	2	3	6	10	20	35

which confirms the following conjecture for  $n = 2, \dots, 7$ .

**Conjecture A.5.1.** For  $n \in \mathbb{N}_{\geq 2}$ , we have

$$l_{0,0}^{(n)} = \frac{1}{2} (3^{\lfloor \frac{n+1}{2} \rfloor} + (-1)^n 3^{\lfloor \frac{n-1}{2} \rfloor}). \quad (\text{A.48})$$

### A.5.2 Principal hamiltonian $h_{-\frac{2}{\delta}}$

For  $n = 2, 3, 4, 5$ , the principal hamiltonian  $h_{n,-\frac{2}{\delta}}$  is given by

$$h_{2,-\frac{2}{\delta}} = e_1, \quad (\text{A.49})$$

$$h_{3,-\frac{2}{\delta}} = -\frac{1}{2\delta}(\delta^2 + 4)(e_1 + e_2) + e_1 e_2 + e_2 e_1, \quad (\text{A.50})$$

$$\begin{aligned} h_{4,-\frac{2}{\delta}} = & \frac{1}{4\delta^2}(\delta^4 + 4\delta^2 + 16)(e_1 + e_3) + \frac{1}{4\delta^2}(\delta^2 + 4)^2 e_2 - \frac{1}{2\delta}(\delta^2 + 4)(e_1 e_2 + e_2 e_1 + e_2 e_3 + e_3 e_2) \\ & - \frac{4}{\delta}e_1 e_3 + e_1 e_2 e_3 + e_3 e_2 e_1 + e_1 e_3 e_2 + e_2 e_1 e_3, \end{aligned} \quad (\text{A.51})$$

$$\begin{aligned} h_{5,-\frac{2}{\delta}} = & -\frac{1}{8\delta^3}(\delta^2 + 4)(\delta^4 + 16)(e_1 + e_4) - \frac{1}{8\delta^3}(\delta^2 + 4)(\delta^4 + 4\delta^2 + 16)(e_2 + e_3) \\ & + \frac{1}{4\delta^2}(\delta^4 + 4\delta^2 + 16)(e_1 e_2 + e_3 e_4 + e_4 e_3 + e_2 e_1) + \frac{1}{4\delta^2}(\delta^2 + 4)^2(e_2 e_3 + e_3 e_2) \\ & + \frac{2}{\delta^2}(\delta^2 + 4)(e_1 e_3 + e_2 e_4) + \frac{8}{\delta^2}e_1 e_4 - \frac{4}{\delta}(e_1 e_2 e_4 + e_1 e_3 e_4 + e_1 e_4 e_3 + e_2 e_1 e_4) \\ & - \frac{1}{2\delta}(\delta^2 + 4)(e_1 e_2 e_3 + e_1 e_3 e_2 + e_2 e_1 e_3 + e_2 e_3 e_4 + e_2 e_4 e_3 + e_3 e_2 e_1 + e_3 e_2 e_4 + e_4 e_3 e_2) \\ & + e_1 e_2 e_3 e_4 + e_1 e_2 e_4 e_3 + e_1 e_3 e_2 e_4 + e_1 e_4 e_3 e_2 + e_2 e_1 e_3 e_4 + e_2 e_1 e_4 e_3 + e_3 e_2 e_1 e_4 + e_4 e_3 e_2 e_1, \end{aligned} \quad (\text{A.52})$$

and for  $\delta$  an indeterminate, its minimal polynomial is given by

$$m_{-\frac{2}{\delta}}^{(2)}(h) = h^2 - \delta h, \quad (\text{A.53})$$

$$m_{-\frac{2}{\delta}}^{(3)}(h) = h^3 + \frac{2\delta}{2\delta}(\delta^2 + 2)h^2 + \frac{1}{(2\delta)^2}(\delta^6 + 3\delta^4 + 12\delta^2 - 16)h, \quad (\text{A.54})$$

$$m_{-\frac{2}{\delta}}^{(4)}(h) = h^6 - \frac{6\delta}{(2\delta)^2}(\delta^4 + \frac{8}{3}\delta^2 + \frac{16}{3})h^5 + \frac{14}{(2\delta)^4}(\delta^{10} + \frac{38}{7}\delta^8 + \dots)h^4 - \frac{16\delta}{(2\delta)^6}(\delta^{14} + \dots)h^3 + \dots, \quad (\text{A.55})$$

$$m_{-\frac{2}{\delta}}^{(5)}(h) = h^{10} + \frac{12\delta}{(2\delta)^3}(\delta^6 + 3\delta^4 + 8\delta^2 + 16)h^9 + \frac{63}{(2\delta)^6}(\delta^{14} + \dots)h^8 + \frac{190\delta}{(2\delta)^9}(\delta^{20} + \dots)h^7 + \dots \quad (\text{A.56})$$

We note that the numerators of the fractions multiplying the even monic  $\delta$ -polynomials in these minimal polynomials are the same as the coefficients to the similar terms in (A.36)–(A.39). We also note that the degree of the monic  $\delta$ -polynomial multiplying  $h^i$  in  $m_0^{(n)}(h)$  is given by  $(n-1)(c_n - i)$ , and that this  $\delta$ -polynomial is even (respectively odd) if the degree is even (respectively odd). For the  $h_{-\frac{2}{\delta}}$  counterpart to (A.43), we conjecture the following expression.

**Conjecture A.5.2.** For  $n \in \mathbb{N}_{\geq 2}$ , we have

$$m_{-\frac{2}{\delta}}^{(n)}(h) = h^{c_n} - (-1)^n \left\lfloor \frac{n}{2} \right\rfloor \frac{c_{n-1}}{2^{n-2}} \left( \delta^{n-1} + \frac{4(n-2)}{n-1} \delta^{n-3} + \dots \right) h^{c_n-1} + \dots \quad (\text{A.57})$$

### A.5.3 Decomposition conjectures

**Conjecture A.5.3.** Let  $n \in \mathbb{N}_{\geq 3}$  and  $\delta$  an indeterminate. Then,  $\tilde{T}_n(x)$  admits a unique decomposition of the form

$$\tilde{T}_n(x) = \left[ \delta U_n\left(\frac{x}{2}\right) + 2U_{n-1}\left(\frac{x}{2}\right) \right] \mathbb{1}_n + (\delta^2 + 2\delta x + 4) \left( x^{n-3} \left[ (\delta - x)h_0 + h_0^2 \right] + \frac{1}{f_{n,0}(\delta)} \sum_{i=1}^{c_{n-1}} \sum_{k=0}^{n-4} \tilde{a}_{i,k}^{n,0}(\delta) x^k h_0^i \right), \quad (\text{A.58})$$

where  $f_{n,0}(\delta)$  is as in Conjecture 6.1.15 and  $\tilde{a}_{i,k}^{n,0}(\delta)$  are polynomials such that no root of  $f_{n,0}(\delta)$  is a root of  $\tilde{a}_{i,k}^{n,0}(\delta)$  for all  $i, k$ .

The form of the contribution  $x^{n-3} \left[ (\delta - x)h_0 + h_0^2 \right]$  follows from continuing the expansion (6.43) to third order in  $\epsilon$ :

$$\begin{aligned} T_n(\epsilon, \delta) = & \left[ \delta + 2\epsilon - (n-1)\epsilon^2 \delta - 2(n-2)\epsilon^3 \right] \mathbb{1}_n \\ & - 2\epsilon \delta h_0 + \epsilon^2 \left[ 2\delta h_0^2 + (\delta^2 - 4)h_0 \right] + \epsilon^3 (4 + \delta^2) (h_0^2 + \delta h_0) + O(\epsilon^4). \end{aligned} \quad (\text{A.59})$$

We have verified Conjecture A.5.3 for  $n = 3, 4, 5, 6$ , finding

$$\tilde{a}_{1,0}^{4,0}(\delta) = \frac{1}{2}\delta^4 - 2\delta^2 + 2, \quad \tilde{a}_{2,0}^{4,0}(\delta) = \frac{7}{4}\delta^3 - \frac{7}{2}\delta, \quad \tilde{a}_{3,0}^{4,0}(\delta) = \frac{9}{4}\delta^2 - \frac{3}{2}, \quad \tilde{a}_{4,0}^{4,0}(\delta) = \frac{5}{4}\delta, \quad \tilde{a}_{5,0}^{4,0}(\delta) = \frac{1}{4}, \quad (\text{A.60})$$

and

$$\tilde{a}_{1,0}^{5,0}(\delta) = 16\delta^{13} - 20\delta^{11} - 1266\delta^9 + \frac{20349}{4}\delta^7 - \frac{16291}{4}\delta^5 - \frac{13207}{4}\delta^3 + 1749\delta, \quad (\text{A.61})$$

$$\tilde{a}_{1,1}^{5,0}(\delta) = -72\delta^{12} + \frac{1085}{2}\delta^{10} - \frac{1541}{4}\delta^8 - \frac{29325}{8}\delta^6 + \frac{49671}{8}\delta^4 - \frac{3815}{8}\delta^2 - \frac{1331}{2}, \quad (\text{A.62})$$

$$\tilde{a}_{2,0}^{5,0}(\delta) = 104\delta^{12} - \frac{57}{2}\delta^{10} - 7996\delta^8 + \frac{46665}{2}\delta^6 - \frac{21031}{2}\delta^4 - \frac{16799}{2}\delta^2 + 1320, \quad (\text{A.63})$$

$$\tilde{a}_{2,1}^{5,0}(\delta) = -460\delta^{11} + \frac{11439}{4}\delta^9 + \frac{1901}{4}\delta^7 - \frac{73429}{4}\delta^5 + \frac{72761}{4}\delta^3 - \frac{3277}{2}\delta, \quad (\text{A.64})$$

$$\tilde{a}_{3,0}^{5,0}(\delta) = 292\delta^{11} + \frac{599}{4}\delta^9 - \frac{88045}{4}\delta^7 + \frac{178239}{4}\delta^5 - \frac{31661}{4}\delta^3 - 7096\delta, \quad (\text{A.65})$$

$$\tilde{a}_{3,1}^{5,0}(\delta) = -1270\delta^{10} + \frac{52157}{8}\delta^8 + \frac{53071}{8}\delta^6 - \frac{291349}{8}\delta^4 + \frac{152711}{8}\delta^2 - \frac{627}{2}, \quad (\text{A.66})$$

$$\tilde{a}_{4,0}^{5,0}(\delta) = 462\delta^{10} + 518\delta^8 - \frac{68991}{2}\delta^6 + \frac{89539}{2}\delta^4 + \frac{1515}{2}\delta^2 - 2134, \quad (\text{A.67})$$

$$\tilde{a}_{4,1}^{5,0}(\delta) = -1977\delta^9 + \frac{16893}{2}\delta^7 + 15452\delta^5 - \frac{73257}{2}\delta^3 + 8347\delta, \quad (\text{A.68})$$

$$\tilde{a}_{5,0}^{5,0}(\delta) = 450\delta^9 + \frac{2813}{4}\delta^7 - 33643\delta^5 + 24358\delta^3 + 3106\delta, \quad (\text{A.69})$$

$$\tilde{a}_{5,1}^{5,0}(\delta) = -1896\delta^8 + \frac{54903}{8}\delta^6 + 17612\delta^4 - 19783\delta^2 + 1254, \quad (\text{A.70})$$

$$\tilde{a}_{6,0}^{5,0}(\delta) = 276\delta^8 + \frac{1021}{2}\delta^6 - \frac{41757}{2}\delta^4 + 6328\delta^2 + 924, \quad (\text{A.71})$$

$$\tilde{a}_{6,1}^{5,0}(\delta) = -1146\delta^7 + \frac{14491}{4}\delta^5 + \frac{45761}{4}\delta^3 - 5432\delta, \quad (\text{A.72})$$

$$\tilde{a}_{7,0}^{5,0}(\delta) = 104\delta^7 + \frac{829}{4}\delta^5 - \frac{32131}{4}\delta^3 + 315\delta, \quad (\text{A.73})$$

$$\tilde{a}_{7,1}^{5,0}(\delta) = -426\delta^6 + \frac{9827}{8}\delta^4 + \frac{34447}{8}\delta^2 - \frac{1177}{2}, \quad (\text{A.74})$$

$$\tilde{a}_{8,0}^{5,0}(\delta) = 22\delta^6 + 44\delta^4 - 1747\delta^2 - 110, \quad (\text{A.75})$$

$$\tilde{a}_{8,1}^{5,0}(\delta) = -89\delta^5 + 247\delta^3 + \frac{1737}{2}\delta, \quad (\text{A.76})$$

$$\tilde{a}_{9,0}^{5,0}(\delta) = 2\delta^5 + \frac{15}{4}\delta^3 - 164\delta, \quad (\text{A.77})$$

$$\tilde{a}_{9,1}^{5,0}(\delta) = -8\delta^4 + \frac{181}{8}\delta^2 + \frac{143}{2}. \quad (\text{A.78})$$

Although the polynomials  $\tilde{a}_{i,k}^{6,0}(\delta)$  are not provided here, we note that, for  $n = 4, 5, 6$  and all  $i, k$ ,

$$\deg(\tilde{a}_{i,k}^{n,0}) = d_{n,0} - i - \frac{1}{2}(1 - (-1)^k), \quad d_{4,0} = 5, d_{5,0} = 14, d_{6,0} = 63, \quad (\text{A.79})$$

and that  $\tilde{a}_{i,k}^{n,0}(\delta)$  is even (respectively odd) if its degree is even (respectively odd). This is seen to correspond to the parity of  $n + i + k + 1$ .

**Conjecture A.5.4.** *Let  $n \in \mathbb{N}_{\geq 3}$  and  $\delta$  an indeterminate. Then,  $\tilde{T}_n(x)$  admits a unique decomposition of the form*

$$\tilde{T}_n(x) = [\delta U_n(\frac{x}{2}) + 2U_{n-1}(\frac{x}{2})] \mathbb{1}_n + \frac{\delta^2 + 2\delta x + 4}{f_{n,-\frac{2}{\delta}}(\delta)} \sum_{i=1}^{c_n-1} \sum_{k=0}^{n-2} \tilde{a}_{i,k}^{n,-\frac{2}{\delta}}(\delta) x^k h_{-\frac{2}{\delta}}^i, \quad (\text{A.80})$$

where  $f_{n,-\frac{2}{\delta}}(\delta)$  is as in Conjecture 6.1.15 and  $\tilde{a}_{i,k}^{n,-\frac{2}{\delta}}(\delta)$  are polynomials such that no root of  $f_{n,-\frac{2}{\delta}}(\delta)$  is a root of  $\tilde{a}_{i,k}^{n,-\frac{2}{\delta}}(\delta)$  for all  $i, k$ .

We have verified Conjecture A.5.4 for  $n = 3, 4, 5$ , where we note that, for all  $i, k$ ,

$$\deg(\tilde{a}_{i,k}^{n,-\frac{2}{\delta}}) = d_{n,-\frac{2}{\delta}} - (n-1)i - k, \quad d_{3,-\frac{2}{\delta}} = 9, d_{4,-\frac{2}{\delta}} = 54, d_{5,-\frac{2}{\delta}} = 235, \quad (\text{A.81})$$

and that  $\tilde{a}_{i,k}^{n,-\frac{2}{\delta}}(\delta)$  is even (respectively odd) if its degree is even (respectively odd). This is seen to correspond to the parity of  $n + i + k$ .



---

# Bibliography

---

- [1] B. Durhuus, X. Poncini, J. Rasmussen, M. Ünel, *Critical behaviour of loop models on causal triangulations*, J. Stat. Mech. (2021) 113102, arXiv:2104.14176 [hep-th].
- [2] X. Poncini, J. Rasmussen, *Integrability of planar-algebraic models*, J. Stat. Mech. (2023) 073101, arXiv:2206.14462 [math-ph].
- [3] X. Poncini, J. Rasmussen, *A classification of integrable planar-algebraic models*, arXiv:2302.11712 [math-ph].
- [4] T. Jones, K. Steven, X. Poncini, M. Rose, A. Fedorov, *Approximations in transmon simulation*, Phys. Rev. Appl. **16**, (2021) 054039, arXiv:2102.09721 [quant-ph].
- [5] V.I. Arnold, *Mathematical Methods of Classical Mechanics*, Springer-Verlag (1978).
- [6] D.V. Schroeder, *An Introduction to Thermal Physics*, Addison-Wesley (2000).
- [7] M. Reed, B. Simon, *Analysis of Operators*, Academic Press (1978).
- [8] D.J. Griffiths, *Introduction to Quantum Mechanics*, Cambridge University Press (1995).
- [9] M. Henkel, *Conformal Invariance and Critical Phenomena*, Springer (1999).
- [10] M. Nielsen, I. Chuang, *Quantum Computation and Quantum Information*, Cambridge University Press (2000).
- [11] R.J. Baxter, *Exactly Solved Models in Statistical Mechanics*, Academic Press (1982).
- [12] J. Rasmussen, Lecture notes, University of Queensland (2016).
- [13] V.F.R. Jones, *Planar algebra, I*, New Zealand J. Math. **52** (2021) 1–107, arXiv:math/9909027 [math.QA].
- [14] V.F.R. Jones, *A polynomial invariant for knots via von Neumann algebras*, Bull. Amer. Math. Soc. **12** (1985) 103–111.
- [15] L.H. Kauffman, *State models and the Jones polynomial*, Topology **26** (1987) 395–407.

- [16] S. Morrison, E. Peters, N. Snyder, *Knot polynomial identities and quantum group coincidences*, Quantum Topol. **2** (2011) 101–156, arXiv:1003.0022 [math.QA].
- [17] H.N.V. Temperley, E.H. Lieb, *Relations between the ‘percolation’ and ‘colouring’ problem and other graph-theoretical problems associated with regular planar lattices: Some exact results for the ‘percolation’ problem*, Proc. Roy. Soc. A **322** (1971) 251–280.
- [18] V. Kodiyalam, V. Pati, V.S. Sunder, *Subfactors and 1+1-dimensional TQFTs*, Int. J. Math. **18** (2007), arXiv:math/0507050 [math.QA].
- [19] Ö. Ceyhan and M. Marcolli, *Open string theory and planar algebras*, J. Phys. A: Math. Theor. **43** (2010), arXiv:0907.5330 [math.QA].
- [20] V.F.R. Jones, *A no-go theorem for the continuum limit of a periodic quantum spin chain*, Commun. Math. Phys. **357** (2018) 295–317.
- [21] P.A. Pearce, J. Rasmussen, J.-B. Zuber, *Logarithmic minimal models*, J. Stat. Mech. (2006) P11017, arXiv:hep-th/0607232.
- [22] Z. Liu, S. Morrison, D. Penneys, *Lifting shadings on symmetrically self-dual subfactor planar algebras*, Contemp. Math. Amer. Math. Soc. **747** (2020) 51–61, arXiv:1709.05023 [math.OA].
- [23] V.F.R. Jones, *Lecture notes on planar algebras*, Vanderbilt University (2011), available at <https://math.berkeley.edu/~vfr/VANDERBILT/p121.pdf>.
- [24] V. Jones, V. S. Sunder, *Introduction to Subfactors*, Cambridge University Press (2009).
- [25] V.F.R. Jones, *The planar algebra of a bipartite graph*, in Knots in Hellas '98, pp. 94–117, World Scientific (2000).
- [26] V.F.R. Jones, *Index for subfactors*, Invent. Math. **72** (1983) 1–25.
- [27] V.F.R. Jones S.A. Reznikoff, *Hilbert space representations of the annular Temperley–Lieb algebra*, Pac. J. Math. **228** (2006) 219–249.
- [28] K. Iohara, G.I. Lehrer, R.B. Zhang, *The Jones quotients of the Temperley–Lieb algebras*, arXiv:1702.08128 [math.QA].
- [29] D. Bisch, V. Jones, *Singly generated planar algebras of small dimension*, Duke Math. J. **101** (2000) 41–75.
- [30] D. Bisch, V. Jones, *Singly generated planar algebras of small dimension, part II*, Adv. Math. **175** (2003) 297–318.
- [31] D. Bisch, V.F.R. Jones, Z. Liu, *Singly generated planar algebras of small dimension, part III*, Trans. Amer. Math. Soc. **369** (2017) 2461–2476, arXiv:1410.2876 [math.QA].

- [32] J.B. McGuire, *Exactly soluble one-dimensional  $N$ -body problems*, J. Math. Phys. **5** (1964) 622–636.
- [33] C.N. Yang, *Some exact results for the many-body problem in one dimension with repulsive delta-function interaction*, Phys. Rev. Lett. **19** (1967) 1312–1315.
- [34] R.J. Baxter, *Eight-vertex model in lattice statistics*, Phys. Rev. Lett. **26** (1971) 832–833.
- [35] V. Chari, A.N. Pressley, *A Guide to Quantum Groups*, Cambridge University Press (1995).
- [36] C.N. Yang, M.L. Ge, *Braid Group, Knot Theory and Statistical Mechanics*, World Scientific (1991).
- [37] L.D. Faddeev, *Integrable models in 1+1 dimensional quantum field theory*, Les Houches Lectures (1982).
- [38] V.F.R. Jones, *Baxterization*, Int. J. Mod. Phys. B **4** (1990) 701–713.
- [39] Z. Liu, *Yang–Baxter relation planar algebras*, arXiv:1507.06030 [math.OA].
- [40] V.F.R. Jones, *The annular structure of subfactors*, Monogr. Enseign. Math. **38** (2001) 401–463, arXiv:math/0105071.
- [41] S.K. Ghosh, *Planar algebras: a category theoretic point of view*, J. Alg. **339** (2011) 27–54, arXiv:0810.4186 [math.QA].
- [42] R.E. Behrend, P.A. Pearce, D.L. O’Brien, *Interaction-round-a-face models with fixed boundary conditions: the ABF fusion hierarchy*, J. Stat. Phys. **84** (1996) 1–48, arXiv:hep-th/9507118.
- [43] L.D. Faddeev, E.K. Sklyanin, L.A. Takhtajan, *Quantum inverse problem. I*, Theor. Math. Phys. **40** (1979) 688–706.
- [44] E.K. Sklyanin, *Boundary conditions for integrable quantum systems*, J. Phys. A: Math. Gen. **21** (1988) 2375–2389.
- [45] V.E. Korepin, N.M. Bogoliubov, A.G. Izergin, *Quantum Inverse Scattering Method and Correlation Functions*, Cambridge University Press (1993).
- [46] P.A. Pearce, J. Rasmussen, *Solvable critical dense polymers*, J. Stat. Mech. (2007) P02015, arXiv:hep-th/0610273.
- [47] P.M. Neumann, C.E. Praeger, *Cyclic matrices over finite fields*, J. London Math. Soc. **52** (1995) 263–284.
- [48] F.R. Gantmacher, *The Theory of Matrices*, vols. I and II, Chelsea Publishing Company (1959).
- [49] T.Y. Lam, *A First Course in Noncommutative Rings*, Springer (2001).

- [50] L.V. Ahlfors, *Complex Analysis: An Introduction to the Theory of Analytic Functions of One Complex Variable*, 3rd edition, McGraw-Hill (1979).
- [51] J.J. Graham, G.I. Lehrer, *Cellular algebras*, Invent. Math. **123** (2006) 1–34.
- [52] H. Wenzl, *On sequences of projections*, C. R. Math. Rep. Acad. Sci. Canada **9** (1987) 5–7.
- [53] V. Kodiyalam, S. Tupurani, *Universal skein theory for finite depth subfactor planar algebras*, Quantum Topol. **2** (2011) 157–172, arXiv:1003.4577 [math.QA].
- [54] D. Bisch, V. Jones, *Algebras associated to intermediate subfactors*, Invent. Math. **128** (1997) 89–157.
- [55] P. Di Francesco, *New integrable lattice models from Fuss–Catalan algebras*, Nucl. Phys. B **532** (1998) 609–634, arXiv:hep-th/9807074.
- [56] H. Wenzl, *Quantum groups and subfactors of type B, C, and D*, Commun. Math. Phys. **133** (1990) 383–432.
- [57] H.R. Morton (with A.J. Wassermann), *A basis for the Birman–Wenzl algebra*, arXiv:1012.3116 [math.QA].
- [58] L.H. Kauffman, *An invariant of regular isotopy*, Trans. Amer. Math. Soc. **318** (1990) 417–471.
- [59] J.S. Birman, H. Wenzl, *Braids, link polynomials and a new algebra*, Trans. Amer. Math. Soc. **313** (1989) 249–273.
- [60] Y. Cheng, M.L. Ge, K. Xue, *Yang–Baxterization of braid group representations*, Commun. Math. Phys. **136** (1991) 195–208.
- [61] P.A. Pearce, J. Rasmussen, E. Tartaglia, *Logarithmic superconformal minimal models*, J. Stat. Mech. (2014) P05001, arXiv:1312.6763 [hep-th].
- [62] D. Ridout, Y. Saint-Aubin, *Standard modules, induction, and the structure of the Temperley–Lieb algebra*, Adv. Theor. Math. Phys. **18** (2014) 957–1041, arXiv:1204.4505 [math-ph].
- [63] B. Westbury, *The representation theory of the Temperley–Lieb algebras*, Math. Z. **219** (1995) 539–565.
- [64] P.A. Pearce, J. Rasmussen, S.P. Villani, *Solvable critical dense polymers on the cylinder*, J. Stat. Mech. (2010) P02010, arXiv:0910.4444 [hep-th].
- [65] V. Pasquier, H. Saleur, *Common structures between finite systems and conformal field theories through quantum groups*, Nucl. Phys. B **330** (1990) 523–556.
- [66] C. Fan, F.Y. Wu, *General lattice model of phase transitions*, Phys. Rev. B **2** (1970) 723–733.

- [67] B. Sutherland, *Two-dimensional hydrogen bonded crystals without the ice rule*, *J. Math. Phys.* **11** (1970) 3183–3186.
- [68] H. Gould, J. Quaintance, *Double fun with double factorials*, *Mathematics Magazine* **85** (2012) 177–192.
- [69] V.A. Kazakov, *Ising model on a dynamical planar random lattice: Exact solution*, *Phys. Lett. A* **119** (1986) 140–144.
- [70] M. Staudacher, *The Yang-Lee edge singularity on a dynamical planar random surface*, *Nucl. Phys. B* **336** (1990) 349–362.
- [71] J.-M. Daul,  *$Q$ -states Potts model on a random planar lattice*, arXiv:hep-th/9502014.
- [72] P. Zinn-Justin, *The dilute Potts model on random surfaces*, *J. Stat. Phys.* **98** (2000) 245–264, arXiv:cond-mat/9903385 [cond-mat.stat-mech].
- [73] I.K. Kostov, M. Staudacher, *Multicritical phases of the  $O(n)$  model on a random lattice*, *Nucl. Phys. B* **384** (1992) 459–483, arXiv:hep-th/9203030.
- [74] J. Ambjørn, B. Durhuus, T. Jonsson, *Quantum Geometry: A Statistical Field Theory Approach*, Cambridge University Press (1997).
- [75] V.G. Knizhnik, A.M. Polyakov, A.B. Zamolodchikov, *Fractal structure of 2d-quantum gravity*, *Mod. Phys. Lett. A* **3** (1988) 819–826.
- [76] Y. Watabiki, *Analytic study of fractal structure of quantized surface in two-dimensional quantum gravity*, *Prog. Theor. Phys. Suppl.* **114** (1993) 1–17.
- [77] J. Ding, S. Goswami, *Upper bounds on Liouville first-passage percolation and Watabiki’s prediction*, *Commun. Pure Appl. Math.* **72** (2019) 2331–2384, arXiv:1610.09998 [math.PR].
- [78] J. Ding, E. Gwynne, *The fractal dimension of Liouville quantum gravity: universality, monotonicity, and bounds*, *Commun. Math. Phys.* **374** (2020) 1877–1934, arXiv:1807.01072 [math.PR].
- [79] J. Ambjørn, R. Loll, *Non-perturbative Lorentzian quantum gravity, causality and topology change*, *Nucl. Phys. B* **536** (1998) 407–434, arXiv:hep-th/9805108.
- [80] J. Ambjørn, Y. Watabiki, *Scaling in quantum gravity*, *Nucl. Phys. B* **445** (1995) 129–142, arXiv:hep-th/9501049.
- [81] P. Chassaing, G. Schaeffer, *Random planar lattices and integrated superBrownian excursion*, *Probab. Theory Relat. Fields* **128** (2004) 161–212, arXiv:math/0205226 [math.CO].
- [82] B. Durhuus, T. Jonsson, J.F. Wheater, *On the spectral dimension of causal triangulations*, *J. Stat. Phys.* **139** (2010) 859–881, arXiv:0908.3643 [math-ph].

- [83] J. Ambjørn, K.N. Anagnostopoulos, R. Loll, *A new perspective on matter coupling in 2D quantum gravity*, Phys. Rev. D **60** (1999) 104035, arXiv:hep-th/9904012.
- [84] J. Ambjørn, K.N. Anagnostopoulos, R. Loll, I. Pushkina, *Shaken, but not stirred—Potts model coupled to quantum gravity*, Nucl. Phys. B **807** (2009) 251–264, arXiv:0806.3506 [hep-lat].
- [85] J. Ambjørn, S. Jordan, J. Jurkiewicz, R. Loll, *Second-order phase transition in causal dynamical triangulations*, Phys. Rev. Lett. **107** (2011) 211303, arXiv:1108.3932 [hep-th].
- [86] M.R. Atkin, S. Zohren, *An analytical analysis of CDT coupled to dimer-like matter*, Phys. Lett. B **712** (2012) 445–450, arXiv:1202.4322 [hep-th].
- [87] J. Ambjørn, B. Durhuus, J.F. Wheater, *A restricted dimer model on a two-dimensional random causal triangulation*, J. Phys. A: Math. Theor. **47** (2014) 365001, arXiv:1407.6782 [hep-th].
- [88] P. Di Francesco, E. Guitter, C. Kristjansen, *Integrable 2D Lorentzian gravity and random walks*, Nucl. Phys. B **567** (2000) 515–553, arXiv:hep-th/9907084.
- [89] H.N.V. Temperley, E.H. Lieb, *Relations between the ‘percolation’ and ‘colouring’ problem and other graph-theoretical problems associated with regular planar lattices: Some exact results for the ‘percolation’ problem*, Proc. Roy. Soc. A **322** (1971) 251–280.
- [90] A. Morin-Duchesne, P.A. Pearce, J. Rasmussen, *Modular invariant partition function of critical dense polymers*, Nucl. Phys. B **874** (2013) 312–357, arXiv:1303.4895 [hep-th].
- [91] B. Duplantier, *Exact critical exponents for two-dimensional dense polymers*, J. Phys. A: Math. Gen. **19** (1986) L1009–L1014.
- [92] H. Saleur, *Conformal invariance for polymers and percolation*, J. Phys. A: Math. Gen. **20** (1987) 455–470.
- [93] H. Saleur, B. Duplantier, *Exact determination of the percolation hull exponent in two dimensions*, Phys. Rev. Lett. **58** (1987) 2325–2328.
- [94] H.W.J. Blöte, B. Nienhuis, *Critical behaviour and conformal anomaly of the  $O(n)$  model on the square lattice*, J. Phys. A: Math. Gen. **22** (1989) 1415–1438.
- [95] B. Nienhuis, *Critical and multicritical  $O(n)$  models*, Physica A **163** (1990) 152–157.
- [96] B. Eynard, C. Kristjansen, *Exact solution of the  $O(n)$  model on a random lattice*, Nucl. Phys. B **455** (1995) 577–618, arXiv:hep-th/9506193.
- [97] P. Di Francesco, E. Guitter, C. Kristjansen, *Fully packed  $O(n=1)$  model on random Eulerian triangulations*, Nucl. Phys. B **549** (1999) 657–667, arXiv:cond-mat/9902082.

- [98] G. Borot, J. Bouttier, E. Guitter, *Loop models on random maps via nested loops: case of domain symmetry breaking and applications to the Potts model*, J. Phys. A: Math. Theor. **45** (2012) 494017, arXiv:1207.4878 [math-ph].
- [99] V. Malyshev, A. Yambartsev, A. Zamyatin, *Two-dimensional Lorentzian models*, Mosc. Math. J. **1** (2001) 439–456.
- [100] B. Durhuus, M. Ünel, *Trees with exponential height dependent weight*, arXiv:2112.06570 [math.pr].
- [101] M. Drmota, *Random Trees: An Interplay between Combinatorics and Probability*, Springer Science & Business Media (2009).
- [102] I.M. Gel'fand, N.Ya. Vilenkin, *Generalized Functions, Vol. 4: Applications of Harmonic Analysis*, Academic Press (1964).
- [103] B. Durhuus, G.M. Napolitano, *Generic Ising trees*, J. Phys. A: Math. Theor. **45** (2012) 185004, arXiv:1107.2964 [cond-mat.stat-mech].
- [104] R. Haag, D. Kastler, *An algebraic approach to quantum field theory*, J. Math. Phys. **5** (1964).
- [105] R. Haag, *Local Quantum Physics: Fields, Particles, Algebras*, Springer (1996).
- [106] H. Araki, *Mathematical Theory of Quantum Fields*, Oxford University Press (1999).
- [107] V.F.R. Jones, *Some unitary representations of Thompson's groups F and T*, J. Comb. Algebra **1** (2017) 1–44, arXiv:1412.7740 [math.GR].
- [108] T.J. Osborne, D.E. Stiegemann, *Dynamics for holographic codes*, JHEP **04** (2020) 154, arXiv:1706.08823 [quant-ph].
- [109] J.W. Cannon, W.J. Floyd, W.R. Parry, *Introductory notes on Richard Thompson's groups*, Enseign. Math. **42** (1996) 215–256.
- [110] K.S. Brown, *Finiteness properties of groups*, J. Pure Appl. Algebra **44** (1987) 45–75.
- [111] D. Zhuang, *Irrational stable commutator length in finitely presented groups*, J. Mod. Dyn. **2** (2008) 499–507.
- [112] R. Bieri, R. Strebel, *On Groups of PL-homeomorphisms of the Real Line*, American Mathematical Society (2016), arXiv:1411.2868 [math.GR].
- [113] D.E. Stiegemann, *Approximating diffeomorphisms by elements of Thompson's groups F and T*, Morfismos **23** (2019) 1–10, arXiv:1810.11041 [math-ph].
- [114] A. Kliesch, R. Koenig, *Continuum limits of homogeneous binary trees and the Thompson group*, Phys. Rev. Lett. **124** (2020) 010601.

[115] V.F.R. Jones, *Scale invariant transfer matrices and Hamiltonians*, J. Phys. A: Math. Theor. **51** (2018) 104001, arXiv:1706.00515 [math.OA].

[116] P.A. Pearce, A. Klümper, *Finite-size corrections and scaling dimensions of solvable lattice models: an analytic method*, Phys. Rev. Lett. **66** (1991) 974–977.

[117] A. Klümper, P.A. Pearce, *Conformal weights of RSOS lattice models and their fusion hierarchies*, Physica A **183** (1992) 304–350.

[118] A.B. Zamolodchikov, *On the thermodynamic Bethe ansatz equations for reflectionless ADE scattering theories*, Phys. Lett. B **253** (1991) 391–394.

[119] A.B. Zamolodchikov, *Thermodynamic Bethe ansatz for RSOS scattering theories*, Nucl. Phys. B **358** (1991) 497–523.

[120] A. Kuniba, T. Nakanishi, J. Suzuki, *T-systems and Y-systems in integrable systems*, J. Phys. A: Math. Theor. **44** (2011) 103001, arXiv:1010.1344 [hep-th].

[121] P.A. Pearce, J. Rasmussen, I.Yu. Tipunin, *Critical dense polymers with Robin boundary conditions, half-integer Kac labels and  $\mathbb{Z}_4$  fermions*, Nucl. Phys. B **889** (2014) 580–636, arXiv:1405:0550 [hep-th].

[122] A. Morin-Duchesne, P.A. Pearce, J. Rasmussen, *Fusion hierarchies, T-systems, and Y-systems of logarithmic minimal models*, J. Stat. Mech. (2014) P05012, arXiv:1401.7750 [math-ph].

[123] P. Zinn-Justin, *Combinatorial point for fused loop models*, Commun. Math. Phys. **272** (2007) 661–682, arXiv:math-ph/0603018.

[124] V.V. Bazhanov, N. Reshetikhin, *Critical RSOS models and conformal field theory*, Int. J. Mod. Phys. A **4** (1989) 115–142.

[125] P. Fendley, N. Read, *Exact S-matrices for supersymmetric sigma models and the Potts model*, J. Phys. A: Math. Gen. **35** (2002) 10675, arXiv:hep-th/0207176.

[126] J. Murakami, *The Kauffman polynomial of links and representation theory*, Osaka J. Math. **24** (1987) 745–758.

[127] E.H. Lieb, *Residual entropy of square ice*, Phys. Rev. **162** (1967) 162–172.

[128] G.E. Andrews, R.J. Baxter, P.J. Forrester, *Eight-vertex SOS model and generalized Rogers-Ramanujan-type identities*, J. Stat. Phys. **35** (1984) 193–266.

[129] P.J. Forrester, R.J. Baxter, *Further exact solutions of the eight-vertex SOS model and generalizations of the Rogers-Ramanujan identities*, J. Stat. Phys. **38** (1985) 435–472.

[130] A. Brothier, *Forest-skein groups I: between Vaughan Jones' subfactors and Richard Thompson's groups*, arXiv:2207.03100 [math.GR].

[131] A. Brothier, *Forest-skein categories II: construction from homogeneously presented monoids*, arXiv:2212.01993 [math.GR].